

**Structural Controls on Mineralisation of the
Coronation Hill Deposit and Surrounding Area.
Record 1991/107.**

**A contribution to the BMR Kakadu
Conservation Zone Project 1987-1992**

R.K. Valenta

Department of Earth Sciences, Monash University



* R 9 1 1 0 7 0 1 *

DEPARTMENT OF PRIMARY INDUSTRIES AND ENERGY

Minister: The Hon. Alan Griffiths

Secretary: G.L. Miller

BUREAU OF MINERAL RESOURCES, GEOLOGY AND GEOPHYSICS

Executive Director: R.W.R. Rutland AO

© Commonwealth of Australia, 1991.

ISSN 0811 062X

ISBN 0 642 16997 7

This work is copyright. Apart from any fair dealing for the purpose of study, research, criticism, or review, as permitted under the Copyright Act, no part may be reproduced by any process without written permission. Copyright is the responsibility of the Director, Bureau of Mineral Resources. Inquiries should be directed to the Principal Information Officer, Bureau of Mineral Resources, GPO Box 378, Canberra City, ACT, 2601.

These three reports were prepared by Dr R.K.Valenta of Monash University, whilst acting as contractor to the Bureau of Mineral Resources, Geology and Geophysics, for the BMR Kakadu Project from 1987 to 1990. They are the actual reports as prepared by the contractor with no modifications to the text.

Part 1, 'Structure and mineralization in the South Alligator Valley, N.T.', is a combination of two reports, resulting from two contracts carried out over the 1987-1988 period. The purpose of the contracts was to determine the relationship between geological structure, rock alteration, and mineralisation of the Coronation Hill type, based on fieldwork carried out in the South Alligator Valley between the Rockhole and Coronation Hill deposits.

Part 2, 'Structure and Mineralization in the Mundogie and Eastern Stow areas, Kakadu Stage III, N.T. 1989 ', results from a contract issued in 1989 to map the extensions of the major structures which control mineralization in the Coronation Hill - Rockhole area, into the western and eastern part of the former ~2300km² South Alligator Conservation Zone where exposure is poor.

Part 3, 'Geological and Structural constraints on the Resource Potential of the Kakadu Conservation Zone.', was carried out as part of the 1990 BMR program to determine the inferred and potential resources of the 47 km² Kakadu Conservation Zone, for the Resource Assessment Commission. The report is based on the examination of drill core and surface structural features, and the Coronation Hill, El Sherana and Palette areas are examined in particular detail.

L.Wyborn

Kakadu Project Manager

1987-1991.

Table of contents

Summary.....	1
Objectives	1
Scope	1
Conclusions.....	1
Introduction.....	3
Structural Studies	4
Regional Structural Pattern.....	4
Summary of Structural Setting	4
Early Proterozoic Rocks.....	5
Outcrop Pattern	5
D ₁	5
D ₂	5
D ₃	5
D ₄	6
Mid Proterozoic Rocks	6
Outcrop Pattern	6
Folds.....	6
Faults	7
Fault Kinematics	7
Summary.....	10
Mineralization	11
Rockhole.....	11
El Sherana.....	12
Palette.....	13
Scinto VI and V	14
Saddle Ridge.....	14
Coronation Hill.....	15
Timing of mineralization relative to structures.....	17
Geometry of dilatant sites	17
Predictive model.....	18
Alteration.....	19
Discussion	20
Uplift/Subsidence related to fault movement.....	20

Estimation of displacement.....	20
Structural Controls on Mineralization.....	20
Structural/fluid circulation model.....	21
Gold-platinoid potential away from Coronation Hill.....	22
Conclusions	23
Recommendations	24
Acknowledgements.....	25
References	26
Appendix I - Samples collected, 1988	
Appendix II - Structural Data	
Appendix III - Selected thin section descriptions	
Appendix IV - Extract on types of alteration from an earlier report by R.K.Valenta	

Summary

Objectives

The general objective of this study has been to determine the deformation kinematics and structural setting of U-Au-P.G.E. mineralization in the South Alligator Valley. This study forms a background and a structural framework for associated studies of mineralization, alteration, sedimentology and geophysics within the Kakadu Stage 3 conservation zone.

Scope

Data and interpretations presented in this report are the result of two seasons of field work in the South Alligator Valley (08/87-09/87, 07/88) (figure 1), as well as preliminary knowledge of geochemical results from sampling performed in the first field season. An earlier report (Valenta, 1988) dealt with: a) the general history of folding and cleavage development; b) fault geometry and kinematics; c) the relationship between structure and U-Au-PGE mineralization; d) preliminary examination of variations in El Sherana Group stratigraphy relative to regional faults; and e) general definition of alteration types based on hand specimen characteristics.

This report is a general expansion and re-evaluation of some results from Valenta (1988), containing: a) more constraints on the timing and controls on mineralization; b) more information on specific deposits; c) and update of the predictive model for U-Au-PGE mineralization; d) a preliminary examination of the overall setting of structures in the South Alligator Valley within a regional context; e) re-evaluation of alteration studies in light of preliminary geochemical results; f) more detailed information on the timing, relative movements and possible fluid circulation patterns associated with regional faults; g) speculation on areas which are unevaluated and may be prospective based on present models; and h) possible extensions to the present mineralization model and related implications for relatively unexplored areas within the conservation zone.

Conclusions

1) The main northwest-trending dextral strike-slip fault system has controlled patterns of sedimentation and mineralization in the South Alligator Valley.

2) The relationship of this strike-slip system to regional framework of late faulting in the Pine Creek Geosyncline is still unclear.

3) U-Au-PGE mineralization occurred in the later stages of fault movement, in structurally-controlled dilation sites.

4) Orebody geometries vary systematically as a function of small scale variations in geometry of the major northwest-trending fault set.

5) The Early Proterozoic-Late Early Proterozoic unconformity is the most chemically favorable site for localization of mineralization, though similar sites within the basement cannot be ruled out.

6) Field evaluation of alteration types based on hand specimen characteristics has been shown to be ineffective.

7) Silicification patterns may be a guide to two dimensional fluid circulation patterns on major faults in the South Alligator Valley

Introduction

The South Alligator Valley contains numerous small uranium deposits, most of which were mined in the 1960's (Needham, 1987). The area has seen a recent resurgence in exploration activity and geological interest because of the discovery of a deposit of gold and platinoids associated with uranium mineralization in the area of the Coronation Hill mine. Thus, there is a strong possibility that similar gold-platinoid mineralization occurs in association with other small uranium deposits in the area. It has long been realized that structure has played an important role in both mineralization and sedimentation in the South Alligator Valley (Matheson, 1960; Ayres and Eadington, 1975; Needham, 1987; Crick et al, 1980). The aim of this project is to determine the structural framework of the South Alligator Valley, and to assess models of mineralization and sedimentation as they relate to structure. Critical questions which require structural input include: a) what is the timing of mineralization relative to sedimentation and structure; b) how much movement has there been on the major northwest-trending fault set; c) what was the regional tectonic regime during late faulting in the Pine Creek Geosyncline; d) what is the general predictive model for U-Au-PGE mineralization, and what areas fit this model; and e) What is the detailed history of deformation, mineralization, alteration and sedimentation in the South Alligator Valley.

Data presented in this report has been collected in two seasons of regional structural mapping and detailed pit mapping. This project is part of the ongoing B.M.R. resource assessment of the Kakadu Stage 3 Conservation Zone.

This report begins with a summary of the structural setting of the South Alligator Valley, and an examination of various implications of the dextral strike-slip model. More details on specific deposits are provided in a section on mineralization, along with a modified general predictive model for U-Au-PGE mineralization. This is followed by a brief evaluation of the results of preliminary alteration studies, and the report ends with discussions of the regional geological history, fluid circulation models, and identification of areas of Au-PGE potential.

Structural Studies

Regional Structural Pattern

The strike pattern of major faults in the Pine Creek Geosyncline-McArthur River area is summarized in figure 2. The three major fault sets cutting cover rocks in this area are: a) northwest-trending faults (eg. South Alligator, Bulman, Calvert Faults); b) north-trending faults (eg. Emu, Bath Range, Koolatong, Parsons Range Faults); and c) a series of faults within 20° of east-west (eg. Flying Fox, Jumb Faults). In most cases it is difficult to estimate fault displacements from map patterns, but it would appear that many of these show small displacements relative to their size. The main faults in the South Alligator Valley are part of the major northwest-trending set.

Summary of Structural Setting

Rocks in the South Alligator Valley are divisible into two main structural-lithological groups, which are separated by the Nimbuwah Event, the main structural-metamorphic event of the Top End Orogeny (Needham et. al., 1988):

1) Early Proterozoic rocks of the Namoonna, Mount Partridge, South Alligator and Finnis River Groups consist mainly of shales, quartzites and volcanic rocks which have been metamorphosed to greenschist facies and polydeformed. In the South Alligator Valley area, they strike northwest, dip near vertical and lie on the northeast limb of a major regional anticline.

2) Late Early Proterozoic to Middle Proterozoic rocks of the El Sherana, Edith River and Katherine River Groups consist mainly of felsic volcanics and coarse clastic sediments which lie unconformably on older rocks. They are unmetamorphosed and folded into gentle to tight folds.

There are two main fault zones in the South Alligator Valley (figure 3). The Rockhole-El Sherana-Palette fault system extends from north of Rockhole to well south of Coronation Hill. Most of the uranium deposits in the area occur on or near this fault system, which is well exposed within the El Sherana Group and in Early Proterozoic rocks. The South Alligator Fault extends from Rockhole to south of Coronation Hill. It forms the northeast outcrop limit of the Edith River Group, and is poorly exposed.

Four deformation episodes have been recognized in Early Proterozoic rocks of the South Alligator Valley. The structures show a progression from subhorizontal bedding-parallel fabrics, to upright and penetrative regional folds, to locally developed inclined and often shear-associated folds. This progression is similar to that recognized by Needham et al. (1988) and Johnston (1984).

Early Proterozoic Rocks

Outcrop Pattern

Bedding orientations in Early Proterozoic rocks are shown in figure 6. Bedding strikes consistently northwest, dips steeply southwest or northeast, and youngs consistently to the northeast. The Early Proterozoic stratigraphy of the Pine Creek Geosyncline has been summarized in Needham et al. (1988).

D₁

D₁ structures take the form of isoclinal folds, bedding-parallel fabrics, and rare transposed zones (Davies, 1981). Isoclinal folds are best developed in cherty ferruginous layers of the Koolpin Formation (figure 7a). They are usually subparallel to bedding and show a large variation in fold axis orientation. Vergence is usually difficult to determine, and appears to be inconsistent. D₁ bedding-parallel fabrics are developed within carbonaceous units of the Koolpin Formation, quartzites of the Mundogie Formation, red slates of the Masson Formation, and slates of the Kapalga Formation. Bedding-parallel fabrics within the Koolpin formation take the form of elongate pods of quartz-rich material, separated by zones of closely spaced opaque seams (possibly graphite) (figure 8b). Bedding-parallel fabrics are sometimes defined by the shape-preferred orientation of chert nodules in cherty ferruginous lithologies (figure 8a).

D₂

The D₂ deformation episode produced regional anticlines and synclines. Early Proterozoic rocks southwest of the Palette Fault lie on the northeast limb of a large scale D₂ anticline (figure 4), while those northeast of the Palette Fault are folded into a series of tight to isoclinal northwest-trending anticlines and synclines (figure 4). S₂ cleavage is regionally extensive in some phyllosilicate-bearing lithologies (eg. figure 7d), and is generally northwest-trending and subvertical (figure 5). F₂ fold axes plunge shallow northwest or southeast, and vergences are generally to the southwest. Where younging is visible, D₂ structures are consistently upward-facing.

D₃

D₃ structures take the form of small scale asymmetric folds (eg. figures 6e,f), sometimes associated with high strain zones (figure 9c). F₃ folds show steep plunges (figure 4) and cleavages are variably oriented (figure 5) and generally non-penetrative. F₃ folds show both northeast and

southwest vergences. A 20 to 30m wide D₃ high strain zone occurs within millimetre-scale boudinaged and transposed psammitic and pelitic units of the Koolpin Formation. Poorly developed S-C planes and shear bands in this area indicate dextral movement, with a major strike-slip component indicated by subhorizontal lineations. In thin section, this zone takes the form of a quartz-sericite rock with a penetrative foliation (figure 8b). Small scale extensional shear bands suggest a dextral sense of shear (appendix III). The rock is cut by numerous deformed quartz veins.

D₄

D₄ structures are spatially associated with shear zones, and take the form of polyclinal disharmonic folds which refold S₂ and S₃ (figure 9b). D₄ shear zones are strongly weathered phyllonitic zones (figure 9c) which show long histories of movement and internal deformation (figures 9d,f). The latest D₄ structures are small scale faults which show extensional offsets in both northwest-southeast and vertical directions (figure 9e). Faults of this type appear to have formed synchronously with faulting in the younger sequences (figure 9a).

Mid Proterozoic Rocks

Outcrop Pattern

The South Alligator River cuts down through the Mid Proterozoic sequences into the vertically-dipping Early Proterozoic sequence. In the study area (figure 4), the El Sherana group is mainly exposed on isolated hilltops, in fault-bounded inliers, and at lower levels of the main escarpment. The El Sherana Group thickens and becomes more continuous to the north of the South Alligator Fault (figure 4). The Edith River Group outcrops only to the south of the South Alligator Fault in the study area.

Folds

Bedding orientations for rocks of the El Sherana, Edith River and Katherine River Groups are shown in figure 6, in which it can be seen that all three groups are folded about a northwest-trending subhorizontal axis. Rocks of the El Sherana Group show the tightest folding, while rocks of the Katherine River Group show steep dips only in close proximity to fault zones. Small scale folds are absent in all three groups, probably because of their coarse grained, thickly-bedded nature.

Faults

Fault orientations for the entire South Alligator Valley are summarized in figure 10. The major fault orientation is northwest-trending, steeply dipping (eg. South Alligator Fault, Palette Fault, Rockhole Fault) (figure 8). Faults of this set are up to 20 km in length. Faults of 1-2km length occur in north-south (eg. Scinto Plateau area and Coronation Hill area in figure 10) and east-west (eg. Saddle Fault, figure 10) orientations. Faults ranging from 1m to 100m have been measured in exposures at Rockhole, Scinto Plateau, El Sherana, Saddle Ridge, Coronation Hill and Scinto VI (figure 10). Faults at this scale show large variation in orientation and movement sense. Faults with similar orientations sometimes show both normal and reverse movement in the same area (eg. figure 17), and in some cases striations indicate both strike-slip and dip-slip movement on the same plane. In figure 10 it can be seen that minor fault orientations vary from place to place in the South Alligator Valley. Reverse faults and flats dominate in the Rockhole area, while subparallel normal and reverse faults occur in the El Sherana pit. Dextral and reverse faults appear to predominate in the Scinto Plateau area, while the main fault in the Saddle Ridge pit is a reverse fault. Two generations of flat reverse faults occur in the Scinto VI mine, as well as steep faults in various orientations. Strike-slip faults and normal faults predominate in the Coronation Hill area.

Faults show a large variation in mesoscopic character. Movement lineations are well-developed in some cases (figure 12b), and absent in others. Fabrics associated with faults (figure 5) range in character from crenulation cleavage (figure 12e) to discontinuous fracture cleavage (figure 13 a,c,d) to phyllonite (figure 13b). In areas where major faults are not exposed, evidence for faulting takes the form of wide zones of crush brecciation (figure 12f) and/or pervasive microfracturing (figure 12c). Zones of shear-parallel veining (figure 12d) develop rarely.

Fault Kinematics

Major faults in the Kakadu Stage 3 area of the Pine Creek Geosyncline are summarized in figure 3. The major fault orientations in the South Alligator Valley are:

a) Northwest-trending faults which show both extensional and contractional offsets in cross section, and have movement lineations indicating both strike-slip and dip-slip movement (eg. Palette Fault, Rockhole Fault, South Alligator Fault).

b) North-trending faults which show either strike-slip or extensional offsets (eg. Coronation Hill, Scinto Plateau areas).

c) East-trending faults which show either strike-slip or contractional offsets (eg. Saddle Ridge Fault)

A possible kinematic interpretation of faulting in the South Alligator Valley is shown in figure 11, in which the major northwest-trending faults are interpreted as dextral strike-slip faults, and observed variations in outcrop level (and to a certain extent sediment thickness) are interpreted in terms of small scale geometrical effects associated with strike-slip movement. It should be stressed that the overall setting appears to be one of *divergent* wrench faulting (Harding et al., 1985), with most of the major faults showing a component of southwest-block-down movement. Using this model, it is possible to explain many of the observed outcrop and fault patterns:

1) Reverse faulting in the Rockhole area appears to have been due to the transpressional effects of a slight bend in the Palette Fault-Rockhole Fault system (figures 2, 11).

2) Normal and reverse faulting in the El Sherana pit is slightly removed from the main Palette-Rockhole fault system (figure 10). It is possible that normal faulting occurred on an earlier strand of this system in a releasing bend geometry, with reverse faulting taking precedence when the main strand of the Palette-Rockhole system became active.

3) The Scinto Plateau area contains an extensional duplex (Woodcock and Fisher, 1986) with at least for north-trending faults showing small dextral strike-slip displacements (figures 2,10). Slickensides are generally well-developed on this fault set (figure 12b) and veining is relatively common (figure 12d).

4) This system is bounded to the south in the Saddle Ridge pit by a subvertical east-west fault showing north-block-down displacement. There is abundant folding, fracturing and cleavage development associated with this fault, and it has been interpreted as one of a set of east-trending oblique contractional faults.

5) Further to the southeast, movement on this set has produced the downfaulted Pul Pul Hill block which is bounded to the northwest and southeast by upfaulted blocks.

6) The Coronation Hill area shows abundant evidence of long-lived (including synsedimentary) fault movement. The overall geometry is consistent with a releasing overstep (Christie-Blick and Biddle, 1985) where the Palette Fault transfers displacement to the South Alligator Fault and a slightly offset extension of the Palette Fault. This has resulted in a basin centered around the rhomb-shaped overstep, with both dip-slip and strike-slip bounding faults.

7) Mineralization in the Slesbeck area is associated with north-block-up reverse faulting on an east-trending fault set which occurs at the southeast end of the Palette-South Alligator Fault system (figure 3, 29). This is interpreted to be a contractional fault setting similar to the Saddle Ridge fault geometry.

A schematic cross-section interpretation of the South Alligator Valley is shown in figure 14. This interpretation is once again based on general strike-slip basin models (Christie-Blick and Biddle, 1985). Evidence in favour of this interpretation is as follows:

1) The range of major fault orientations and movement directions is consistent with shortening in a north-south direction and extension in an east-west direction. Vertical northwest-trending faults within this kinematic framework should show dextral strike-slip movement.

2) There is a change in basement type across the South Alligator Valley. The transition from Koolpin to Kapalga is a fundamental regional change in both geologically and geophysically (Stuart Smith et al., 1980).

3) There is a change in style of pre-fault structures across the South Alligator Valley. Rocks on the southwest side lie on one limb of a large scale F_2 anticline, while rocks on the northwest side are folded into a series of tight to isoclinal F_2 folds. The transition between these two structural styles occurs abruptly across the Palette Fault.

4) Most large scale faults in the area are steep. There is no evidence for listric faulting.

5) Normal and reverse faults appear to coexist both temporally and spatially within the valley, indicating a complex history of shortening and extension similar to that reported in many strike slip basins.

6) Offsets on single faults vary from unit to unit (figure 14), indicating some combination of synsedimentary fault movement and movement out of the plane of section.

7) Individual units show marked thickness and facies variations across faults. An example of this is the change in thickness of the lower El Sherana group across the Palette and Fisher Faults.

8) Conglomerates of the El Sherana Group commonly show diverse sources (Needham and Stuart Smith, 1985), including nearly coeval volcanics from adjacent fault blocks.

Regional thickness variations indicate that the thickest accumulation of El Sherana Group sediments was in a restricted basin bounded by the South Alligator and Fisher Faults, as suggested by Needham and Stuart Smith (1985). The area of deposition of the Edith River Group was mostly south of the South Alligator Fault. Fault movement continued into post-Kombolgie time, as indicated by fault-associated folding in the Kombolgie Formation.

Summary

Early Proterozoic rocks in the South Alligator Valley have been affected by three main folding events. D₁ takes the form of rare isoclinal folds developed within cherty ferruginous units of the Koolpin formation. Some bedding-parallel fabrics may be related to D₁ as well. D₂ produced the regional anticlinal axis to the southwest of the South Alligator Valley, and takes the form of west-verging folds and cleavage in the South Alligator Valley. D₃ produced minor northeast-verging folds and cleavage in the South Alligator Valley. Minor late folds occur in a number of orientations.

Early Proterozoic rocks in the South Alligator Valley can be divided into two main structural domains. Rocks on the southwest side of the Rockhole-El Sherana-Palette Fault system strike northwest and are generally subvertical in the area between Rockhole and Coronation Hill. Rocks on the northeast side of this fault system are cut by numerous dykes and sills of Zamu dolerite. They are folded into a series of smaller amplitude folds and display a subhorizontal form surface. These two domains are separated by a poorly-outcropping high strain zone which shows S-C planes consistent with dextral movement. This high strain zone is folded by F₃ folds.

High strain zones have also been noted near the Koolpin/Mundogie boundary in the northwest part of the Conservation Zone (Johnston, 1984; Davies, 1981). Strong folding is common in cherty ferruginous layers of the Koolpin Formation, suggesting that these layers may have been zones of movement during the Nimbuwah Event as well.

Rocks above the Early Proterozoic unconformity consist of three groups, separated by angular unconformities (Needham et. al., 1988). The El Sherana Group is present with varying thickness throughout the South Alligator Valley, and is a sequence of bimodal volcanics and high energy clastic rocks. The El Sherana Group appears to have been deposited during extension on the main northwest-trending fault set. Deposition of the El Sherana Group was followed by the Maud Creek Event, which produced gentle to close northwest-trending folds. The Edith River Group, a sequence of rhyolitic volcanics and coarse clastics, was deposited following the Maud Creek Event. The Edith River Group is not present on the northeast side of the South Alligator Fault, implying erosion or non-deposition in this area. The Edith River Group was gently folded about northwest-trending axes during the Shoobridge Event, and deposition of the Katherine River Group followed this. Rocks of the Katherine River Group have been gently folded about northwest-trending axes as well. This sedimentation-deformation history implies alternating extension and contraction in a northeast direction. An alternate explanation is that basin formation and folding about the same axis were related to an ongoing process of strike slip movement on the two major fault systems.

Mineralization

Characteristics of the uranium major deposits have been discussed by a number of authors (e.g. Matheson, 1960; Threadgold, 1960; Ayres and Eadington, 1975; Crick et al., 1980; Needham, 1987; Needham and Stuart-Smith, 1987; Valenta, 1988). The purpose of the following sections is to provide more detail on the structural setting, alteration, orebody geometry, and structural timing of the major uranium deposits in the South Alligator Valley.

Rockhole

Information on the Rockhole deposit is based on published data as well as surface and underground mapping and sampling in the Rockhole area.

The main fault in the Rockhole area is a northwest striking, steep southwest-dipping reverse fault. On the surface, rocks of the Koolpin Formation outcrop to the southwest of this fault and rocks of the Coronation sandstone and Pul Pul Rhyolite outcrop to the northeast. Subsurface control (eg. Ayres and Eadington, 1975) shows that the unconformity is gently northeast-dipping and is displaced up to the southwest across a series of northwest-striking reverse faults. The main faults also show horizontally pitching bends to a gentler southwest dip. The main fault is exposed in the upper adit. In this area, there is a set of flat fractures associated with the fault, and a set of synthetic shears consistent with a component of dextral strike slip. In other underground exposures the fault contact can be a single sharp zone, a zone of minor faulting or a zone of cataclasite up to 1-2 m in thickness.

The Koolpin Formation near the Rockhole fault shows a number of late structures in addition to early isoclinal and west-verging folds. These include west-verging kink folds and shallow southwest-plunging reverse faults. The timing of these structures relative to the Rockhole Fault is unclear.

Mineralization occurs in shallow bends, on flat fractures, and on the unconformity. The uranium orebodies generally define subhorizontal pipes or flat ribbons on a large scale (Ayres and Eadington, 1975). All these features are associated with extension in a vertical direction. The localization of orebodies on faults indicates a syn- to post-fault timing for uranium mineralization. The systematic localization of mineralization on features related to vertical extension suggests that mineralization occurred during faulting, rather than later. Rhyolites in and around the upper adit are strongly altered to sericite and clay minerals. No samples have been taken from below the weathered zone.

El Sherana

Information on El Sherana is based on mapping in the El Sherana and El Sherana West pits, as well as geological reconnaissance around the pit areas. Rock types exposed in the El Sherana area include cherty ferruginous and carbonaceous rocks of the Koolpin Formation, conglomerates and sandstones of the Coronation Sandstone formation, and altered volcanic rocks of the Pul Pul Rhyolite. The plan and cross section geology of the El Sherana pit is shown in figures 18 and 17 respectively. In these it can be seen that there are two main fault types present: a) a steep southwest-dipping normal fault; and b) a set of moderate to shallow southwest-dipping reverse faults. On the northeast side of the pit, Pul Pul Rhyolite directly overlies the Koolpin Formation, while on the southwest side the Koolpin Formation is overlain by Coronation Sandstone. An interpretation of this fault geometry involving fault movement and erosion during El Sherana Group deposition is shown in figure 19. The three stages shown in this model are: a) movement on the steep southwest-dipping normal fault following deposition of the Coronation Sandstone; b) erosion of the Coronation Sandstone on the northeast side of the fault, followed by deposition of the Pul Pul Rhyolite on the eroded surface; and c) southwest-block-up movement on shallow southwest-dipping reverse faults. The end result of this movement history is a net downthrow on the unconformity and a net upthrow on the Pul Pul Rhyolite.

Mineralization at El Sherana occurs in a tabular body which tapers at depth (Ayres and Eadington, 1975), parallel to the northwest-striking subvertical Koolpin Formation. Mineralization is mainly concentrated in carbonaceous layers within the Koolpin Formation. Rocks of the Pul Pul Rhyolite are strongly altered in and around the El Sherana pit. A sample taken from the northwest end of the pit shows strong desilicification and sodium depletion (L. Wyborn, pers. comm.).

It is difficult to place a timing on mineralization in the El Sherana area. The tabular shape of the orebody does not suggest a relationship with a specific structural feature. The control in this case appears to be more chemical in nature. It is, however, likely that an extensional setting would favour dilation on bedding and the resultant formation of tabular orebodies. The profound alteration of Pul Pul Rhyolite suggests that mineralization postdates El Sherana Group deposition, but the timing relative to Kombolgie deposition is unknown.

Future work on this deposit should include drill core examination and sampling, more detailed surface mapping and examination of underground mapping and sampling data.

Palette

Work in the Palette area has been confined to preliminary reconnaissance of surface exposures and adit entrances in the mine area. Some structural interpretations are therefore based on plans and cross sections by other workers (eg. Matheson, 1960; UUNL company maps).

The Palette deposit occurs on and near the Palette Fault on the northeast side of the Scinto Plateau. The Scinto Plateau contains a thinned section of El Sherana Group and is capped by Kombolgie Sandstone. A plan of the Palette area is shown in figure 21. From this, it can be seen that the Palette deposit lies in an area of intersection of three major fault sets:

a) The main fault is the Palette Fault, which is steeply northeast-dipping in this area and now shows a relative northeast-block-up displacement in vertical section. The El Sherana Group is thinned on the southwest side of this fault, suggesting a period of erosion related to southwest-block-up movement prior to deposition of the Kombolgie Sandstone. The latest movement on this fault resulted in folding of the Kombolgie sandstone into a doubly plunging, basin-like synform which is cut by north-trending dextral faults. Rocks of the Pul Pul Rhyolite are strongly altered and sheared near this fault. Two cleavages are visible in deformed volcanics in the northern adits of the Palette mine.

b) A series of north-striking subvertical dextral strike slip faults occur in the Scinto Plateau area. This set displaces the Palette Fault, and shows well developed subhorizontal movement lineations in a number of areas. A fault of this set is well-exposed in the upper drill pad in the Palette mine area, where it forms the contact between Coronation Sandstone and highly deformed bleached carbonaceous Koolpin Formation.

c) Shallow southwest-dipping reverse faults bring carbonaceous Koolpin Formation over Coronation Sandstone in the area of the Palette mine. These faults are not well-exposed, so it is difficult to determine their true movement vector. Faults of this set are interpreted to postdate the Palette Fault and north-striking dextral faults.

Mineralization occurs along the Palette Fault, the north-striking dextral fault and the unconformity, but is not present on the southwest-dipping reverse fault (Matheson, 1960). Thus, the latest fault movement appears to postdate mineralization. The overall shape of the orebodies is not known. Most samples of Pul Pul Rhyolite in the area are strongly altered to sericite and clay minerals, though it is not known what form this alteration takes at depth. It is likely that mineralization occurred during movement on the Palette Fault and the north-striking dextral fault set, in an overall setting of constriction perpendicular to the Palette Fault. The obvious control is dilation on the north-striking dextral fault set, a geometry similar to that developed at Coronation Hill.

The Skull mine (figure 22) is a small deposit (3t U₃O₈) in which mineralization and alteration occur in a zone of northeast-trending fractures associated with a north-trending dextral strike-slip fault. The occurrence of mineralization on faults of only this orientation would suggest that mineralization occurred during fault movement, and the northeast-trending fractures were in an orientation favorable for tensile failure.

Scinto VI and V

Fault geometry in the Scinto VI mine is schematically shown in figure 23. Secondary U mineralization and sericitic alteration are associated with subvertical faults which are cut by at least one set of shallow reverse faults. This indicates that in some cases reverse faulting continued after mineralization.

Structures in the Scinto V mine are schematically summarized in figure 24. The pit coincides with a northwest-trending quartz-filled fault of unknown movement, which cuts a zone of doubly-plunging folds and cleavage. Folds change in dip from 52°N at the northern end of the pit to 17°S near the southern end. The detailed distribution of mineralization relative to this feature is unknown, but it is possible that the structural control in this case was fluid channelling into the top of the doubly-plunging anticline.

Saddle Ridge

Work done in the Saddle Ridge area includes detailed pit mapping and reconnaissance of the geology around the pit. Volcanics and minor sandstone layers of the El Sherana Group outcrop on the north side of the pit, and polydeformed and faulted rocks of the Koolpin Formation outcrop on the south side. They are separated by a major east-striking, south-block-up reverse fault which occurs in the center of the pit. Volcanics of the El Sherana Group are strongly altered to a bottle green colour associated with surface sericitization. Sandstone lenses within the El Sherana Group are south-dipping and overturned in the pit.

Mineralization occurred mainly within the altered volcanics, and was almost entirely secondary in origin (Matheson, 1960; Needham, 1987). The extent of alteration in the Pul Pul Rhyolite in the Saddle Ridge area is not known, nor is it possible to say whether this alteration was related to earlier primary mineralization or secondary mineralization only.

The east-striking fault in the Saddle Ridge pit is an oblique contractional fault associated with the main Palette Fault system. In this setting it is likely that any primary mineralization would be

located on subhorizontal east-striking pipe-like or ribbon-like features, similar to those developed at Rockhole.

Coronation Hill

Work done in the Coronation Hill area includes detailed mapping of the original pit, surface mapping in the Coronation Hill area, and preliminary sampling and reconnaissance in the area of recent bench development.

The large scale fault geometry of the Coronation Hill area is shown in figure 26. The Coronation Hill area occurs at the meeting point between two slightly offset branches of the Palette Fault. The Palette Fault Crosses the northern margin of Coronation Hill and continues southeast from the center of Coronation Hill. The main faults on Coronation Hill strike north, east and north-northwest. Faults occurring in the pit include (figure 27):

a) an east-trending fault which separates debris flow conglomerates from volcanics of the Coronation Sandstone. Movement on this fault appears to be north-block-down, though the actual slip vector is not known. Faults of this type occur in various locations away from the pit on the north side of Coronation Hill, where they are generally offset by north-trending faults. The debris flow conglomerate may be a fault scarp deposit, though it is clearly deformed by the latest movement on the east-trending fault set.

b) a north-trending fault which separates debris flow conglomerate to the west from green tuffaceous siltstone to the east. This fault is generally poorly exposed. Where visible, movement lineations are subvertical and the inferred displacement is east-block-up. This fault truncates and therefore postdates the east-trending normal fault. Rocks which are mapped as "green tuffaceous siltstone" are still somewhat enigmatic. They appear to be volcanic in origin and therefore correlatable with the El Sherana Group, yet they contain up to three cleavages and abundant deformed veins in the Coronation Hill Pit. These rocks were previously interpreted as El Sherana Group by the author (Valenta, 1988), though the occurrence of a nearly identical rock type in the Early Proterozoic sequence at the north end of the Scinto Plateau suggests that they may instead be part of the Early Proterozoic sequence.

c) The north-trending fault is cut by a 3-5 m spaced set of north-northwest trending faults which display movement lineations and geometries consistent with dextral strike-slip movement. This series of stepping faults appears to define an overall north-trending zone, in which individual faults are connected by releasing oversteps. Uranium and gold-platinoid mineralization appear to be spatially related to this fault set, though more information is needed in order to test this hypothesis.

The general fault progression, therefore, is from north-trending and east-trending dip slip faults to north-trending dextral strike slip faulting. The latest movement on all these faults postdates El Sherana Group deposition, though the profound stratigraphic changes across fault blocks in the Coronation Hill area suggests that faults were active during sedimentation as well. The fault interpretation presented here is based on surface mapping only. It is expected that additional subsurface information will allow a much more detailed interpretation of the fault history of the Coronation Hill area, and may cause major modification to some of the interpretations presented in this report.

Uranium mineralization occurs in carbonaceous fragments within the debris flow conglomerate (Needham et al, 1987), while gold-platinoid mineralization occurs in almost all rock types in the area (BHP geologists, pers. comm.). Data on the detailed distribution of gold and platinoid mineralization has not been made available to the author, though it would appear that mineralization on the surface is elongate parallel to the type "c" large scale north-trending fault set described above. There is no data presently available on the shape or distribution of gold-platinoid mineralization in the subsurface.

Mineralization appears to have occurred during or after fault movement, as indicated by the fact that it occurs in lithologies of various ages in association with the main north-trending fault zone. Once again, the fact that this would have been a zone of dilation within the large scale fault framework suggests that mineralization occurred during, rather than after fault movement.

Orientations of veins in the Coronation Hill area are shown in figure 28. It can be seen that veins cover a wide range of orientations, although it appears that many veins lie on a northeast-trending great circle and vary from horizontal to steeply northeast-dipping. The three sets defined do not appear to show significant differences in orientation, even though the earliest veins probably formed during deposition of the El Sherana group while the latest veins probably formed much later.

A set of geochemical samples were taken in the area of gold-platinoid mineralization, but the results have not yet been processed. The effects of surface weathering are strong in this area, so any detailed study of alteration associated with gold-platinoid mineralization will require the collection of fresh samples from drill core.

Much more data is needed before a detailed model of the genesis of the Coronation Hill deposit can be produced. This should include examination and sampling of drill core, detailed bench mapping, and smaller scale and more detailed surface mapping.

Timing of mineralization relative to structures

In almost all uranium deposits in the South Alligator Valley, mineralization is localized around fault zones. This indicates that fluid permeability was probably a major factor in localization, and it also indicates that mineralization must have formed during or after fault movement. Mineralization is also often localized in zones which are clearly associated with dilatancy during fault movement. Perhaps the best example of this is the occurrence of mineralization in pipe-like subhorizontal features on the Rockhole reverse fault (cf. Johnston and Wall, 1983). This indicates that mineralization probably formed during fault movement, since increased permeability in dilatant zones is likely to have been transient. In most deposits there is clear evidence of significant post-El Sherana group deformation. In fact, at the Palette mine there is abundant primary U mineralization in rocks of the El Sherana Group (Crick et al., 1980). This would suggest that U mineralization postdated deposition of the El Sherana Group. Mineralization is often associated with faults which have deformed and displaced rocks of the El Sherana Group and the Katherine River Group. An example of this is the Palette mine, where a north-trending dextral fault clearly post-dates Kombolgie deposition and contains primary mineralization. There is no evidence for a component of pre-Kombolgie movement on this fault. This suggests that mineralization, in this case, postdates Kombolgie deposition.

It is also important to note that there appears to have been more than one generation of mineralization at Rockhole (Threadgold, 1960) and Coronation Hill (Needham and Stuart Smith, 1980), suggesting the possibility of evolving mineralization systems and/or late remobilization of pre-existing mineralization. Structural observations at Coronation Hill suggest that there was a significant component of syndepositional deformation which predated intrusion of the quartz feldspar porphyry, though it is also clear that mineralized structures postdated this intrusive event.

In summary, it is difficult to constrain the structural timing of mineralization any more than from syn-El Sherana Group deposition to post-Kombolgie deposition, and any attempt to do so must take into account the possibility of remobilization and/or long-lived multi-stage mineralization.

Geometry of dilatant sites

The variations in shape and orientation of dilatant sites are summarized in figure 33. The main uranium deposits in the South Alligator Valley can be divided into two types based on their setting within the strike-slip system:

- 1) Rockhole and Saddle Ridge occur on features which are contractional within the framework of the strike slip system. That is, movement on the strike-slip system would result in a major buildup of compressive stress in the horizontal plane in these zones. The result of this is that the rocks must extend in a vertical direction, so dilation and tensile fracturing is favoured on planes which are close

to horizontal. Mineralization at Rockhole occurs in subhorizontal pipe-like or ribbon-like orebodies, while the shape of primary mineralization at Saddle Ridge is not known. Late faulting at El Sherana is also contractional, though the timing of this faulting relative to mineralization is still unclear.

2) Palette and Coronation Hill occur on features which are dilatant within the framework of the strike-slip system. They occur in areas in which any strike-slip movement would produce tensile stresses in the horizontal plane perpendicular to the maximum principal stress. Mineralization in this setting therefore tends to occur on subvertical features which are subparallel to the maximum principal stress. This explains the localization of mineralization on north-trending subvertical faults at Palette and Coronation Hill.

Predictive model

Needham (1987) proposed a general set of characteristics for uranium deposits in the South Alligator Valley. In this section, these will be extended to include structural observations and preliminary observations on gold-platinoid mineralization.

1) Uranium deposits generally occur in cherty ferruginous units of the carbonaceous Koolpin Formation, below the Early Proterozoic-Middle Proterozoic unconformity. Gold-platinoid mineralization occurs below and above the unconformity, and is hosted in a wide range of rock types (BHP geologists, pers. comm.)

2) Uranium mineralization never occurs greater than 100 m below the unconformity and never more than a few metres above it. Gold-platinoid mineralization appears to be much more widely distributed, though precise distances above and below the unconformity are not known.

3) Uranium mineralization is localized in brittle features. Gold-platinoid mineralization appears to share this control. Mineralization is localized on subhorizontal brittle features in contractional areas and on subvertical features in extensional areas.

4) Primary uranium mineralization occurs as uraninite in veins and lenses. Uranium mineralization is generally in restricted and easily recognized positions, while gold-platinoid mineralization appears to be associated with larger scale fluid circulation systems, possibly cogenetic with uranium. Minor gold-bearing quartz veins are known to occur in the area of uranium mineralization at Coronation Hill (Needham and Stuart-Smith, 1987), but there is otherwise little information available on the mineralogy and petrography of gold-platinoid mineralization.

5) Chlorite and hematite are common gangue minerals associated with uranium mineralization. Gangue minerals associated with gold-platinoid mineralization are not known, though the general

alteration pattern associated with mineralization appears to involve desilicification and sodium depletion. Sericitic and clay-rich surface alteration is well-developed in the Coronation Hill area, though the character of this alteration at depth is not known. Chloritic, kaolinitic and sericitic lithologies are all possibilities.

Alteration

In the 1987 field season, four separate alteration types were identified on the basis of hand specimen characteristics[†]. Regional types were subdivided into a widespread hematitic alteration and a more restricted joint-related sericitic alteration. Alteration types associated with mineralization were subdivided into weakly sericitic rocks and strongly sericitic, clay-rich lithologies. It was recognized in Valenta (1988) that there were a number of problems with this classification, including:

- 1) It was based on characteristics of rocks which have undergone surface weathering.
- 2) It was mainly applicable to altered volcanics of the El Sherana Group.

Results of geochemical analyses have subsequently shown that the four alteration types are chemically indistinguishable. The following possible conclusions can be drawn from this:

- 1) The classification system was not useful.
- 2) A broad range of hand specimen types have similar chemistry, suggesting that other methods must be used to determine alteration patterns.
- 3) All samples have probably been subjected to some degree of chemical modification due to surface weathering. Evaluation of alteration patterns in deeply weathered rocks is not particularly useful.
- 4) The alteration system associated with the Rockhole-El Sherana-Palette system is regional in extent, and must have involved large volumes of focussed fluid.

A more detailed evaluation of the existing geochemical database is needed before more conclusions can be drawn regarding the nature and extent of alteration in the South Alligator Valley.

[†] See Appendix 4 for a description of the 4 alteration types identified in the field, extracted from a previous report.

Discussion

Uplift/Subsidence related to fault movement

Variations in thickness of the El Sherana Group in the South Alligator Valley are shown in figure 31. In the Rockhole and El Sherana areas, the Coronation sandstone is thinned or absent on the northeast side of the fault. This indicates that in these areas, rocks on the northeast side of the fault were uplifted during deposition of the El Sherana Group. Later movement on the Rockhole-El Sherana-Palette fault system in both areas shows the opposite sense, with southwest-block-up displacement on northwest-trending reverse faults. The same fault set approximately 2 km southeast of El Sherana shows northeast-block-down movement during El Sherana Group deposition. Thus, the overall movement in this area following deposition of the Coronation Sandstone changed laterally from northeast-block-up to northeast-block down. One interpretation of this pattern is that minor fault irregularities were responsible for local variations in uplift during fault movement. This is consistent with a strike-slip interpretation for the major fault systems.

Estimation of displacement

At present there are no markers which can be used to place a figure on the amount of movement on the Rockhole-El Sherana-Palette fault system. However, overall relationships across the fault can be used to make a qualitative estimate of the displacement which occurred at various times in the fault history. The Rockhole-El Sherana-Palette fault system juxtaposes Early Proterozoic rocks of different stratigraphic groups and different structural style. It is possible that dextral strike-slip movement on this fault system prior to El Sherana Group deposition may have been as much as 10's of kilometres. In contrast to this, rocks of the El Sherana Group often change in thickness but are similar in characteristics on either side of the Rockhole-El Sherana-Palette fault system. This indicates that strike-slip displacement during and after deposition of the El Sherana Group was probably much less than earlier displacement, possibly on the order of 3-5 km.

Structural Controls on Mineralization

The most comprehensive work on structural controls on South Alligator River Uranium Field or related deposits has been done by Johnston (1984), who proposed a model involving fluid focussing in dilatant fault jogs at or near the unconformity in various deposits of the East Alligator River Uranium Field.

Ore localization at the unconformity is clearly due to a combination of chemical and structural factors. Carbonaceous lithologies are not uncommon in the lower Proterozoic rocks, and therefore it is likely that the final localization of ore is essentially a structural process. The role of deformation in this setting would be to set up fluid pressure gradients and permeability patterns suitable for fluid focussing. The structural processes producing these variations include: 1) the effects of displacement on irregular faults; 2) dilation on pre-existing fractures or foliations; 3) enhancement of permeability due to faulting; and strain incompatibility between basement and cover rocks.

1) Displacement on irregular faults is an effective means of producing permeability and fluid pressure gradients (eg. Guha et al., 1983; Sibson, 1987; Cox et al., 1987). An example of this is the occurrence of ore in more gently dipping portions of the Rockhole reverse fault.

2) Ore deposition commonly occurs on minor fractures or pre-existing foliations rather than on major structures with significant movement (eg. Robert and Brown, 1986). This is evident in the South Alligator Valley on both macroscopic and mesoscopic scales. Most of the relatively large deposits (eg. El Sherana, Palette, Saddle Ridge, Coronation Hill) occur on macroscopic faults which are not parallel to the major northwest-trending fault set. Similar effects are visible on a mesoscopic scale at Rockhole (figure 16) and Skull (figure 22). This localization of mineralization is due to the fact that minor faults are more likely to occur in orientations favorable for dilation, and faults with small offset are more likely to preserve large fault surface irregularities which can dilate during movement.

3) It is common to see wide zones of variably intense crush brecciation associated with major faults (figures 11f, 12a, 12d). Rocks within these zones would be much more permeable than their undeformed equivalents.

4) Late structures within the Lower Proterozoic sequence take the form of small scale (and possibly large scale) faults with extensional offsets in both northwest and vertical directions. Coeval structures in the Mid-Proterozoic sequence take the form of subhorizontal northwest-trending folds. The incompatibility between these two macroscopic deformation styles is likely to have resulted in large variations in stress and permeability during deformation.

Structural/fluid circulation model

Uranium-gold-platinoid mineralization is localized in dilatant features, and desilicification associated with mineralization indicates that ore-bearing fluids probably flowed downward. The simplest hydrodynamic model based on this is as follows: a) dilatancy associated with movement on major faults caused the formation of downward-sucking fluid pressure gradients. b) fluid flowing down from upper levels in the area caused desilicification and deposited uranium, gold and platinoids

in areas of suitable chemistry (e.g. carbonaceous lithologies, reduced fluids, calcareous lithologies...). c) sealing of dilatant features caused a reversion to normal fluid pressure gradients, causing a return flow of fluid toward the surface. Upward-flowing fluids are likely to have deposited quartz, rather than dissolving it. A schematic diagram of this system is shown in figure 34. Using this model, mineralization may be related to dilation at the unconformity or below the unconformity within basement rocks. Fluid is focussed into the zone of mineralization in the first case, while in the second case the zone of mineralization is simply a pathway to the deeper dilatant zone.

The Palette Fault to the southeast of Coronation Hill takes the form of a wide zone of silicification and abundant quartz veining. The unconformity is not exposed in this area. A detailed sampling traverse has been performed over this part of the fault, in order to determine the patterns of alteration associated with it. It is possible that this strongly siliceous fault represents a zone of large scale fluid upflow. Quartz veins in similar orientations cut the Scinto Breccia at the north end of the Scinto Plateau, but their timing relative to fault movement is not known. It is possible that fluid circulation on major faults in the South Alligator Valley may be responsible for an overall upward transfer of silica during deformation and mineralization. In this case, the buried unconformity in the silicified portion of the Palette Fault may be mineralized at depth.

Gold-platinoid potential away from Coronation Hill

It is important to note that there are no major differences between Coronation Hill and other uranium deposits in the South Alligator Valley. Uranium mineralization is associated with faults, hosted by carbonaceous lithologies, and the area contains a broadly similar assemblage of rock types. Gold-platinoid mineralization is hosted in a wide range of lithologies (BHP geologists, pers. comm.). Alteration in the Coronation Hill area seems to be chemically consistent with the penetrative desilicification and sodium depletion noted over most of the South Alligator Valley.

Rockhole, Palette and El Sherana all contained minor amounts of gold associated with the uranium orebodies (Needham, 1987), and this was also the case in the Coronation Hill uranium deposit. A possible interpretation of this is that each of these uranium deposits represents a uranium-bearing portion of a much larger gold-platinoid bearing alteration system. This could have the following implications:

- 1) Significant gold-platinoid mineralization may occur in altered areas which contain little or no significant uranium mineralization.
- 2) Gold-platinoid mineralization may occur at a significant distance above or below the unconformity.

If these prove to be correct, large areas in which the unconformity is eroded away or buried may be prospective for Coronation Hill-style gold-platinoid mineralization. In addition to this, areas within the South Alligator Valley with no major uranium deposits may be prospective for gold-platinoid mineralization. These two possibilities open up a large area of the conservation zone outside the present area of main interest.

The critical need at this point is for a better understanding of the detailed relationship between gold-platinoid and uranium mineralization at Coronation Hill. It is possible that the structural/chemical controls for gold-platinoid mineralization may be slightly different, and the only way to examine this is a detailed study of the Coronation Hill deposit.

Conclusions

1) The main northwest-trending mineralized fault system in the South Alligator Valley shows a long movement history, beginning prior to deposition of the El Sherana Group and ending after deposition of the Katherine River Group. Movement on this fault set had a major influence on patterns of sedimentation and mineralization in the South Alligator Valley. Pre-El Sherana Group dextral strike-slip movement on this system may have been up to 10's of kilometres, while strike-slip movement during and after El Sherana Group deposition probably totalled less than 5-10 kilometres. Only minor late stage strike slip displacement would have been required to produce the observed patterns of dilation related to mineralization.

2) The South Alligator Valley contains one of the major northwest-trending fault sets of the Pine Creek Geosyncline. The regional importance of the dextral strike slip model, and the potential for its extension to other areas of the Pine Creek Geosyncline, is still unclear. Sinistral movement reported for faults of similar orientation (eg. the Jim Jim Fault) may imply that the overall setting during post-Kombolgie fault movement was one of "minor readjustment" rather than large scale non-coaxial deformation.

3) U-Au-PGE mineralization occurred during fault movement in structurally-controlled sites of dilation. It is likely that mineralization occurred after deposition of the Kombolgie sandstone. Late mineralization is consistent with observations of alteration distribution, deformation patterns, vein orientations and distribution of mineralization relative to large and small scale structures.

4) Structural features and geometries vary significantly from deposit to deposit. This is to be expected in a setting where the deformation is discontinuous, and the resultant patterns of stress and strain are strongly heterogeneous. Orebodies are localized in both contractional and extensional

features associated with the main NW-trending dextral strike-slip system, and orebody geometries vary systematically as a function of their location relative to the large scale fault system.

5) The general model for mineralization requires a dilation site near a zone which juxtaposes rocks of different composition. Contrasts in oxidation state seem to be the most important chemical control. The best site for this requirement is the Mid Proterozoic-Early Proterozoic unconformity, though the occurrence of similar lithological distributions in basement rocks cannot be ruled out. This implies that areas in which the unconformity is above erosion level may still be prospective for Coronation Hill style U-Au-PGE mineralization.

6) The South Alligator Valley is a major area of strong alteration. Field evaluation of alteration types based on hand specimen characteristics has been shown to be ineffective. The masking effects of deep surface weathering are likely to render useless any study of alteration distribution using surface samples. Remote sensing and bedrock geochemistry may still be useful in evaluating alteration patterns around deposits, and should therefore not be discounted because of the discouraging nature of the hand specimen geochemistry results.

7) The Palette fault system is a zone of desilicification in the Palette/Coronation Hill area, and a zone of strong silicification at higher structural levels further south, where the unconformity occurs at depth. It is possible that the Palette/Coronation Hill area is a zone of fluid downflow, while the area further south is a zone of fluid upflow. This lateral variation may be a result of dilation-driven, two dimensional fluid circulation on this fault system.

Recommendations

1) Structural study should be extended to cover the entire conservation zone. This will be necessary in order to trace major faults from the South Alligator Valley into areas of less exposure, and will also allow a more detailed evaluation of potential mineralisation outside the South Alligator Valley.

2) Observations of fault kinematics in the South Alligator Valley should be placed within a regional context. This will improve the understanding of late stage deformations in the Pine Creek Geosyncline, and will also help define possible prospective areas outside the present boundaries of the Conservation Zone.

3) More detailed work is required in order to assess surface alteration patterns associated with U-Au-PGE mineralisation. This should include more detailed sampling control and possible assessment of remote sensing methods...

4) Structural interpretations should be combined with results of the recent aeromagnetic survey over the Conservation Zone. This will aid geophysical interpretation, and should also improve geological understanding of the area.

5) More detailed work should be undertaken on the stratigraphy and sedimentology of the El Sherana and Edith River Groups, in order to refine models for tectonics and sedimentation in the Conservation Zone.

6) Any detailed examination of alteration and mineralisation in specific deposits will require drill core sampling and general company information on subsurface lithologies and grade distributions.

Acknowledgements

Field work which forms the basis for this report was performed while the author was employed as a contract geologist by the Bureau of Mineral Resources. The following are acknowledged:

- Stuart Needham, Lesley Wyborn and Gladys Warren for logistical assistance.
- Stuart Needham, Peter Stuart-Smith, Mike Etheridge, Lesley Wyborn, Gladys Warren, Vic Wall, Rod Page and Andy Wilde for useful geological discussions.
- Foy Leckie and the other BHP geologists (Alan, Dean, Jeff and Colin) for useful discussions, provision of company maps, and for sharing their knowledge of mineralization in the South Alligator area. Thanks to Dean and Jeff for putting up us a second time.
- Neil Holzapfel and John Hawke for invaluable field assistance
- Draga Gelt for drafting assistance

References

- Ayres, D.E. and Eadington, P.J., 1975. Uranium mineralization in the South Alligator Valley. *Mineralium Deposita*, 10: 27-41.
- Christie-Blick, N.H. and Biddle, K.T., 1985. Deformation and basin formation along strike-slip faults. In Biddle, K.T. and Christie-Blick, N. (eds.), *Strike-Slip Deformation, Basin Formation, and Sedimentation: Society of Economic Paleontologists and Mineralogists Special Publication no. 37*: pp. 1-34.
- Cox, S.F., Etheridge, M.A., and Wall, V.J., 1987. The role of fluids in syntectonic mass transport, and the localization of metamorphic vein-type ore deposits. *Ore Geology Reviews*, 2: 65-86.
- Crick, I.H., Muir, M.D., Needham, R.S. and Roarty, M.J., 1980. The geology and mineralization of the South Alligator Uranium Field. In Ferguson, J., and Goleby, A.B., (editors), *Uranium in the Pine Creek Geosyncline. International Atomic Energy Agency, Vienna*. 273-285.
- Davies, H.E., 1981. A structural and stratigraphic study of the Lower and Middle Proterozoic sequences in the South Alligator Valley, Northern Territory. *Hons. Thesis, Monash University*.
- Guha, J., Archambault, G. and Leroy, J., 1983. A correlation between the evolution of mineralizing fluids and the geomechanical development of a shear zone as illustrated by the Henderson 2 mine, Quebec. *Economic Geology*, 78: 1605-1618.
- Hammond, R.L., Nisbet, B.W., Etheridge, M.A. and Wall, V.J., 1984. The Litchfield Complex, northwest Northern Territory: Archaean basement or Proterozoic cover? *Australian Journal of Earth Sciences*, 31: 485-496.
- Guha, J., Archambault, G. and Leroy, J., 1983. A correlation between the evolution of mineralizing fluids and the geomechanical development of a shear zone as illustrated by the Henderson 2 mine, Quebec. *Economic Geology*, 78: 1605-1618.
- Harding, T.P., Vierbuchen, R.C. and Christie-Blick, N., 1985. Structural styles, plate-tectonic settings, and hydrocarbon traps of divergent (transtensional) wrench faults. In Biddle, K.T. and Christie-Blick, N. (eds.), *Strike-Slip Deformation, Basin Formation, and Sedimentation: Society of Economic Paleontologists and Mineralogists Special Publication no. 37*, pp. 51-77.
- Johnston, D.J. and Wall, V., 1984. "Why unconformity-related uranium deposits are unconformity-related." *Abs. Geol. Soc. Aust.* v. 12, 285-287.
- Johnston, J.D., 1984. Structural evolution of the Pine Creek Inlier and mineralization therein, N.T., Australia. Ph.D. thesis, Monash University, Clayton, Victoria, 268pp.
- Matheson, R.S., 1960. Report on holdings of United Uranium, N.L., South Alligator River area, N.T. Unpublished company report.
- Needham, R.S., 1987. Review of mineralization in the South Alligator Valley. *BMR Record* 1987/52.
- Needham, R.S. and Stuart-Smith, P.G., 1985. Stratigraphy and tectonics of the Early to Middle Proterozoic transition, Katherine-El Sherana area, N.T. *Australian Journal of Earth Sciences*, 32: 219-230.
- Needham, R.S., Stuart-Smith, P.G. and Page, R.W., 1988. Tectonic Evolution of the Pine Creek Inlier, Northern Territory. *Precambrian Research*, 40/41: 543-564.
- Robert, F., and Brown, A.C., 1986. Archean gold-bearing quartz veins at the Sigma mine, Abitibi greenstone belt, Quebec: Part I. Geologic relations and formation of the vein system. *Economic Geology*, 81: 578-592.
- Sibson, R.H., 1987. Earthquake rupturing as a mineralising agent in hydrothermal systems. *Geology*, 15: 701-704.
- Stuart-Smith, P.G., Wills, K., Crick, I.H. and Needham, R.S., 1980. Evolution of the Pine Creek Geosyncline. In Ferguson, J., and Goleby, A.B., (editors), *Uranium in the Pine Creek Geosyncline. International Atomic Energy Agency, Vienna*. 23-38.

Threadgold, I.M., 1960. The mineral composition of some uranium ores from the South Alligator River area, N.T. *C.S.I.R.O., Melbourne, Mineragraphic Technical Investigations Technical Paper 2*, 53.

Valenta, R.K., 1988.[†] A report on mineralization and structure in the South Alligator Valley. Unpublished report to the Bureau of Mineral Resources.

Woodcock, N.H. and Fischer, M. 1986. Strike-slip duplexes. *Journal of Structural Geology*. 8: 725-735.

[†] The findings of the unpublished 1988 report are incorporated in this manuscript.

Figure 1. Simplified map of the South Alligator Valley (after Needham and Stuart-Smith, 1987, showing mineral deposits referred to in text.

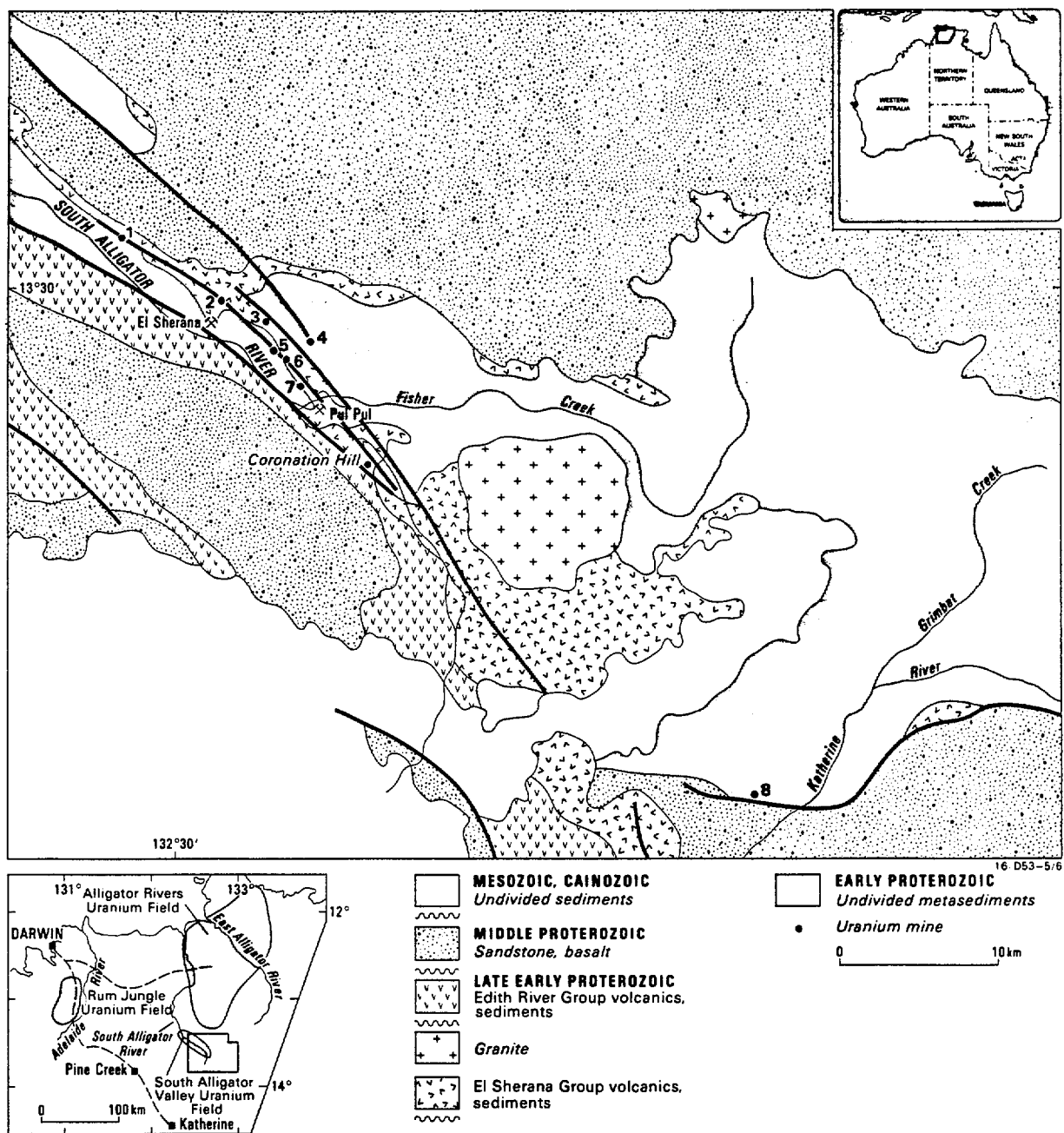


Figure 2. Major fault orientations in the Pine Creek Geosyncline and McArthur Basin.

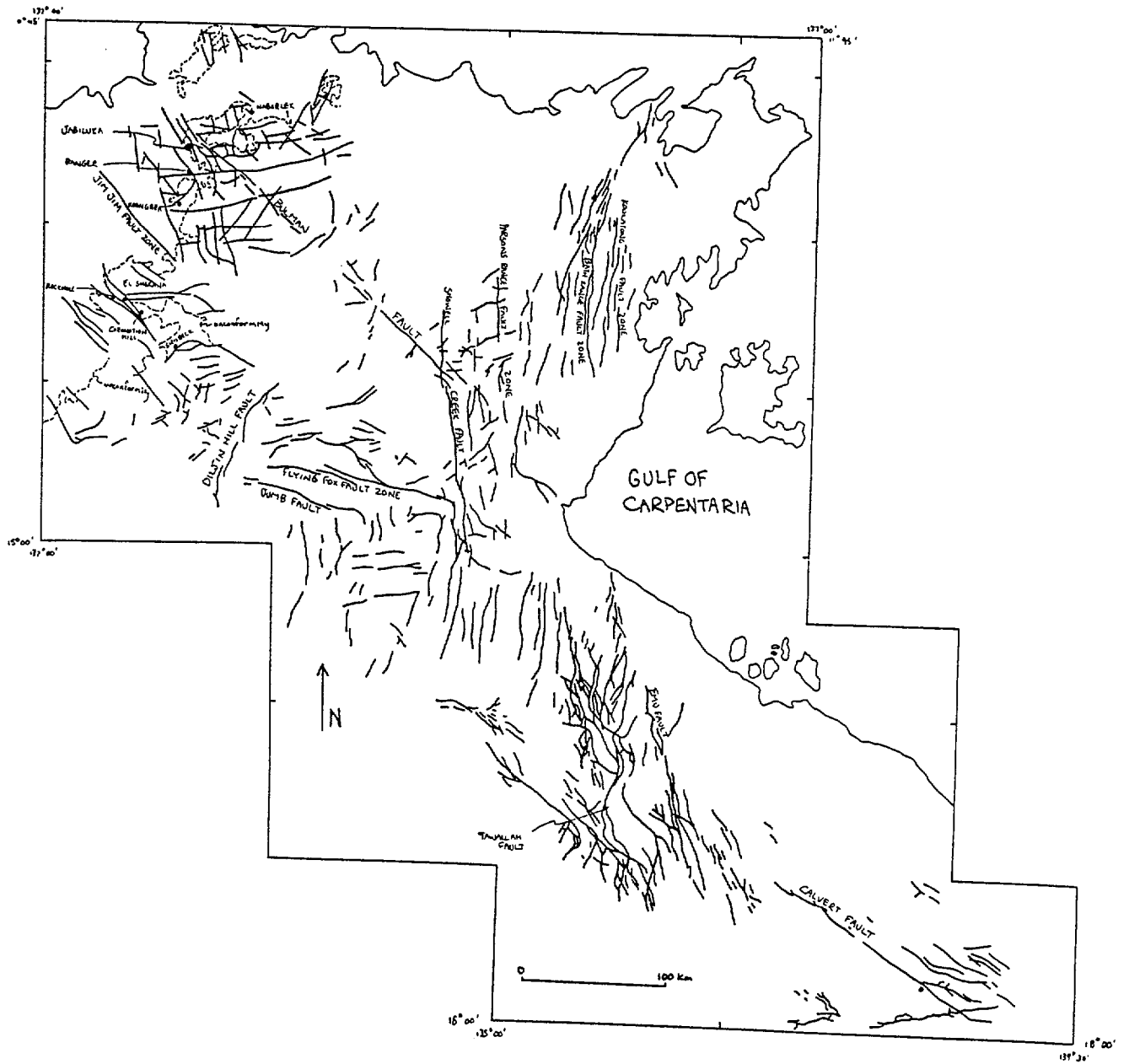


Figure 3. Major fault orientations in the area of the Kakadu Stage 3 conservation zone.

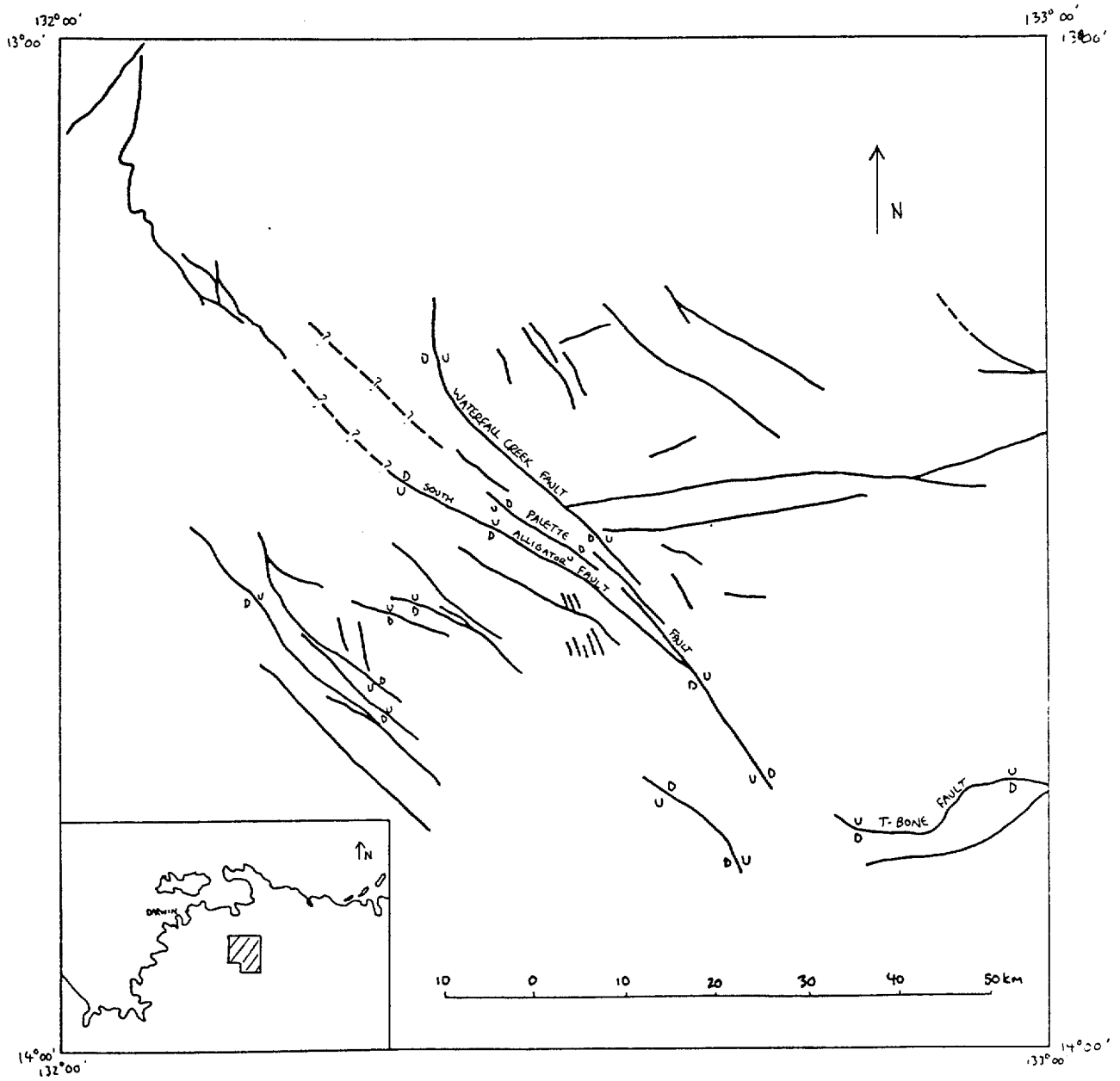
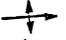
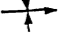
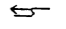
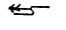
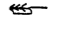
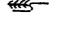

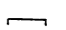
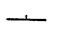
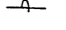
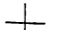




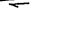


Figure 4. a) Geological map of the South Alligator Valley.
b) Insert shows detailed geology of the Scinto Plateau area.

Figure 4a.

-  anticline
-  syncline
-  F1 fold with vergence
-  F2 fold with vergence
-  F3 fold with vergence
-  F4 fold with vergence
-  S2 cleavage in basement
-  S3 cleavage in basement
-  cleavage in cover
-  strike and dip of bedding
-  overturned bedding
-  horizontal bedding
-  vertical bedding
-  normal fault, ball on downthrown side
-  reverse fault, barbs on upthrown side
-  strike-slip fault



0 1 2 km

SCALE: 1:60,000

1:60,000 ~ 1:60,000

Figure 4b.

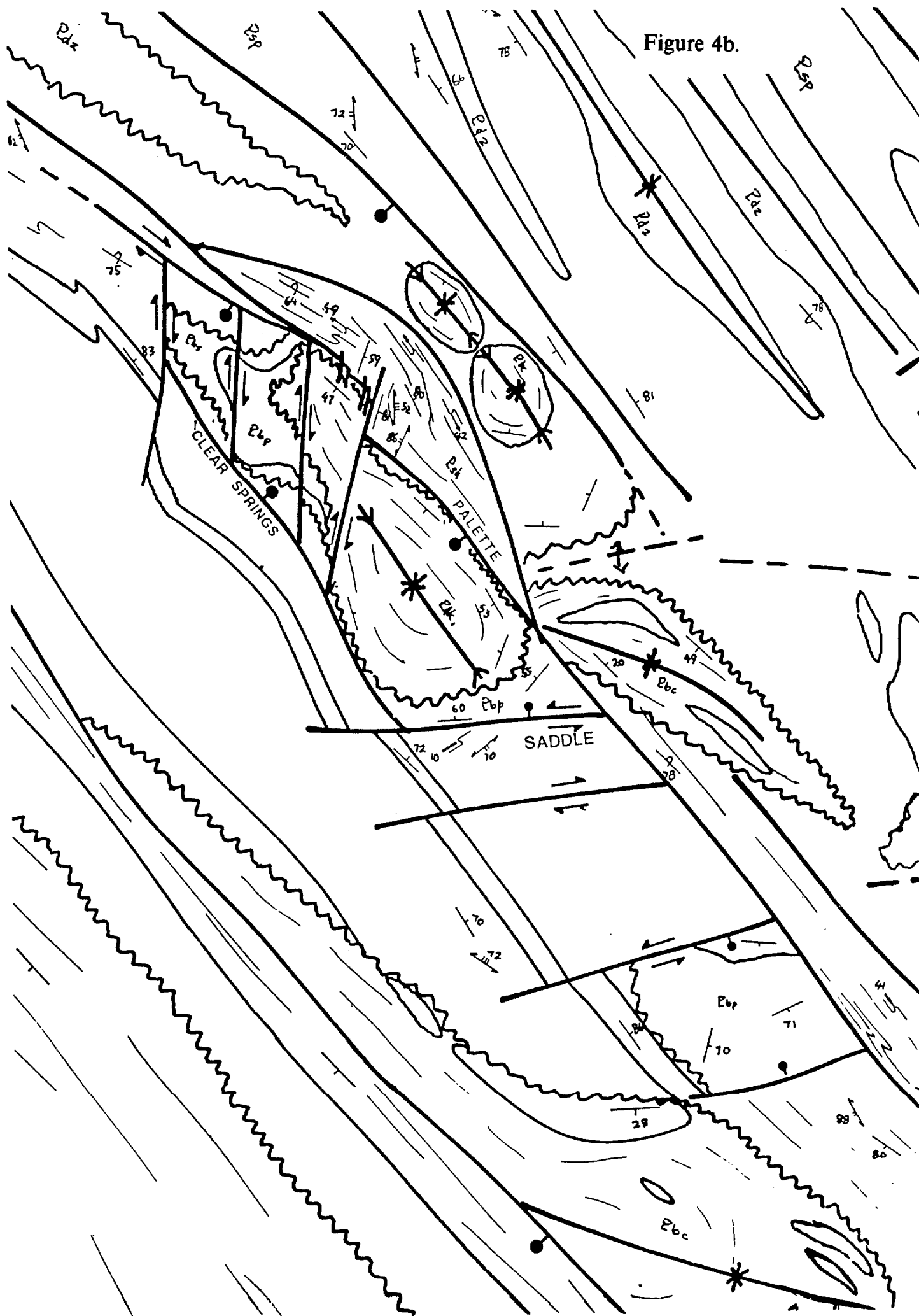


Figure 5. Schematic cross sections through the South Alligator Valley.

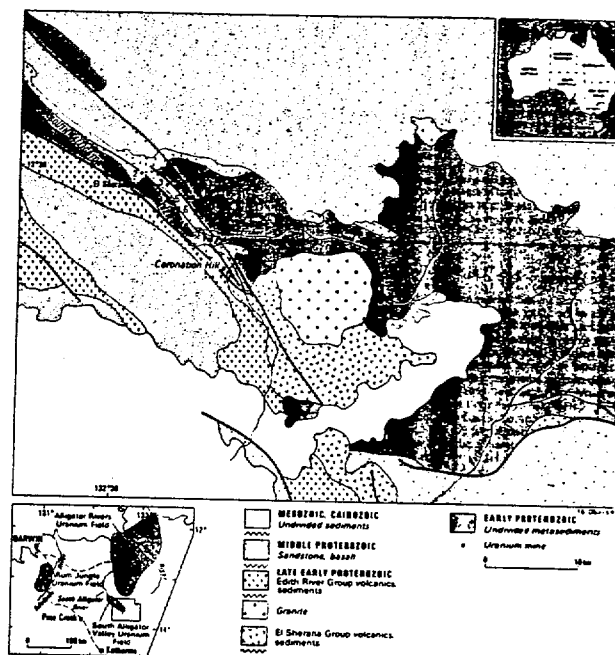
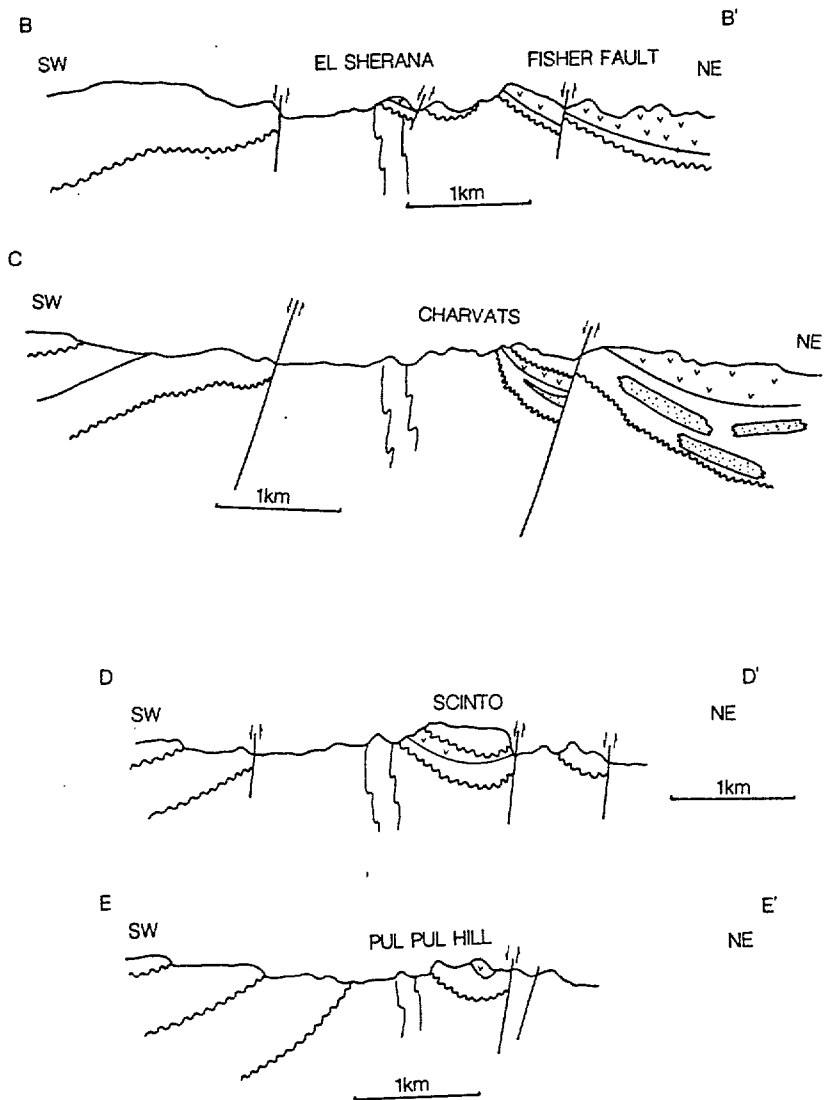
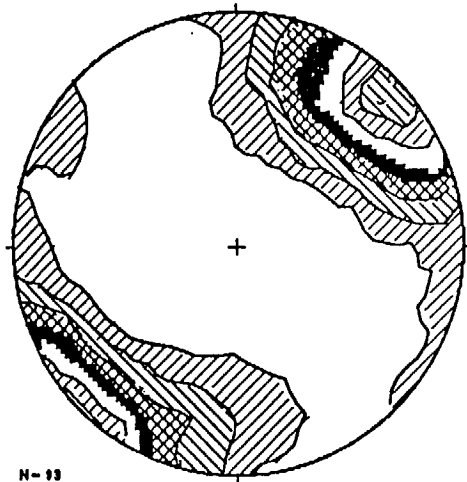
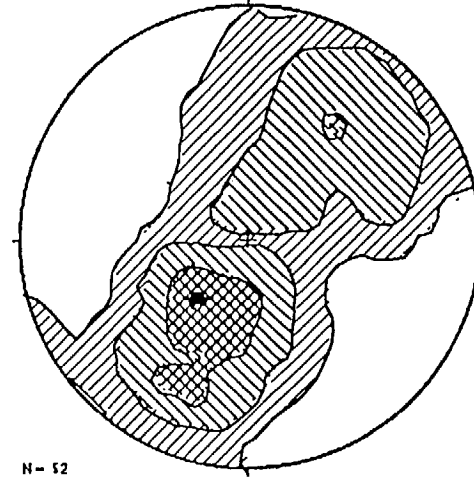


Figure 1. Carbonates HMI mine locations and regional geology.
 1—Ranchbore mine, 2—El Sherana, El Sherana West mine, 3—Lookout mine, 4—Scinto VI mine, 5—Scinto V mine, 6—Pattie, 7—Sally, 8—Shedrick mine.

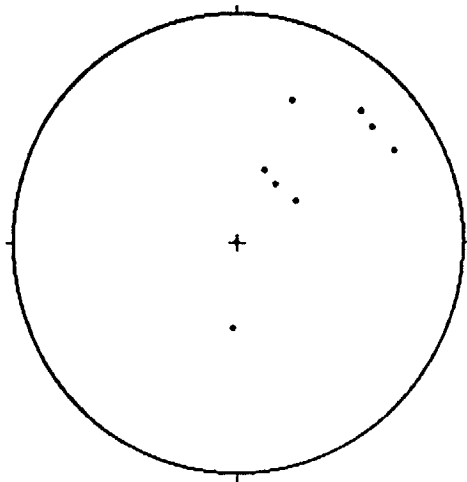
SOUTH ALLIGATOR VALLEY, BEDDING



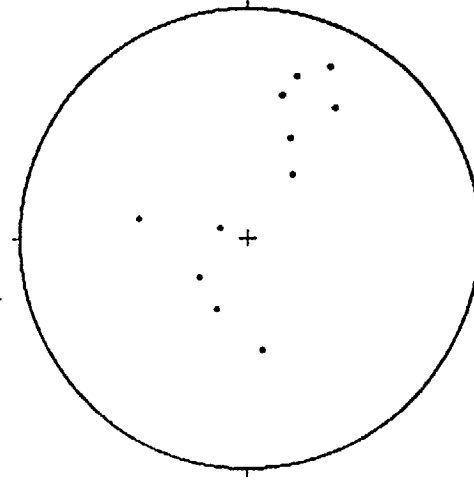
S.A.G. bedding



E.S.G. bedding



E.R.G. bedding



K.R.G. bedding

Figure 6a. South Alligator Valley stereonet data: Bedding

SOUTH ALLIGATOR VALLEY, FOLD AXES

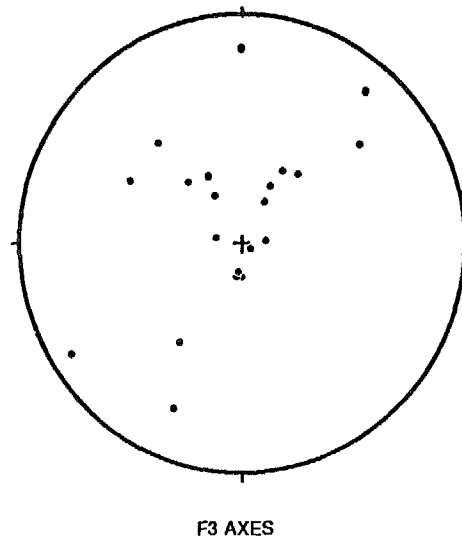
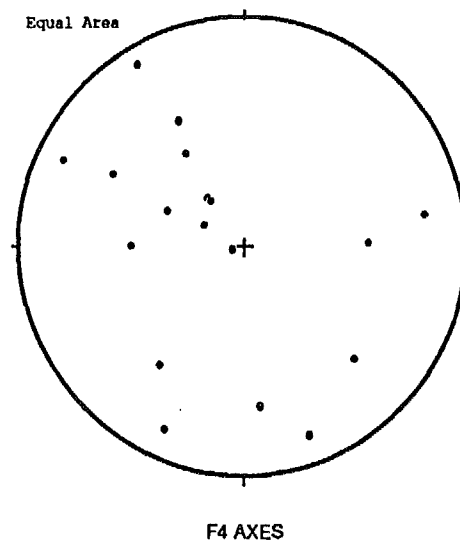
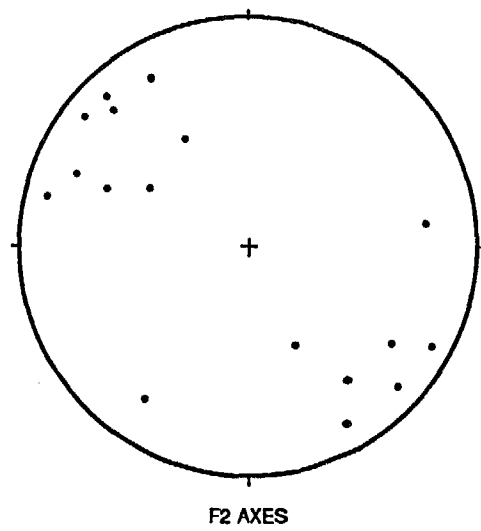
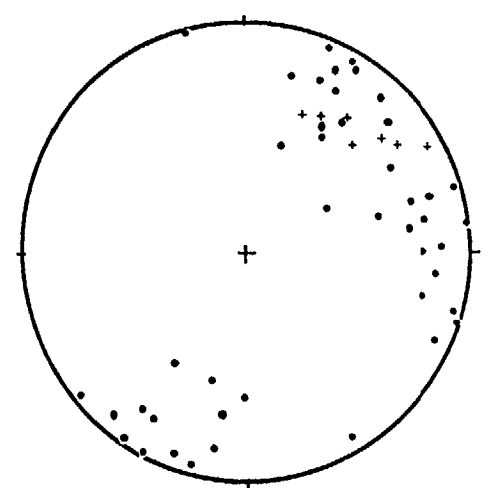
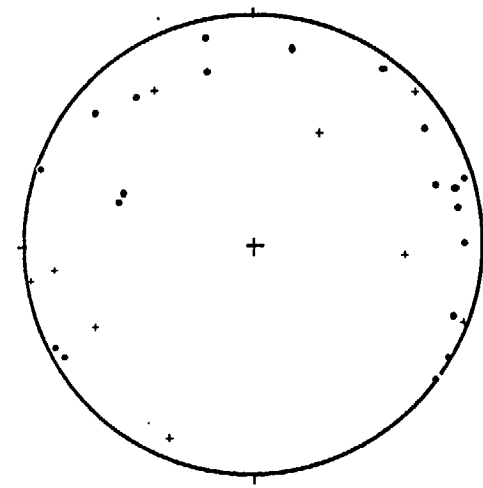


Figure 6 b. South Alligator Valley stereonet data: Fold Axes.

Figure 6 c. South Alligator Valley stereonet data: Cleavages.

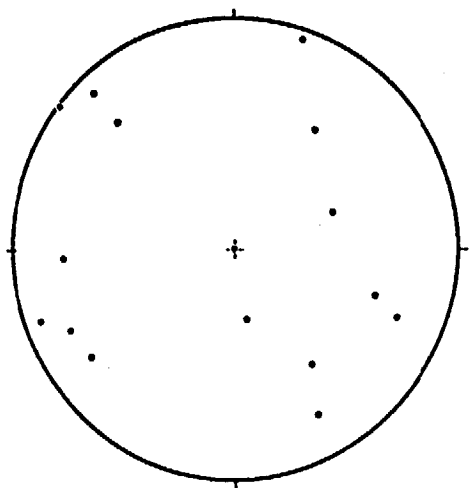


+ F2 axial surfaces
• S2

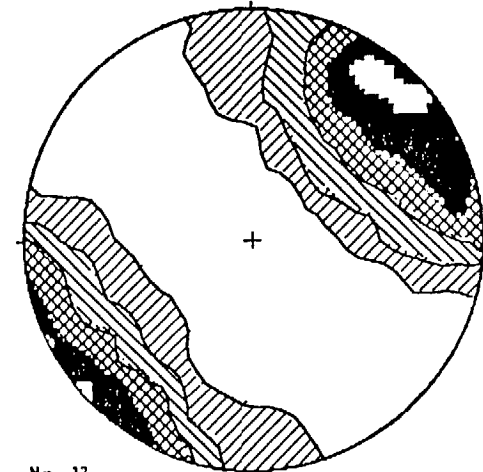


+ F3 axial surfaces
• S3

CLEAVAGES



• S4



N= 12

El Sherana Group-cleavage

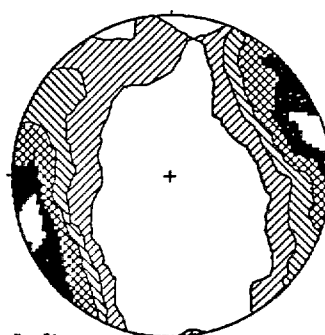
Figure 6 d.

POLES TO FAULTS-SOUTH ALLIGATOR VALLEY



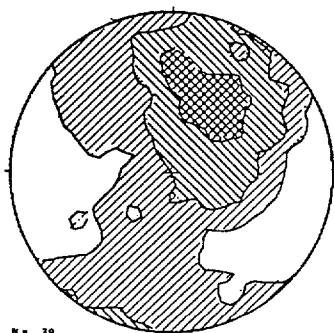
N = 22

normal faults



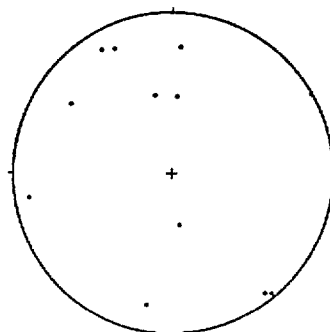
N = 54

dextral faults



N = 38

reverse faults



sinistral faults

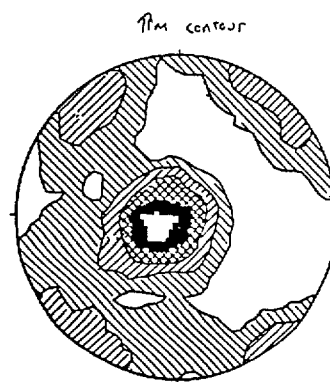
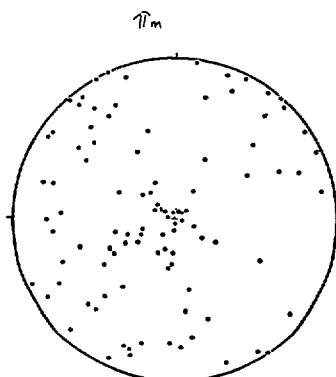
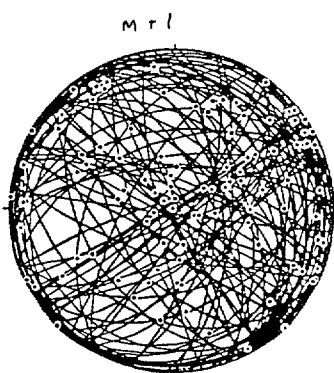
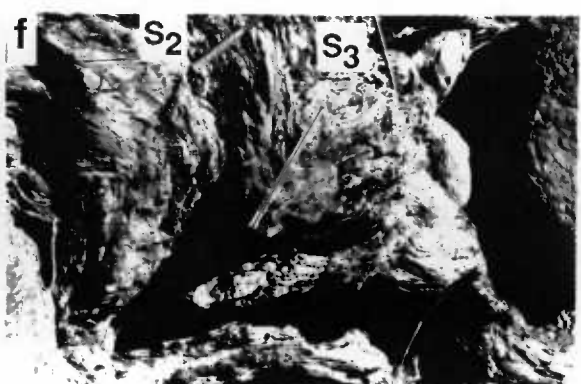
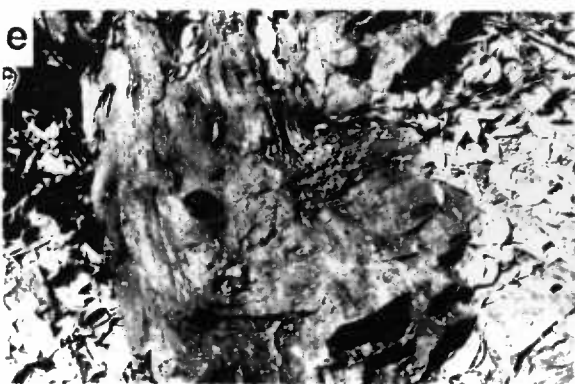
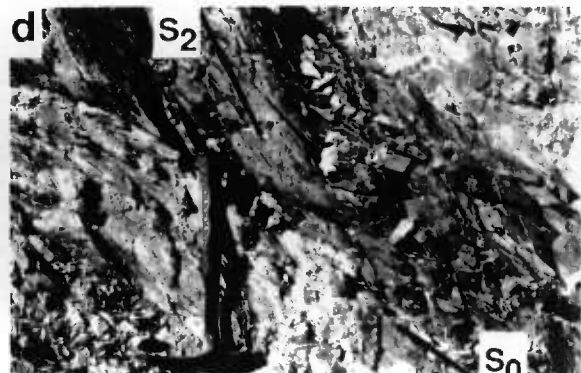
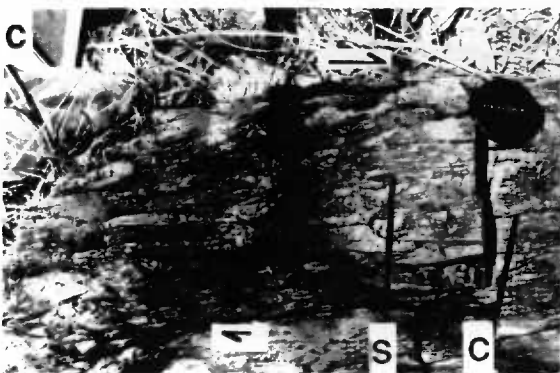
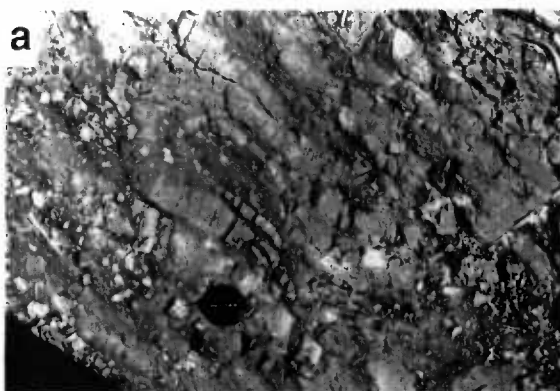


Figure 7a. Isoclinal F_1 in cherty ferruginous Koolpin Formation. **b.** Southwest-verging F_2 in overturned cherty ferruginous Koolpin Formation. **c.** D_3 high strain zone (ESE of Pul Pul Hill) showing dextral movement. **d.** S_2 cleavage, Saddle Ridge mine. **e.** Steeply-plunging F_3 fold. **f.** F_3 fold showing folded S_2 and axial plane S_3 .



* R 9 1 1 0 7 0 2 *

Figure 8a. Preferred orientation of chert nodules in Koolpin Formation. **b.**
Photomicrograph of well-foliated Koolpin formation, Palette mine. (4X, plane polarized light).



* R 9 1 1 0 7 0 3 *

Figure 8a. Preferred orientation of chert nodules in Koolpin Formation. **b.** Photomicrograph of well-foliated Koolpin formation, Palette mine. (4X, plane polarized light).

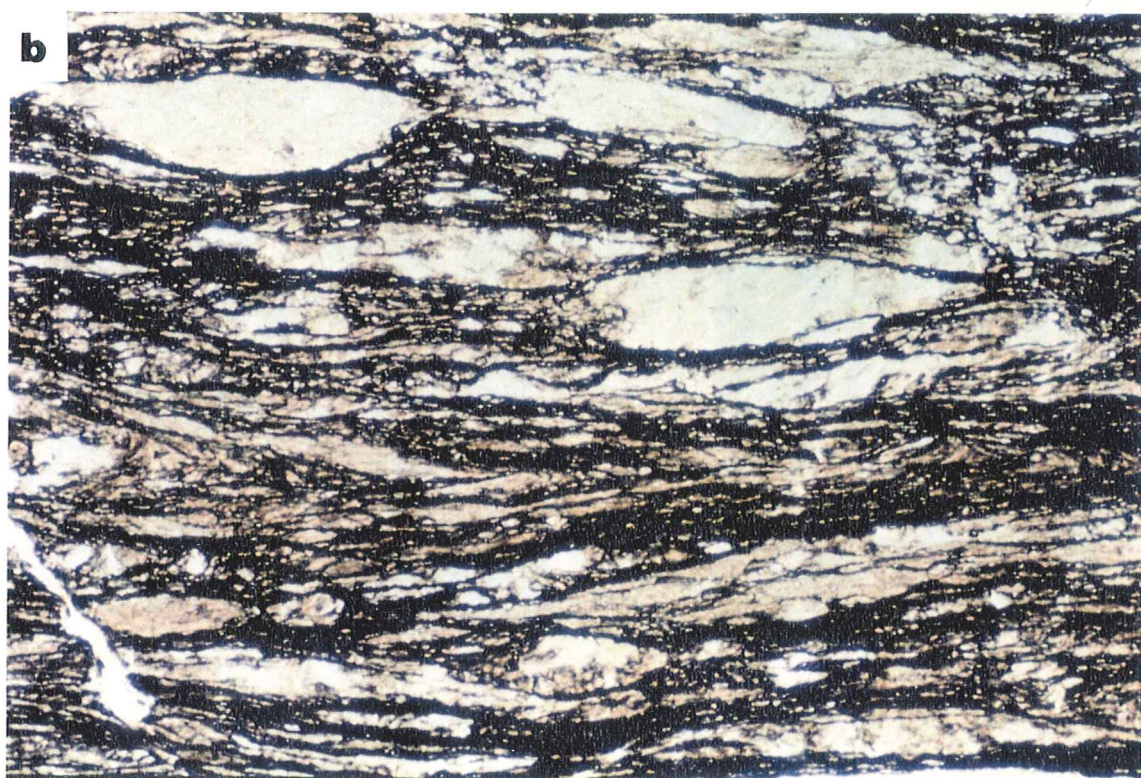
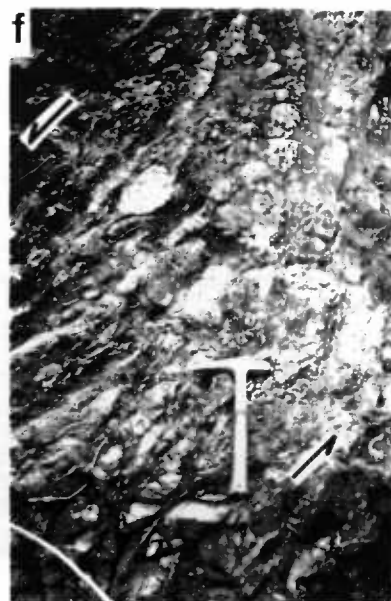
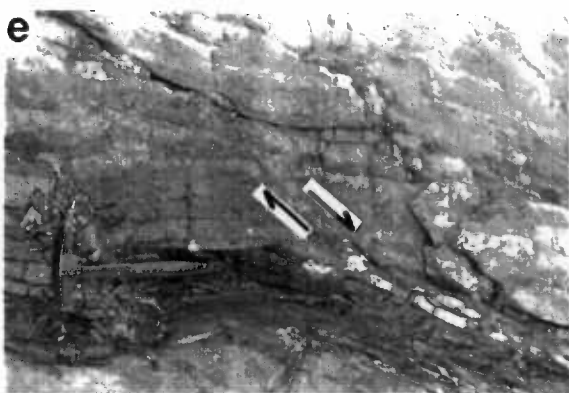
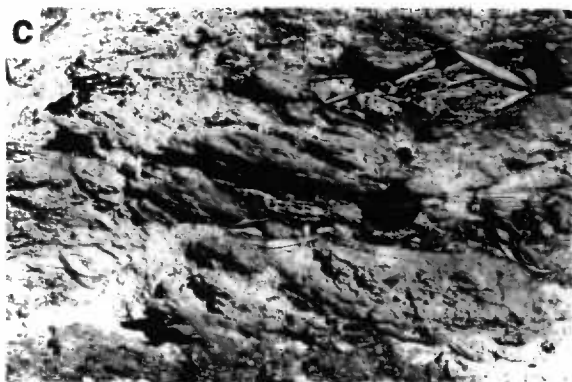
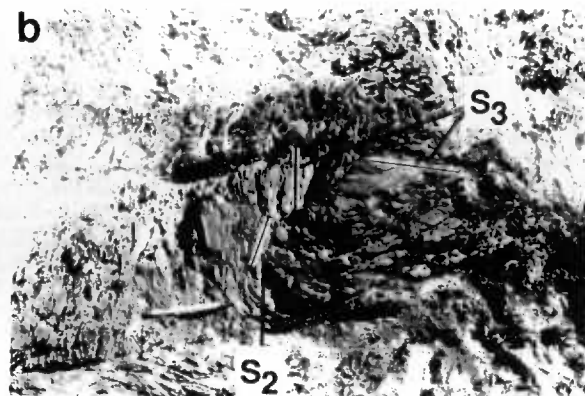
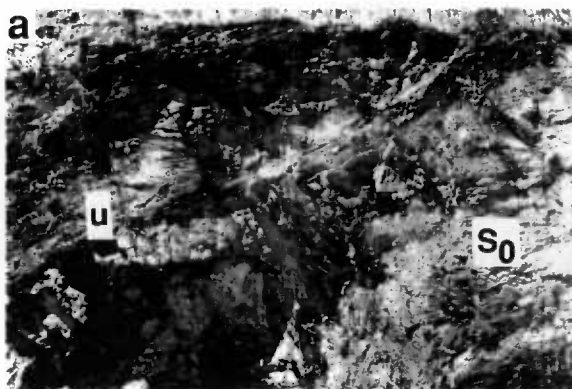


Figure 9a. Unconformity-parallel fault (labelled "u") in Koolpin Formation, El Sherana Mine. Bedding surface (S_0) shown. **9b.** F_4 fold, showing folded S_2 and S_3 . **9c.** D_4 phyllonite, El Sherana dam area. **9d.** Multiple fold generations in phyllonitic foliation (outlined), El Sherana dam area. **7e.** Late extensional fault in cherty ferruginous Koolpin formation, east of Scinto V. **7f.** Phyllonitic high strain zone in Koolpin formation, southeast of Rockhole.



* R 9 1 1 0 7 0 5 *



* R 9 1 1 0 7 0 6 *

Figure 10. South Alligator Valley Faults by locality. F+l denotes lineations and poles to faults.



* R 9 1 1 0 7 0 7 *

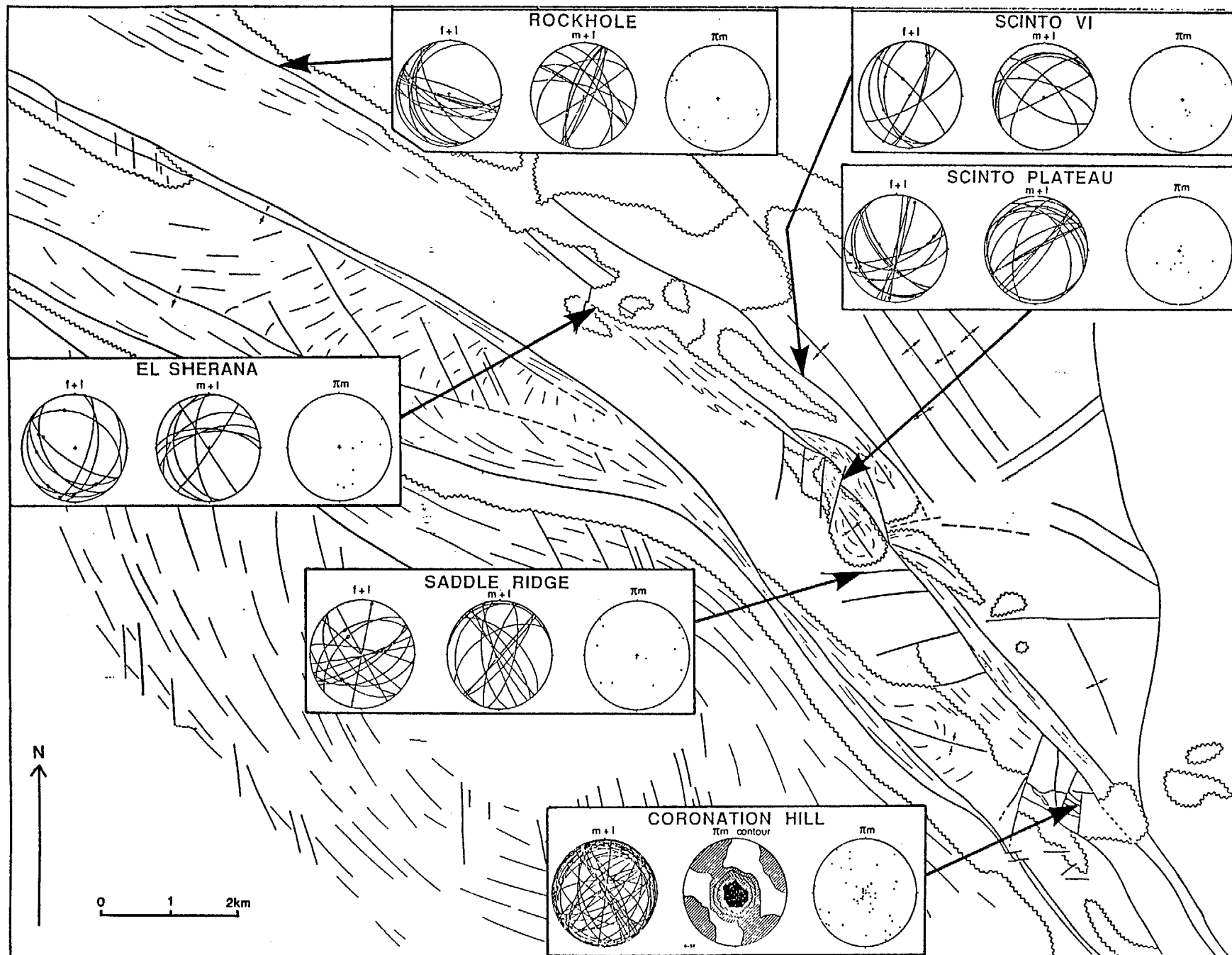


Figure 11. Kinematic interpretation of South Alligator Valley fault geometry.

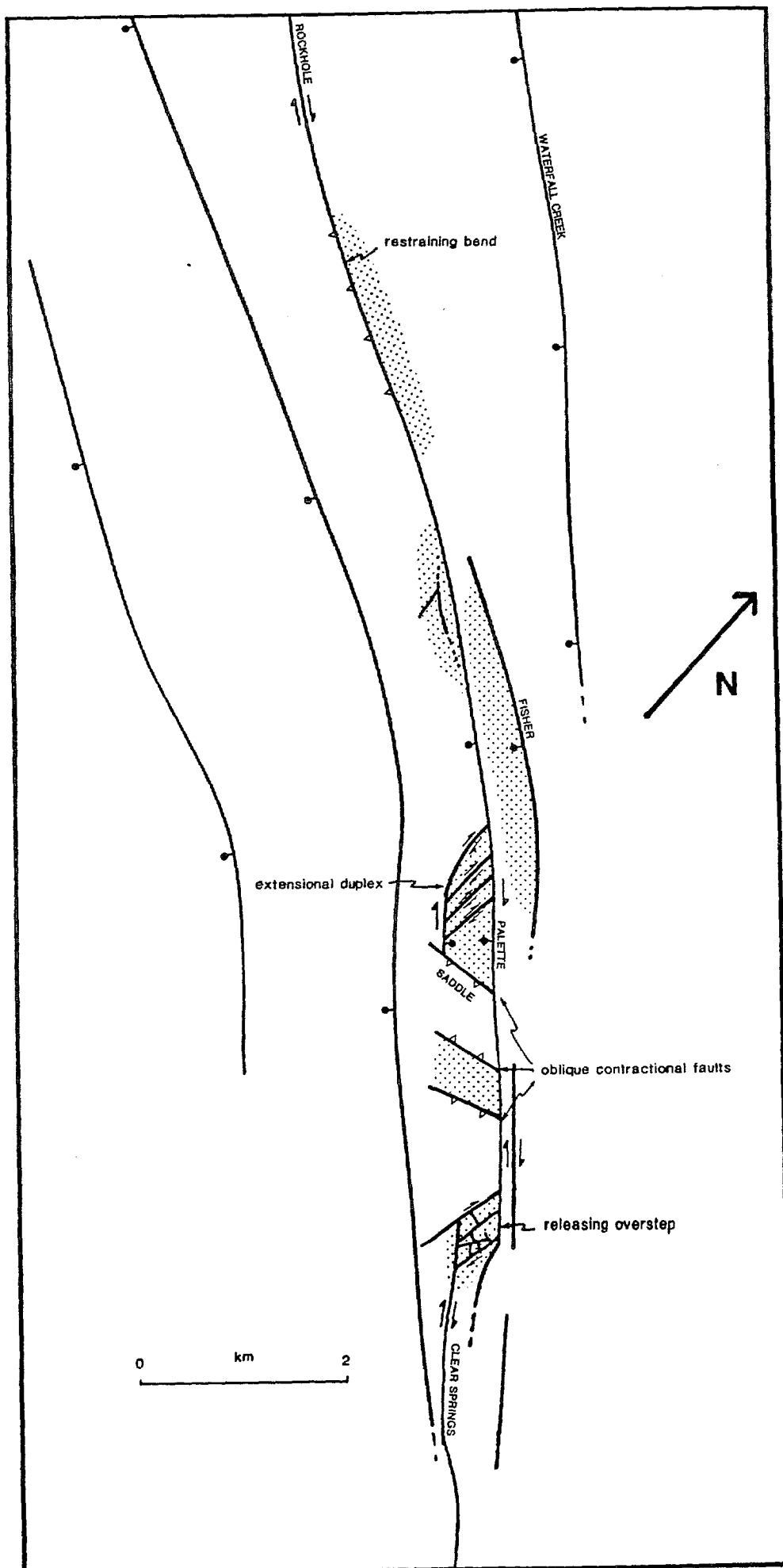
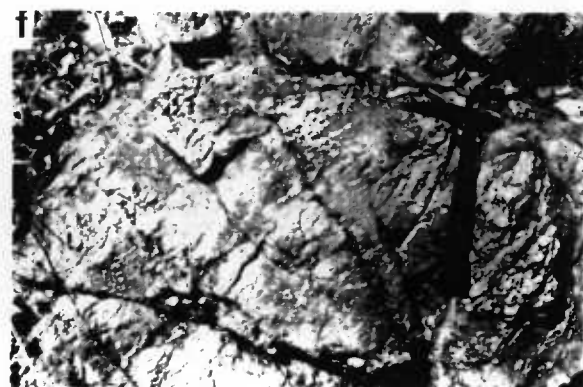
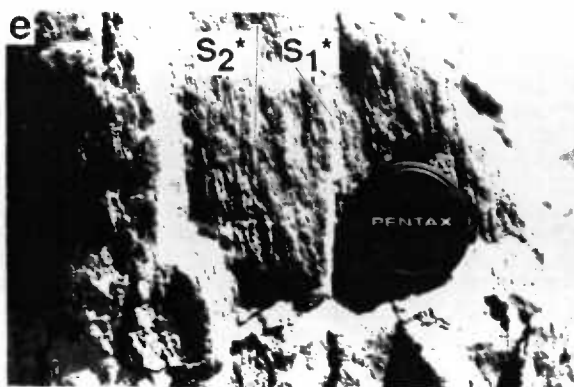
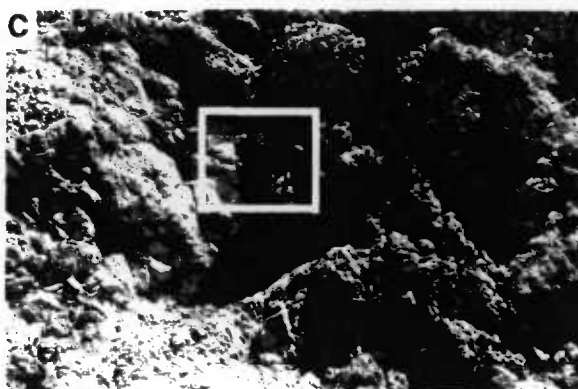
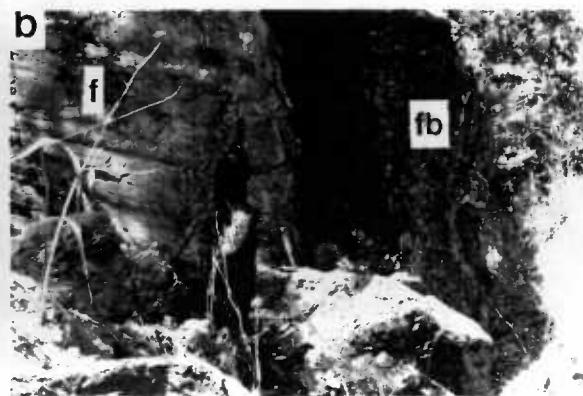


Figure 12a. Densely fractured Pul Pul rhyolite, El Sherana pit, looking north. **12b.** Gently north-dipping slickensides on dextral fault, Cliff Face mine. **12c.** Highly fractured debris flow conglomerate, Coronation Hill Mine. Note carbonaceous fragment and hammer scale within box. **12d.** Multiple veins in north-trending fault zone, Cliff Face Mine. **12e.** Multiple cleavages and deformed veins (left of lens cap) in Green Tuffaceous Siltstone, Coronation Hill Mine. **12f.** Weak crush brecciation in Coronation Sandstone near Fisher Fault.



* R 9 1 1 0 7 0 8 *

Figure 13a. Penetrative microfractures in El Sherana Group volcanics, Monolith Prospect. **13b.** Phyllonitic fault zone, Saddle Ridge Mine. **12c.** Weak cleavage and anastomosing shear zones in Coronation Volcanics, Palette area. **12d.** Spaced fracture cleavage, Rockhole Mine upper adit.

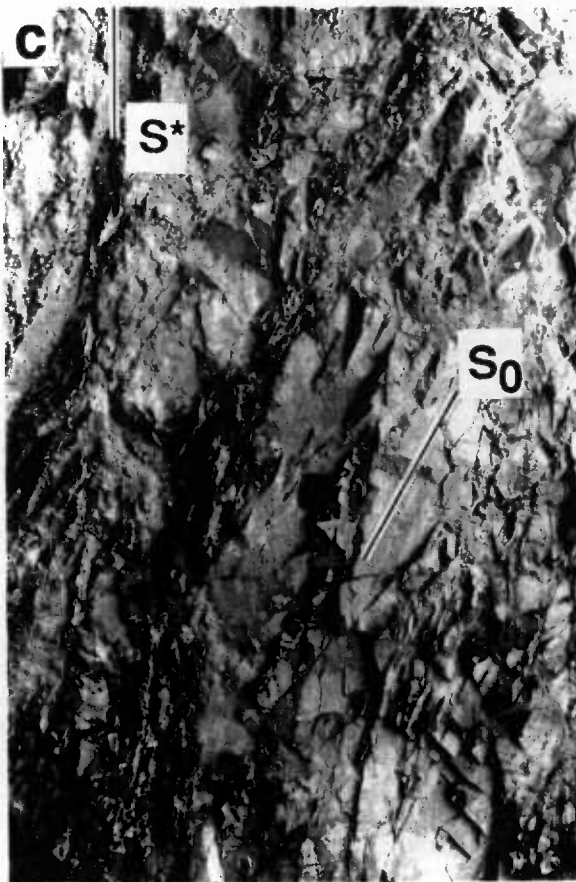


Figure 14. Interpretive schematic cross section of South Alligator Valley, looking northwest.



* R 9 1 1 0 7 0 9 *

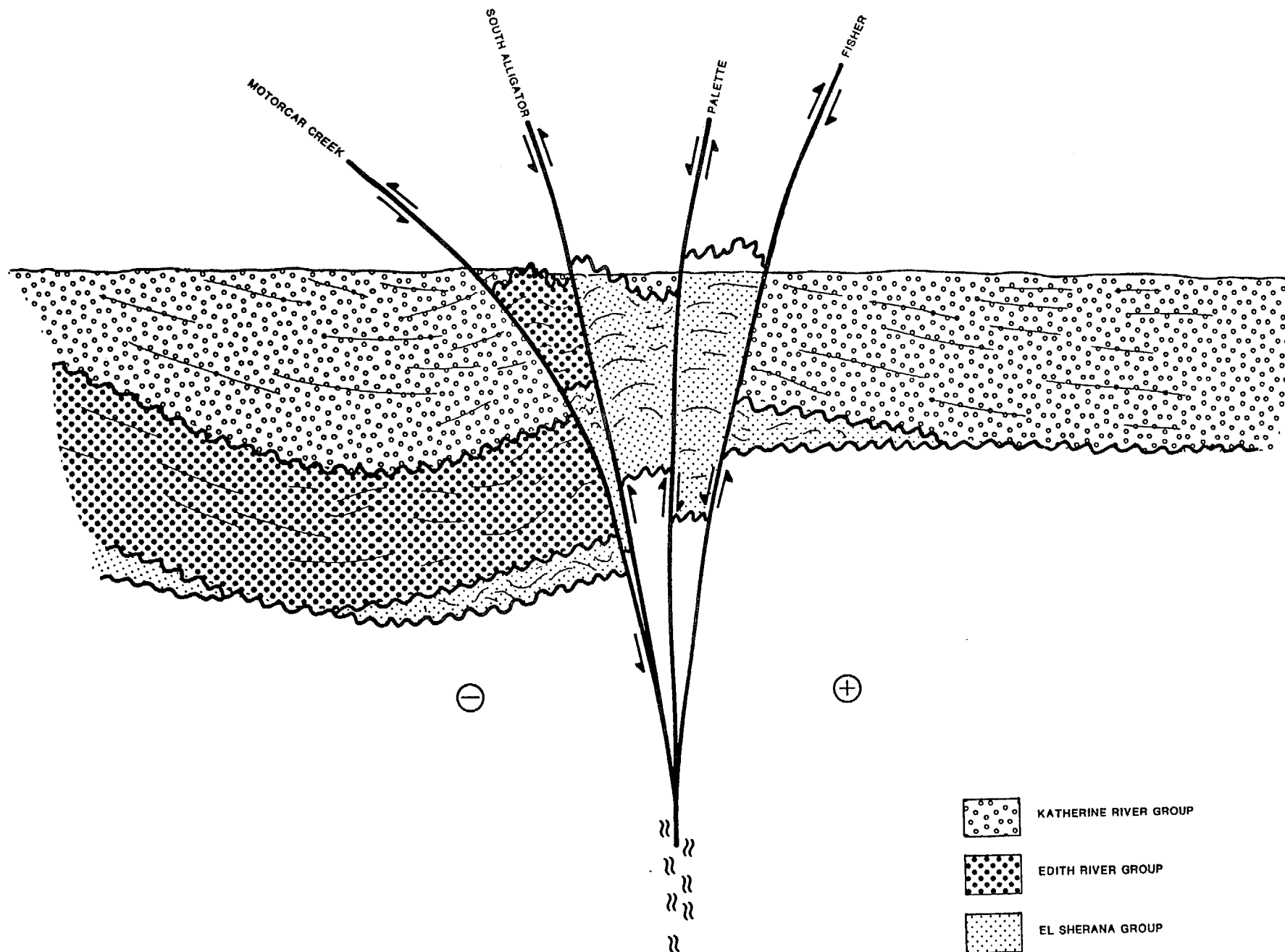
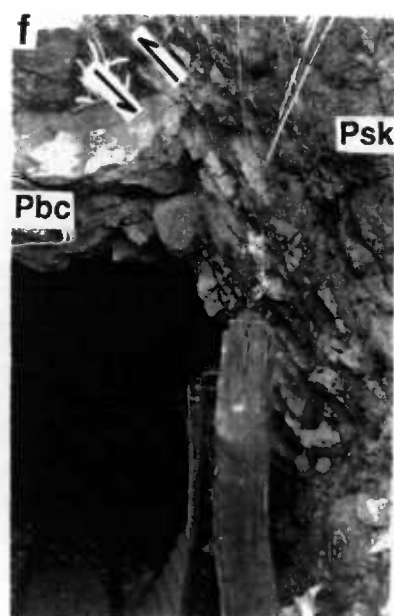
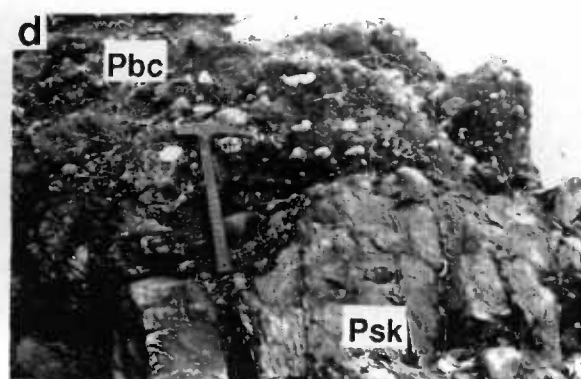
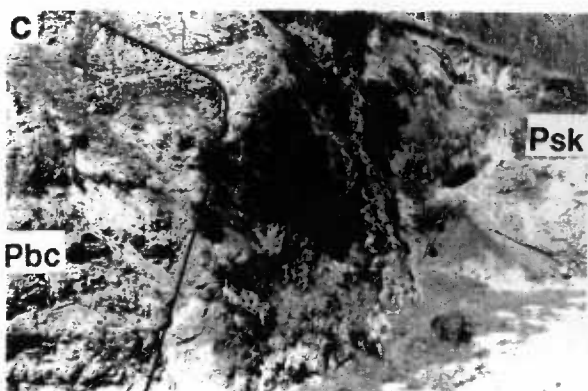
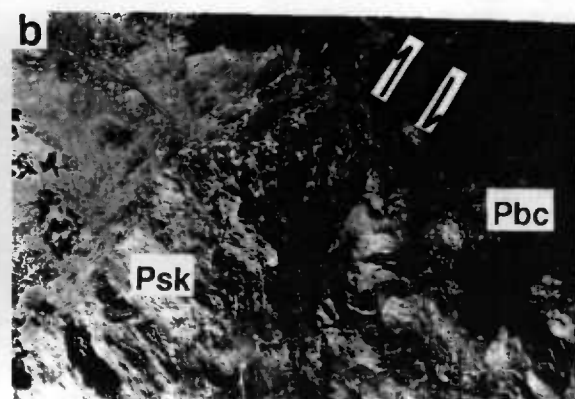
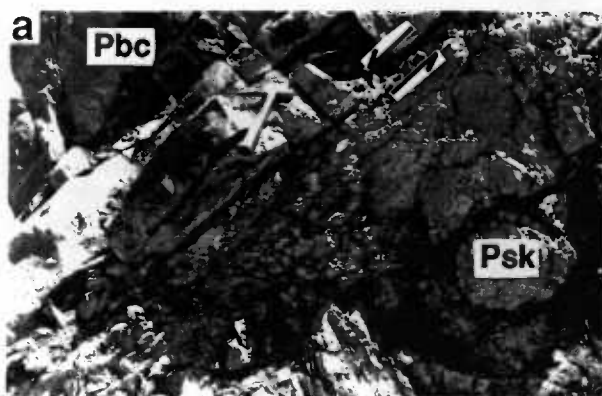


Figure 15a. Normal fault contact between Coronation Sandstone and Koolpin Formation. Note the zone of penetrative fracturing in the Koolpin formation. **15b.** Reverse fault contact between foliated and deformed carbonaceous Koolpin Formation and relatively undeformed Coronation Sandstone, Palette Mine. **15c.** Unconformity surface (outlined) exposed at El Sherana. **15d.** Conglomerate of the El Sherana Group overlying vertically-dipping Koolpin Formation, O'Dwyers (just south of Rockhole). **15e.** Same contact as 15d, but more steeply-dipping. **15f.** Reverse fault contact between Koolpin Formation (right) and Coronation Sandstone (left), Rockhole upper adit.



* R 9 1 1 0 7 1 0 *

Figure 16. Schematic cross section showing Rockhole fault geometry, with an equal area plot of poles to flats and reverse faults.

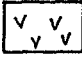
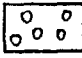



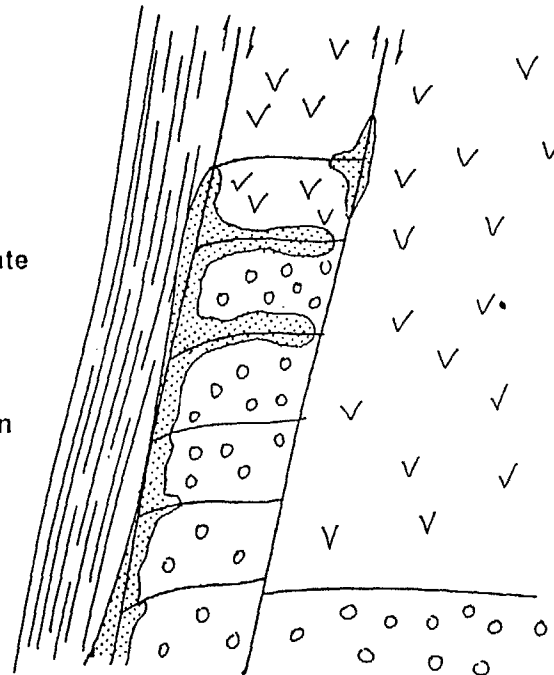
* R 9 1 1 0 7 1 1 *

ROCKHOLE, UPPER ADIT

SW

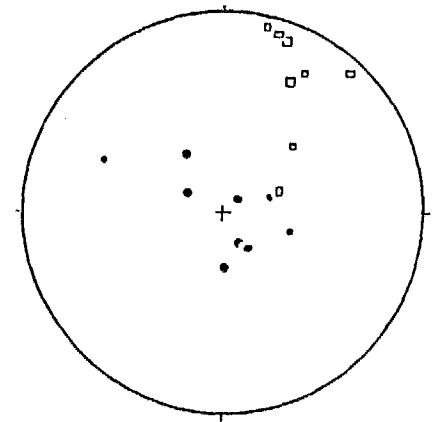
NE

-  green sericitized rhyolite
-  sandstone and conglomerate
-  Koolpin formation
- intense hematitic alteration
+ U mineralization (?)



5m

ROCKHOLE



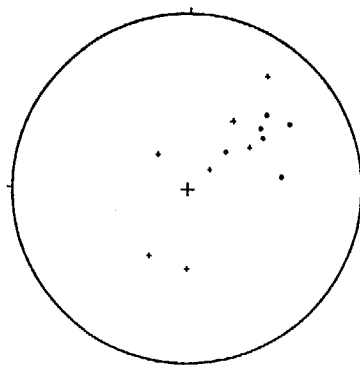
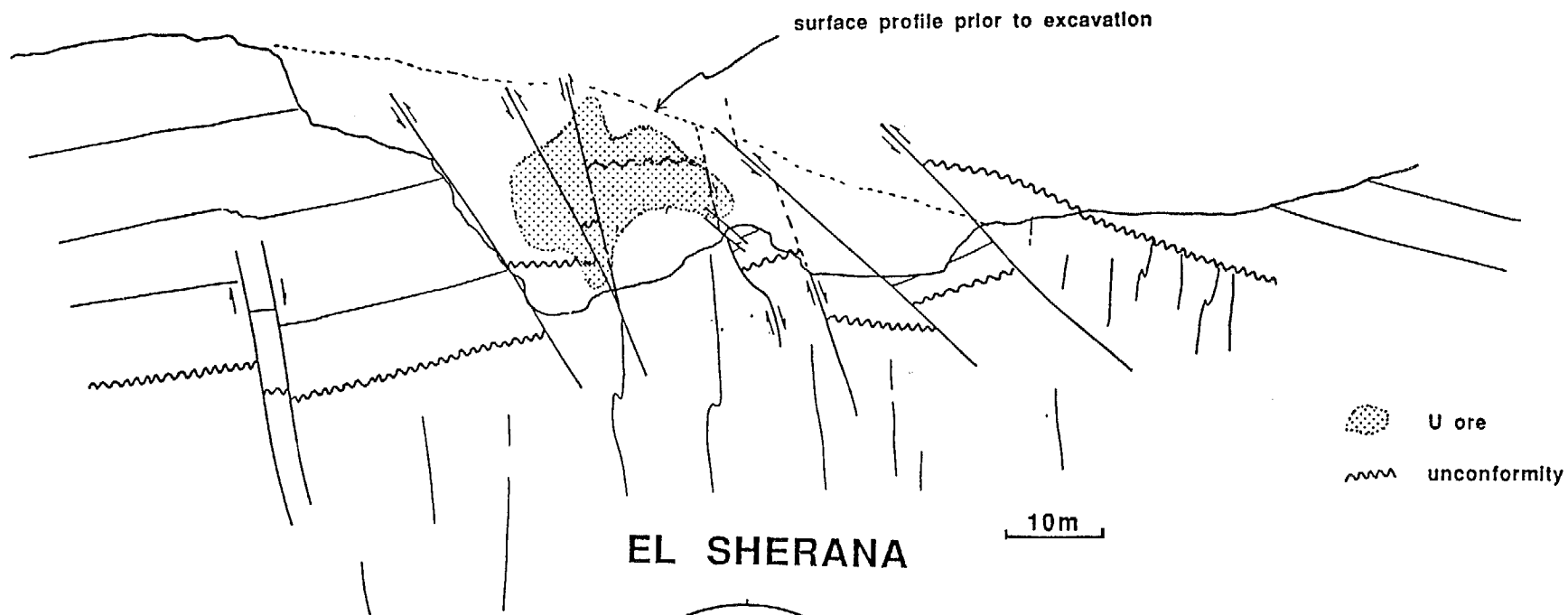
- flats
- reverse faults

Figure 17. Schematic cross section showing the interpreted El Sherana Fault geometry, with an equal area plot of poles to normal and reverse faults.

EL SHERANA, CROSS SECTION LOOKING SE

NE

SW



- REVERSE FAULTS
- NORMAL FAULTS

Figure 18. Geological map of the El Sherana pit.

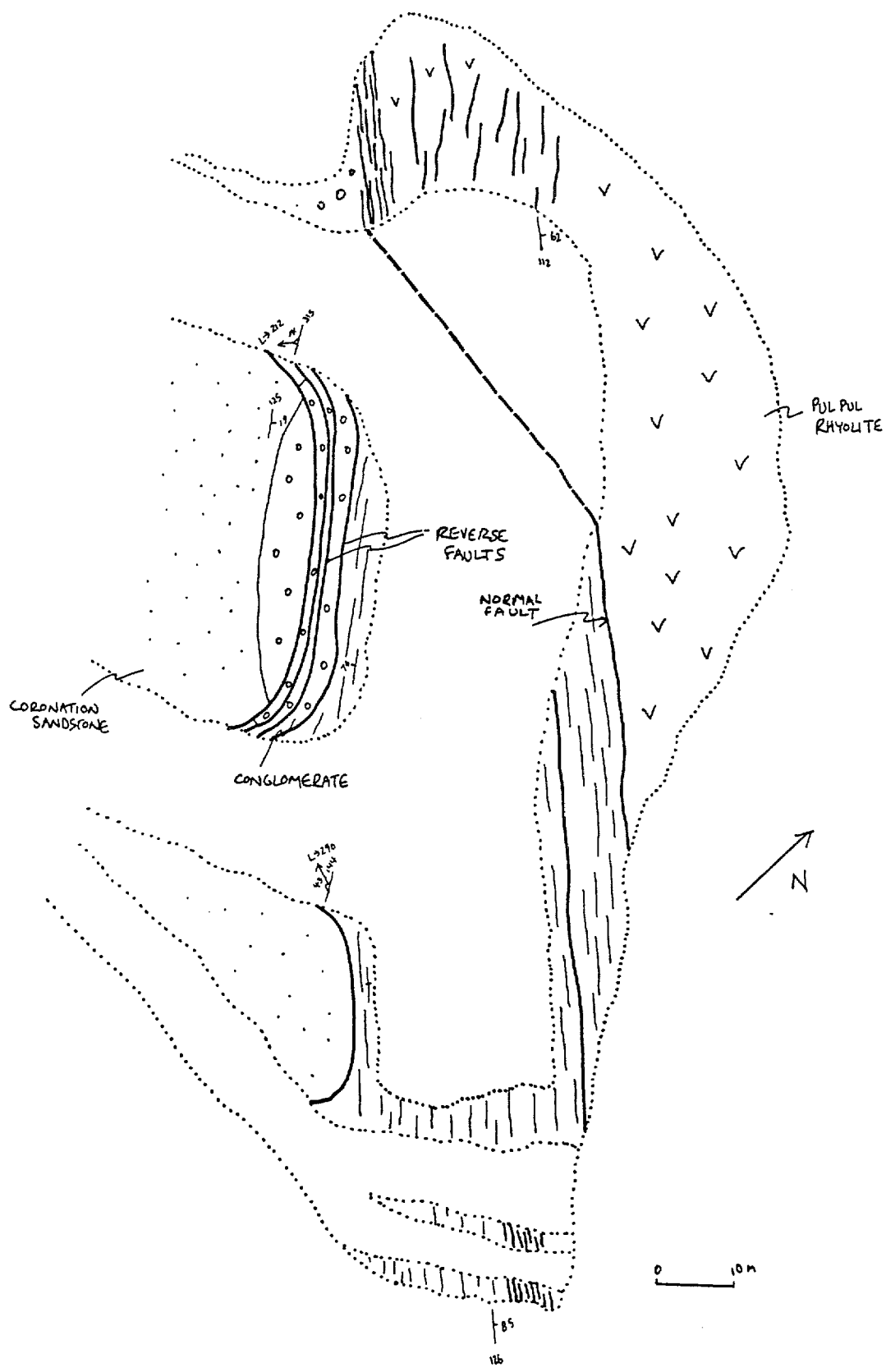
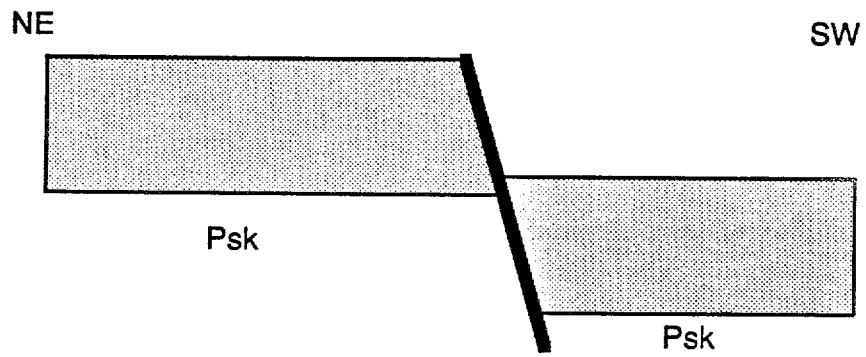
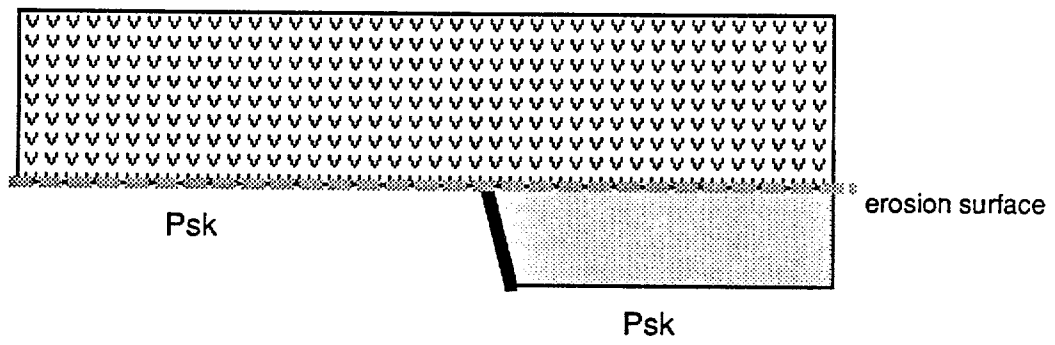


Figure 19. Three stage model used to explain the El Sherana cross section geometry. **a.** Movement on a steep southwest-dipping normal fault causes a south-block-down displacement on the unconformity contact between Coronation Sandstone (stippled) and Koolpin Formation. **b.** Coronation Sandstone is eroded away on the north side of the fault, followed by deposition of the Pul Pul Rhyolite. **c.** South-block-up movement occurs on moderately southwest-dipping reverse faults.

a)



b)



c)

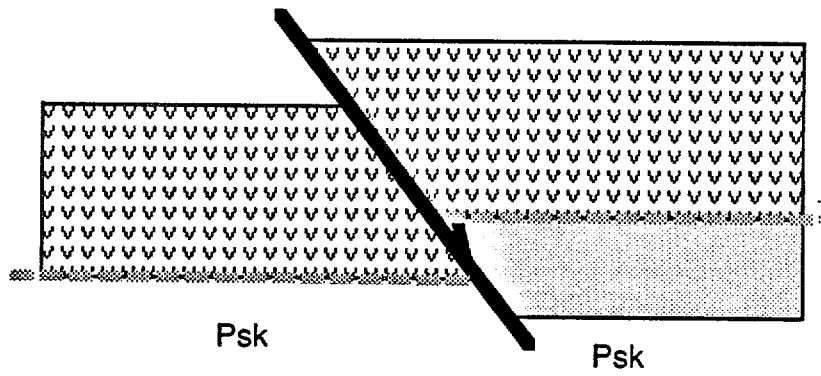


Figure 20. Outcrop geology of the Scinto Plateau area (based on Stuart-Smith et al., 1988), showing the locations of more detailed figures of individual deposits.

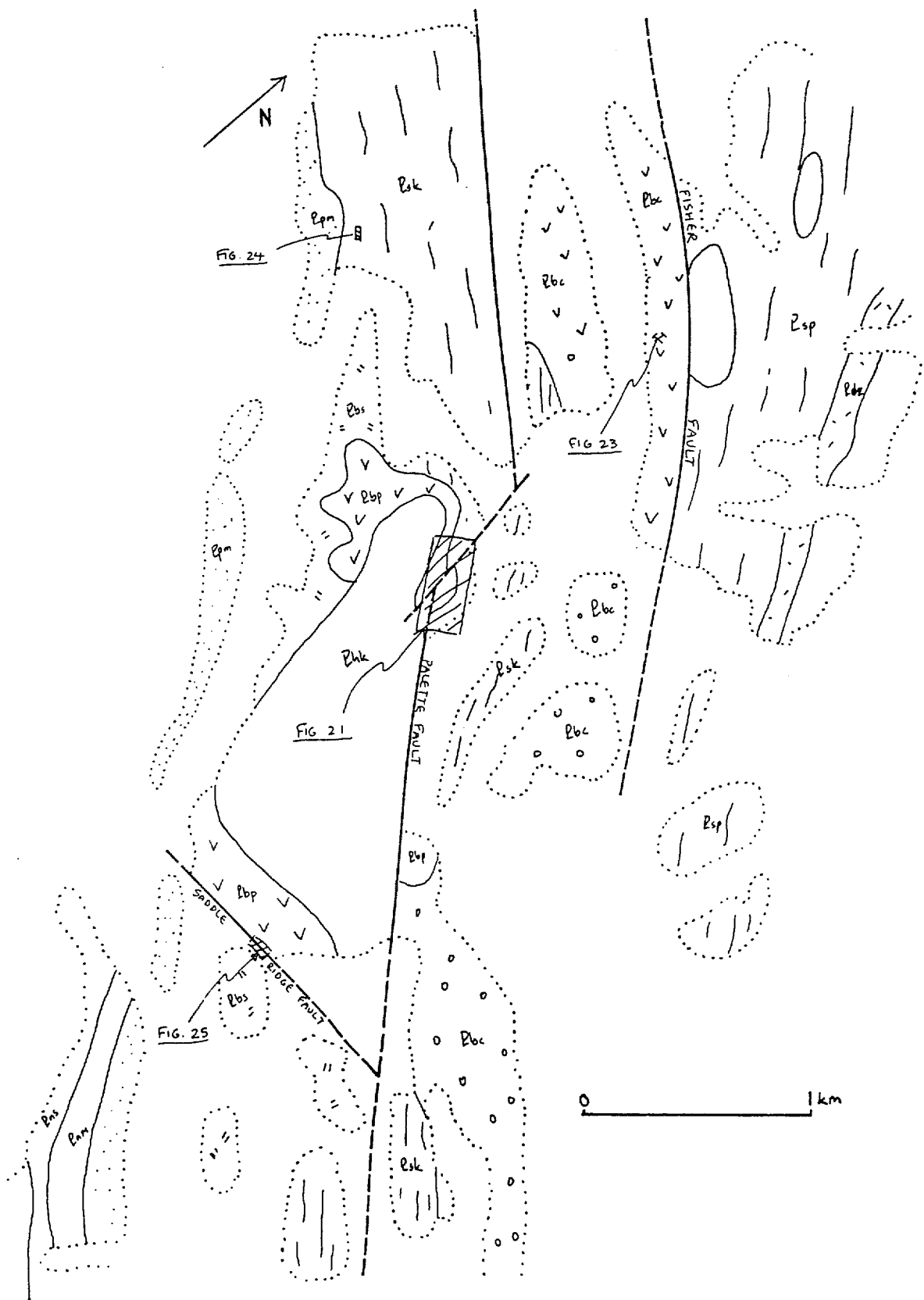


Figure 21. Fault geometry in the Palette-Skull area.

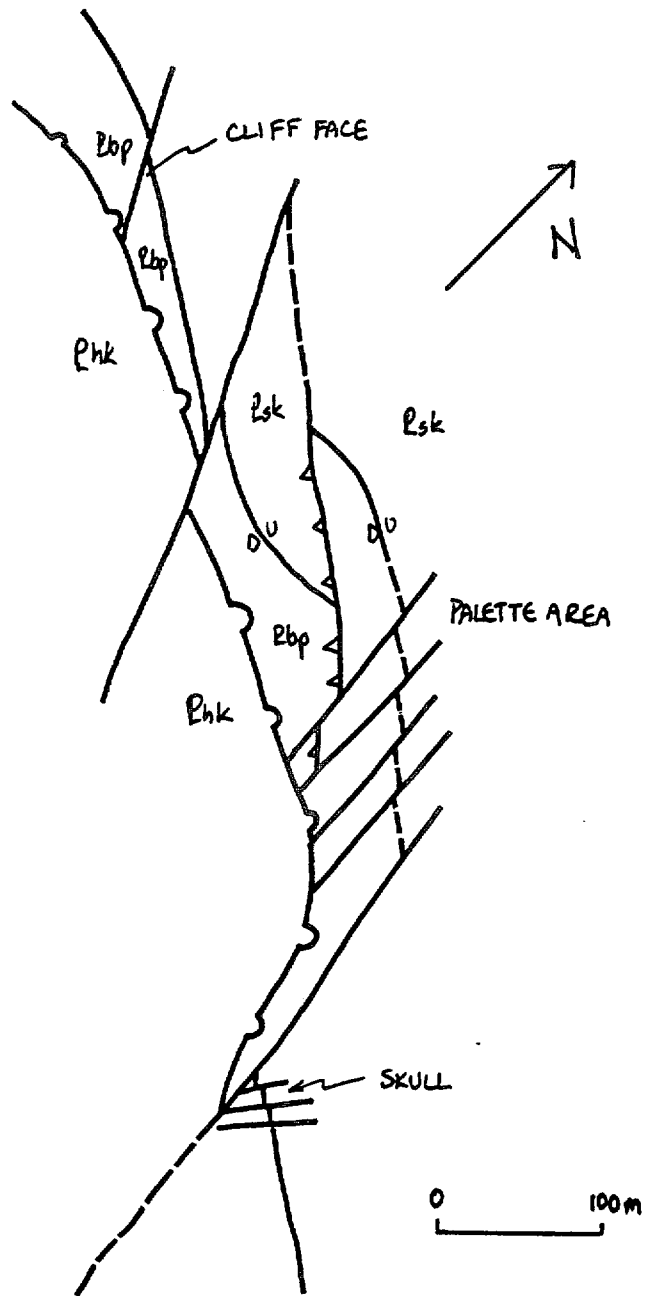
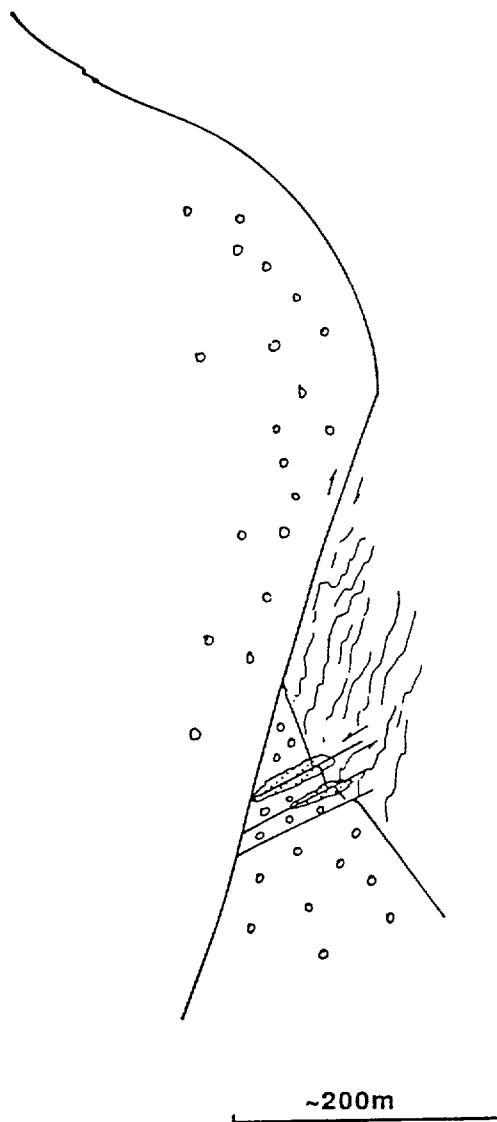


Figure 22. Schematic plan view of fault geometry and distribution of mineralization in the Skull Mine.



SKULL MINE, FAULT GEOMETRY



Coronation sandstone



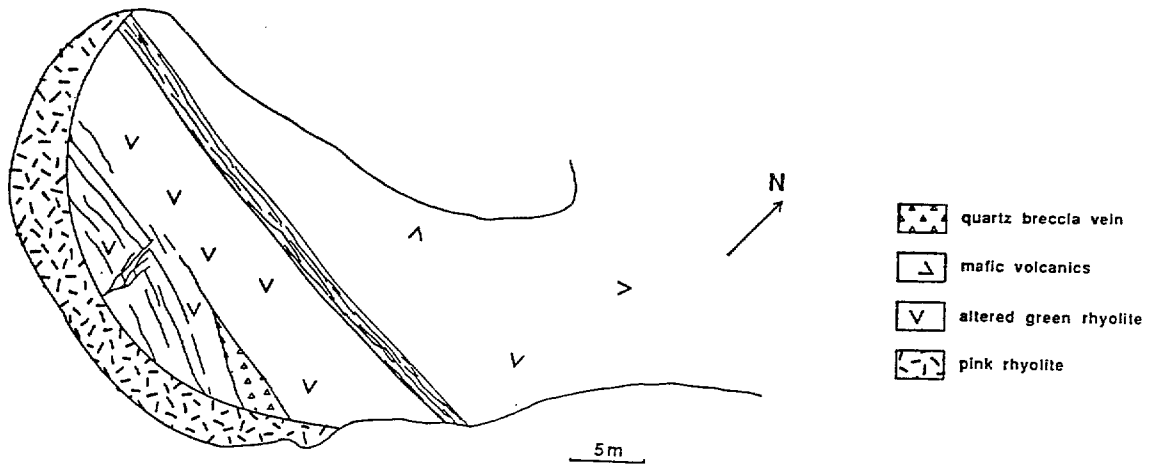
Koolpin formation



alteration, mineralization

Figure 23. Schematic plan and section of the Scinto VI mine.

SCINTO VI, PLAN



SCINTO VI, LOOKING SE

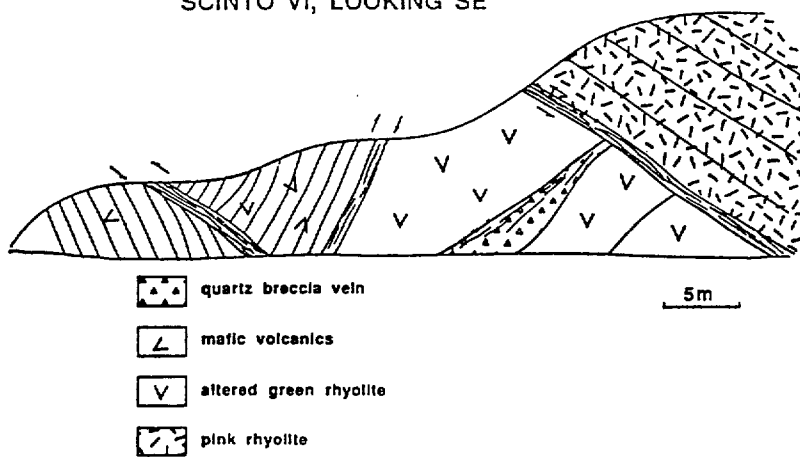
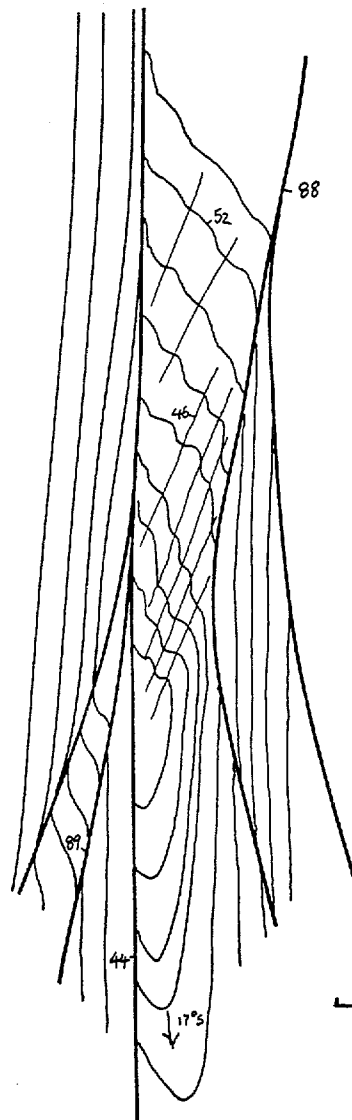


Figure 24. Schematic section, Scinto V mine.

NW



FAULT, DIP
So, DIP
CLEAVAGE, DIP

~10 m

SE

Figure 25. Simplified geological map of the Saddle Ridge pit.

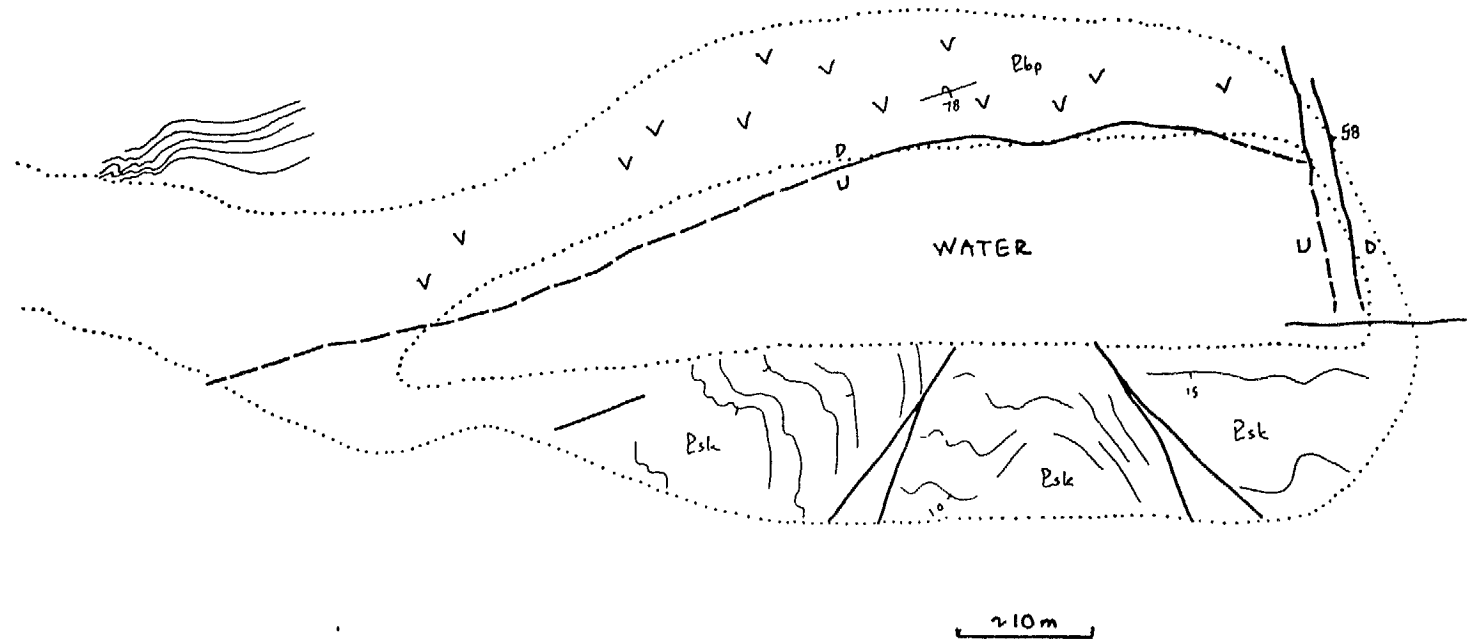


Figure 26. Summary of Coronation Hill fault geometry. Arrows show strike-slip movement sense, ball and spikes show downthrow block of normal fault.

CORONATION HILL FAULT GEOM

N

pit

1km

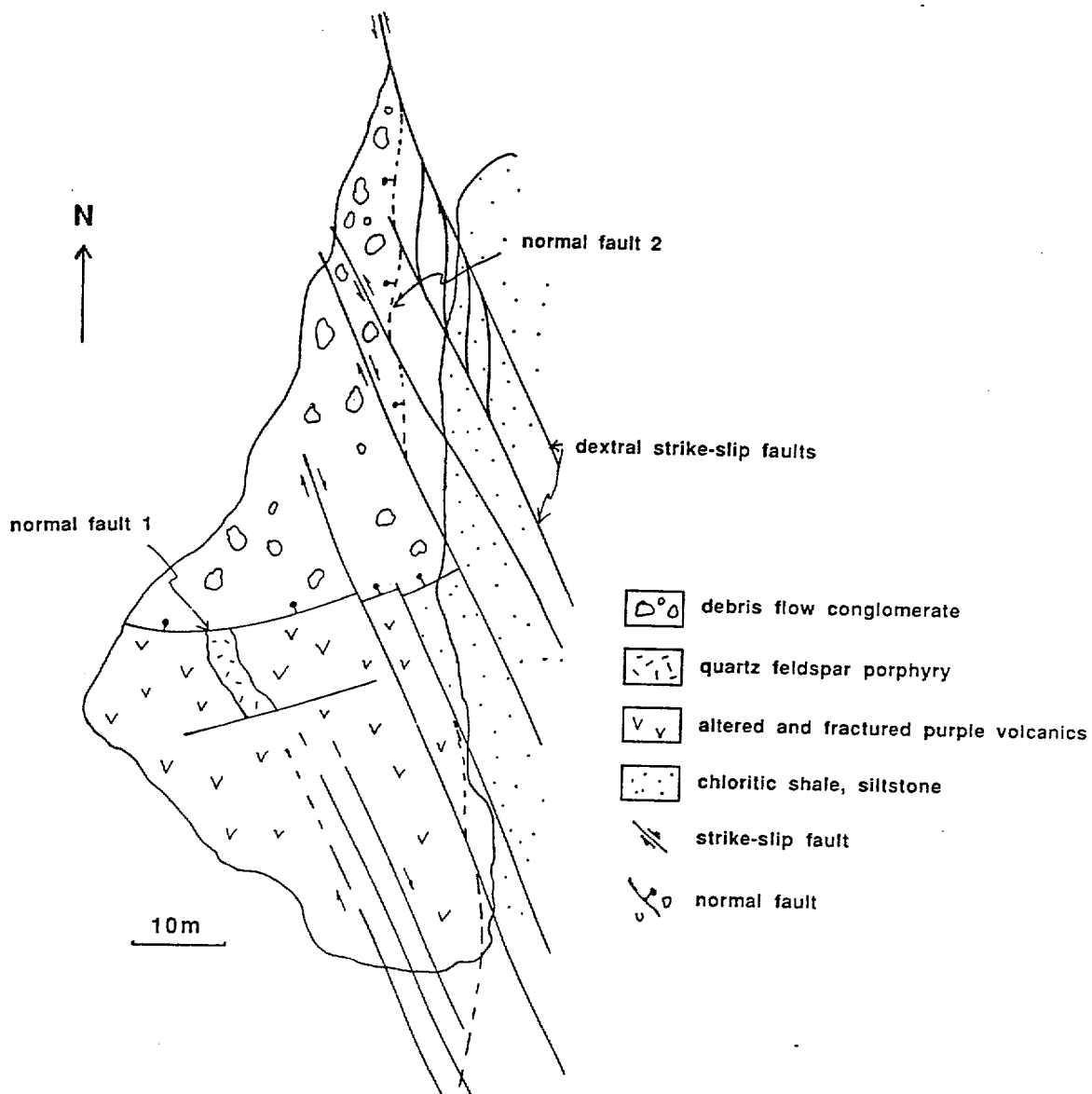
N

pit

1km

Figure 27. Fault geometry in the Coronation Hill pit, with equal area plots of fault orientations.

CORONATION PIT



CORONATION HILL - FAULTS

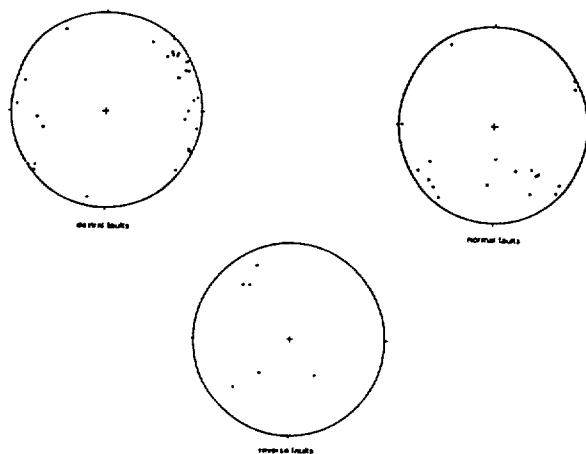
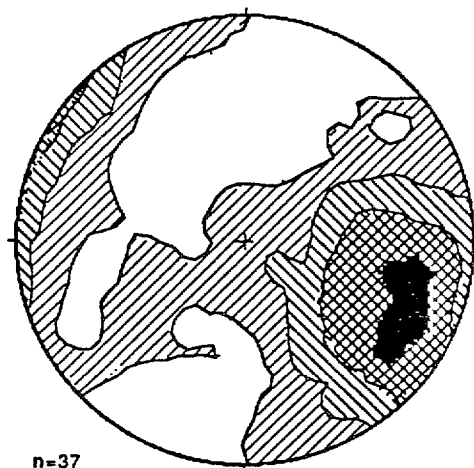
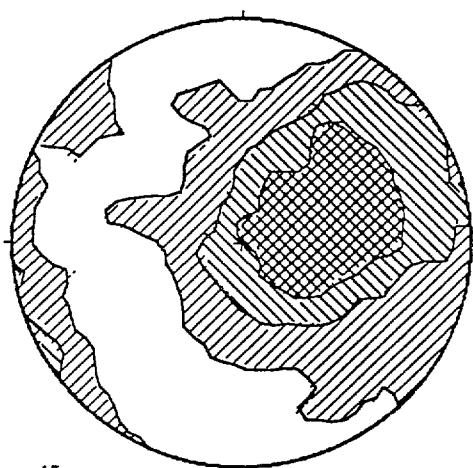


Figure 28. South Alligator Valley vein data. Top plot shows poles to veins in the Mundogie Sandstone. Middle plot is of all veins in the Coronation Hill area. Bottom plot divides vein types into early deformed veins (QVE), late undeformed veins (QVL) and veins occurring within the quartz feldspar porphyry unit (QFP).



n=37



n=45

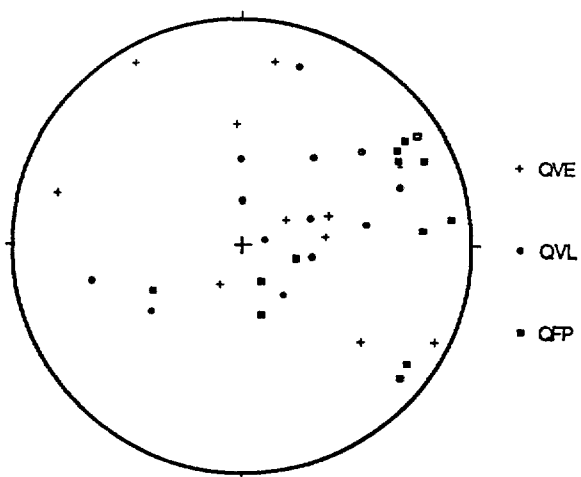


Figure 29. Geology of the Slesbeck area (based on Stuart Smith et al., 1988). Inset show structures developed in the open pit.

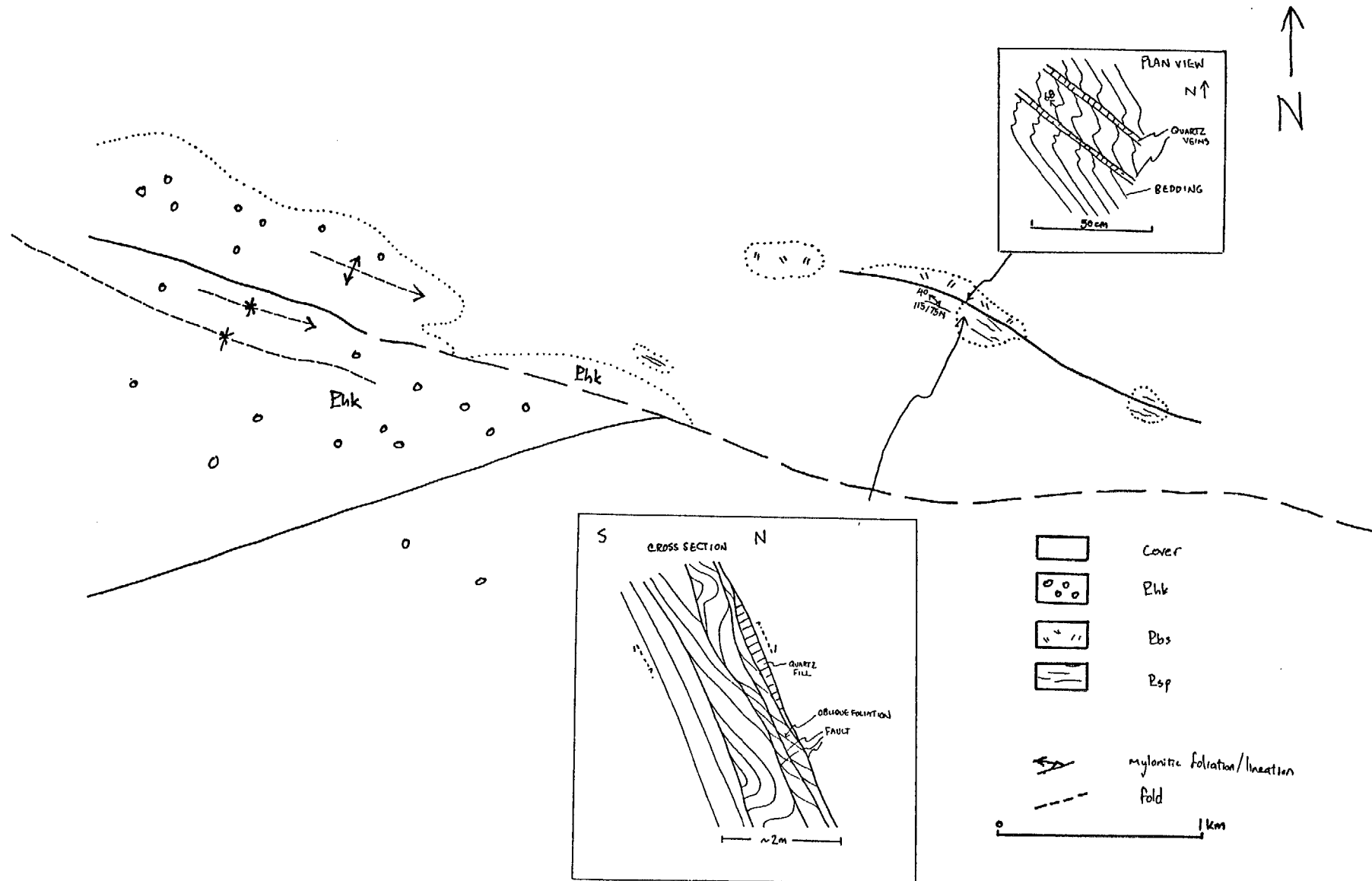
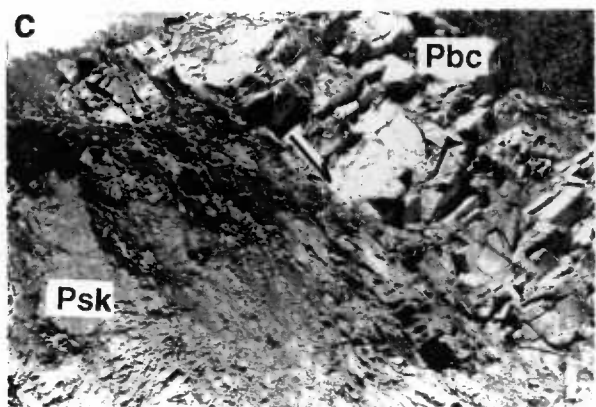
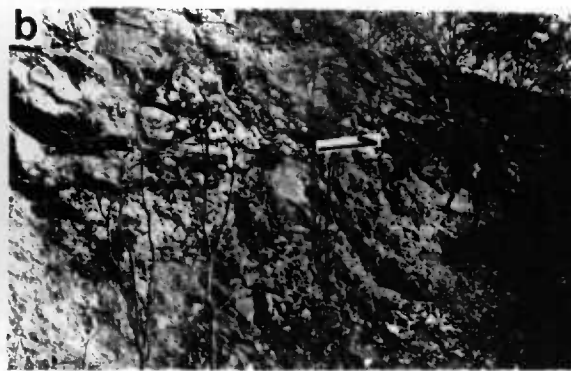


Figure 30a. Koolpin Mine geometry. Mineralization is associated with a north-trending oblique-slip fault zone. **30b.** Shallow reverse fault, Scinto VI mine. **30c.** Normal fault, El Sherana mine. **30d.** Possible overprinting between early steep normal faults and late shallow reverse faults, El Sherana Mine. **30e.** Reverse faults, El Sherana Mine. **30f.** 2-3m wide foliated zone at the normal fault contact between Coronation volcanics (v) and debris flow conglomerate (c), Coronation Hill pit.



* R 9 1 1 0 7 1 2 *

Figure 31. Summary diagram of variations in El Sherana group stratigraphy in the South Alligator Valley.



* R 9 1 1 0 7 1 3 *

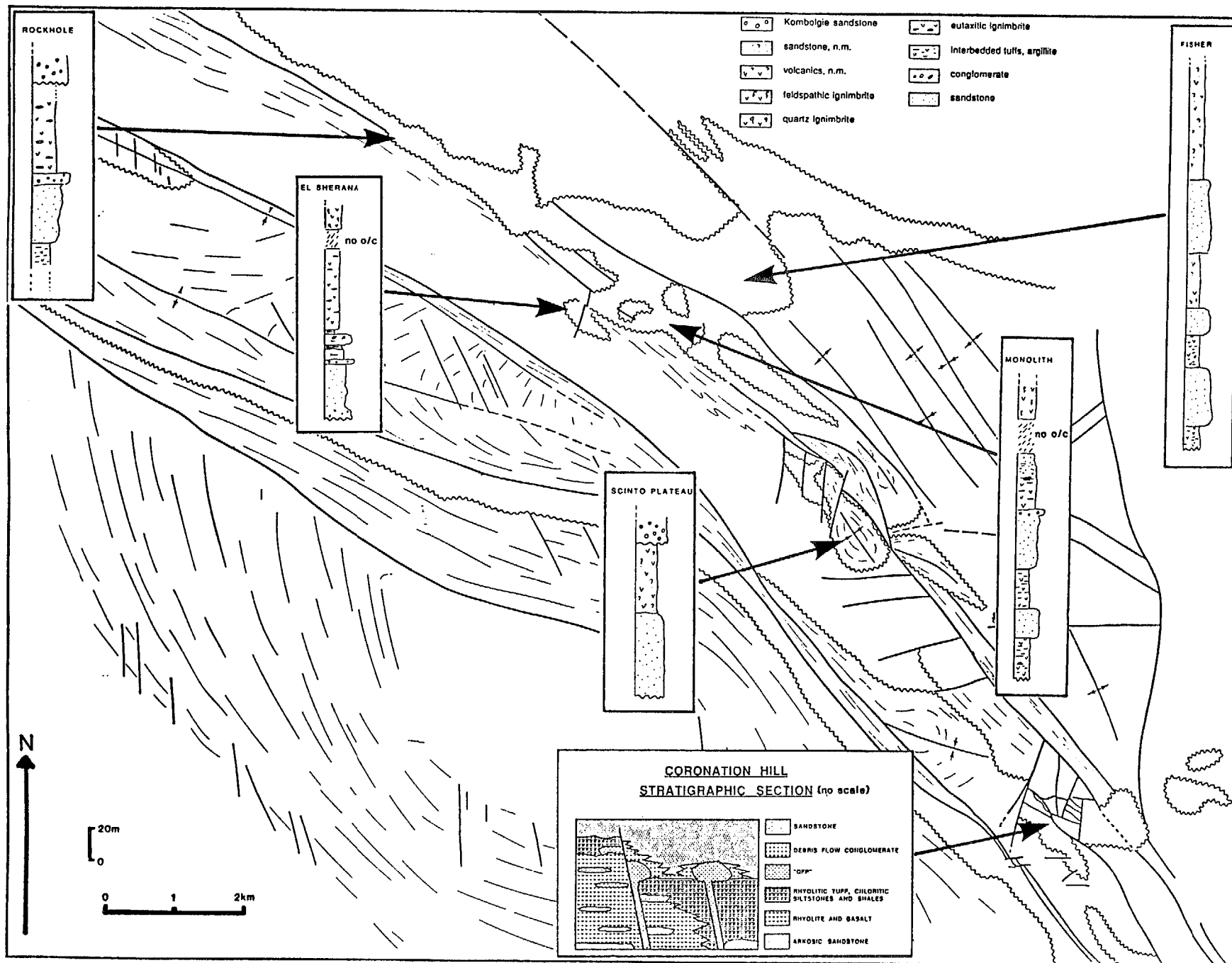
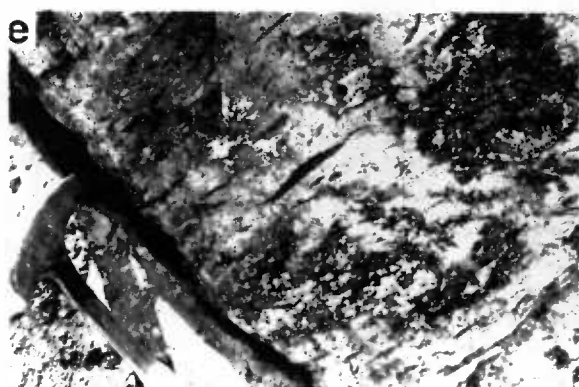
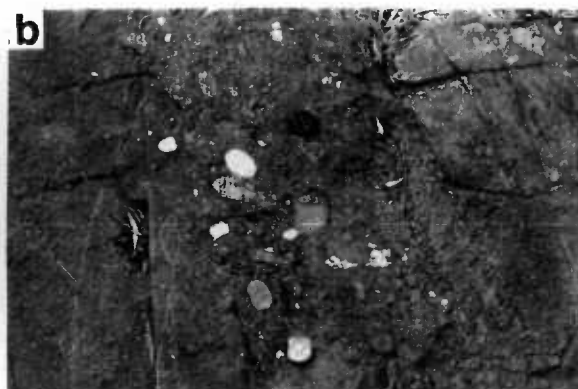


Figure 32a. Debris flow conglomerate unit in the Coronation Sandstone, south of El Sherana. The ground surface is parallel to bedding. **32b.** Pebbly layer in Coronation Sandstone, El Sherana area. **32c.** Carbonaceous shale fragments in debris flow conglomerate, Coronation Hill Mine. **32d.** Fold in flow banded Coronation Volcanics, south of Coronation Hill. **32e.** Fiamme in Pul Pul rhyolite, Fisher Fault area. **32f.** Rotated and foliated clasts of green tuffaceous siltstone (GTS) in intrusive quartz feldspar porphyry (QFP), Coronation Hill Mine.



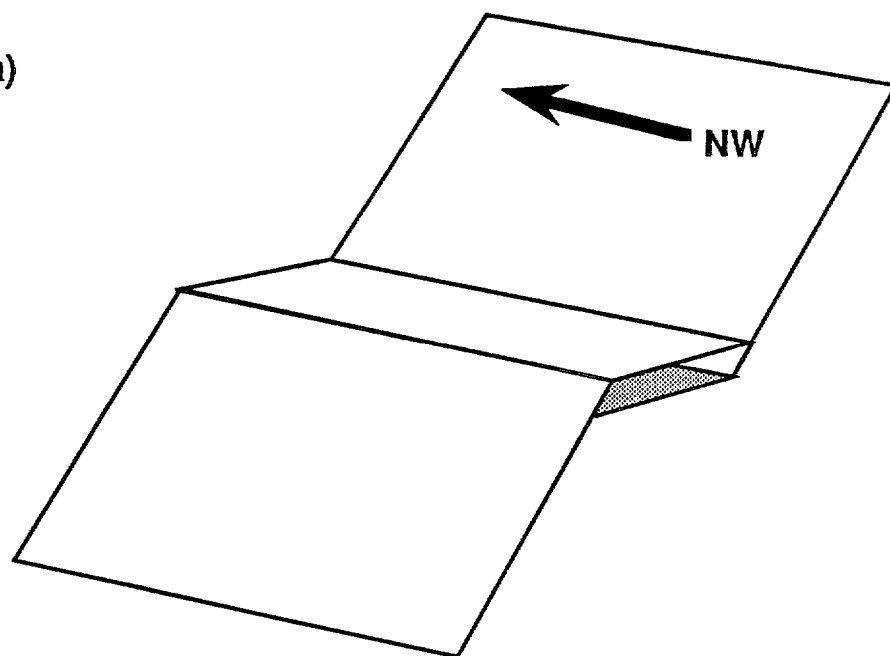
* R 9 1 1 0 7 1 4 *

Figure 33. End member spatial variations in the geometry of dilatant sites. **a.** Steep reverse fault with flat dilatant site (eg. Rockhole, ?Saddle Ridge, ?Sleisbeck). **b.** Steep strike-slip fault with steep dilatant site (eg. Coronation Hill, Palette area, Skull).



* R 9 1 1 0 7 1 5 *

a)



b)

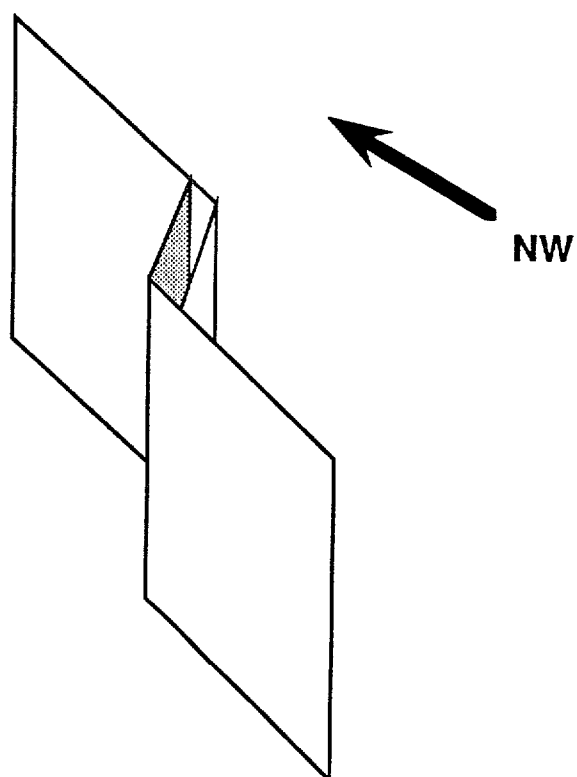
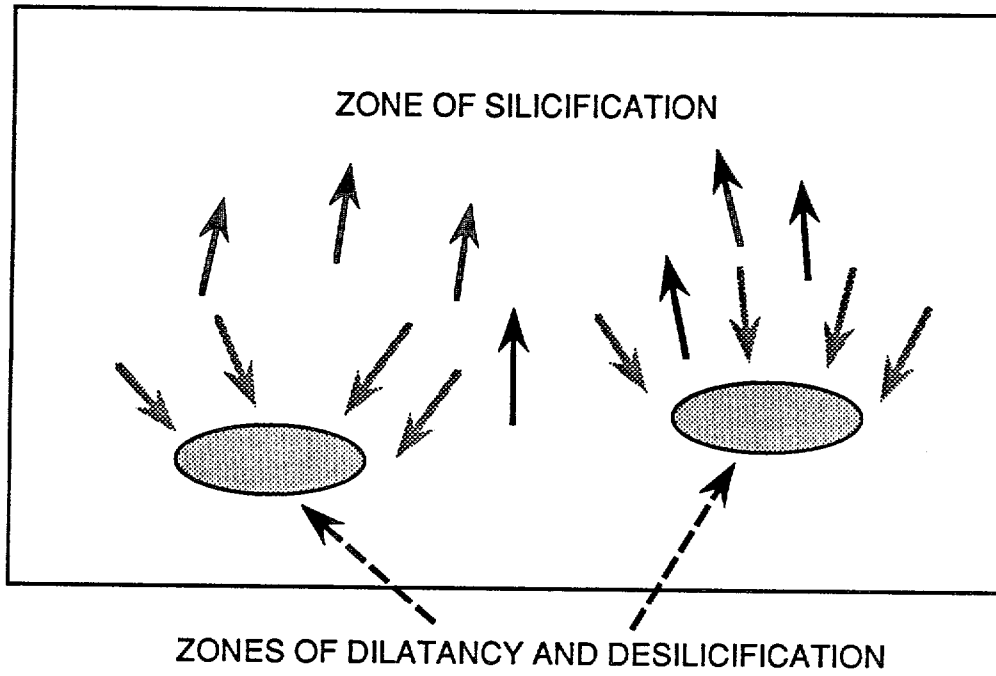


Figure 34. Schematic summary of fluid flow and silicification patterns expected in a dilatancy-driven fault-controlled fluid circulation system. Fluid sucked downwards into a dilatant site (eg. a fault-unconformity intersection) causes desilicification on its downward path. Dissolved silica is deposited at higher structural levels (eg. the Palette Fault system southeast of Coronation Hill) once normal upward fluid flow is restored.



APPENDIX I: SAMPLES TAKEN, 1988 SEASON

APPENDIX I : SAMPLES TAKEN, 1988 SEASON

2

SAMPLE	: S1/33/24A	SAMPLE	: S4/155/24
GRID REFERENCE	: 5470-352024	GRID REFERENCE	: 5470-460904
FORMATION	: Scinto Breccia	FORMATION	: Pul Pul Rhyolite
DESCRIPTION	: Veined Scinto breccia, quartz veins, saddle reefs	DESCRIPTION	: Banded rhyolite with brick-red (quartz-rich) lenses
ACTION	: T.S., Fluid inclusions	ACTION	: T.S., geochem.
SAMPLE	: S1/33/24B	SAMPLE	: S4/155/23B
GRID REFERENCE	: 5470-352024	GRID REFERENCE	: 5470-460903
FORMATION	: Scinto Breccia	FORMATION	: Pul Pul Rhyolite
DESCRIPTION	: Veined Scinto breccia, quartz veins, saddle reefs	DESCRIPTION	: Banded rhyolite, with gray-green fragment containing coarse-grained fluorite
ACTION	: T.S., Fluid inclusions	ACTION	: T.S., geochem.
SAMPLE	: S1/33/24C	SAMPLE	: S4/155/23A
GRID REFERENCE	: 5470-352024	GRID REFERENCE	: 5470-460903
FORMATION	: Scinto Breccia	FORMATION	: Pul Pul Rhyolite
DESCRIPTION	: Veined Scinto breccia, quartz veins, saddle reefs	DESCRIPTION	: Banded rhyolite with brick red (quartz-rich) lenses
ACTION	: T.S., Fluid inclusions	ACTION	: T.S., geochem.
SAMPLE	: S1/33/24D	SAMPLE	: S4/155/22
GRID REFERENCE	: 5470-352024	GRID REFERENCE	: 5470-459902
FORMATION	: Scinto Breccia	FORMATION	: Pul Pul Rhyolite
DESCRIPTION	: Veined Scinto breccia, quartz veins, saddle reefs	DESCRIPTION	: Rhyolite with fiamme
ACTION	: T.S., Fluid inclusions	ACTION	: T.S., geochem
SAMPLE	: S1/33/23B	SAMPLE	: S4/155/16a
GRID REFERENCE	: 5470-352024	GRID REFERENCE	: 5470-457900
FORMATION	: Koolpin Formation	FORMATION	: Pul Pul Rhyolite
DESCRIPTION	: Highly chloritic (GTS-like) foliated Koolpin formation	DESCRIPTION	: Breccia veining in sericitized ?crystal tuff, southern arm of Palette Fault.
ACTION	: T.S.	ACTION	: T.S., geochem.
SAMPLE	: S1/33/23C	SAMPLE	: S4/155/16B
GRID REFERENCE	: 5470-352024	GRID REFERENCE	: 5470-457900
FORMATION	: Koolpin Formation	FORMATION	: n/a
DESCRIPTION	: Bleached surface of Koolpin Formation	DESCRIPTION	: Massive quartz reef on Palette Fault
ACTION	: T.S.	ACTION	: T.S., Fluid Inclusions.
SAMPLE	: S1/33/25A	SAMPLE	: S4/155/16C
GRID REFERENCE	: 5470-347028	GRID REFERENCE	: 5470-457900
FORMATION	: n/a	FORMATION	: Pul Pul Rhyolite
DESCRIPTION	: Quartz vein along major fault in Scinto V pit	DESCRIPTION	: Veined, altered ?ignimbrite on Palette Fault
ACTION	: T.S., Fluid Inclusions	ACTION	: T.S., geochem, fluid inclusions
SAMPLE	: S1/33/23B	SAMPLE	: S4/155/17
GRID REFERENCE	: 5470-347028	GRID REFERENCE	: 5470-457900
FORMATION	: Koolpin Formation	FORMATION	: Pul Pul Rhyolite
DESCRIPTION	: Cleavage perpendicular to bedding in Scinto V pit		
ACTION	: T.S.		

APPENDIX I : SAMPLES TAKEN, 1988 SEASON

3

DESCRIPTION	: Altered crystal tuff near Palette Fault	DESCRIPTION	: Actinolite-bearing medium grained dolerite
ACTION	: T.S., geochem.	ACTION	: T.S.
SAMPLE	: S4/155/18	SAMPLE	: S2/84/35A
GRID REFERENCE	: 5470-458901	GRID REFERENCE	: 5470-431010
FORMATION	: Pul Pul Rhyolite	FORMATION	: Zamu dolerite
DESCRIPTION	: Altered crystal tuff 125m from Palette Fault	DESCRIPTION	: Black, hornblende-bearing coarse-grained dolerite
ACTION	: T.S., geochem.	ACTION	: T.S.
SAMPLE	: S4/155/19	SAMPLE	: S2/84/35B
GRID REFERENCE	: 5470-458901	GRID REFERENCE	: 5470-431010
FORMATION	: Pul Pul Rhyolite	FORMATION	: Zamu dolerite
DESCRIPTION	: Altered eutaxitic ignimbrite, 150m from Palette Fault	DESCRIPTION	: Quartz-?barite vein material
ACTION	: T.S., geochem.	ACTION	: T.S.
SAMPLE	: S4/155/20	SAMPLE	: S1/32/29A
GRID REFERENCE	: 5470-458902	GRID REFERENCE	: 5470-344067
FORMATION	: Pul Pul Rhyolite	FORMATION	: Coronation Sandstone
DESCRIPTION	: Altered eutaxitic ignimbrite, 235m from Palette Fault	DESCRIPTION	: Conglomerate with abundant rhyolite clasts
ACTION	: T.S., geochem.	ACTION	: T.S., geochem.
SAMPLE	: S4/155/21	SAMPLE	: S1/32/29B
GRID REFERENCE	: 5470-459902	GRID REFERENCE	: 5470-344067
FORMATION	: Pul Pul Rhyolite	FORMATION	: Coronation Sandstone
DESCRIPTION	: "Unaltered" eutaxitic ign- imbrite, 335m from Palette Fault	DESCRIPTION	: Massive hematite-calcite rock
ACTION	: T.S., geochem.	ACTION	: T.S., geochem.
SAMPLE	: S4/156/1	SAMPLE	: S1/32/29C
GRID REFERENCE	: 5470-472905	GRID REFERENCE	: 5470-344067
FORMATION	: ?Dolerite	FORMATION	: Coronation Sandstone
DESCRIPTION	: Fine-grained black dolerite cutting Pul Pul Rhyolite	DESCRIPTION	: "Conglomerate" with "breadcrusted" rounded fragments (possibly an agglomerate..)
ACTION	: T.S.	ACTION	: T.S., geochem.
SAMPLE	: S4/156/2	SAMPLE	: S1/32/29E
GRID REFERENCE	: 5470-474906	GRID REFERENCE	: 5470-344067
FORMATION	: Malone Creek Granite	FORMATION	: Coronation Sandstone
DESCRIPTION	: K-spar-rich granite with quartz-amphibole clots	DESCRIPTION	: Fragment of purple volcanic rock, taken from the conglomerate.
ACTION	: T.S.	ACTION	: T.S., geochem.
SAMPLE	: S2/84/33	SAMPLE	: S1/36/19
GRID REFERENCE	: 5470-431010	GRID REFERENCE	: 5470-411053
FORMATION	: Zamu dolerite	FORMATION	: Coronation Sandstone
DESCRIPTION	: Actinolite-bearing dolerite	DESCRIPTION	: Green, quartzose, veined Coronation Sandstone volcanic.
ACTION	: T.S.	ACTION	: T.S., geochem.
SAMPLE	: S2/84/34	SAMPLE	: S1/36/20
GRID REFERENCE	: 5470-431010		
FORMATION	: Zamu dolerite		

GRID REFERENCE	: 5470-411054	DESCRIPTION	: Chlorite-muscovite schist with S ₂ differentiated crenulation cleavage.
FORMATION	: Coronation Sandstone		
DESCRIPTION	: Conglomerate		
ACTION	:	ACTION	: T.S.
SAMPLE	: S1/36/21	SAMPLE	: S2/84/26
GRID REFERENCE	: 5470-410053	GRID REFERENCE	: 5470-456014
FORMATION	: Coronation Sandstone	FORMATION	: Burrell Creek
DESCRIPTION	: Volcanic, purple, with abundant lithic fragments.	DESCRIPTION	: Dark shale layer with two cleavages.
ACTION	: T.S., geochem.	ACTION	: T.S.
SAMPLE	: S2/84/19	SAMPLE	: S2/84/27
GRID REFERENCE	: 5470-455008	GRID REFERENCE	: 5470-456014
FORMATION	: Burrell Creek	FORMATION	: Burrell Creek
DESCRIPTION	: Kinked chlorite-muscovite schist.	DESCRIPTION	: Chlorite-muscovite schist with S ₂ differentiated crenulation cleavage. May contain andalusite and/or staurolite
ACTION	: T.S. (both cut lines).		
SAMPLE	: S2/84/19	ACTION	: T.S. (both cut lines).
GRID REFERENCE	: 5470-455010		
FORMATION	: Burrell Creek	SAMPLE	: S2/84/28
DESCRIPTION	: Box-like kinks in chlorite-muscovite schist.	GRID REFERENCE	: 5470-457015
ACTION	: T.S. (both cut lines).	FORMATION	: Burrell Creek
		DESCRIPTION	: Lower grade chloritic schist.
SAMPLE	: S2/84/21	ACTION	: T.S.
GRID REFERENCE	: 5470-456011		
FORMATION	: Burrell Creek	SAMPLE	: S2/84/29
DESCRIPTION	: Chlorite-muscovite schist with well-developed differentiated crenulation cleavage.	GRID REFERENCE	: 5470-456016
ACTION	: T.S.	FORMATION	: Burrell Creek
		DESCRIPTION	: Chlorite-muscovite schist with S ₂ and S ₃ differentiated crenulation cleavages.
SAMPLE	: S2/84/22	ACTION	: T.S. (both cut lines)
GRID REFERENCE	: 5470-456011		
FORMATION	: Zamu Dolerite	SAMPLE	: S2/84/30
DESCRIPTION	: Collected by R.G.W..	GRID REFERENCE	: 5470-457019
ACTION	:	FORMATION	: Burrell Creek
		DESCRIPTION	: Red-green fine grained sandstone with ~30 cm-scale pencil structure.
SAMPLE	: S2/84/23	ACTION	: T.S.
GRID REFERENCE	: 5470-456012		
FORMATION	: Zamu Dolerite	SAMPLE	: S2/84/32
DESCRIPTION	: Collected by R.G.W.	GRID REFERENCE	: 5470-458025
ACTION	:	FORMATION	: Burrell Creek
		DESCRIPTION	: Medium-grained siliceous rock with abundant biotite flecks.
SAMPLE	: S2/84/24	ACTION	: T.S.
GRID REFERENCE	: 5470-456012		
FORMATION	: Zamu Dolerite	SAMPLE	: S1/37/1
DESCRIPTION	: Dolerite with strong S ₂ cleavage.	GRID REFERENCE	: 5470-461031
ACTION	: T.S.	FORMATION	: Burrell Creek
SAMPLE	: S2/84/25		
GRID REFERENCE	: 5470-456013		
FORMATION	: Burrell Creek		

DESCRIPTION	: Vine to medium grained sandstone with strong S ₂ .	FORMATION	: Kapalga
ACTION	: T.S. (both cut lines).	DESCRIPTION	: Mylonitized siltstone, Sleisbeck pit.
SAMPLE	: S1/37/2	ACTION	: T.S. (both cut lines)
GRID REFERENCE	: 5470-461032	SAMPLE	: M8/220/65
FORMATION	: Burrell Creek	GRID REFERENCE	: 5731-103282
DESCRIPTION	: Breccia vein in sandstone.	FORMATION	: Gerowie Tuff
ACTION	: T.S.	DESCRIPTION	:
SAMPLE	: S2/88/22	ACTION	: T.S., geochem
GRID REFERENCE	: 5470-371981	SAMPLE	: M10/193/32A,B,C,D
FORMATION	: ?Pul Pul Rhyolite	GRID REFERENCE	: 5731-124222
DESCRIPTION	: Rhyolitic volcanic with abundant lithic fragments and quartz phenocrysts.	FORMATION	: Zamu dolerite
ACTION	: T.S., geochem.	DESCRIPTION	: A set of samples showing large variations in K-feldspar and ferromagnesian mineral content.
SAMPLE	: S2/88/23	ACTION	: T.S.
GRID REFERENCE	: 5470-378978	SAMPLE	: S1/32/30
FORMATION	: Coronation Sandstone	GRID REFERENCE	: 5471-343062
DESCRIPTION	: Mafic volcanic with hematite-calcite±pyrite clots.	FORMATION	: Pul Pul Rhyolite
ACTION	: T.S., geochem.	DESCRIPTION	: Red micaceous siltstone.
SAMPLE	: M13/53/13	ACTION	: T.S.
GRID REFERENCE	: 5731-248096	SAMPLE	: S1/32/31
FORMATION	: Coronation Sandstone	GRID REFERENCE	: 5471-320064
DESCRIPTION	: Flow banded lava, strongly weathered.	FORMATION	: Pul Pul Rhyolite
ACTION	: ?geochem.	DESCRIPTION	:
SAMPLE	: M13/53/14	ACTION	: T.S., geochem.
GRID REFERENCE	: 5470-245093	SAMPLE	: S1/32/33
FORMATION	: Koolpin	GRID REFERENCE	: 5470-319051
DESCRIPTION	: Folds in cherty ferruginous rock.	FORMATION	: Pul Pul Rhyolite
ACTION	: cut only.	DESCRIPTION	:
SAMPLE	: M12/77/27B	ACTION	: T.S., geochem.
GRID REFERENCE	: 5731-210119	SAMPLE	: S1/32/32A
FORMATION	: Koolpin?	GRID REFERENCE	: 5470-331056
DESCRIPTION	: Green tuffaceous sandstone.	FORMATION	: Coronation Sandstone
ACTION	: T.S.	DESCRIPTION	: Foliated crush breccia in rhyolite, strong surface weathering.
SAMPLE	: M12/77/27C	ACTION	: T.S., ?geochem.
GRID REFERENCE	: 5731-210119	SAMPLE	: S1/32/32B
FORMATION	: Gerowie Tuff?	GRID REFERENCE	: 5470-331056
DESCRIPTION	: Fine grained jointed siliceous rock, stained white on weathered surface.	FORMATION	: Coronation Sandstone
ACTION	: T.S., geochem,	DESCRIPTION	: Less deformed rhyolite, strong surface weathering.
SAMPLE	: S8/91/5	ACTION	: T.S., ?geochem.
GRID REFERENCE	: 5470-648755	SAMPLE	: S2/88/24
		GRID REFERENCE	: 5470-364017
		FORMATION	:

APPENDIX I : SAMPLES TAKEN, 1988 SEASON

6

DESCRIPTION	: Deformed El Sherana
ACTION	: T.S., geochem.
SAMPLE	: S2/88/25A,B,C,D
GRID REFERENCE	: 5470-363018
FORMATION	: Kombolgie
DESCRIPTION	: Conglomerate and purple "vesicular" siltstone and mudstone near unconformity.
ACTION	: T.S., geochem.
SAMPLE	: S2/84/33
GRID REFERENCE	: 5470-498012
FORMATION	: Coronation Sandstone
DESCRIPTION	: Volcanic sampled from boulder, strong surface weathering.
ACTION	: T.S., ?geochem.
SAMPLE	: S5/203/14A,B
GRID REFERENCE	: 5470-464891
FORMATION	: mixed
DESCRIPTION	: Breccia vein in southern arm of Palette Fault.
ACTION	: T.S., geochem., fluid inclusions
SAMPLE	: S4/155/25
GRID REFERENCE	: 5470-441918
FORMATION	: mixed
DESCRIPTION	: Breccia vein in southern arm of Palette Fault.
ACTION	: T.S., geochem., fluid inclusions
SAMPLE	: S1/34/29
GRID REFERENCE	: 5471-360025
FORMATION	: Coronation Sandstone
DESCRIPTION	: Green, foliated, coarse grained quartz-rich volcanic.
ACTION	: T.S. (cut both lines)

Structural Data Set

Formatted Field Data

strike or dip	dip or plunge	dip dir planes	pitch	vergence	feature	location
283	73	S			AS1	RH
288	82	S			AS1	RH
341	70	W			AS1	ES
137	?				AS1	ESG
300	58	S			AS2	RH
293	55	S			AS2	RH
140	68	S			AS2	RHS
128	64	S			AS2	RHS
145	71	S			AS2	ESN
315	56	W			AS2	PN1M
330	83	W			AS2	EOP
343	86	W			AS3	RH
165	81	W			AS3	RHS
40	79	E			AS3	ES
216	90	W			AS3	ES
20	89	E			AS3	ES
200	83	W			AS3	ES
170	80	W			AS3	ES
77	83	S			AS3	ES
330	86	E			AS3	ES
30	88	W			AS3	ES
162	73	W			AS3	ESN
75	67	S			AS3	SRM
18	52	E			AS3	SRM
22	51	E			AS3	SRM
52	71	S			AS3	SRM
360	82	W			AS3	SRM
307	85	S			AS3	ESWM
282	76	S			AS3	GIM
146	84	N			AS3	GIM
327	79	S			AS3	CH
153	87	N			AS3	CFM
306	53	S			AS4	RH
243	71	W			AS4	RH
109	86	S			AS4	RHS
38	90	S			AS4	RHLA
357	66	E			AS4	RHLA
23	68	W			AS4	ES
160	39	W			AS4	ES
236	52	N			AS4	KGR
227	64	S			AS4	PM
227	81	S			AS4	PN2M
312	?				AS4	CHM
18	56	W			AS4	ESG
260	26	N			AS4	CHM
160	83	E			AS4	CHM
323	69	E			AS4	CHM
334	71	E			AS4	CHM
190	88	W			ASFLOW	CHS
57	80	N			BV	CLRSP
128	77	E			BV	CF
154	53	E			BZ	RH
330	27				CHL01	CHM
164	88	E	29		CHL02	CHM
45	86	N	75		CHL02	CHM
134	39	E	38		CHL02	CHM
180	55	W			CHS1	CHM
123	73	S			CHS1	CHM
160	63	E			CHS1	CHM
330	75	E			CHS1	CHM
330	70	W			CHS1	CHM
300	48	W			CHS1	CHM
325	60	W			CHS1	CHM
157	62	W			CHS2	CHM
160	65	N			CHS2	CHM
142	88	W			CHS2	CHM
160	83	W			CHS2	CHM
324	90				CHS2	CHM
334	72	W			CHS2	CHM
320	64	W			CHS2	CHM
325	65	W			CHS2	CHM
323	80	E	50		CHS2	CHM
330	80	W			CHS2	CHM
290	90				CHS2	CHM

strike or dip	dip or plunge	dip dir planes	pitch	vergence	feature	location
332	73	E			CHS3	CHM
356	80	E			CHS3	CHM
90	65	S			CHS3	CHM
147	69	S	86		D3NF	RHS
164	59	W			D3NF(OBL)	RHS
168	58	W			D3NF(OBL)	RHS
110	79	N			DF	RH
200	28	W			DF	RH
340	40	W	30		DF	RHLA
346	31	W			DF	RHLA
318	62	W			DF	KM
198	69	E	5		DF	ESS
190	55	E	13		DF	ESS
17	74	E	20		DF	SC6M
29	90	W			DF	SC6M
20	72	E	13		DF	SC6M
60	73	S	3		DF	SC6M
74	79	S	38		DF	SKM
84	69	S	24		DF	SKM
80	56	S	166		DF	SKM
66	46	S	141		DF	SKM
135	90		25		DF	CHM
135	90		146		DF	CHM
352	87	W	174		DF	CHM
322	83	N			DF	CHM
165	58	E			DF	CHM
140	79	S			DF	CHM
62	81	S	166		DF	CHM
142	78	W			DF	CHM
173	82	W	172		DF	CHM
156	72	W	170		DF	CHM
184	84	E	0		DF	CHM
11	87	W	8		DF	CHM
25	86	W	1		DF	CHM
40	87	W	170		DF	CHM
160	62	E	144		DF	CLRSP
345	81	E			DF	CLRSP
168	89	W			DF	CFM
355	62	E	140		DF	CHM
102	81	N	33		DF	CHM
325	90		3		DF	CHM
323	83	W			DF	CHM
154	82	W	173		DF	CHM
320	72	W	1		DF	CHM
335	85	W	3		DF	CHM
180	76	W	9		DF	CHM
6	73	W	12		DF	CHM
144	81	W	174		DF	CHM
330	87	W			DF	CHM
126	72	S			DF	CHM
320	88	E	2		DF	CHM
26	88	W	2		DF	CHM
20	80	E	3		DF	CHM
330	88	W	177		DF	CHM
330	88	W	28		DF	CHM
330	88	W	137		DF	CHM
11	90	E	4		DF	SRM
170	58	E			DF	SRM
317	66	S			DF	SRM
167	82	E			DF	SRM
7	88	E	173		DF	SP
22	81	E	5		DF	SP
16	89	W	21		DF	SP
13	83	E	17		DF	SP
130	85	E			DF?	CF
278	47	S			DFC/JT	CHM
279	90				DFC/JT	CHM
290	23	N			DFC/JT	CHM
352	87	W	174		DFC/JT	CHM
253	85				DFL	RH
305	27				DFL	RH
114	13				DFL	RHLA
29	23				DFL	SC6M
203	?				DFL	SKM

strike or dip	dip or plunge	dip dir plane	pitch	vergence	feature	location
192	18				DFL	SRM
330	45	W			EF	ESG
320	84	S			EF	ESM
153	37	W			EF	ESM
200	?				EFL	ESM
250	?				EFL	ESM
164	88	E			F	CHM
265	50				F1	RH
275	34				F1	RH
338	21				F1	ES
330	77	E	95		F1	GIM
121	78	S	158		F1	ESG
284	10			S	F2	RH
293	20			S	F2	RH
119	9			S	F2	RHS
143	28			S	F2	RHS
155	51			S	F2	ESN
214	21				F2	SRM
300	49			S	F2	PN1M
330	16			S	F2	EOP
180	78			S	F3	RH
189	78			N	F3	RHS
40	57			N	F3	ES
212	47			N	F3	ES
28	67			S	F3	ES
30	59			S	F3	ES
186	78			N	F3	ES
84	81			S	F3	ES
331	70			S	F3	ES
30	73			S	F3	ES
334	63			S	F3	ESN
238	10			E	F3	SRM
50	31				F3	SRM
203	23				F3	SRM
40	13				F3	SRM
360	15				F3	SRM
300	42			E	F3	ESWM
284	81			N	F3	GIM
320	41			N	F3	GIM
320	60			W	F3	CH
115	86				F3	CFM
295	12			S	F4	RH
254	86			N	F4	RH
300	74			S	F4	RHS
204	14				F4	RHLA
174	30				F4	RHLA
323	68				F4	ES
298	34				F4	ES
328	50			W	F4	KGR
88	43			N	F4	PM
216	36			N	F4	PN2M
324	70				F4	CHM
270	48				F4	CHM
80	18				F4	CHM
295	59				F4	ESG
135	30				F4	CHM
160	13				F4	CHM
332	38				F4	CHM
329	8				F4	CHM
51	51	N			FB	CHS
20	52	E			FB	CHS
349	84	W			FB	CHS
94	26	N			FB	CHS
60	90				FB	PPH
153	41	E			FB	PPH
25	87	E			FB	PPH
11	48	E			FB	PPH
40	60	E			FB	PPH
60	72	E			FB	PPH
172	79	E			FB	CHS
112	62	N			FB	ESM
81	14	N			FF	RHUA
24	55	E			FF	RHUA
58	28	S			FF	RHUA

strike or dip	dip or plunge	dip dir plane	pitch	vergence	feature	location
162	20	W			FF	RHUA
56	17	N			FF	RHUA
16	29	W			FF	RHUA
54	18	N			FF	RHUA
190	76			E	FFLOW	CHS
52	69	N			JT	SC6
93	61	N			JT	SC6
80	90	S			JT	SC6
113	77	N			JT	SC6
110	90	N			JT	SC6
116	60	N			JT	SC6
74	84	N			JT	SC6
153	75	E			JT	SC6
242	89	S			JT	SC6
308	90				JT	SC6
22	87	E			JT	SC6
291	13				L02	RH
57	27				L02	ES
97	84				L02	ES
104	30				L02	ES
300	1				L02	ESS
318	36				L02	CHAR
108	20				L02	SR
233	7				L02	SRM
48	354				L02	CHS
152	36				L02	KGR
232	48				L02	KGR
168	60				L02	KGR
190	53				L02	KGR
272	23				L02	ESWM
96	54				L02	ES
110	27				L03	RH
294	8				L03	RH
323	46				L03	KGR
336	48				L03	CHS
360	70				L2	SR
252	58	S			NF	RH
138	83	N			NF	FF
116	82	N	157		NF	FF
120	43	N	97		NF	FF
280	84	N			NF	SRM
136	80	E	117		NF	SC6M
31	63	E			NF	SC6M
154	90		71		NF	CHM
360	88	E	69		NF	CHM
60	82	S			NF	CHM
40	82	W	99		NF	CHM
96	51	N	88		NF	CHM
60	68	N	90		NF	CHM
225	59	N	99		NF	CHM
228	58	N	115		NF	CHM
243	43	N	100		NF	CHM
228	51	N	97		NF	CHM
45	86	N			NF	CHM
149	82	E	98		NF	CHM
320	78	E	54		NF	CHM
128	84	N	74		NF	CHM
335	85	W	87		NF	CHM
150	67	E	69		NF	CHM
315	79	E	83		NF	CHM
330	88	W	71		NF	CHM
102	88	N			NF	SRM
310	89	W			NF	SRM
47	55	N			NF	SRM
62	43	N			NF	SRM
100	82	N	67		NF	SRM
145	44	S			NF	ESM
144	43	S			NF	ESM
135	63	S	73		NF	SP
142	71	S	112		NF	SP
137	66	S	90		NF	SP
170	80	W	82		NF?	CF
40	89				NFL	SRM
319	?				NFL	SRM

strike or dip	dip or plunge	dip dir plane:	pitch	vergence	feature	location
323	?				NFL	SRM
279	?				NFL	ESM
290	?				NFL	ESM
175	57	E			PLF	CHS
350	75	W			PLF	CHS
131	63	E			PLF	CHS
80	84	S			PLF	CHS
120	76	E			PLF	CHS
164	81	E			PLF	CHS
76	60	N			PLF	CLRSP
75	51	S			PLF	ES
110	79	N			QV	RH
170	66	E			QV	RH
335	29	N			QV	RH
345	58	W			QV	RH
42	65	N			QV	RH
215	68	W			QV	RH
155	29	W			QV	ES
12	43	W			QV	ES
84	9	N			QV	ES
18	43	W			QV	ES
163	37	W			QV	ES
342	62	W			QV	ESS
189	69	W			QV	ESS
200	42	W			QV	ESS
205	55	W			QV	ESS
197	60	W			QV	ESS
196	86	E			QV	ESS
195	69	W			QV	ESS
200	90	W			QV	ESS
318	22	N			QV	KGATE
348	73	N			QV	KGATE
36	20	E			QV	KGATE
342	70	W			QV	KGATE
228	57	S			QV	CHS
67	74	S			QV	PM
300	48	E			QV	PM
20	85	E			QV	CLRSP
40	90				QV	CLRSP
58	88	N			QV	CLRSP
48	81	N			QV	CLRSP
10	62	W			QV	CLRSP
64	73	N			QV	CLRSP
148	50	W			QV	CH
148	33	W			QV	CH
120	89	S			QV	CH
238	47	N			QV	CH
162	22	W			QV	CH
226	34	S			QV	CH
13	48	W			QV	ESG
37	57	W			QV	ESG
50	44	W			QV	CHM
15	20	W			QV(QFP)	CHM
75	26	N			QV(QFP)	CHM
154	36	E			QV(QFP)	CHM
62	14	N			QV(QFP)	CHM
332	67	W			QV(QFP)	CHM
352	81	W			QV(QFP)	CHM
327	73	W			QV(QFP)	CHM
355	68	W			QV(QFP)	CHM
328	79	W			QV(QFP)	CHM
328	68	W			QV(QFP)	CHM
335	76	W			QV(QFP)	CHM
40	80	W			QV(QFP)	CHM
36	77	W			QV(QFP)	CHM
10	26	W			QVE	CHM
310	41	W			QVE	CHM
270	31	S			QVE	CHM
346	8	W			QVE	CHM
322	56	W			QVE	CHM
338	27	W			QVE	CHM
82	16	S			QVE	CHM
333	67	W			QVE	CHM
229	23	N			QVE	CHM

strike or dip	dip or plunge	dip dir plane	pitch	vergence	feature	location
144	41	E			QVE	CHM
288	72	S			QVE	CHM
340	63	W			QVE	CHM
170	46	W			QVE	CHM
167	58	E			QVE	CH
326	19	W			QVL	CHM
352	30	W			QVL	CHM
338	33	W			QVL	CHM
16	74	E			QVL	CH
26	83	W			QVL	CH
100	73	S			QVL	CHS
60	84	S			QVL	CHS
123	15	N			QVL	CHS
36	56	W			QVL	CHS
87	45	S			QVL	CHS
34	60	W			QVSET	RH
196	22	W			QVSET	RHS
340	25	W			RF	RH
318	8	S			RF	RH
120	70	S	150		RF	RH
264	22	N			RF	RHLA
124	69	S	142		RF	ESM
144	36	S			RF	ES
230	22	S			RF	ESS
301	66	N			RF	SRM
337	42	W			RF	SC6M
354	48	W			RF	SC6M
330	24	S			RF	SC6M
8	60	E			RF	PM
232	45	S			RF	PM
300	60	S			RF	PN2M
321	32	W			RF	PN2M
53	61	E	140		RF	CHM
235	38	N	90		RF	CHM
140	67	E	57		RF	CHM
134	39	E			RF	CHM
229	65	E	119		RF	CHM
65	75	S	90		RF	CHM
117	63	S	87		RF	RHUA
136	40	S			RF	RHUA
132	84	S			RF	RHUA
110	81	S	85		RF	RHUA
107	83	S	106		RF	RHUA
103	86	S	112		RF	RHUA
80	88	S	118		RF	SRM
70	87	S	96		RF	SRM
56	70	S	56		RF	SRM
68	48	S			RF	SRM
137	40	S			RF	SRM
94	41	S			RF	SRM
240	46	S			RF	SRM
315	14	S			RF	ESM
302	40	S			RF	ESM
120	36	N			RF	ESM
89	37	N			RF	ESM
137	20	S	84		RF	SP
141	18	S	102		RF	SP
152	23	S	91		RF	SP
100	56	S	110		RF	RHLA
30	18	S			RF(OBL)	RHLA
128	81	N	139		RF(OBL)	ESM
170	?				RFL	RH
125	?				RFL	RH
328	?				RFL	ESS
242	38				RFL	SC6M
306	37				RFL	SC6M
340	?				RFL	SC6M
330	?				RFL	CHM
127	?				RFL	SRM
220	?				RFL	SRM
207	?				RFL	SRM
212	?				RFL	ESM
264	?				RFL	ESM
346	?				RFL	ESM

strike or dip	dip or plunge	dip dir plane	pitch	vergence	feature	location
176	43	W			S(OFP)	CHM
292	70	W			S0B	RH
330	77	E			S1	GIM
128	90				S1	GIM
283	64	N			S1	GIM
122	54	S			S2	RH
60	83	N			S2	ES
124	88	N			S2	ES
280	76	N			S2	ES
300	70	S			S2	ESS
165	51	W			S2	CHAR
320	87	E			S2	ESN
105	69	S	28		S2	KGATE
132	79	S			S2	KGATE
163	88	S			S2	KGATE
120	86	S			S2	KGATE
163	86	W			S2	KGATE
300	72	N			S2	SR
6	74	W			S2	SRM
25	82	W			S2	SRM
271	54	N			S2	CHS
113	87	S			S2	SR
151	63	W			S2	KGR
75	90	S			S2	KGR
172	63	W			S2	KGR
180	68	W			S2	KGR
170	71	W			S2	KGR
114	70	S			S2	KGR
173	90	W			S2	KGR
178	77	W			S2	KGR
164	75	W			S2	KGR
16	86	W			S2	SKM
332	34	S			S2	ESWM
110	83	N			S2	ES
304	72	N			S2	ES
285	85	N	107		S2	GIM
302	83	S	81		S2	GIM
117	78	S			S2	GIM
279	61	N			S2	GIM
106	49	N		S	S2	CHS
109	41	S			S2	CH
128	60	S			S2	ESG
18	89	W			S2	ESG
123	48	E			S2	OD
125	50	W			S2	ESS
298	89	N			S2	PPH
130	82	N			S2	CC
139	74	S			S2	CHS
14	70	W			S2	CHS
114	80	N			S3	RH
120	48	S			S3	RH
58	70	E			S3	SRM
20	87	W			S3	SRM
172	89	E			S3	SR
183	56	W			S3	KGR
360	52	E			S3	SKM
137	88	S			S3	PPB
354	78	E			S3	CHS
154	67	E			S3	OD
294	69	N			SC	SRM
286	53	N			SC	SRM
144	86	S			SC	SC6
286	59	W			SC	PN1M
285	88	S			SC	PN1M
275	83	W			SC	PN1M
118	62	S			SC	PN2M
15	88	W			SC	CH
330	52	W			SC	CHM
140	80	S			SC	MON
106	83	S			SC	RH
180	90				SC1	MON
150	60	W			SC2	MON
170	81	E			SF	RH
94	68	S	44		SF	RHLA

strike or dip	dip or plunge	dip dir planes	pitch	vergence	feature	location
80	27	N			SF	SRM
78	41	S			SF	SRM
94	40	S	164		SF	CFM
150	90				SF	SRM
232	85	W	16		SF?	CHM
214	66	E	160		SF?	CHM
50	88	W	177		SF?	CHM
65	75	S	169		SF?	CHM
100	73	N			SF?	SRM
60	78	E	170		SF?	SRM
150	36				SFL	SRM
340	?				SFM	SRM
110	?				SFM	SRM
107	44	N			SOA	RH
126	50	N			SOA	RH
98	38	S			SOA	PTC
102	50	N			SOA	RHS
114	39	N			SOA	RHS
120	57	N			SOA	RHLA
319	86	N			SOA	SR
277	7	N			SOA	SR
110	83	N			SOA	KGR
308	64	W			SOA	SC6M
333	73	W			SOA	SC6M
320	59	E			SOA	SC6M
342	27	W			SOA	PM
320	67	W			SOA	PN1M
273	49	W			SOA	PN1M
271	51	S			SOA	PN2M
160	70	S			SOA	CHM
130	79	N			SOA	CHM
146	48	W			SOA	CH
126	25	E			SOA	CH
187	67	W			SOA	CH
147	43	E			SOA	CH
141	40	W			SOA	CH
162	53	W			SOA	CH
20	77	E			SOA	CH
277	60	S			SOA	CH
258	69	S			SOA	CH
32	8	E			SOA	CHS
20	63	E			SOA	ES
340	53	E			SOA	CHM
125	19	N			SOA	ESM
257	34	N			SOA	MON
253	16	N			SOA	MON
118	88	N			SOA	ESS
127	49	N			SOA	ESS
115	65	S			SOA	ES
180	18	E			SOA	ES
92	33	S			SOA	PPH
140	70	S			SOA	CC
76	60	N			SOA	SR
37	55	N			SOA	SR
266	41	N			SOA	SR
310	44	W			SOA	SRE
280	37	N			SOA	PPH
110	40	N			SOA	STER
102	78	N			SOA	CHS
133	52	W			SOA	CHS
132	54	S			SOA	CHE
32	8	E			SOA	CHS
58	12	S			SOA	CHS
91	43	N			SOA	CHS
272	31	N			SOAA	MESA
325	26	S			SOAA	MESA'
111	28	S			SOAA	MESA
140	68	S			SOAA	CC
134	69	S			SOAA	CC
124	25	W			SOAA	CHS
150	70	W			SOAA	CH
292	57	W			SOAA	CHS
140	22	N			SOAAA	CHAR
124	58	W			SOAAA	SR

strike or dip	dip or plunge	dip dir plane:	pitch	vergence	feature	location
10	40	E			SOAAA	SR
113	39	S			SOAAA	SR
82	41	N			SOAAA	SR
113	28	N			SOAAA	SR
125	28	S			SOAAA	MESA
107	63	S			SOAAA	MCC
104	54	S			SOAAA	MCC
116	72	S			SOAAA	MCC
21	10	E			SOAAA	MCC
310	67	S			SOB	RH
295	70	S			SOB	RH
132	56	S			SOB	RH
295	63	S			SOB	RH
128	74	S			SOB	RH
116	89	S			SOB	RH
291	87	S			SOB	RH
136	60	S			SOB	RHS
270	66	S			SOB	RHS
102	48	S			SOB	MESA
102	46	S			SOB	MESA
96	63	S			SOB	RHLA
139	76	S			SOB	ES
324	69	W			SOB	ES
226	79	W			SOB	ES
314	79	W			SOB	ES
240	71	N			SOB	ES
156	90	W			SOB	ES
82	63	N			SOB	ES
314	79	W			SOB	ES
320	86	N			SOB	ES
292	76	N			SOB	ES
255	89	S			SOB	KM
300	75	S			SOB	SCS
296	90	S			SOB	ESS
291	49	S			SOB	ESS
304	79	N			SOB	ESS
140	88	S			SOB	CHAR
120	71	N			SOB	ESN
150	82	W			SOB	ESN
130	81	S			SOB	KGATE
157	76	S	148		SOB	KGATE
297	90	S			SOB	KGATE
59	77	W			SOB	KGATE
320	88	E			SOB	KGATE
172	47	W			SOB	SRM
27	48	W	3		SOB	SRM
43	77	S			SOB	SRM
134	30	E			SOB	CHS
147	81	N			SOB	CHS
285	50	N			SOB	CHS
165	68	S			SOB	CHS
140	70	S			SOB	SR
174	80	W			SOB	KGR
100	78	N	135		SOB	KGR
148	87	W			SOB	KGR
150	72	W			SOB	KGR
153	82	W			SOB	KGR
152	70	W	90		SOB	KGR
146	66	W			SOB	KGR
143	89	E			SOB	KGR
24	81	E			SOB	SKM
126	14	S			SOB	SKM
24	81	E			SOB	SKM
12	81	E			SOB	PM
40	59	S			SOB	PM
12	85	E			SOB	PM
150	64	S			SOB	ESWM
131	68	S			SOB	ESWM
136	55	S			SOB	ESWM
273	65	N			SOB	ESWM
100	70	N	177		SOB	ES
340	80	E			SOB	EOP
325	70	E			SOB	ES
102	50	S			SOB	PPB

strike or dip	dip or plunge	dip dir plane	pitch	vergence	feature	location
142	48	W			SOB	PPB
114	80	S	78		SOB	PPB
274	69	N			SOB	CH
148	72	S			SOB	CH
218	77	W			SOB	CH
100	53	N			SOB	CHS
148	57	N			SOB	CHS
135	85	E	117		SOB	CH
102	58	N	7		SOB	CH
140	82	S			SOB	CFM
121	78	S	157		SOB	ESG
180	73	W			SOB	ESG
100	85	E			SOB	RHUA
138	76	S			SOB	ESM
147	81	E			SOB	KGR
150	78	E			SOB	KGR
116	59	W			SOB	ESS
107	69	S			SOB	ESS
128	83	N			SOB	PPH
132	86	E			SOB	PPH
131	72	E			SOB	PPH
168	88	E			SOB	CC
144	85	W			SOB	SR
302	78	W			SOB	SRE
145	73	E			SOB	CHS
96	58	N			SOB	CHS
130	83	W			SOB	CHS
139	80	N			SOB	CH
346	32				STRETCH	GIM
341	28				STRETCH	GIM
320	19				STRETCH	GIM
136	32	E	90		VOLCF	RHS
100	51	S	140		VOLCF	RHS
106	31	N			VOLCF	RHS
348	36	E			VOLCF	RHS
122	41	S			VOLCF	RHS
182	76	W	72		VOLCF	ESM
162	60	W	63		VOLCF	ESM
334	90	W	90		VOLCF	ESM
320	76	E	65		VOLCF	ESM
104	78	N	117		VOLCF	ESM
50	31	W	2		VOLCF	ESM
109	76	N	81		VOLCF	ESM
129	79	N	147		VOLCF	ESM
14	90	W	167		VOLCF	ESM
142	64	N	3		VOLCF	ESM
110	68	S			VOLCF	ESM
315	69	W	85		VOLCF	ESM
94	64	S	50		VOLCF	ESM
67	41	W	162		VOLCF	ESM
351	51	W			VOLCF	ESM
40	86	W	75		VOLCF	ESM
66	57	S	40		VOLCF	ESM
133	63	N	55		VOLCF	ESM
360	75	W	62		VOLCF	ESM
198	30	E			VOLCF	ESM
162	16	W			VOLCF	ESM
54	?				VOLCFL	RHS
48	?				VOLCFL	RHS
204	?				VOLCFL	RHS
235	?				VOLCFL	ESM
250	?				VOLCFL	ESM
120	?				VOLCFL	ESM
242	?				VOLCFL	ESM

strike or dip dir	dip or plunge	dip dir plane on	pitch	vergence	feature	location
283	73	S			AS1	RH
288	82	S			AS1	RH
341	70	W			AS1	ES
300	58	S			AS2	RH
293	55	S			AS2	RH
140	68	S			AS2	RHS
128	64	S			AS2	RHS
145	71	S			AS2	ESN
343	86	W			AS3	RH
165	81	W			AS3	RHS
040	79	E			AS3	ES
216	90	W			AS3	ES
020	89	E			AS3	ES
200	83	W			AS3	ES
170	80	W			AS3	ES
077	83	S			AS3	ES
330	86	E			AS3	ES
030	88	W			AS3	ES
162	73	W			AS3	ESN
075	67	S			AS3	SRM
018	52	E			AS3	SRM
022	51	E			AS3	SRM
052	71	S			AS3	SRM
360	82	W			AS3	SRM
306	53	S			AS4	RH
243	71	W			AS4	RH
109	86	S			AS4	RHS
038	90	S			AS4	RHLA
357	66	E			AS4	RHLA
023	68	W			AS4	ES
160	39	W			AS4	ES
236	52	N			AS4	KGR
154	53	E			BZ	RH
147	69	S	86		D3NF	RHS
164	59	W			D3NF(OBL)	RHS
168	58	W			D3NF(OBL)	RHS
110	79	N			DF	RH
200	28	W			DF	RH
340	40	W	30		DF	RHLA
346	31	W			DF	RHLA
318	62	W			DF	KM
198	69	E	6		DF	ESS
190	55	E	13		DF	ESS
253	85				DFL	RH
305	27				DFL	RH
114	13				DFL	RHLA
265	50				F1	RH
275	34				F1	RH
338	21				F1	ES
284	10			S	F2	RH
293	20			S	F2	RH
119	9			S	F2	RHS
143	28			S	F2	RHS
155	51			S	F2	ESN
214	21				F2	SRM
180	78			S	F3	RH
189	78			N	F3	RHS
040	57			N	F3	ES
212	47			N	F3	ES
028	67			S	F3	ES
030	59			S	F3	ES
186	79			N	F3	ES
084	81			S	F3	ES
331	70			S	F3	ES
030	73			S	F3	ES
334	63			S	F3	ESN
238	10			E	F3	SRM
050	31				F3	SRM
203	23				F3	SRM
040	13				F3	SRM
360	15				F3	SRM
295	12			S	F4	RH
254	86			N	F4	RH
300	74			S	F4	RHS

strike or dip dir	dip or plunge	dip dir planes on	pitch	vergence	feature	location
204	14				F4	RHLA
174	30				F4	RHLA
323	68				F4	ES
298	34				F4	ES
328	50			W	F4	KGR
051	51	N			FB	CHS
020	52	E			FB	CHS
349	84	W			FB	CHS
094	26	N			FB	CHS
291	13				L02	RH
057	27				L02	ES
097	84				L02	ES
104	30				L02	ES
300	01				L02	ESS
318	36				L02	CHAR
108	20				L02	SR
233	?				L02	SRM
48	354				L02	CHS
152	36				L02	KGR
232	48				L02	KGR
168	60				L02	KGR
190	53				L02	KGR
110	27				L03	RH
294	8				L03	RH
323	46				L03	KGR
360	70				L2	SR
252	58	S			NF	RH
138	83	N			NF	FF
116	82	N	157		NF	FF
120	43	N	97		NF	FF
280	84	N			NF	SRM
175	57	E			PLF	CHS
350	75	W			PLF	CHS
131	63	E			PLF	CHS
080	84	S			PLF	CHS
120	76	E			PLF	CHS
164	81	E			PLF	CHS
110	79	N			QV	RH
170	66	E			QV	RH
335	29	N			QV	RH
345	58	W			QV	RH
042	65	N			QV	RH
215	68	W			QV	RH
155	29	W			QV	ES
012	43	W			QV	ES
084	9	N			QV	ES
018	43	W			QV	ES
163	37	W			QV	ESS
342	62	W			QV	ESS
189	69	W			QV	ESS
200	42	W			QV	ESS
205	55	W			QV	ESS
197	60	W			QV	ESS
196	86	E			QV	ESS
195	69	W			QV	ESS
200	90	W			QV	ESS
318	22	N			QV	KGATE
348	73	N			QV	KGATE
036	20	E			QV	KGATE
342	70	W			QV	CHS
228	57	S			QVSET	RH
034	60	W			QVSET	RHS
196	22	W			RF	RH
340	25	W			RF	RH
318	8	S			RF	RH
120	70	S	150		RF	RH
264	22	N			RF	RHLA
124	69	S	142		RF	ESP
144	36	S			RF	ES
230	22	S			RF	ESS
301	66	N			RF	SRM
100	56	S	110		RF	RHLA
030	16	S			RF(OBL)	RHLA
128	81	N	139		RF(OBL)	ESP

strike or dip dir	dip or plunge	dip dir planes on	pitch	vergence	feature	location
170	?				RFL	RH
125	?				RFL	RH
328	?				RFL	ESS
292	70	W			S0B	RH
122	54	S			S2	RH
060	83	N			S2	ES
124	88	N			S2	ES
280	76	N			S2	ES
300	70	S			S2	ESS
165	51	W			S2	CHAR
320	87	E			S2	ESN
105	69	S	28		S2	KGATE
132	79	S			S2	KGATE
163	88	S			S2	KGATE
120	86	S			S2	KGATE
163	66	W			S2	KGATE
300	72	N			S2	SR
006	74	W			S2	SRM
025	82	W			S2	SRM
271	54	N			S2	CHS
113	87	S			S2	SR
151	63	W			S2	KGR
075	90	S			S2	KGR
172	63	W			S2	KGR
180	68	W			S2	KGR
170	71	W			S2	KGR
114	70	S			S2	KGR
173	90	W			S2	KGR
178	77	W			S2	KGR
164	75	W			S2	KGR
114	80	N			S3	RH
120	48	S			S3	RH
058	70	E			S3	SRM
020	87	W			S3	SRM
172	89	E			S3	SR
183	56	W			S3	KGR
294	69	N			SC	SRM
286	53	N			SC	SRM
170	81	E			SF	RH
094	68	S	44		SF	RHLA
080	27	N			SF	SRM
078	41	S			SF	SRM
340	?				SFM	SRM
110	?				SFM	SRM
107	44	N			SOA	RH
126	50	N			SOA	RH
098	38	S			SOA	PTC
102	50	N			SOA	RHS
114	39	N			SOA	RHS
272	31	N			SOA	MESA
325	26	S			SOA	MESA
111	28	S			SOA	MESA
120	57	N			SOA	RHLA
319	86	N			SOA	SR
277	7	N			SOA	SR
110	83	N			SOA	KGR
310	67	S			SOB	RH
295	70	S			SOB	RH
132	56	S			SOB	RH
295	63	S			SOB	RH
128	74	S			SOB	RH
116	89	S			SOB	RH
291	87	S			SOB	RH
136	60	S			SOB	RHS
270	66	S			SOB	RHS
102	48	S			SOB	MESA
102	46	S			SOB	MESA
096	63	S			SOB	RHLA
139	76	S			SOB	ES
324	69	W			SOB	ES
226	79	W			SOB	ES
314	79	W			SOB	ES
240	71	N			SOB	ES
156	90	W			SOB	ES

strike or dip dir	dip or plunge	dip dir planes onl	pitch	vergence	feature	location
082	63	N			SOB	ES
314	79	W			SOB	ES
320	86	N			SOB	ES
292	76	N			SOB	ES
255	89	S			SOB	ES
300	75	S			SOB	KM
296	90	S			SOB	SC5
291	49	S			SOB	ESS
304	79	N			SOB	ESS
140	88	S			SOB	ESS
120	71	N			SOB	CHAR
150	82	W			SOB	ESN
130	81	S			SOB	ESN
157	76	S	148		SOB	KGATE
297	90	S			SOB	KGATE
059	77	W			SOB	KGATE
320	88	E			SOB	KGATE
172	47	W			SOB	KGATE
027	48	W	03		SOB	SRM
043	77	S			SOB	SRM
134	30	E			SOB	SRM
147	81	N			SOB	CHS
285	50	N			SOB	CHS
165	68	S			SOB	CHS
140	70	S			SOB	CHS
174	80	W			SOB	SR
100	78	N	135		SOB	KGR
148	87	W			SOB	KGR
150	72	W			SOB	KGR
153	82	W			SOB	KGR
152	70	W	90		SOB	KGR
146	66	W			SOB	KGR
143	89	E			SOB	KGR
136	32	E	90		VOLCF	RHS
100	51	S	140		VOLCF	RHS
106	31	N			VOLCF	RHS
348	36	E			VOLCF	RHS
122	41	S			VOLCF	RHS
182	76	W	72		VOLCF	ESP
162	60	W	63		VOLCF	ESP
334	90	W	90		VOLCF	ESP
320	76	E	65		VOLCF	ESP
104	78	N	117		VOLCF	ESP
050	31	W	02		VOLCF	ESP
109	76	N	81		VOLCF	ESP
129	79	N	147		VOLCF	ESP
014	90	W	167		VOLCF	ESP
142	64	N	3		VOLCF	ESP
110	68	S			VOLCF	ESP
315	69	W	85		VOLCF	ESP
094	64	S	50		VOLCF	ESP
067	41	W	162		VOLCF	ESP
351	51	W			VOLCF	ESP
040	86	W	75		VOLCF	ESP
066	57	S	40		VOLCF	ESP
133	63	N	55		VOLCF	ESP
360	75	W	62		VOLCF	ESP
198	30	E			VOLCF	ESP
162	16	W			VOLCF	ESP
054	?				VOLCFL	RHS
048	?				VOLCFL	RHS
204	?				VOLCFL	RHS
235	?				VOLCFL	ESP
250	?				VOLCFL	ESP
120	?				VOLCFL	ESP
242	?				VOLCFL	ESP

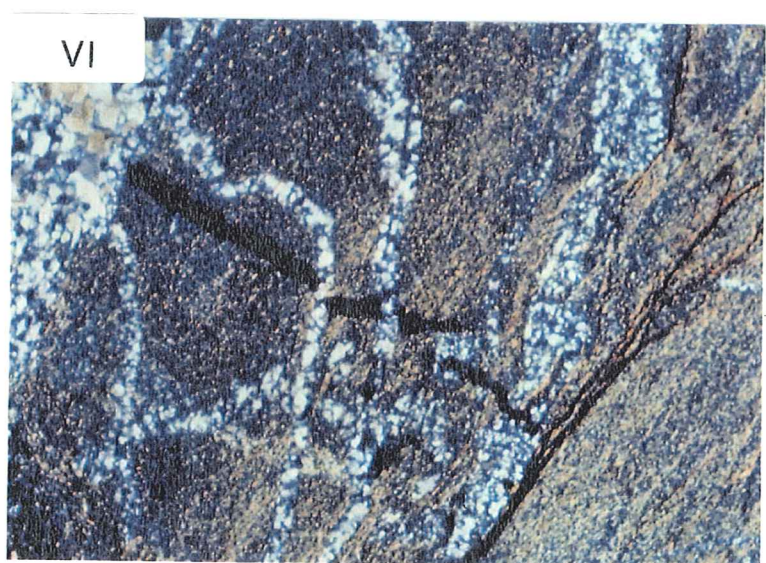
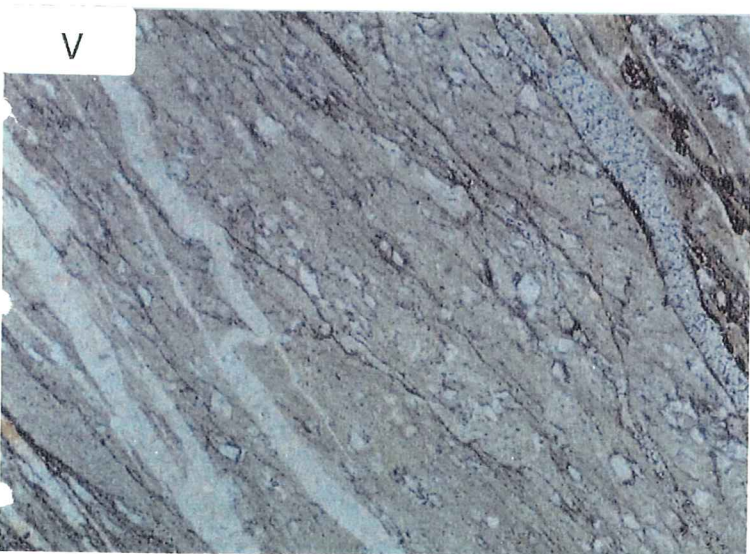
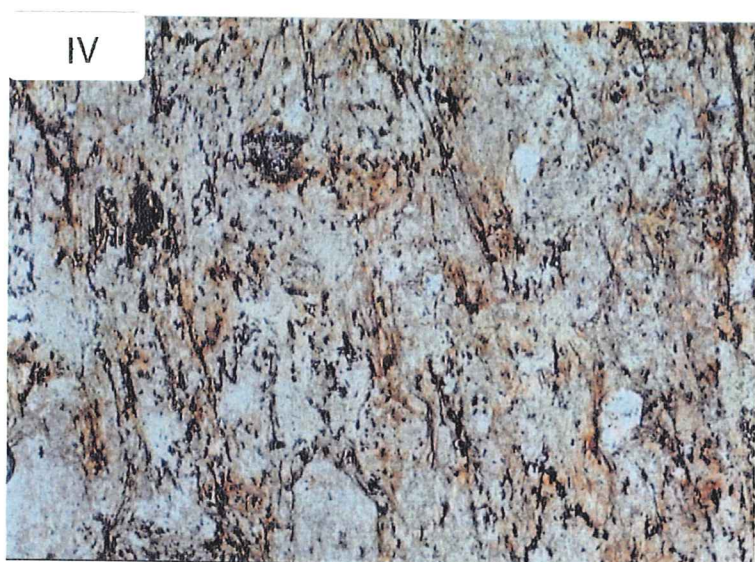
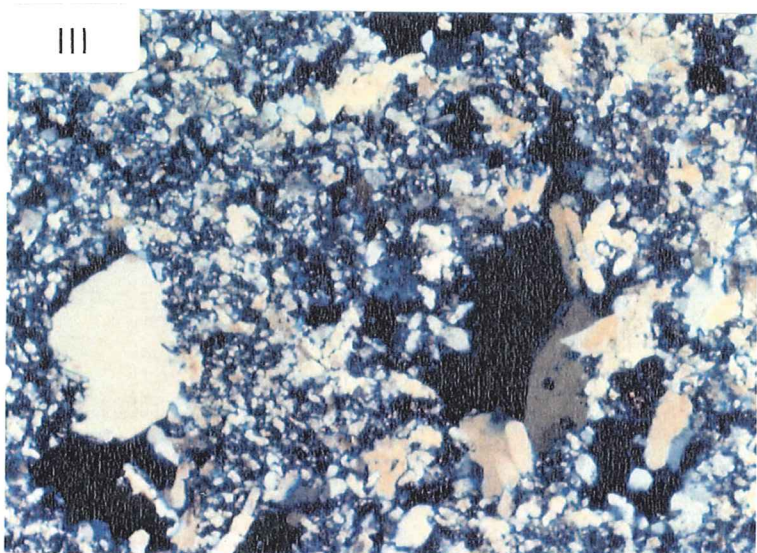
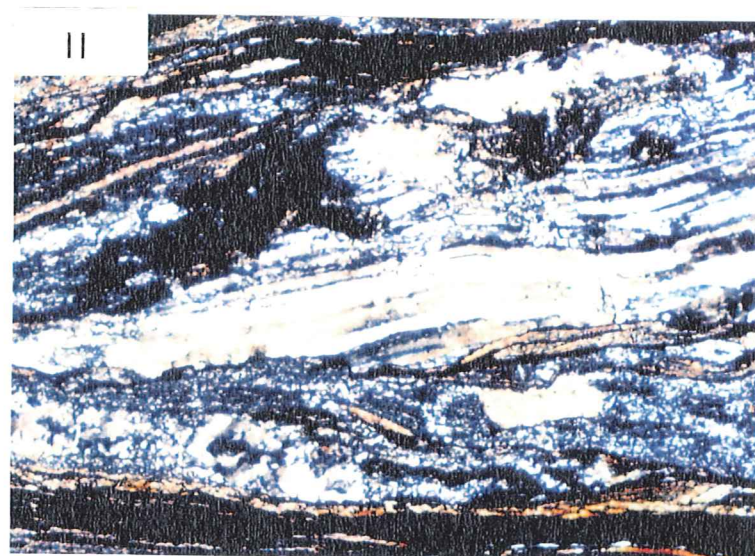
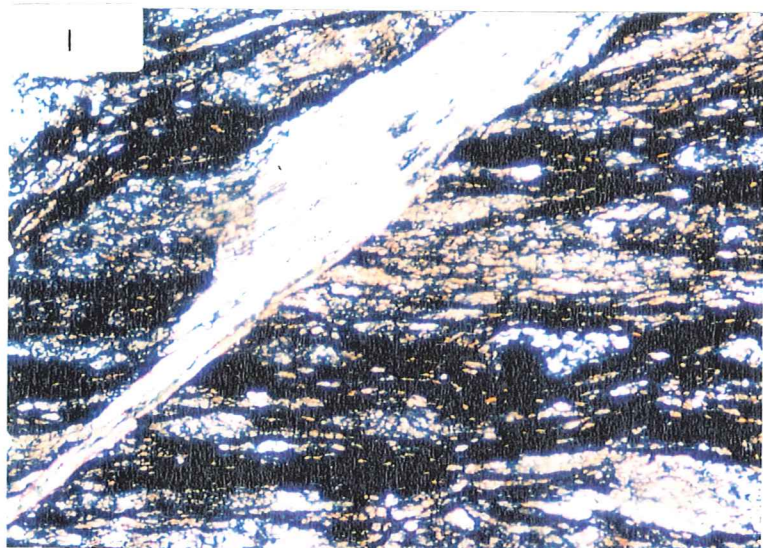
**APPENDIX III: SELECTED THIN SECTION
DESCRIPTIONS**

Sample number	: 8712044
Photo reference	: M13/54/5
Formation	: Koolpin Formation from O'Dwyers mullock heap
Hand Specimen	: carbonaceous shale
Thin section	: a fine grained carbonaceous shale with 2 cleavages and strong quartz (\pm sericite) veining. The rock is composed of carbonaceous material, quartz, chlorite and muscovite. Bedding is defined by a single cherty layer, and the main cleavage is at approximately 20° to bedding. Quartz veins are generally at a high angle to cleavage and appear to be partly post-cleavage, though quartz veins are displaced by thicker and more widely spaced dark cleavage seams. Compound breccia veins occur in places.
Comments	: Collected as a sample of "typical" Koolpin formation below the oxidized zone. This sample shows that carbonaceous Koolpin formation is intensely deformed, possibly due in part to the ductile nature of this rock type.
Photomicrograph ref.	:
Sample number	: 8712045
Photo reference	: S1/34/22b
Formation	: Koolpin Formation from Palette mullock heap
Hand Specimen	: A well foliated, highly strained and folded, banded carbonaceous-quartzose rock.
Thin section	: the specimen is made up of elongate quartz-sericite pods separated by highly carbonaceous domains. The pods are sometimes isoclinally folded and cut by deformed quartz-sericite veins. Stepped microfractures show highly fibrous quartz-sericite infill on oversteps.
Comments	: Collected as a sample of "typical" Koolpin formation below the oxidized zone, similar to the previous sample. This sample is slightly more quartz-rich, but still shows evidence of intense strain.
Photomicrograph ref.	: Figure 8b, plate I (10x, P.P)
Sample number	: 8712046
Photo reference	: S1/34/22c
Formation	: Koolpin Formation from Palette lower adit, near the Koolpin/Coronation Sandstone contact.
Hand Specimen	: A banded carbonate-quartz rock with angular quartz breccia clasts, cut by a convolute (~1-2mm) sericite seam.
Thin section	: the specimen is made up of rotated clasts and pods of: a) massive quartz-sericite; b) banded quartz-sericite; c) partially recrystallized quartz vein material; d) well-foliated highly sericitic material; and e) "cherty" quartz. The foliation, defined by sericite and carbonaceous material, is polyclinally folded. The foliation within clasts is often rotated with respect to the external foliation.
Comments	: This sample is interpreted as a multiply veined and brecciated highly strained rock, showing that the "unconformity" in this area is a zone of intense deformation.
Photomicrograph ref.	:
Sample number	: 8712047
Photo reference	: M13/55/22b
Formation	: Mixed Koolpin Formation and Coronation Sandstone from Rockhole lower adit, near the Koolpin/Coronation Sandstone contact.
Hand Specimen	: Dark graphitic fault gouge – brecciated and veined. Bedding is recognizable and rotated in clasts, absent in matrix.
Thin section	: A highly strained rock made up of sericite and carbonaceous material with small cherty nodules and rotated clasts separated by carbonaceous seams and vein zones, folded and cut by multiple generations of quartz veins. Veins are usually subperpendicular to, and cross cut the foliation. At the same time, some quartz veins terminate against thicker cleavage seams. Minor sulphides (mainly pyrite) are present in some veins.
Comments	: This sample was collected from a shallower-dipping portion of the Rockhole Fault, but failed to show significant Uranium mineralization.

- Structures developed within the sample show a progression from early ductile high strain to later cataclasis and penetrative veining, suggesting that the Rockhole Fault in this area was a relatively long-lived feature.
- Photomicrograph ref. :
- Sample number : 8712048
 Photo reference : S3/11/21g
 Formation : Koolpin Formation from Coronation Hill Uranium pit.
 Hand Specimen : A pale grey weakly foliated sericitic rock with multiple generations of quartz veining.
 Thin section : Sericite is the dominant mineral in this sample. There is no carbonaceous material present. There is a strong foliation defined by the preferred orientation of sericite, and this foliation is folded in places. The sample is cut by quartz veins which are strongly folded and/or boudinaged in places.
 Comments : This sample was taken from a lens of probable Koolpin Formation occurring within a fault zone on the east wall of the Coronation Hill Uranium pit. It is much less carbonaceous than other Koolpin Formation samples, though the intensity of deformation is similar.
- Photomicrograph ref. :
- Sample number : 8712049
 Photo reference : S3/11/21i
 Formation : ?
 Hand Specimen : Green tuffaceous siltstone.
 Thin section : a well-foliated high strain sericite-chlorite rock with strong (patchy) red staining. Quartz-rich lenses are common, with very long fibres subparallel to the foliation.
 Comments : This sample shows a strong ductile foliation similar to those seen in samples of Koolpin Formation.
- Photomicrograph ref. : Plate II
- Sample number : 8712050
 Photo reference : M13/55/22g
 Formation : altered Koolpin Formation from near the Rockhole Fault, Rockhole lower adit.
 Hand Specimen : Coarse-grained pyrite with ≤ 1 cm clasts of subangular quartz.
 Thin section : The sample consists of subhedral to euhedral pyrite overgrowing sutured but detrital-looking quartz.
 Comments : The sample is either quartz-rich Koolpin Formation or Coronation Sandstone. In either case, the strong pyrite alteration is probably associated with the Rockhole Fault.
- Photomicrograph ref. :
- Sample number : 8712088
 Photo reference : M13/55/19
 Formation : Coronation Sandstone volcanic, south of Rockhole area.
 Hand Specimen : Fragmental volcanic rock.
 Thin section : the specimen is made up of abundant euhedral quartz phenocrysts in a strongly ferroan matrix. Other phenocrysts include chlorite after feldspar, and chert after igneous quartz. The matrix is sericitic in places, and also contains irregular areas of silicification.
 Comments : This sample was taken from just above the Koolpin/Coronation Sandstone unconformity.
- Photomicrograph ref. :
- Sample number : 87120090
 Photo reference : S2/84/7
 Formation : Koolpin Formation, north of Pul Pul bioherm.
 Hand Specimen : highly silicified and veined rock of unknown origin (dolomite?).
 Thin section : The sample is a highly siliceous rock with a regular dusting of fine opaque material. Quartz varies in grain size from ≤ 5 cm to fine grained and cherty.

Comments	Quartz occurs in both fibrous and equigranular habits, both as replacement and open space precipitation into cavities. : The common association in this area between rocks of this type and dolomite suggests that this is a cap overlying dolomitic rocks at depth. This is supported by the occurrence of dolomitic Koolpin Formation immediately to the south.
Photomicrograph ref.	: Plate III (10x, X.P.)
<u>Sample number</u>	: 87120091
Photo reference	: S1/34/19e
Formation	: Coronation Sandstone volcanic, Scinto VI.
Hand Specimen	: Fine grained veined purple volcanic rock.
Thin section	: The sample consists of a fine grained hematitic matrix with clay-altered, lath-shaped partially-resorbed opaque phenocrysts. Quartz phenocrysts ($\leq 3\text{mm}$) are highly sutured, recrystallized and fractured.
Comments	: This rock is highly altered to iron oxides, but relict phenocrysts are visible, confirming a volcanic origin.
Photomicrograph ref.	:
<u>Sample number</u>	: 87120093
Photo reference	: S1/33/16b
Formation	: Coronation Sandstone volcanic, below Monolith sandstone lens.
Hand Specimen	: Fine grained veined purple volcanic rock.
Thin section	: This rock is made up of a clay-altered chert-sericite matrix with abundant subhedral phenocrysts of quartz and K-feldspar. Quartz crystals are sometimes embayed. The sample contains dark areas caused by a dusting of a fine black prismatic opaque mineral.
Comments	: As in the previous sample, this rock is highly altered to iron oxides, but relict phenocrysts are visible, confirming a volcanic origin.
Photomicrograph ref.	:
<u>Sample number</u>	: 87120094
Photo reference	: S3/11/21h
Formation	: ?Coronation Sandstone, Coronation Hill Uranium pit.
Hand Specimen	: Green tuffaceous siltstone with abundant graphitic shale fragments.
Thin section	: This rock is a siltstone with abundant quartz grains, abundant slivers of carbonaceous shale, and minor sericitic fragments. Carbonaceous fragments are undeformed, show a weak preferred dimensional orientation parallel to bedding, and tend to occur in layers. The matrix is mainly fine grained quartz, with very little chlorite.
Comments	: The bedded and undeformed nature of the carbonaceous fragments in this sample suggests that the rock is a post-unconformity sediment, rather than a fault rock with mixed Koolpin-Coronation Sandstone lithologies. The sample does not contain the intense cleavage displayed by some other green tuffaceous siltstone samples.
Photomicrograph ref.	:
<u>Sample number</u>	: 87120095
Photo reference	: S3/11/21d
Formation	: ?; Coronation Hill Uranium pit.
Hand Specimen	: Veined and foliated green tuffaceous siltstone next to fault zone.
Thin section	: The sample is a quartz-chlorite-biotite rock with a well-developed anastomosing foliation defined by biotite seams. There is a fine dusting of hematite throughout the sample. The main foliation is quite variable in orientation, and it is difficult to pinpoint a single earlier foliation. Veins consist of equigranular recrystallized quartz. The veins are cross-cut and are deformed by the cleavage, suggesting that they are partly syn-cleavage. The foliation bends around ~equant rounded cherty domains, possibly original nodules.
Comments	: This rock is an example of multiply deformed green tuffaceous siltstone occurring in the Coronation Hill area. The presence of one or more strong

	foliations as well as deformed veins suggests that this rock is pre-El Sherana Group.
Photomicrograph ref.	: Plate IV (4x, X.P.)
<u>Sample number</u>	: 87120099
Photo reference	: S2/88/21A
Formation	: Scinto Breccia.
Hand Specimen	: Hematitic breccia showing numerous episodes of veining.
Thin section	: The sample is made up of red and clear angular veined clasts cut by large (≤ 1 cm) quartz vein networks. Minor sericite is present in the veins as well. Quartz grains increase in size toward vein centers. Multiple episodes of veining are indicated by cross-cutting relationships, and the presence of early folded veins.
Comments	: The presence of folded quartz veins indicates that veining in this sample is not simply related to post-deformation weathering processes. This lends support to the idea that some occurrences of Scinto Breccia are associated with fault zones.
Photomicrograph ref.	:
<u>Sample number</u>	: 87120100
Photo reference	: S2/87/6A
Formation	: Koolpin.
Hand Specimen	: Strongly veined gray layered siltstone, with veins parallel and perpendicular to the main foliation.
Thin section	: This rock consists mainly of sericite and minor quartz. There is a strong foliation, defined by the preferred orientation of sericite. Quartz veins parallel are relatively undeformed, while those perpendicular to the foliation are strongly folded. Dissolution seams are well-developed in the sample, and veins are often rotated parallel to the foliation in sericite-rich zones of volume loss.
Comments	: This rock occurs near the pre-El Sherana Group fault which separates Koolpin Formation from Kapalga Formation. While this rock shows evidence of high strain, it does not appear to be a true mylonite. No sense of shear indicators were noted.
Photomicrograph ref.	: Plate V (4x P.P.), Plate VI (4x, X.P.)
<u>Sample number</u>	: 87120101
Photo reference	: S2/87/6B
Formation	: Koolpin.
Hand Specimen	: see 87120100.
Thin section	: This sample is similar to 87120100, except for the occurrence of extensional shear bands confirming the dextral sense of shear observed in outcrop..
Comments	:
Photomicrograph ref.	:



APPENDIX IV: ALTERATION TYPES



* R 9 1 1 0 7 1 7 *

Four general alteration types have been recognised. Types I and II occur mainly associated with mineralization, while types III and IV are more regional in extent. It should be stressed that this alteration scheme is based on weathered surface or near surface exposures and as such should be considered only as a rough guideline for possible future subsurface and core studies. This scheme is most easily applied to volcanics (and to a lesser extent sandstone) of the El Sherana Group. Rocks of the Koolpin Formation do not appear to show significant visible alteration effects, aside from surface bleaching of carbonaceous lithologies. The widespread nature of visible alteration in rocks of the El Sherana Group would suggest that rocks of the Koolpin Formation have been altered, but this alteration may be cryptic or visible only in thin section.

Type I

Type I alteration occurs associated with mainly primary U and Au mineralization at Rockhole, El Sherana and Coronation Hill. It is distinguished by the penetrative alteration of original volcanic rocks to buff or white chalky clay-rich lithologies. Mineralogy at the surface appears to be mainly clay minerals, although at depth there may be a significant chlorite component. Quartz phenocrysts are commonly preserved even in areas of most intense alteration. Type I alteration is spatially associated with faults though affected areas are large in the case of Coronation Hill, El Sherana, Palette and Rockhole.

Type II

Type II alteration is associated with both primary and secondary mineralization, and is the more widespread of the two mineralization-associated alteration types. Rocks of this alteration type commonly show a distinctive pea green colour, though buff colours occur as well. Altered volcanics of this type generally display partial sericitization of the groundmass as well as complete sericitization of feldspar phenocrysts. Quartz phenocrysts are generally unaffected. Altered sandstones show a framework of sericitized feldspar and rock fragments in a fine grained green sericitic matrix.

Type III

Type III alteration takes the form of patchy (commonly circular patches) sericitization of volcanics and arkosic sandstones. Alteration ranges in intensity from a few isolated patches to pervasive sericitization, commonly associated with fractures. Areas of intense type III alteration commonly display symmetrical zoning into weakly altered to unaltered rocks, with the transition zone defined by gradual coalescence of sericitic patches. This alteration type shows no spatial association with mineralization, and is distinguished from type II alteration by its distribution and generally non-penetrative nature. The obvious mineralogical similarities between types II and III suggest a genetic or temporal link between the two.

Type IV

Type IV is the most widespread and penetrative of the alteration types. It generally takes the form of intense fracture-controlled hematite and/or hematite-carbonate alteration, giving the affected rock a brick-red colour. Alteration of this type is generally overprinted by the other three alteration types, though in some cases it is clear that some hematite alteration is a late surface feature.

Structure and Mineralization In the Mundogie
and Eastern Stow areas, Kakadu Stage III,
N.T.

R. K. Valenta

June, 1990

Table of Contents

Summary.....	2
Objectives.....	2
Scope.....	2
Conclusions.....	2
Structure of the Mundogie Area.....	3
Previous Work.....	3
Structural Elements.....	4
Area 1.....	4
Area 2.....	7
Area 3.....	7
Area 4.....	8
Area 5.....	8
Area 6,7.....	8
Area 8.....	9
Area 9.....	9
Summary.....	10
Interpretation.....	11
<i>Comparison with the South Alligator Valley</i>	12
Mineralization.....	12
The Malone Creek Granite Area.....	13
Mineralization.....	14
3/171.....	15
Zamu.....	15
Discussion.....	15
Conclusions.....	16
Recommendations.....	17
Acknowledgements.....	18
References.....	18

Summary

Objectives

The objective of field study in 1989 was to assess the structural setting and mineralization potential of outlying areas in the Kakadu Stage III conservation zone. These areas consisted mainly of the Mundogie region to the west of Rockhole, and the portion of the Stow sheet to the east of Coronation Hill. These areas were examined in light of the structural model for U-Au-PGE mineralization developed based on experience in the South Alligator Valley. In addition, other types of mineralization were examined in order to determine their structural timing, structural setting, and lithological controls.

Scope

Data presented in this report were mainly collected during the 1989 field season, though many interpretations have built on previous investigations in the area (Valenta....). A general reconnaissance of the Mundogie area was carried out, and selected areas were remapped in more detail. These areas included the zone extending from Shovel Billabong to Rockhole, the Coirwong Gorge area and an area of apparent folded thrusts approximately 10 kilometres southwest of anomaly 5C. On the Stow sheet, traverses were carried out in areas to the north and east of the Malone Creek Granite. Detailed examination of selected minor deposits and prospects was carried out as well. These included anomaly 2J, Minglo, Namoon, Zamu and anomaly 3/171. Regional sampling of quartz fault fill was carried out for possible regional stable isotope study.

Conclusions

1) Late faults in the South Alligator Valley region are laterally continuous with fault repeats of stratigraphy in the Mundogie area. Faults are generally poorly exposed, so in many cases it is difficult to determine their geometry and timing. Isolated exposures of early high strain zones suggest that at least some of these faults may be early thrusts.

2) There is some evidence for reactivation of early high strain zones during later brittle faulting.

3) Early thrust faults are clearly folded in some areas, and appear to show complicated subsurface geometries. These subsurface geometries may have important implications for the localization of U-Au-PGE deposits.

4) Interpreted large scale thrust geometries show a ramping and change in style from southeast to northwest. In the northwest, the main detachment is below the Mundogie Sandstone and there are multiple thrust repeats of the Gerowie Tuff - Shovel Billabong Andesite - Koolpin Formation sequence. Further to the southeast, the Gerowie Tuff is absent and there do not appear to be thrust repeats of the Mundogie Sandstone.

5) The general lack of evidence of significant Uranium deposits in the Mundogie area provides at least partial confirmation of the crucial role played by the unconformity surface in Uranium localization. It is, however, possible to predict favourable structural geometries and host rock distributions in basement-only settings.

6) Field observations show that deformation and veining were synchronous in the contact aureole of the Cullen granite. This may have important implications for potential thermal aureole type gold mineralization.

7) Lead mineralization in the Namoon area occurs on northwest-trending fractures which, from their relationships to folds and cleavage, appear to have formed relatively early in the deformation history.

Structure of the Mundogie Area

Previous Work

Studies of the structure of the Mundogie region have been carried out by the Bureau of Mineral Resources and by Nisbet, Johnston and Davies of Monash University. Johnston (1983) recognized three main sets of structures:

- 1) D₁ structures take the form of a locally developed bedding perpendicular foliation.

2) D₂ structures take the form of foliations and isoclinal folds developed in bedding-parallel high strain zones.

3) D₃ structures take the form of upright north- to northwest-trending folds and associated cleavage.

Johnston described a major bedding-parallel high strain zone near the top of the Wildman Siltstone. This high strain zone is folded and cuts up and down section from area to area. The area is also thought to contain southwest-verging thrusts and reverse faults.

Structural Elements

Bedding strikes northwest in most parts of the Mundogie sheet within the Conservation Zone. Rock types which contain phyllosilicates often display a bedding-parallel fabric which can be correlated with the S₂ fabric of Johnston (1983). Mineral lineations associated with the bedding-parallel fabric are rare, and are generally downdip where they are developed. The early cleavage recognized as S₁ by Johnston (1983) was not recognized in the course of this study. Northwest-trending folds with shallow southeast or northwest-trending plunges are common. Fold axes tend to be steeper in areas of more intense strain, typified by intense foliation development and tight to isoclinal fold axes. Northwest-trending folds are refolded in one area by northeast-trending folds and a non-penetrative crenulation cleavage. In the Shovel Billabong-South Alligator Valley area there are a series of repeats of consistently-younging stratigraphic packages. The actual contacts between these packages are poorly exposed, and they could have two possible geometries: a) high angle reverse faults or b) folded low angle thrusts.

The areas of the Mundogie sheet which were studied as part of this project are shown in figure 1. Each area was studied because of its critical stratigraphic, structural or mineralization features.

Area 1

This area is the northwest continuation of the belt of lower to mid-Proterozoic rocks exposed in the South Alligator Valley. The Rockhole-Palette and South Alligator Faults are traceable up to the southeast corner of the Mundogie sheet, but past this point their nature is not clear. This is also a useful area to study the structural and stratigraphic setting of the Shovel Billabong Andesite and the Gerowie Tuff, both of which are stratigraphically above the Koolpin

Formation. The general stratigraphy of rock units in this area is schematically shown in figure 2. In this figure, it can be seen that the Koolpin Formation outcropping in the Rockhole area continues as a belt into area 1, thickening into a zone of shallow to moderate plunging tight to isoclinal folds at the northwest end of the area. Stratigraphically above this belt there is a zone made up of elongate pods of Gerowie Tuff, Shovel Billabong Andesite and Koolpin Formation surrounded by Zamu dolerite. There is a large lateral variation in the thickness of Zamu dolerite in this zone, and it is thickest in a zone immediately to the southeast of the Kakadu highway.

Outcrop of Koolpin formation, Shovel Billabong Andesite and Gerowie Tuff in *area 1* is discontinuous due to intrusion of Zamu dolerite and alluvial cover. Thus, in this area it is necessary to build up a complete stratigraphy of this interval using sets of incomplete exposures from geographically separated areas. From continuous exposures of the lower contact between the Koolpin Formation and the Mundogie Sandstone, it is possible to build up the following consistent stratigraphy of the lower part of the Koolpin Formation:

- siltstone
- cherty banded iron formation, with .5 to 2cm bands ($k \leq 20000 \times 10^{-6}$)
- thick-bedded (>2cm) cherty banded iron formation, grading at times into nodular banded iron formation.
- Shovel Billabong Andesite (chloritic, deeply weathered volcanic)
- thin-bedded (<.5cm) cherty banded iron formation
- red siltstone
- thick-bedded (>2cm) cherty banded iron formation ($k \leq 80000 \times 10^{-6}$)

A series of exposures at the upper contact between Koolpin Formation and Gerowie Tuff show the following sequence:

- Gerowie Tuff
- moderately bedded (.5-2cm) cherty banded iron formation (high susceptibility)
- thick-bedded cherty banded iron formation
- Shovel Billabong Andesite

From these two sets of observations, it would appear that it is possible to recognize a complete stratigraphy from Koolpin Formation to Gerowie Tuff. In the first case above, the occurrence of rocks mapped as red siltstone may be due to alteration of original Gerowie Tuff. Recognition of a complete internal stratigraphy in the Koolpin Formation is critical for interpretation of structural patterns in this area. It should be noted that there are lateral variations from bedded BIF to nodular BIF. These variations appear to predate deformation, since both bedded and banded rock types are overprinted by deformation features such as folds, bedding-parallel fabrics and cross-cutting fabrics. In some areas, the Koolpin Formation is strongly siliceous, with patchy limonite and variably developed banding. Rocks of this type are often breccias in which rotated and vein-infilled bedding can be seen, suggesting that veining and silicification are associated with alteration during movement on faults.

There are a series of repeats of the Koolpin-Shovel Billabong-Gerowie sequence to the northeast of the first belt of Gerowie Tuff. In each case, the stratigraphy in the Koolpin-Gerowie contact region suggests that the repeats are consistently northeast-facing. This suggests that stratigraphic repeats in this area are thrust-related, rather than being the result of folding. The detailed geometry of this area is shown in figure 3, in which a series of small scale thrust repeats which cut up and down section along strike can be seen. The northernmost exposure of Gerowie Tuff in this area defines a southeast-plunging syncline. In one area in the northern limb, a southwest-dipping thrust repeat can be seen, suggesting that the thrusts are folded by the main northwest-trending fold generation.

The continuation of the Rockhole Fault can be projected along the contact between; a) the main ridge of Koolpin Formation, which is continuous with the belt Koolpin Formation in the Rockhole area, and b) the belt made up of pods of Koolpin Formation, Shovel Billabong Andesite, and Gerowie Tuff. This contact does not correspond to any of the inferred thrusts outlined above. In general, this contact is poorly exposed, and no outcrops of cataclasite or fault-related "quartz-blows" have been identified. Layering is variable but generally steeply-dipping in this zone, so the continuation of the Rockhole Fault may simply be a late reactivation of the contact between these two stratigraphic packages. The South Alligator Fault is also difficult to recognize in this area, but it is continuous with a major fault zone in the Coirwong Gorge area (*area 3*, see below).

On a large scale, this area can be interpreted as a series of thrust repeats of the Koolpin-Gerowie sequence which are folded by northwest-trending F_2 folds. This indicates that the thrusts are associated with D_1 . No clear movement lineations were found, but northeast over

southwest movement can be inferred from the fact that, on a large scale, the metamorphic grade of rocks in this part of the Pine Creek Geosyncline increases to the northeast (Needham et al, 1989).

Area 2

In this area, reconnaissance field checking was carried out in order to determine the stratigraphic and structural relationship between two linear belts of Gerowie Tuff (fig 1). The northeastern belt of Gerowie Tuff (fig 1) dips shallowly northeast and is overlain and underlain by Koolpin Formation. The belt is truncated to the northwest by a northeast-trending fault. A syncline in the Koolpin Formation separates this belt of Gerowie Tuff from the region of Mundogie Sandstone which makes up the Mundogie Inlier. The occurrence of Shovel Billabong Andesite in places on the southwest side of this belt suggests that the Gerowie Tuff is right-way up in this area, and the Koolpin Formation on the northeast side of the belt has been thrust over the belt and is continuous with the inferred overthrust at this stratigraphic level in area 1 (fig 1). The fact that this belt is laterally continuous with a northeast-facing belt of Gerowie Tuff to the southeast also supports this interpretation. A schematic cross-sectional interpretation of this area is shown in figure 4, in which it can be seen that the Gerowie Tuff is interpreted to form an asymmetric anticline-syncline pair. A pinchout of the Gerowie Tuff in section in the area to the southwest of the Mundogie Inlier (fig 4) is necessary in order to explain the lack of Gerowie Tuff in this area, and the pinchout of the belt of Gerowie Tuff to the northwest.

Area 3

Coirwong Gorge was chosen as an area of study because of the multiple repeats of the Mundogie Sandstone mapped in this area. The interpreted cross-sectional geometry of this area is schematically shown in figure 5. The northernmost thrust sheet is continuous with the belt of Mundogie Sandstone and Koolpin Formation extending northwest from the South Alligator Valley (fig 1). The detachment for this sheet is near the top of the Masson Formation. To the south of this sheet, there is a repeat of the Namoon to Masson sequence which is, in turn, thrust over masson, Mundogie and Wildman Siltstone. The restricted northwest and southeast extent of the central thrust sheet suggests that it is limited in vertical extent as well. It has therefore been interpreted as a minor duplex associated with the main thrust in this area (fig 5). Once again, in this area the actual fault surfaces are not exposed, so it is difficult to determine orientations and movement directions. The major thrust interpreted in this area is directly along strike with the

South Alligator Fault, suggesting that the South Alligator Fault could be a later reactivation of this zone.

Area 4

In this area (fig 1), there is an extremely irregular contact between Stag Creek Volcanics/Mundogie Sandstone to the northeast and Wildman Siltstone to the southwest. The Stag Creek/Mundogie side of the contact is part of an upward-facing sequence which extends upwards into the Gerowie Tuff. This suggests that the juxtaposition of Stag Creek Volcanics on Wildman Siltstone is a thrust or reverse fault contact. The contact between these two rock units appears to be folded into a series of anticlines and synclines with unknown fold axes and northeast-striking axial surfaces (fig 1). In hinge regions in which the fault strikes northwest, bedding on both sides of the fault contact is steep, and, in some areas on the southwest side of the fault, bedding is overturned. In some cases, bedding strikes at a high angle to the fault contact. Fold axes vary from subvertical to steep southwest-plunging on the southwest side of the fault. All of these features indicate that the fault is steep in hinge regions, but they appear to be zones of complex deformation possibly postdating the original thrust surface. In limb regions, bedding in the Wildman Siltstone appears to dip under the Stag Creek Volcanics, suggesting a simpler thrust geometry. The fault can be inferred to predate the northeast-trending folds on the basis of: a) large scale map geometry; and b) overprinting of fault breccias by northeast-striking cleavages. The large scale outcrop pattern to the northeast of this area suggests that the northeast trending folds have refolded northwest-trending folds, producing doubly-plunging basins of Gerowie Tuff.

Area 5

Area 5 was briefly visited for reconnaissance sampling of a zone of intense quartz veining within the Mundogie Sandstone. Veining in this area occurs in northwest-striking subvertical ridges. The common occurrence of intense veining within the Mundogie Sandstone may simply be a result of competency contrast between sandstone and surrounding phyllosilicate-rich rocks.

Areas 6, 7

Both of these areas form part of a northwest-striking vein zone which is over 10km in extent and contains numerous small deposits of at least partly vein-hosted lead mineralization. In costean exposures at Namoonna, it can be seen that quartz veins associated with mineralization are

parallel or at a small angle to the main northwest-trending subvertical cleavage (S_2). In one costean, it can be seen that there are two roughly coaxial northwest-trending fold/cleavage generations. Many of the veins associated with mineralization are at least partly deformed in S_2 , suggesting that the veins formed during D_2 . This is in contrast to U-Au-PGE mineralization in the South Alligator Valley, where it can be inferred that mineralization formed much later in the deformation/sedimentation history (eg Valenta, 1989).

Area 8

This area was studied in order to obtain more information on the nature of the Minglo lead deposit, and to assess the geological setting of the aureole of the Cullen Granite. The geology of the Minglo deposit is discussed in more detail in the mineralization section. In this area, some portions of the Wildman Siltstone are made up of porphyroblasts of ?andesite in a highly graphitic matrix (fig 6). The schists contain two foliations, and the andalusite porphyroblasts are overprinted by the latest of these. This indicates that cleavage formation was occurring during thermal metamorphism associated with emplacement of the Cullen Granite.

Area 9

A traverse was undertaken in this area in order to examine the structural and metamorphic setting of the Cullen Granite and to examine the nature of the Koolpin-Namoonna contact in this area. The Koolpin Formation in this area is strongly brecciated and silicified. Ridges of Koolpin Formation are made up of an interlocking network of fractured and silicified rock fragments, and sometimes it is possible to see an irregularly spaced layering which is vein-like, rather than bedding-like. The presence of patchy limonite staining suggests the presence of sulphides at depth. Breccias associated with this rock type are generally matrix-poor and structurally localized. This rock type can be interpreted as a silicified fault rock associated with a northwest-trending fault zone. This is consistent with the occurrence of a "triple point" contact between Koolpin Formation, Gerowie Tuff and Masson Formation. In areas of Masson Formation closer to the Cullen Granite, it is again possible to see porphyroblasts of weathered and retrogressed ?biotite and ?cordierite which appear to be at least partially overprinted by a northwest-trending foliation. In this area, the granite itself is virtually unfoliated, suggesting a complex and possibly long-lived history of emplacement, thermal metamorphism and associated deformation.

Summary

The observations made in the areas described above can be used to build up a consistent interpretation of the structural history and area scale geometry of the northwest portion of the Stage III Conservation Zone. The large scale cross section interpretation for the area is shown in figure 7. The key structural observations for each area can be summarized as follows:

1) Area 1 shows minor thrusting in an overall northeast-facing sequence, which is folded into a syncline at the northeast limit of the area. The Rockhole Fault is not immediately recognizable as one of the thrusts, but it is continuous with the poorly-exposed contact between the main belt of Koolpin Formation and overlying Zamu dolerite.

2) Area 2 shows that this thrust geometry continues to the northwest. There is only one thrust exposed in this area, indicating that the imbricates in area 1 ramp into one thrust in area 2.

3) Area 3 shows that a major thrust with a detachment in the upper Masson Formation separates a mainly steep northeast-dipping zone to the northeast from a zone of flatter form surface to the southwest. This thrust is continuous with the South Alligator Fault, suggesting that this detachment surface passes into the South Alligator Valley.

4) Area 4 shows that this thrust is steeply-dipping, and is overprinted by northeast-trending folds and cleavage, which also appear (from the large scale map pattern) to overprint the main northwest-trending fold/cleavage event.

5) Areas 5, 6 and 7 show the occurrence of extensive northwest-striking vein zones. In the Namoon area, it can be seen that these veins are at least partly syn-S₂, implying that they probably postdate thrusting but formed during the formation of northwest-trending folds and cleavage. This also suggests that these vein systems predate the U-Au-Platinoid mineralization history in the South Alligator Valley.

6) Areas 8 and 9 show that porphyroblasts within the thermal aureole of the Cullen Granite overprint the main northwest-trending foliation, but they are also pre- to syn- a later northwest-trending crenulation. This suggests that the Cullen Granite intruded after the main northwest folding event, but still during northeast shortening. The Cullen Granite in this area is virtually unfoliated, suggesting that it crystallized late in the history of the thermal aureole.

Interpretation

The interpreted cross section geometry of the area is shown in figure 7. In section A-A', it can be seen that the lowest thrust is inferred to cut up section to the southwest, so that the basal detachment in the northeastern block is in the Masson Formation. In the southwestern block, the detachment climbs up as far as the Wildman Siltstone. In most cases, thrusts climb up section in the direction of movement. In this case, this is consistent with southwest-directed thrusting. The large scale metamorphic zoning of the Pine Creek Geosyncline in this area (eg Needham et al, 1989) is also consistent with southwest-directed thrusting. From lateral map constraints, the middle thrust in this section must merge into the basal basal thrust. At the northeast end of the section, the uppermost thrust must form a syncline immediately to the southwest of the Mundogie Inlier. The Gerowie Tuff below this thrust pinches out laterally to the northwest, and must pinch out in the subsurface to the southwest of the Mundogie Inlier as well.

The truncation of the thrust system by the Cullen Granite can be seen in section B-B' (fig 7). It can also be seen in this section that Koolpin Formation is interpreted to directly overlies Masson Formation, with no intervening Mundogie Sandstone and Stag Creek Volcanics. This may be a stratigraphic pinchout (Mundogie notes). The interpreted position of the South Alligator and Rockhole Faults is shown in section B-B'. It can be seen that the South Alligator Fault is continuous with the main basal detachment, while the projected Rockhole Fault does not correspond to any of the inferred thrusts. The syncline at the northeast end of B-B' passes into an area of flatter form surface and exposure of Mundogie Sandstone further to the northeast.

From these observations, it is possible to infer the following structural history for the Mundogie area:

- 1) Early southwest-directed thrusting and formation of a bedding-parallel cleavage (D₁).
- 2) Formation of northwest-trending upright to overturned folds and cleavage (D₂), sometimes with multiple coaxial fold/cleavage events (D₃). Formation of northwest-trending, steeply-dipping vein zones occurred at this time as well. The Cullen Granite was intruded after the main folding event, but still during ongoing northeast-southwest shortening.
- 3) Formation of northeast-trending folds and cleavage, producing dome and basin interference patterns in the northwest part of the area.

4) Reactivation of bedding and/or thrust surfaces during later movement on northwest-trending subvertical faults. Fault movement at this stage probably would have been consistent with the dextral strike-slip displacement inferred for the South Alligator Valley (Valenta, 1988).

Comparison with the South Alligator Valley

The schematic stratigraphic relationships between early-mid Proterozoic basement rocks in the Mundogie and South Alligator Valley areas are shown in figure 2. In the Rockhole area, the Koolpin Formation is the uppermost unit exposed. Further to the southeast, Freidman (pers comm) has re-interpreted a zone of felsic volcanics to be part of the basement sequence. This felsic volcanic is at the same stratigraphic level as the Gerowie Tuff, and is intruded by Zamu Dolerite in a pattern similar to that seen in the Mundogie area. While it is clear that the felsic volcanic and the Gerowie Tuff are different lithologically, they may represent the products of the same volcanic event. In this case, the altered volcanics would be more proximal to the source while the Gerowie Tuff would be more distal. A much more detailed comparison of these two rock units is necessary before more detailed conclusions can be made.

The lateral variation in thrust geometry is summarized in figure 8. In the northwest Mundogie area, there is a detachment in the upper Masson Formation which climbs up section to the southwest. In the southeast Mundogie area, this detachment is not associated with repetition of stratigraphy. There are, however, multiple imbricates at the Koolpin-Gerowie stratigraphic level. Missing stratigraphy at the southwest end of the area may be due to a combination of ramp geometry, stratigraphic pinchout or late faults. In the South Alligator Valley, bedding-parallel high strain zones associated with these thrusts have been recognized (eg Davies, 1981; Valenta, 1988), but there has been no doubling of stratigraphy. This implies that the detachment stayed at the same level *at this level of exposure*, with thrust-related shortening accommodated elsewhere along the movement direction.

Mineralization

There are a number of identified Uranium prospects in the Mundogie area, as well as a number of lead prospects. Field checking of uranium prospects generally revealed little about the geology of these prospects. With the exception of Anomaly 2J, most of the prospects were located around the Koolpin Formation.

Mineralization at Anomaly 2J consists of secondary Uranium minerals concentrated at the contact between the Mundogie Sandstone and a tuffaceous unit of the Stag Creek Volcanics (ref). Mineralization occurs only in the weathered zone. The contact between these two rock types is exposed in the area, and there is no evidence of strong foliation or faulting.

Lead mineralization at the Namoonna prospect is hosted in deformed Masson Formation. In outcrop exposures, mineralization appears to be associated with steep quartz veins (figure 9). No strong gossan development was observed. Quartz veins associated with mineralization are steeply-dipping and trend northwest. They form parallel to S_2 and are sometimes deformed in S_2 , suggesting that the veins formed during D_2 . The vein zones at Namoonna extend for at least 10 km in a northwest direction. Other small lead deposits occur on this trend.

Mineralization at Minglo is hosted in contact-metamorphosed graphitic schist of the Wildman Siltstone. The quartz vein zone which hosts mineralization strikes perpendicular to the margin of the Cullen Granite, and appears to have formed late in the deformation history of the host rocks, possibly late during granite emplacement.

The Malone Creek Granite Area

An area to the north and east of the Malone Creek Granite in the Stow Region was briefly studied as well, in order to: a) assess the structural and metamorphic effects of the Malone Creek Granite; b) assess the general structural elements and form surface of the area; and c) place mineralization at 3/171 and Zamu into a structural context. The structural elements in the area studied can be summarized as follows:

- a bedding-parallel foliation
- a northwest-trending cleavage associated with upright shallow-plunging folds
- later non-penetrative cleavages in north-trending and east-trending orientations.
- northwest-trending quartz vein zones

- the Malone Creek Granite, which is unfoliated and intrudes Pul Pul Rhyolite.

No traceable markers were found within the Burrell Creek Formation in this area. The Zamu Dolerite, however, appears to be concordant with bedding and therefore is the best marker of stratigraphy and structural form surface. There appear to be three main sills of Zamu Dolerite: 1) near the top of the Kapalga Formation; 2) a sill approximately 1 km from the base of the Burrell Creek Formation; and 3) a sill within Burrell Creek above "2". The middle sill defines a synclinal axis to the north of the Malone Creek Granite (Stow Notes). This syncline is cored by Burrell Creek Formation with two irregular limbs of Zamu Dolerite. The reappearance of Zamu Dolerite at the southeast end of the Malone Creek Granite suggests the presence of another syncline in this area, requiring the presence of an anticlinal axis in the area of 3/171.

The Burrell Creek Formation in this area contains a number of northwest-trending quartz breccia zones. These are zones of intense foliation with veins which range in timing from syn- to post-foliation. Breccia clasts within these zones often contain a rotated foliation. These features suggest that the quartz breccia zones represent shear zones which have focussed fluid flow. It is difficult to constrain their timing relative to other structures, but the presence of ductile foliations in these zones suggests that they may have begun forming at the same time as the northwest-trending folds, and continued to form during later deformation.

The Malone Creek Granite is unfoliated, and in this study, thermal aureole features were not observed. The presence of a hornfels zone has, however, been noted by BMR geologists (Stow notes). North-trending and flat veins have been observed at one margin of the Malone Creek Granite. This geometry is kinematically consistent with the pattern of north-trending and flat tensional features observed in the South Alligator Valley (Valenta, 1989). This suggests that intrusion of the Malone Creek Granite postdated the main northwest folding event, but at least partly predated later deformation associated with U-Au-Platinoid mineralization. An additional constraint on the timing of intrusion is the fact that the Malone Creek Granite intrudes Pul Pul Rhyolite.

Mineralization

Two zones of mineralization were studied in the Malone Creek Granite area. Anomaly 3/171 is a uranium-gold-silver show within Burrell Creek Formation immediately to the east of the Malone Creek Granite, and Zamu is a lead-silver show hosted in Zamu Dolerite.

Mineralization at 3/171 is exposed in a series of costeans, and appears to be hosted in and around quartz veins which are oriented subparallel to S_2 . In this case, veins appear to have formed post- S_2 , since they open on S_2 and are undeformed. This is similar to the timing observed for the Malone Creek Granite, suggesting that the veins may have formed during granite intrusion.

Zamu

Lead-silver mineralization at the Zamu mine occurs in veined and altered Zamu Dolerite (fig 10). Mineralization is hosted in a series of quartz vein/breccia zones. These zones are steeply-dipping and strike northeast (fig 10). This vein geometry suggests a possible sinistral displacement on the Zamu-Burrel Creek contact (fig 10), with the concentration of dilation in Zamu Dolerite related to its greater competency. Mineralization appears to be associated with the altered margins of the quartz veins, which take the form of bleaching and limonitic alteration on the surface (fig 10). The general lack of strong foliation in surrounding Zamu Dolerite makes it difficult to determine the timing of mineralization relative to structures.

Discussion

It is clear from the distribution of Uranium deposits in the conservation zone that proximity to the unconformity is a critical component of the U-Au-Platinoid mineralization model (Needham, 1987). From this standpoint, the U-Au-Platinoid mineralization potential of the Mundogie region suffers from the fact that in much of the area the unconformity is above the present level of erosion. The unconformity plays a mechanical role in mineralization in that it is a zone of relatively high permeability during deformation. It also plays a chemical role in that it juxtaposes sandstones or volcanics (ie rocks with little potential to buffer oxygen fugacity) on carbonaceous and/or ferruginous basement rocks. It is possible to envisage similar structural and chemical roles being played by shallow thrust surfaces within the basement, which implies that the existence of a Coronation Hill style orebody in basement rocks of the Mundogie region cannot be ruled out. The lack of any significant Uranium deposits discovered so far in the Mundogie region makes this area unfavourable relative to areas in which the unconformity is below the

present level of erosion. One area which must be judged to show a high potential for further unconformity-related mineralization is the continuation of the Palette Fault system to the south of Coronation Hill. In this area, the unconformity is below an unknown thickness of Pul Pul Rhyolite, yet it may still be possible to locate zones of fluid focussing and mineralization by studying local geochemical patterns in the present geochemical database.

In addition to unconformity environments of mineralization, it should be noted that thermal aureole gold of the type developed in the Pine Creek area (eg Nicholson and Eupene; Wall, 1990) may be developed in the thermal aureoles of the Cullen and Malone Creek Granites. Samples of ferruginous Koolpin Formation should also be routinely analyzed for thermal aureole and/or regional metamorphic gold mineralization.

Conclusions

The following structural history can be inferred for the Mundogie area:

- a) Early southwest-directed thrusting and formation of a bedding-parallel cleavage (D_1).
- b) Formation of northwest-trending upright to overturned folds and cleavage (D_2), sometimes with multiple coaxial fold/cleavage events (D_3). Formation of northwest-trending, steeply-dipping vein zones occurred at this time as well. The Cullen Granite was intruded after the main folding event, but still during ongoing northeast-southwest shortening.
- c) Formation of northeast-trending folds and cleavage, producing dome and basin interference patterns in the northwest part of the area.
- d) Reactivation of bedding and/or thrust surfaces during later movement on northwest-trending subvertical faults. Fault movement at this stage probably would have been consistent with the dextral strike-slip displacement inferred for the South Alligator Valley (Valenta, 1988).

The Rockhole Fault in the South Alligator Valley is laterally continuous with the steeply-dipping contact between Koolpin Formation and a section rich in Zamu dolerite. The South

Alligator Fault, on the other hand, is laterally continuous with a major regional detachment surface near the top of the Masson Formation.

Early thrust faults are clearly folded in some areas, and appear to show complicated subsurface geometries. These subsurface geometries may have important implications for the localization of U-Au-PGE deposits.

Interpreted large scale thrust geometries show a ramping and change in style from southeast to northwest. In the northwest, the main detachment is below the Mundogie Sandstone and there are multiple thrust repeats of the Gerowie Tuff - Shovel Billabong Andesite - Koolpin Formation sequence. Further to the southeast, the Gerowie Tuff is absent and there do not appear to be thrust repeats of the Mundogie Sandstone.

The general lack of evidence of significant Uranium deposits in the Mundogie area provides at least partial confirmation of the crucial role played by the unconformity surface in Uranium localization. It is, however, possible to predict favourable structural geometries and host rock distributions in basement-only settings.

Field observations show that deformation and veining were synchronous in the contact aureole of the Cullen granite. This may have important implications for potential thermal aureole type gold mineralization.

Lead mineralization in the Namoonna area occurs on northwest-trending fractures which, from their relationships to folds and cleavage, appear to have formed relatively early in the deformation history.

Recommendations

1) It is still necessary to do a detailed core-based study on the distribution of features associated with mineralization and alteration and their relationship to large scale and small scale structural features. This represents a chance to use the detailed three dimensional information from the El Sherana, Palette and Coronation Hill areas to test and refine the mineralization model developed during the course of this study.

2) Use airborne magnetic and radiometric data to refine lithological and structural mapping of the conservation zone. The GIS database available in this area, including magnetic susceptibilities, represents an excellent opportunity to combine surface susceptibility measurements with possible gamma ray spectrometry data and available reflectance spectra for different rock and alteration types in order to carry out a remote sensing-based rock classification project which combines TM-based spectral classification with magnetic and radiometric data.

3) Carry out more detailed surface mapping of structural and lithological patterns in the immediate Coronation Hill area. This will yield valuable information on the small scale structural controls on mineralization, as well as important constraints on the history of deformation and sedimentation in this complex area.

Acknowledgements

Field work which forms the basis for this report was performed while the author was employed as a contract geologist by the Bureau of Mineral Resources. The following are acknowledged:

- Lesley Wyborn and Stuart Needham for logistical assistance.
- Lesley Wyborn, Stuart Needham, Peter Stuart-Smith, Julio Friedman, Elisabeth Jagodzinski and Gladys Warren for useful geological discussions.
- Foy Leckie and Dean Carville of BHP for useful discussions.
- John Hawke and Bob Skinner for invaluable field assistance

References

- Ayres, D.E. and Eadington, P.J., 1975. Uranium mineralization in the South Alligator Valley. *Mineralium Deposita*. 10: 27-41.
- Davies, H.E., 1981. A structural and stratigraphic study of the Lower and Middle Proterozoic sequences in the South Alligator Valley, Northern Territory. *Hons. Thesis, Monash University*.

- Johnston, D.J. and Wall, V., 1984. "Why unconformity-related uranium deposits are unconformity-related." *Abs. Geol. Soc. Aust.* v. 12, 285-287.
- Johnston, J.D., 1984. Structural evolution of the Pine Creek Inlier and mineralization therein, N.T., Australia. Ph.D. thesis, Monash University, Clayton, Victoria, 268pp.
- Needham, R.S., 1987. Review of mineralization in the South Alligator Valley. BMR Record 1987/52.
- Needham, R.S. and Stuart-Smith, P.G., 1985. Stratigraphy and tectonics of the Early to Middle Proterozoic transition, Katherine-El Sherana area, N.T. *Australian Journal of Earth Sciences.*, 32: 219-230.
- Needham, R.S., Stuart-Smith, P.G. and Page, R.W., 1988. Tectonic Evolution of the Pine Creek Inlier, Northern Territory. *Precambrian Research.*, 40/41: 543-564.
- Nicholson, P.M. and Eupene, G.S., 1984. Controls on gold mineralization in the Pine Creek Geosyncline. Aus I.M.M. conference proceedings, Darwin. pp 377-395.
- Stuart-Smith, P.G., Wills, K., Crick, I.H. and Needham, R.S., 1980. Evolution of the Pine Creek Geosyncline. In Ferguson, J., and Goleby, A.B., (editors), Uranium in the Pine Creek Geosyncline. *International Atomic Energy Agency, Vienna.* 23-38.
- Threadgold, I.M., 1960. The mineral composition of some uranium ores from the South Alligator River area, N.T. *C.S.I.R.O., Melbourne, Mineragraphic Technical Investigations Technical Paper 2*, 53.
- Valenta, R.K., 1988.[†] A report on mineralization and structure in the South Alligator Valley. Unpublished report to the Bureau of Mineral Resources.
- Valenta, R.K., 1989. Structure and mineralization in the South Alligator Valley, N.T. Part 1 of this volume: *Structural controls on Mineralization of the Coronation Hill Deposit and Surrounding Area.* Record 1991/107.
- Stuart-Smith, P.G., Needham, R.S., and Bagas, L., 1988. Stow, Northern Territory (Sheet 5470). *Bureau of Mineral Resources, Geology and Geophysics, Australia, 1:100 000 Geological Map and Commentary.*
- Wall, V.J., and Valenta, R.K., 1990. Ironstone-related gold-copper mineralisation: Tennant Creek and Elsewhere. AusIMM Pacific Rim Congress, Extended Abstracts, 855-863.
- Wilde, A.R., Bloom, M.S., and Wall, V.J., 1989. Transport and deposition of gold, uranium and platinum group elements in unconformity-related deposits. *Economic Geology Monograph*, 6, 637-650.

[†] The findings of this report are incorporated in Valenta 1989, which is reproduced as part 1 of this record.

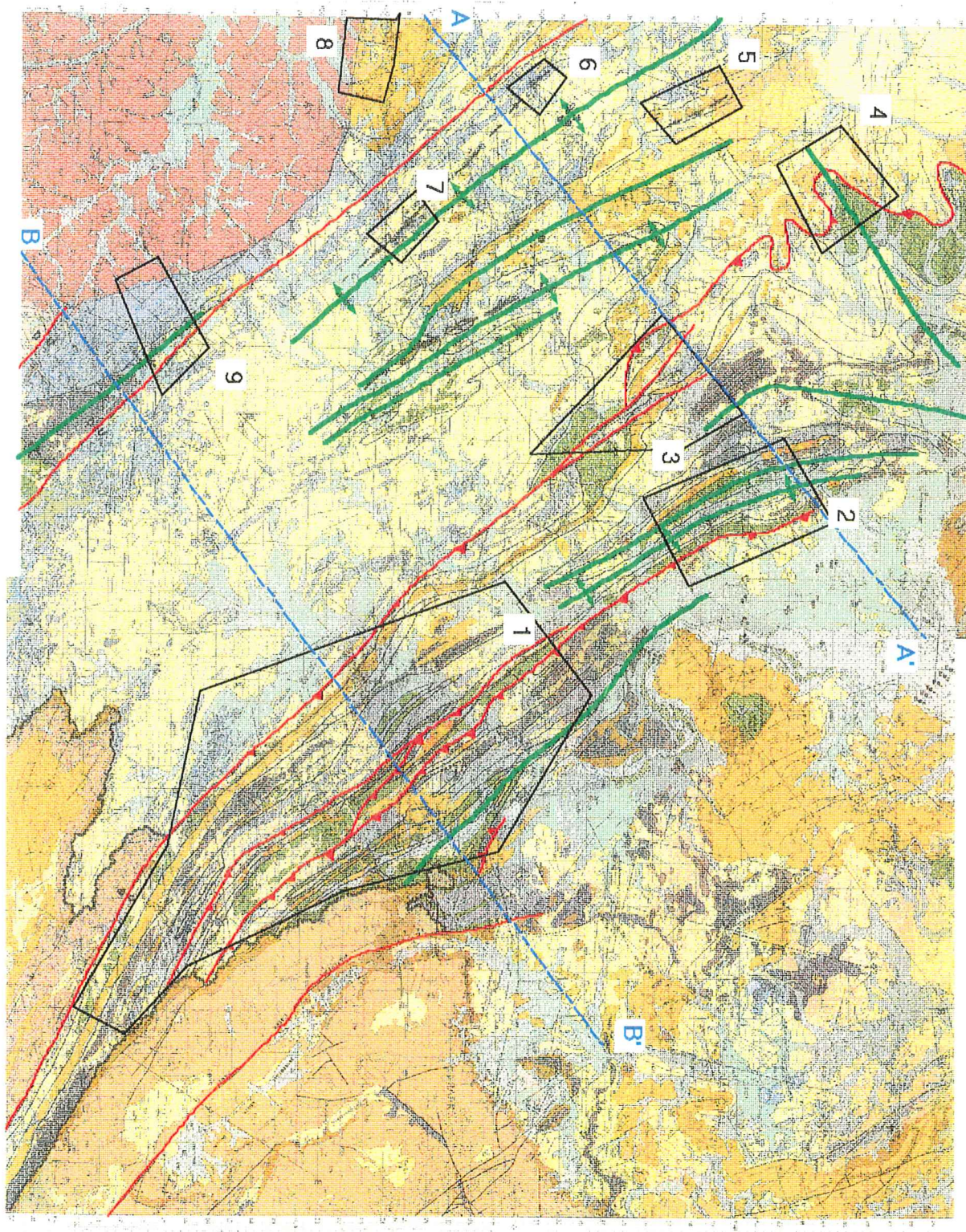
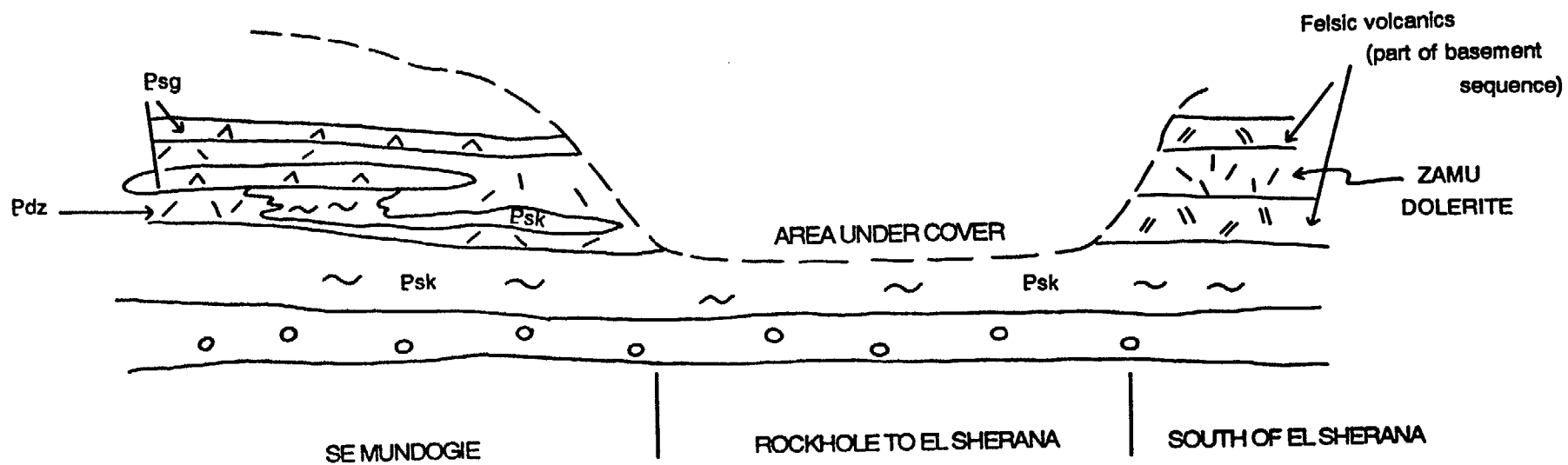


Figure 1. Colour reproduction of the BMR 1:100,000 map of the Mundogie region, with interpreted thrusts in red, interpreted folds in green, study areas enclosed in boxes, and cross section locations shown in blue.



Figure 2. A schematic summary of the distribution of L-M Proterozoic rock units in outcrop from south of El Sherana to north of Rockhole. See text for more detailed discussion.



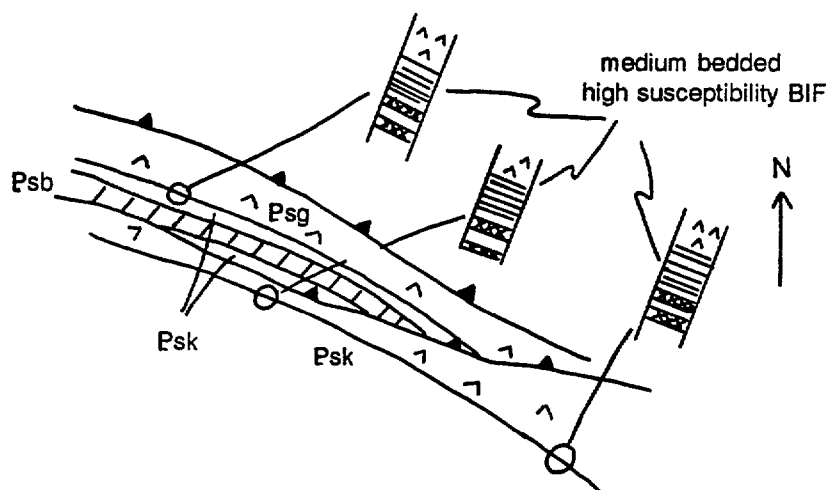


Figure 3. Stratigraphic variations and inferred thrusts in a small portion of area 1. The distinctive medium-bedded high susceptibility BIF at the contact with Gerowie Tuff indicates that both packages are younging north, and therefore must be fault-repeated rather than folded.

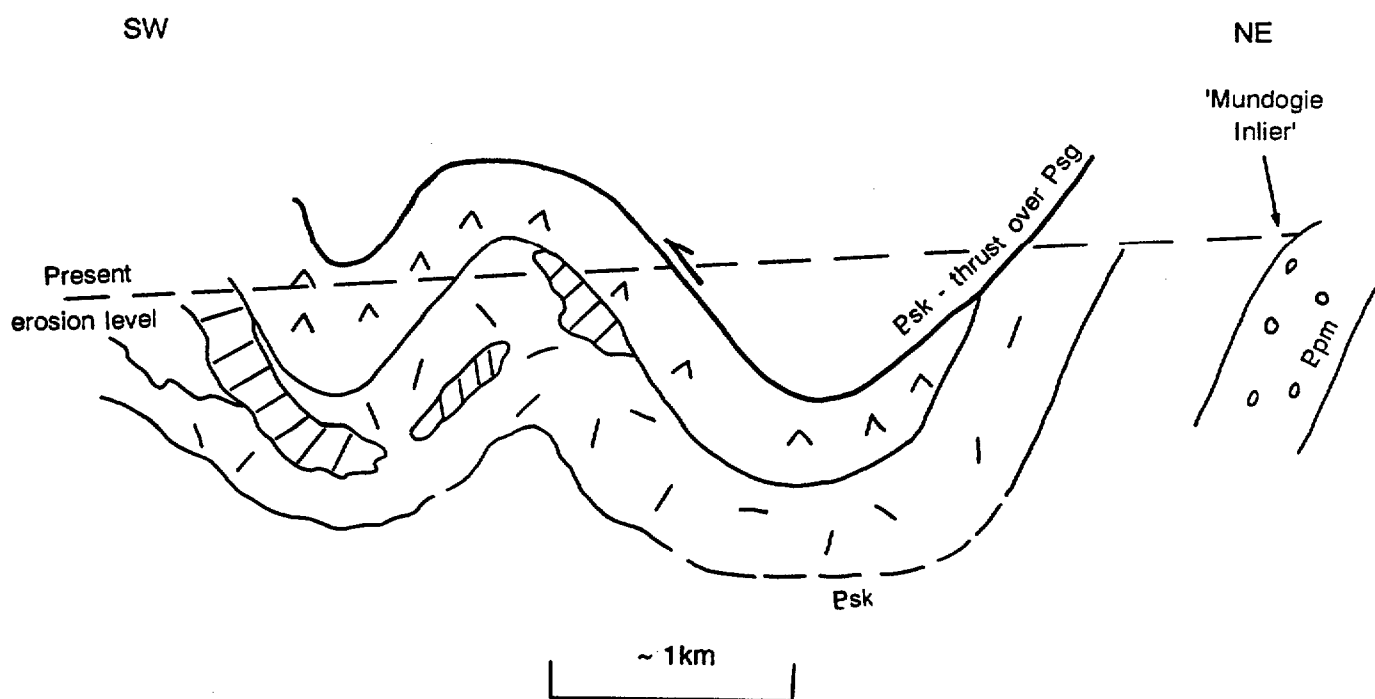


Figure 4. Inferred thrust geometry in area 2. See text for more detailed discussion.

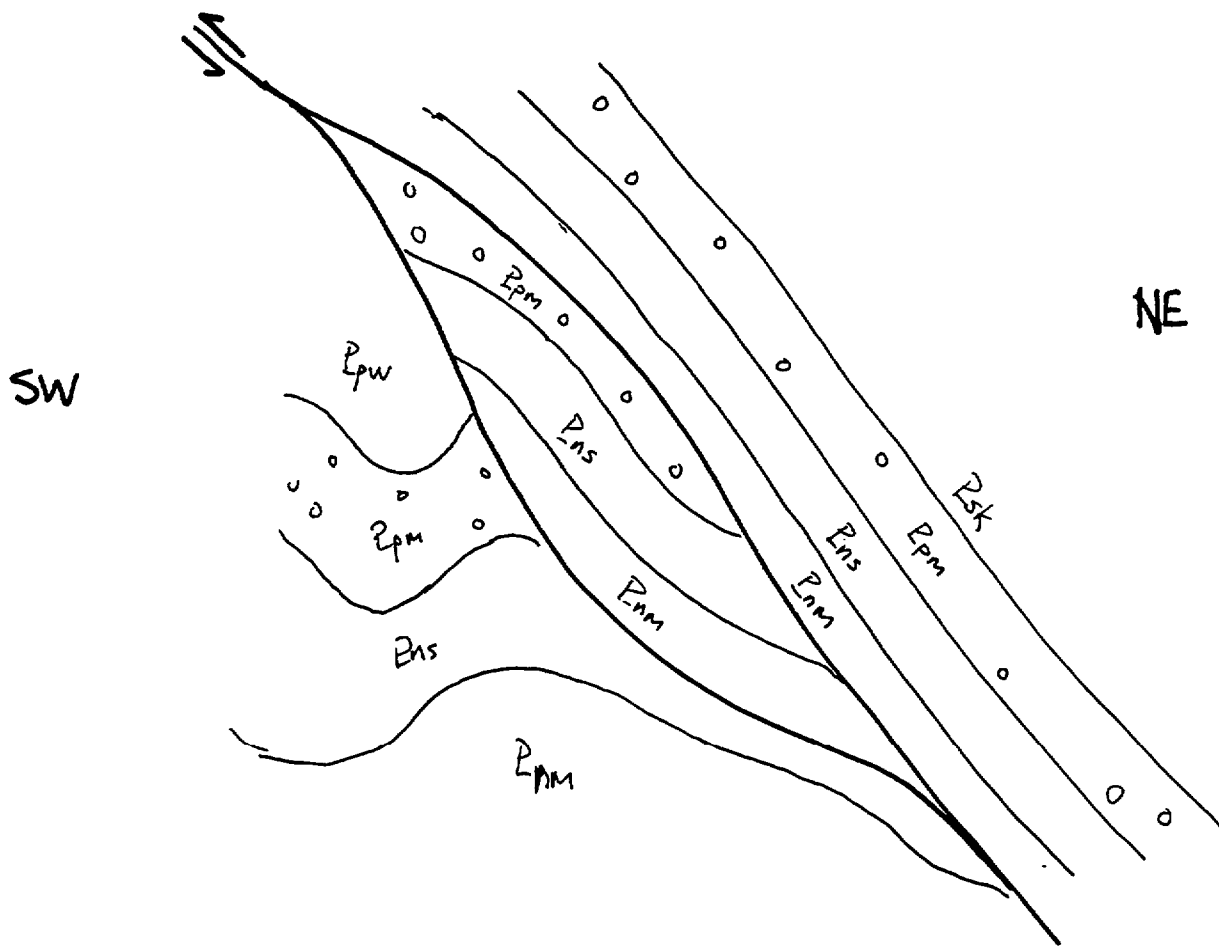


Figure 5. Inferred thrust geometry in area 3. See text for more detailed discussion.

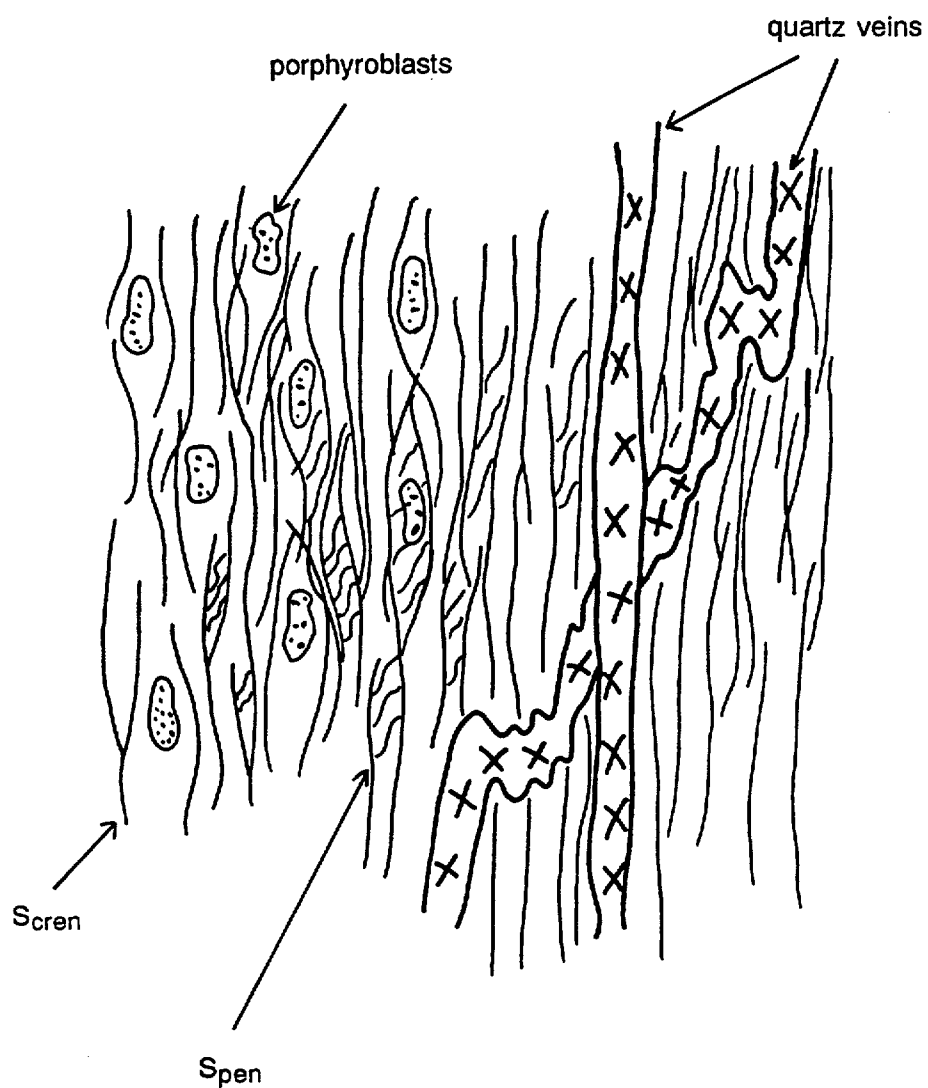


Figure 6. Diagram summarizing timing relationships between veins, porphyroblasts and foliations in the contact aureole of the Cullen Granite. Porphyroblasts postdate the earliest foliation, and are partly overprinted by the latest foliation. Veins are syn- to post- the latest foliation.

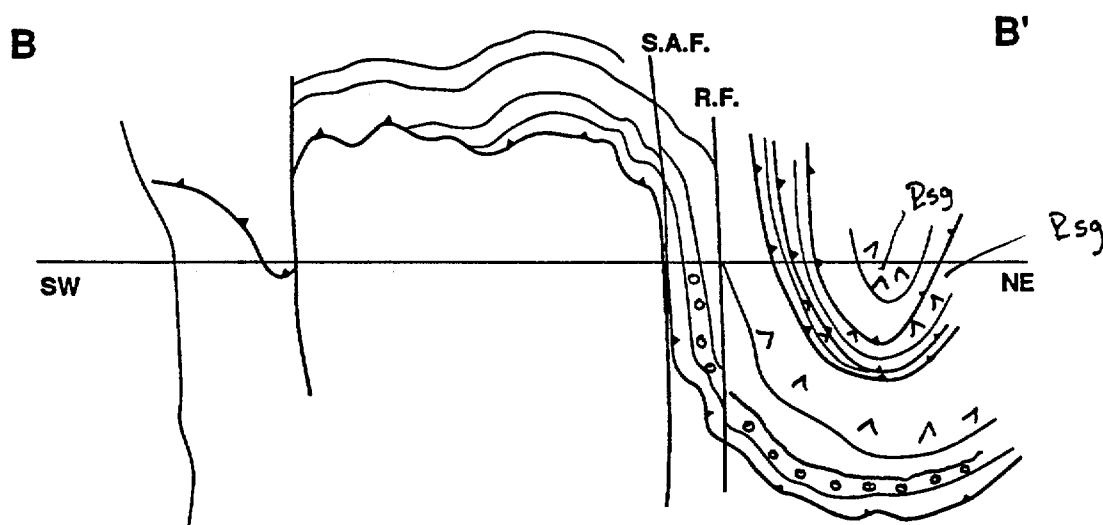
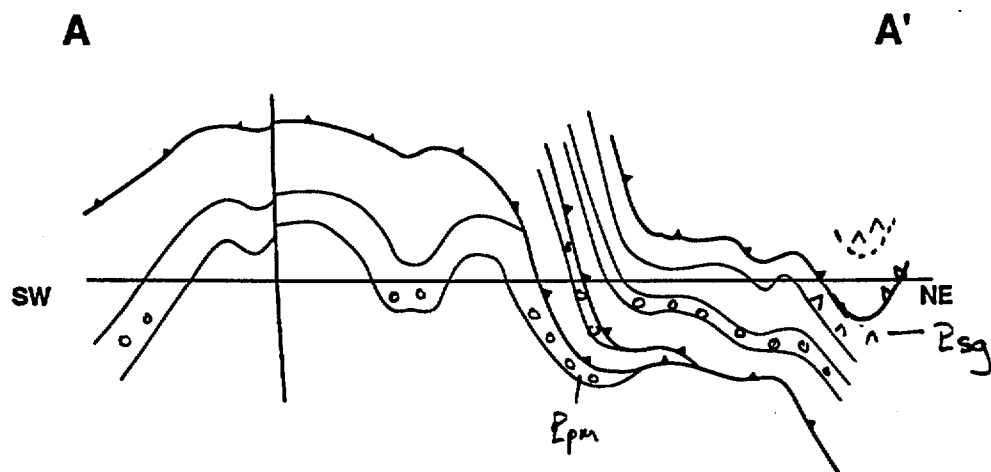


Figure 7. Large scale cross sections across the Mundogie region. See figure 1 for section locations. See text for detailed discussion of sections.

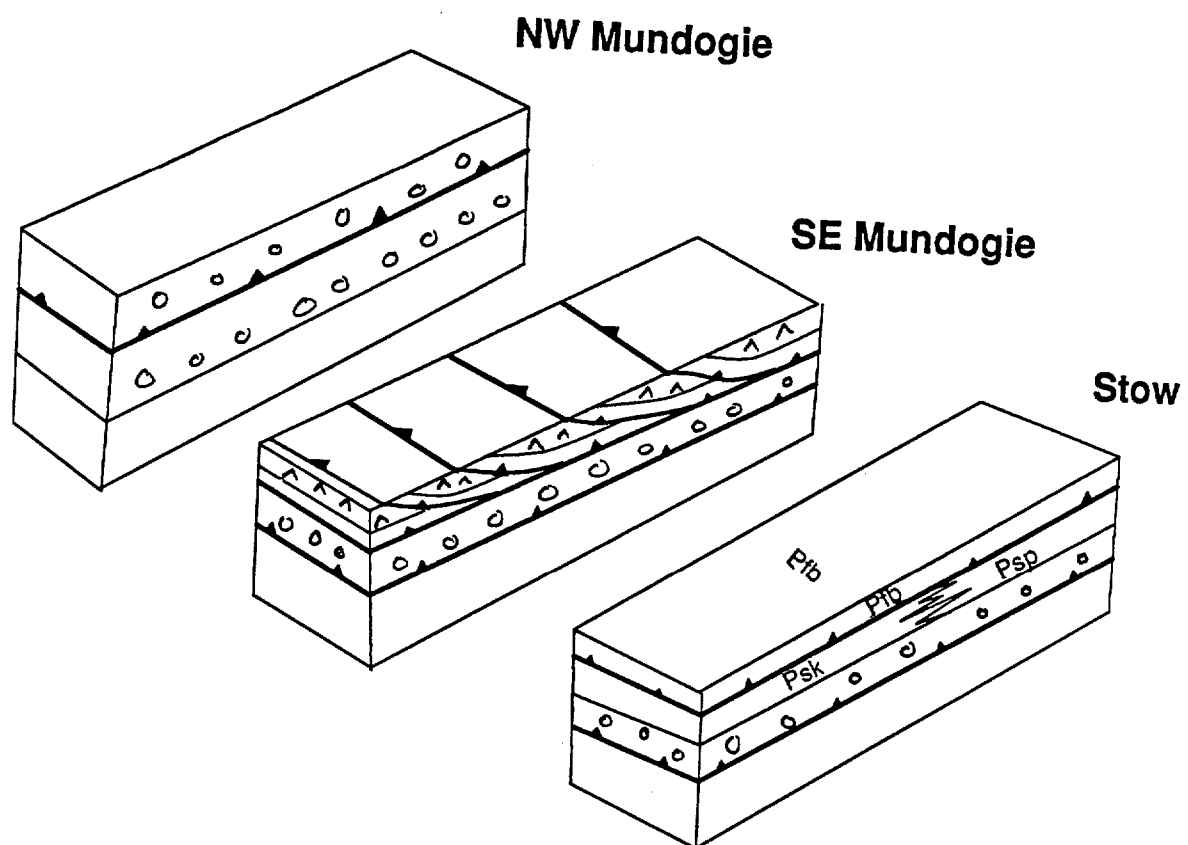


Figure 8. Diagram summarizing the lateral variation in thrust geometry from ar Conservation Zone. See text for detailed discussion.

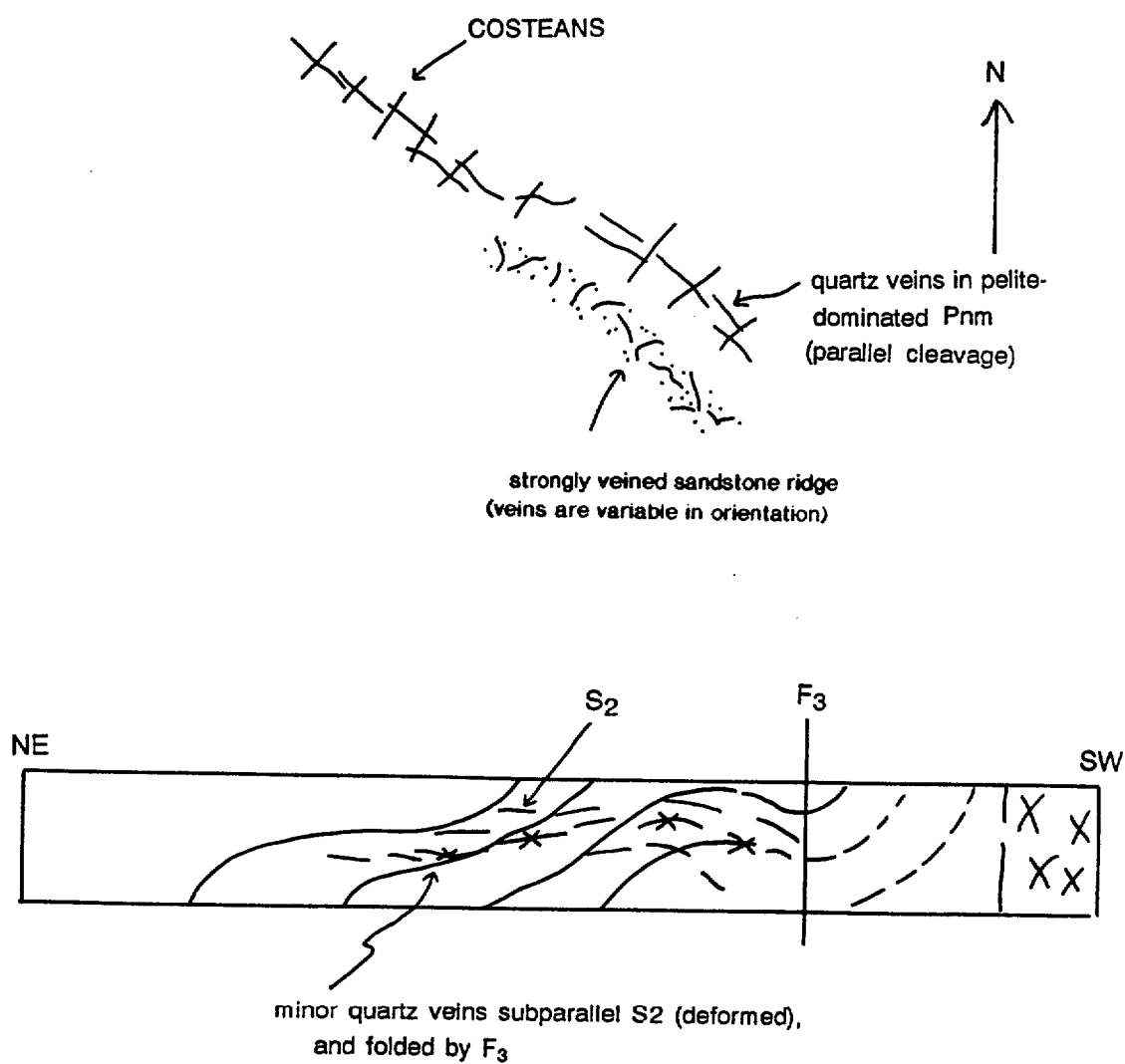


Figure 9. Diagram summarizing the geometry of veins, folds and foliations at Namoon. Veins appear to be at least partly synchronous with the formation of northwest-trending folds during D₂ and D₃.

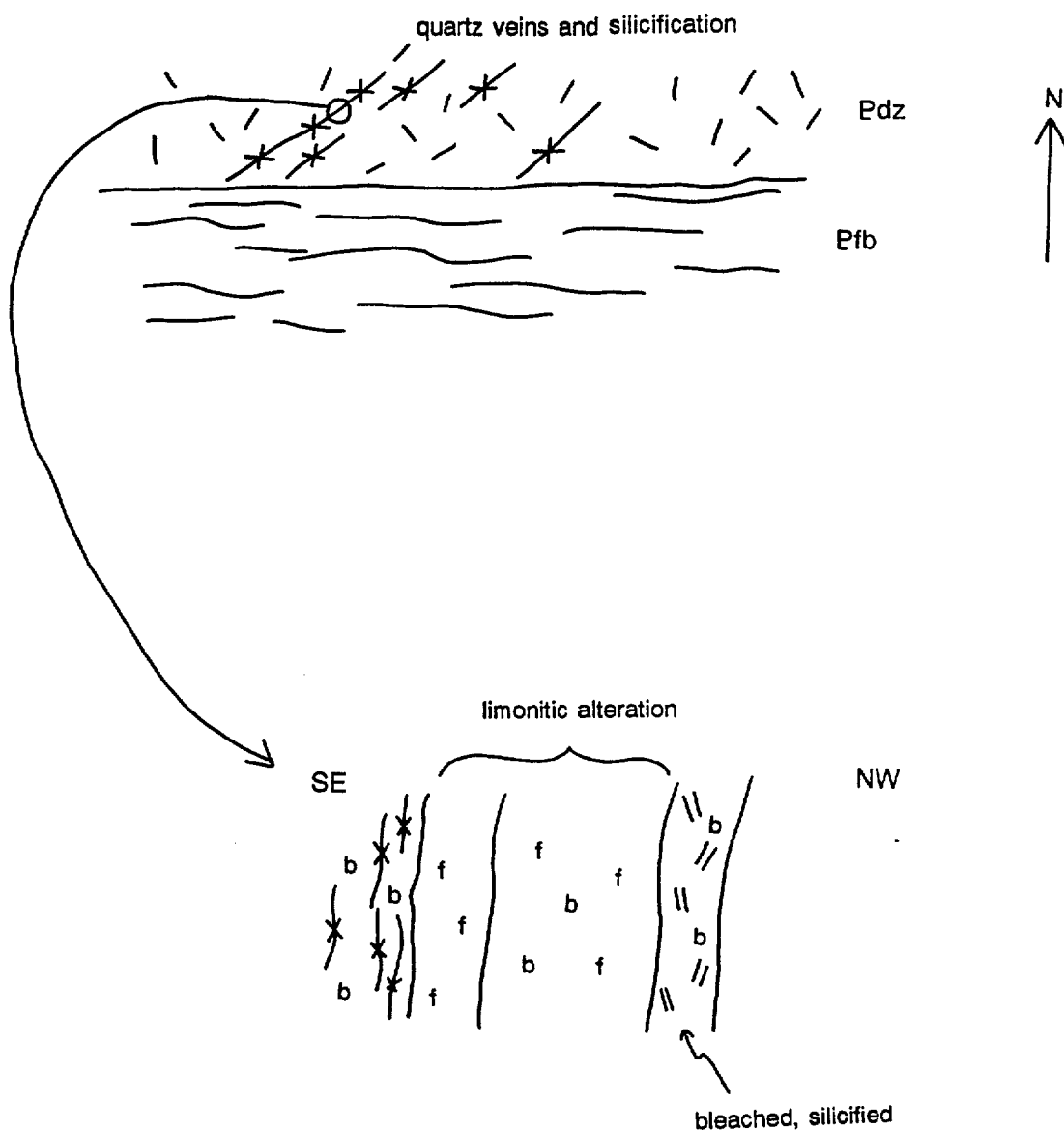


Figure 10. Diagram summarizing the geometry and nature of veins and alteration at the Zamu mine. See text for detailed discussion.

Appendix 1. Structural data

Loc num	Sheet	Dip	Dip az	Feature
1001	M12	80	014	So
1002	M12	75	030	So
1003	M12	74	212	So
1003	M12	64	218	S2
1004	M12	80	218	So
1005	M12	74	120	So
1006	M12	68	221	So
1007	M12	70	235	So
1007	M12	62	270	S2
1008	M12	87	264	So
1009	M12	90	233	So
1010	M11	73	245	So
1011	M11	80	015	So
1012	M11	80	051	So
1013	M11	55	251	So
1014	M11	30	063	So
1015	M11	30	040	So
1016	M11	45	062	So
1017	M11	30	225	So
1018	M11	45	072	So
1019	M11	70	047	So
1020	M11	20	048	FA
1021	M11	40	037	So
1022	M11	15	318	FA
1023	M11	50	202	So
1024	M11	42	278	So
1025	M11	90	020	So
1026	M11	60	034	So
1027	M11	55	027	So
1028	M11	68	128	So
1029	M11	55	200	So
1030	M11	43	271	So
1031	M11	70	080	So
1032	M11	65	061	So
1033	M11	22	135	FA
1034	M11	70	063	So
1035	M11	61	072	So
1035	M11	72	230	S2
1036	M11	40	348	So
1037	M8	65	224	So
1038	M8	85	245	So
1039	M8	90	230	So
1040	M8	84	300	F2
1041	M8	50	135	F2
1042	M8	48	130	F2
1043	M8	50	130	F2
1043	M8	40	270	F3
1044	M8	73	342	F2
1044	M8	75	352	F2
1044	M8	60	115	F3
1044	M8	80	243	So
1044	M8	80	255	So
1045	M10	70	209	So

1046	M10	50	224	So
1047	M10	80	218	So
1048	M10	50	200	So
1049	M10	80	230	So
1050	M10	85	227	S0
1051	M10	90	206	S2
1052	M10	73	189	S2
1053	M10	90	214	S3
1054	ST2	85	225	QV
1055	ST2	27	105	S2
1055	ST2	90	234	S3
1055	ST2	28	141	F3
1055	ST2	25	102	So
1055	ST2	18	131	L2
1055	ST2	33	196	S2
1055	ST2	18	168	F3
1055	ST2	48	090	S3
1056	ST2	31	152	S2
1057	ST2	55	218	S2
1058	ST2	85	252	S2
1059	ST2	60	228	QV
1060	ST2	70	065	So
1060	ST2	81	218	S2
1061	ST2	68	073	So
1062	ST2	77	086	So
1063	ST5	87	012	So
1064	ST5	70	178	So
1064	ST5	90	185	S2
1065	ST5	80	358	S2
1066	ST5	78	232	S2
1067	ST5	75	228	S2
1068	ST5	74	037	SS2
1069	M4	80	050	So
1070	M4	48	025	So
1071	M4	47	015	So
1072	M4	43	052	So
1073	M4	65	076	So
1074	M4	66	220	QV
1074	M4	36	073	So
1075	M4	61	043	So
1076	M4	80	290	So
1077	M4	56	230	So
1077	M4	77	010	S2
1078	M4	90	102	S4
1078	M4	40	006	So
1079	M4	83	105	S4
1079	M4	71	222	So
1080	M4	90	001	So
1080	M4	90	122	S4
1081	M4	81	123	S4
1081	M4	82	183	So
1082	M4	30	150	So
1083	M4	73	117	S4
1084	M4	85	125	S4
1085	M4	57	050	So
1086	M5	64	020	So
1087	M5	66	051	So
1087	M7	84	237	S2

1088	M7	76	241	So
1088	M7	75	027	S2
1089	M7	62	183	S2
1089	M7	90	212	So
1090	M7	55	197	So
1091	M7	40	195	So
1092	M7	88	040	S3
1092	M7	26	130	F3

**GEOLOGICAL AND STRUCTURAL CONSTRAINTS ON THE
RESOURCE POTENTIAL OF THE KAKADU CONSERVATION
ZONE**

by

R.K. Valenta

Part of the Bureau of Mineral Resources submission to the Resource Assessment Commission

Table of Contents

1.	Summary.....	2
2.	Introduction.....	2
3.	Structure of the South Alligator Valley.....	3
4.	Coronation Hill.....	4
4.1	Structural Setting.....	4
4.2	Rock Types.....	5
4.2.1	Green Tuffaceous Siltstone.....	5
4.2.2	Carbonaceous Shale.....	5
4.2.3	Quartz Feldspar Porphyry.....	5
4.2.4	Diorite.....	6
4.2.5	Breccias.....	6
4.2.6	Carbonates.....	8
4.2.7	Distribution of rock types.....	8
4.3	Mineralization.....	9
4.3.1	Large Scale Setting.....	9
4.3.2	Small Scale Setting.....	9
4.3.3	Timing and Controls.....	10
4.4	Alteration.....	10
4.5	Coronation Hill Critical Observation.....	11
4.6	Exploration Model.....	12
4.7	Potential of the Coronation Hill area.....	13
5.	El Sherana.....	13
5.1	Structural Setting.....	14
5.2	Rock Types.....	14
5.2.1	Carbonaceous Shale.....	14
5.2.2	Cherty Ferruginous Shale.....	15
5.2.3	Distribution of Uranium mineralization.....	15
5.2.4	Distribution of Gold Mineralization.....	16
5.2.5	Recent Exploration.....	16
5.3	Summary.....	17
5.4	Exploration Model.....	18
5.5	Potential of the El Sherana area.....	18

6.	Palette.....	18
6.1	Structural Setting.....	18
6.2	Host Rocks.....	19
6.3	Distribution of Mineralization.....	20
6.4	Palette Drilling Program.....	20
6.5	Potential of the Palette area.....	20
7.	The Conservation Zone.....	21
7.1	Types of Mineralization.....	21
7.2	The Role of Structure in Deposit Localization.....	21
7.3	Area-Scale prospectivity.....	22
7.3.1	General.....	22
7.3.2	Saddle Ridge Northeast.....	22
7.3.3	Pul Pul Hill.....	22
7.3.4	Clear Springs.....	22
7.3.5	Stockpile/Flying Fox.....	23
7.3.6	Fisher Fault.....	23
8.	Conclusions.....	23
9.	Acknowledgements.....	24
10.	References.....	25

1 Summary

- 1) The new CZ contains numerous areas which show structures, host rocks and alteration favourable to the occurrence of further uranium-gold-platinoid mineralization of the Coronation Hill type.
- 2) The Coronation Hill deposit contains both uranium-rich and uranium-poor areas. Uranium-poor gold-platinoid mineralization is fracture-controlled and is hosted in a wide range of rock types. Mineralization of this type elsewhere in the new CZ could easily have escaped detection by standard uranium exploration methods.
- 3) NNW-trending fractures which host mineralization in the Coronation Hill area show small displacements and appear to have formed late in the deformation history of the area.
- 4) On a small scale, uranium-gold-platinoid mineralization at Coronation Hill occurs in late veins and breccias containing varying proportions of quartz, calcite and chlorite.
- 5) The presence of carbonaceous shales is not necessary for the occurrence of Coronation Hill style uranium-poor gold-platinoid mineralization.
- 6) The presence of fractured chloritic, K feldspar-bearing or calcareous lithologies may be necessary for the development of mineralization of the uranium-poor Coronation Hill type.
- 7) The Coronation Hill deposit is presently open at depth, and its structural setting suggests that mineralization should persist at depth.
- 8) The Coronation Hill West area is a "mirror image" of the Coronation Hill area, containing similar structures and host rocks. Other areas which must be considered prospective on this basis include Saddle Ridge Northeast, the Pul Pul Hill area, and the length of the Fisher Fault in the new CZ.
- 9) Gold mineralization at El Sherana is often high grade but discontinuous. It occurs in spatial association with, but often slightly removed from uranium mineralization. Both types of mineralization occur in shallow northwest-pitching bodies which do not appear to persist at depth. Recent drilling by the CHJV failed to properly test mineralization at El Sherana, and the area still has a very high potential.
- 10) The Palette area is structurally and stratigraphically complex, and is so far largely untested for gold. Drilling by the CHJV tested a Coronation Hill-like structural target and obtained poor results, but much more work is needed to properly test the potential of this region.

2 Introduction

This report forms part of the BMR submission to the Resource Assessment Commission on the mineral potential of the Kakadu Stage III conservation zone. The detailed aims of this contribution are as follows:

- a) To assist in assessment of potential resources in the new Conservation Zone, including an assessment of El Sherana and Palette.
- b) To identify structural and geological characteristics of the Coronation Hill deposit that could disrupt or change geostatistical trends.

c) To examine the number, nature and distribution of orebodies to develop the most appropriate computer database structure for the evaluation

d) To identify structural features inferring extensions.

This work builds on and draws heavily from three geological field seasons carried out by the author in the conservation zone. Geological study during these field seasons was confined to mapping of surface geology and pit exposures, since drill core was unavailable.

Work carried out as part of this study included:

a) Detailed examination of selected diamond drill holes from Coronation Hill, El Sherana and Palette.

b) Detailed surface mapping in the Coronation Hill and Palette areas.

c) Examination of drill hole and surface assay results from Coronation Hill, El Sherana and Palette.

d) Examination of other BHP-sponsored reports and reviews of previous exploration activity.

3 Structure of the South Alligator Valley

The new CZ occurs within the Pine Creek Geosyncline, a sequence of early to middle Proterozoic ensialic sediments and igneous rocks (Needham et al, 1988)(fig 1). Needham et al (1988) describe a main rift sequence of pre-1880ma rift, sag and orogenic phases of sedimentation and igneous activity, which are overprinted by the "Nimbuwah Event", a phase of low to moderate pressure metamorphism and crustal shortening involving tectonic transport from northeast to southwest. The new CZ straddles the boundary between greenschist and amphibolite facies matamorphism in the main rift sequence (Warren and Kamprad, 1990). Needham et al (1988) described two later "episodes" of rifting separated by "episodes" of crustal shortening, implying alternating shortening and extension about northeast-southwest axes on faults parallel to the northwest-trending structural grain of the pre-Nimbuwah basement. The El Sherana Group and Edith River Group "rift fill" sequences show sediment transport parallel to northwest-trending faults (Needham et al, 1988; Friedmann, 1990). Structural study in the South Alligator Valley suggests that the new CZ occurs within a zone of complex and long-lived reactivation of the basement structural grain, producing spatially and temporally coexisting zones of shortening about northeast-trending axes. The pattern of late faults in the South Alligator Valley (fig 1) is kinematically consistent with late dextral strike slip displacement on northwest-trending faults (eg Christie-Blick and Biddle, 1985; Harding et al, 1985). Alternating shortening and extension on these faults may be due to lateral variations in fault geometry during strike-slip displacement.

4 Coronation Hill

4.1 Structural setting

The structural setting of Coronation Hill can be summarized as follows.

- 1) The Coronation Hill area occurs in a zone of complex dip slip and strike slip faulting, which is located in a large scale dilational offset on the Palette Fault System (Valenta, 1988;1989)(fig 1).
- 2) Basement rocks strike northwest and are steeply-dipping to vertical (fig 2). They contain multiple crenulation cleavages and early deformed veins in suitable rock types.
- 3) Faults in a number of orientations post-date these deformation features. They include: a) north-trending/subvertical; b) northwest-trending/75°S; c) east-trending/70°S; d) northeast-trending/subvertical; and e) NNW-trending/subvertical.
- 4) The widespread occurrence of talus breccias in the Coronation Hill area suggests that some of these faults were active during sedimentation, though in their present form the faults truncate and displace breccia bodies, suggesting that fault movement continued after sedimentation
- 5) On the map it can be seen that most of the topographically high areas of Coronation Hill are occupied by variably brecciated "capping sandstone" (fig 2), which is tentatively correlated with the Kombolgie Formation (fig 3). Surface mapping and subsurface drilling shows that this body is mainly bounded by faults – northwest-trending faults to the north and south and north-trending faults to the east and west. In addition, an outlier of type "A" and "B" breccia occurs in the northwest part of the Coronation Hill pit, where it is bounded on all sides by steep faults.
- 6) The zone of mineralization is bounded to the west by a steep fault separating qfp/gts/dior from breccias and capping sandstone (fig 4). The subsurface geometry of this fault is slightly variable from section to section, suggesting that it may be offset by minor faults at an angle to the section. In some cases, a fragment of the capping sandstone unconformity is preserved on the east side of this fault. Constraints from the 6640 (fig 4) section suggest that this fault has a displacement on the order of 250m in vertical section, bringing the west block down.
- 7) Mineralization on surface and in drill holes occurs mainly along NNW-trending zones of distributed fracturing and quartz/carbonate/chlorite veining (fig 2). These zones appear to have little or no displacement. In the Coronation Hill pit, they clearly postdate the north-trending fault which separates gts from the breccias, yet the north-trending fault is not significantly displaced (fig 2).
- 8) The Calannans fault occurs as an east-trending quartz blow at the surface (fig 2), where it contains minor gold mineralization. It dips approximately 70°S, and forms the boundary between a package dominated by gts, qfp and diorite above and carbonaceous, dolomitic Koolpin formation below, separated by a zone of type C breccia. This contact has been interpreted by BHP geologists as a reverse fault bringing gts/qfp/di over breccias which are unconformably overlying basement lithologies. If this is the case, then the Calannans Fault must have on the order of 500m displacement in vertical section.

4.2 Rock Types

Drilling at Coronation Hill has shown a complicated geometry of rock types in the subsurface, some of which are poorly represented in surface exposure. The main rock types exposed on the surface are green tuffaceous siltstones, sandstones, type "A" and "B" breccias, quartz feldspar porphyry and diorite. Previous studies have placed all of these rock types within the El Sherana Group (eg Needham and Stuart-Smith, 1987; Valenta, 1988; 1990). An exception to this is the green tuffaceous siltstone, which has been interpreted by Valenta (1988; 1990) as being part of the basement sequence.

Relationships observed at Coronation Hill have necessitated a modification of this stratigraphic framework (fig 3). The rock types described below are easily identifiable in core, and they have distinctive characteristics which allow them to be, in some cases, uniquely placed within a stratigraphic framework.

4.2.1 *Green Tuffaceous Siltstone*

Rocks in this category consist of bedded to massive chloritic shales, siltstones and sandstones. Sandstones commonly contain porphyry fragments, but these are scoriaceous fragments which are clearly different from and easily distinguished from quartz feldspar porphyry. Rare quartz feldspar porphyry fragments are present as well. Green tuffaceous siltstone commonly displays at least one foliation, and is usually as highly strained as carbonaceous shales which are clearly part of the Koolpin Formation.

4.2.2 *Carbonaceous Shale*

This rock type is fine grained and highly carbonaceous, with siliceous layers and nodules. It is similar in composition, texture and structure to Koolpin Formation carbonaceous shales outcropping throughout the CZ. The stratigraphic relationship between carbonaceous shale and green tuffaceous siltstone has not been observed at Coronation Hill, but interbedding of the two lithologies at Palette suggests that they are different "facies" of the same rock unit.

4.2.3 *Quartz Feldspar Porphyry*

This rock type occurs throughout the Coronation Hill area, and is especially widespread in the southern drill sections. It consists of a fine grained pink to purple (hematite-altered) matrix with abundant quartz and feldspar phenocrysts, in which feldspars are altered to chlorite, sericite, or hematite depending on the overall alteration type. Quartz feldspar porphyry clearly intrudes GTS, cross cutting it and sometimes causing ?K-feldspar alteration (~pink baking) in some GTS layers. QFP is therefore clearly post-GTS and post-CARBONACEOUS SHALE. Qfp is generally devoid of internal structure, but in rare cases it is possible to see flow banding indicative of either emplacement as a lave or simply flow during intrusion.

Multiple generations of quartz feldspar porphyry are suggested because of the fact that some QFP is cut by diorite and other QFP cuts diorite. QFP which is cut by Zamu-age diorite clearly must be part of the basement. This presents an area scale paradox. On one hand, QFP is lithologically and geochemically similar to obvious post-

unconformity rock types such as Pul Pul Rhyolite and even some examples of the Plum Tree Creek Volcanics. In fact, there is little evidence that the QFP at Pul Pul Hill has undergone one less "history" of deformation and metamorphism than the QFP at Coronation Hill. All rocks of the Pul Pul Rhyolite are metamorphosed and weakly deformed as well as being altered in the South Alligator Valley, but they are still clearly less deformed and altered than pre-El Sherana Group basement rocks. At the same time, however, examples of deformed and altered felsic volcanics concordant with pre-El Sherana Group basement have been identified in an area stretching from El Sherana North to Scinto 6 (Friedmann, 1990), so it can be said that felsic volcanics do occur in the basement sequence. In the Mundogie area, these appear to be mainly concentrated in the upper Koolpin – Gerowie Tuff interval. At the same time, observations of mutual overprinting between ?Zamu dolerite and QFP suggest that at least some of the QFP has to predate El Sherana Group volcanism. One possibility is that intrusion of the porphyries continued throughout the relatively short time period separating deposition, deformation and metamorphism of the South Alligator Group from deposition of the El Sherana Group. If so, it should be possible to distinguish different porphyries based on their degree of alteration, deformation and metamorphism. Surface mapping of these variations is impeded by deep weathering, and differentiation of these types in core would require more detailed study, if indeed it is possible at all. Initial observations made as part of this study suggest that the variation in alteration, deformation and metamorphism in QFP is not great enough to suggest that there are distinct pre-unconformity and post-unconformity associations.

4.2.4 *Diorite*

This rock consists of coarse grained chloritized amphiboles and minor pyroxene in a matrix of feldspar±quartz. The chloritized amphiboles are ≤5 cm in length and form an interlocking ?ophitic network which is texturally very similar to that developed in samples of Zamu dolerite. Diorite also shows variation in grain size and igneous fractionation similar to that observed in Zamu dolerite. In some cases diorite clearly intrudes QFP, while the opposite intrusive relationship has also been observed, suggesting that QFP and diorite were at least partially synchronous.

4.2.5 *Breccias*

A whole range of rocks with clast-matrix textures are found in drill core at Coronation Hill. A complete synthesis of the origin, timing and distribution of these rock types will require more careful study, but some clear distinctions can be made (eg Carville et al, 1990). Breccias have been differentiated based on characteristics such as clast:matrix ratio, clast size, clast composition, matrix composition and timing. Using these criteria, Carville et al have defined four different breccia types: a) a polymict sedimentary breccia containing clasts of QFP, GTS, carbonaceous shale and minor diorite; b) a "monomict" sedimentary breccia consisting mainly of QFP fragments; c) a polymict sedimentary breccia containing abundant clasts of amygdaloidal basalt; and d) a late sandstone pebble conglomerate.

Polymict sedimentary breccia is a clast-supported conglomerate made up of angular clasts (≤50cm) of QFP, GTS and carbonaceous shale. This rock type occurs mainly in and under the Coronation Hill uranium pit area at the north end of the area of gold mineralization. In the pit, this rock type is in fault contact with GTS to the west and

QFP to the south. It is truncated to the north by the Callanans Fault and to the west by an unnamed north-trending fault. Diorite clasts are generally not present in this rock type, but this may not be the case universally. The ratios of various clast types are variable from place to place. Some sedimentary breccias contain clasts of quartz sandstone, possibly indicating that this rock type formed after deposition and induration of part of the Coronation Sandstone.

Monomict sedimentary breccia is a subtype of the polymict breccia which contains abundant QFP clasts. Monomict breccia has roughly the same areal distribution as polymict breccia. Monomict and polymict breccias are compositional end members, and it is very rare to find breccias in which the clasts are truly monomict. Monomict breccias can be clast-supported or matrix supported. The matrix is generally made up of finer grained clasts of qfp, gts, carbonaceous shale and sandstone. QFP clasts are often angular and sometimes display altered rinds.

Polymict basalt breccia occurs in a zone in the deeper parts of the Coronation Hill deposit, beneath the Callanans Fault and above the Koolpin unconformity. This breccia is characterized by an abundance of vesicular basalt of the type occurring within the Coronation Sandstone through the CZ (Noranda maps; Friedmann, 1990). These breccias are generally clast-supported, though medium grained sandstones of similar composition with few or no clasts occur as well. The matrix of these breccias is generally polymict, with detrital qfp, gts, carbonaceous shale etc...

Sandstone pebble conglomerate occurs as part of the capping sandstone sequence which unconformably overlies the sequence which hosts mineralization.

In addition to these sedimentary breccia types, there are a number of tectonic breccias which occur on surface and in drill core. Of these, hematite-quartz breccias are the most volumetrically significant, though hydrothermal breccias with quartz-carbonate-chlorite matrices are also common and appear to be significant for gold-platinoid mineralization.

Hematite-quartz breccia is made up of angular, silicified clasts of qfp, gts, diorite, Coronation Sandstone and vein quartz in a matrix of quartz-hematite which is cut by veins of quartz and/or earthy/specular hematite. This breccia type is very similar to Scinto Breccia. The variation in clast type seen in core is very similar to that observed on the surface around Coronation Hill. The linear distribution of Scinto Breccia on the surface, and its clearly cross-cutting and hydrothermal nature in drill core, suggest that hematite-quartz breccias formed as tectonic breccias on fault zones, rather than as siliceous cappings related to regolith formation. Breccias of this type clearly cross-cut and overprint the sedimentary breccias described above, and in some cases appear to overprint chlorite alteration associated with gold mineralization.

Quartz-carbonate-chlorite breccias take the form of zones of closely spaced, irregular and angular veins cutting qfp, diorite or gts. Quartz and chlorite in these veins is generally equigranular and almost undeformed. Veins of this type often occur in zones of gold-platinoid mineralization, and sometimes contain visible gold mineralization. In areas of uranium-gold mineralization, this vein type tends to be more chloritic and in some cases contains pitchblende and visible gold in addition to quartz, calcite and chlorite. Breccias of this type clearly postdate foliations and syndeformational veins in basement rocks. Chloritic alteration which is sometimes associated with breccias of this type overprints early chlorite and hematite alteration.

4.2.6 *Carbonates*

Deep drilling (holes 100 to 105) has intersected dolomitic/siliceous carbonate rocks at depth under the Coronation Hill deposit. These rocks are on strike with the Pul Pul Bioherm, and are therefore correlated with the carbonate facies of the Koolpin Formation. The occurrence of siliceous/dolomitic carbonates in the Koolpin Formation to the south and southeast of Coronation Hill suggests that there must be a structural repeat of calcareous Koolpin Formation in the Coronation Hill area. Gold mineralization occurs within carbonate rocks of the Koolpin formation. Rocks of this type are often siliceous and strongly recrystallized, though in some cases it is still possible to identify stromatolites and halite casts (Carville, pers comm), confirming the fringing reef/shallow water association proposed by Muir and Jackson (professional opinion...).

4.2.7 *Distribution of rock types*

1) The "dolomite-carbonaceous shale" zone occurs in the deepest drilling in the Coronation Hill area, and sits unconformably below a zone of "type C" breccia (fig 4; 5). It is made up of silicified dolomitic Koolpin Formation and minor amounts of carbonaceous shale, and is laterally equivalent to the Pul Pul Bioherm. This zone is on strike with the Pul Pul Bioherm (fig 2), but is separated from it at shallower depths by north-trending faults on both the western and eastern flanks of Coronation Hill.

2) Below and to the north of the Callanans Fault is a zone of "type C" sedimentary breccias (fig 4; 5). These breccias contain abundant clasts of basalt from the El Sherana Group, as well as other basement lithologies and lithologies from the qfp-dior-gts zone, suggesting that the qfp-dior-gts zone has been thrust or reverse faulted above the "type C" breccia zone. The "type C" breccia zone is truncated to the west by a fault contact with capping sandstone, and sits unconformably on top of dolomites and carbonaceous shales of the basement. The eastern extent of the "type C" breccia zone is unclear. "Type C" breccia has also been drilled in DDH106, which was drilled west from the north end of the Coronation Hill mineralized zone.

3) The qfp-dior-gts hosts a large proportion of the known mineralization at Coronation Hill (fig 4; 5). This is a zone in which QFP and diorite intrude GTS and minor carbonaceous shale. Contacts between rock types are often irregular, though bedding in gts is often steep northeast-dipping. This package is bounded to the north and below by the Callanan's Fault, and is separated from capping sandstone in the west by an unconformity/fault contact (fig 4). The exact nature of the eastern termination of this zone is unclear, though it appears to be laterally continuous with a zone of Pul Pul rhyolite which is clearly unconformably overlying the South Alligator Group basement.

4) Breccias of type "A" and "B" occur in and under the Coronation Hill pit (fig 2). This zone is bounded on all sides by steep faults which postdate breccia deposition. It is distinguishable from the zone of "type C" breccia by its position and by the lack of basalt clasts (Carville et al, 1990).

5) The capping sandstone zone lies to the west of the main Coronation Hill mineralization (fig 4). The eastern boundary of this zone appears to be partly faulted and partly unconformable, while the north, south and west boundaries are formed by variably silicified fault zones. The capping sandstone shows steep to moderate dips which

vary in direction across fault-bounded rock packages. Tectonic brecciation and associated hematite veining are common in this zone, though mineralization does not occur in this rock unit (Carville et al, 1990).

4.3 Mineralization

4.3.1 *Large Scale Setting*

Mineralization occurs in a broadly north-trending zone which extends approximately 300m south of the Callanans Fault (fig 2). This zone is at least partially closed off by drilling to the north and south, but has not been closed off at depth. In section, mineralization occurs in a series of relatively continuous subvertical bodies which cut across lithological boundaries.

Surface line sampling for gold, palladium and platinum has been carried out by the CHJV between 6830N and 6420N. Areas of ≥ 5 ppm gold define a northwest-trending body which begins at ~6700N/40790E and ends at ~6520N/41060E. This trend corresponds well with the main zones of high grade gold defined by drilling. The area of high grade gold passes through breccia and GTS, through a small inlier of carbonaceous Koolpin Formation, and on into qfp and diorite. This surface trend is clearly independent of rock type, though it is clearly parallel to a NNW-trending fault set which is mapped as having minor sinistral displacement in the Pit (Valenta, 1987). Fractures of this set occur elsewhere in the benches as well. The sampling shows a pattern of three main structural trends associated with gold mineralization. These trends are associated with zones of distributed fracturing on the surface, and are often associated with zones of distributed veins and breccias in the subsurface. Minor gold mineralization also occurs within the east-trending Callanans Fault. Gold mineralization does not occur to the north of this feature, but it clearly extends under it in the subsurface.

4.3.2 *Small Scale Setting*

The textural settings of selected visible gold occurrences are shown in figure 6. In Au-PGE-only mineralization, visible gold occurs as disseminated specks in irregular quartz-carbonate-chlorite veins or breccias (figs 6b,c,d), and as flattened flecks in chloritic seams cutting green tuffaceous siltstones (fig 6a). An example of visible gold associated with uranium mineralization is shown in figure 6e. In this setting, high grade disseminated gold occurs in pitchblende-chlorite-quartz breccias cutting and altering quartz feldspar porphyry. A complex alteration zoning associated with uranium mineralization is shown in figure 6f. In this sample, a central seam of chlorite + pitchblende is surrounded by an inner zone with a hematitic matrix and chloritized feldspar phenocrysts. This passes outward into a zone of pale green matrix with chloritized feldspar phenocrysts, and finally into the pre-existing purple hematitic matrix with hematite-altered feldspar phenocrysts. In this case, mineralization is clearly associated with chloritization of feldspar phenocrysts.

In summary, visible gold occurs in association with late veins and breccias containing varying proportions of quartz, carbonate, chlorite and pitchblende. In some cases, there is significant chloritization of the groundmass associated with mineralization. The veins postdate most deformation features, and vein fills are generally undeformed, suggesting a late timing for mineralization. These textures indicate that fracturing on a small scale controlled the focussing of mineralizing fluids, confirming observations of fracture control on larger scales.

4.3.3 *Timing and Controls*

The localization of uranium, gold and platinumoids at Coronation Hill is clearly related to NNW-trending subvertical zones of distributed fracturing, veining and hydrothermal brecciation. Evidence for the timing of these features is as follows:

- a) NNW-trending fractures post-date the north-trending east block-up fault in the Coronation Hill uranium pit (fig 2). This constrains the timing of mineralization to relatively late in the faulting history.
- b) Veins and fractures associated with this set cut across sedimentary breccias which contain clasts of El Sherana Group lithologies. This indicates that mineralization occurred after deposition, erosion and re-deposition of El Sherana Group lithologies.
- c) The NNW-trending fracture/vein set clearly postdates ductile fabrics and deformed veins in green tuffaceous siltstone and carbonaceous shale.
- d) Gold mineralization also occurs on the Callanan's Fault, which does not appear to be displaced by NNW-trending features.

These lines of evidence suggest that NNW-trending fracture zones and the Callanan's Fault formed relatively late in the deformation history of the Coronation Hill area, certainly after or late during deposition of the El Sherana Group. It is difficult to determine the temporal relationship between mineralization and the Capping Sandstone, since they are spatially separated at Coronation Hill and elsewhere in the South Alligator Valley.

Unlike other uranium-gold-platinumoid deposits in the Conservation Zone, gold-platinumoid mineralization at Coronation Hill does not show a clear association with a specific lithology such as carbonaceous shales which appear to localize mineralization elsewhere in the South Alligator Valley. Both uranium-gold-platinumoid and gold-platinumoid-only mineralization types occur in all rock types, not just in or near carbonaceous shales. So, while the structural control is similar to that observed elsewhere in the valley, the chemical cause of metal precipitation is not so clear. Possible alternatives to the accepted model involving redox control by black shales include: i) redox by mixing with methane-rich fluids (eg Wilde et al, 1990); ii) redox by interaction between fluids and chloritic lithologies (eg diorite, gts, and qfp in places; or iii) increase in fluid pH associated with buffering by K-feldspar-rich or carbonate-rich lithologies.

4.4 **Alteration**

Carville et al (1990) described a series of alteration mineralogies which varied from rock type to rock type (table x), which were overprinted by a late and areally extensive earthy hematite alteration. They concluded that there was no spatial or temporal relationship between alteration and mineralization. The following main types of alteration were observed during the course of this study:

- a) Early chlorite alteration occurs in gts and dior and is associated with the development of ductile foliations which predate the El Sherana Group elsewhere in the valley. This alteration type is clearly pre-mineralization, and is probably associated with metamorphism and metasomatism of basement lithologies occurring prior to deposition of the El Sherana Group.

b) In some places, gts and diorite show a red, hematitic coloration. This alteration appears to pseudomorphously overprint early chloritic alteration, and is also clearly replaced by chloritic alteration envelopes associated with mineralized veins. This suggests that this alteration type also predates mineralization.

c) Chloritic alteration envelopes occur in some cases in association with mineralized veins, especially those associated with high grade uranium mineralization. In fig x, there is a clear chloritic alteration envelope in which feldspars are hematized in the hematite zone and chloritized in the chloritic envelope. This indicates that chlorite alteration in this case postdates hematite alteration.

d) Late veins of earthy and/or specular hematite occur in mineralized host rocks and in capping sandstone.

In addition to these alteration types, Warren and Kamprad (1990) have identified a regional-scale carbonate alteration, which is also evident in some parts of the Coronation Hill deposit. As well as this, the overall pyrite content of the Coronation Hill host rocks is much greater than the regional pyrite content for the same rock types. For example, qfp is normally devoid of pyrite, while in some areas of the Coronation Hill deposit pyrite contents in qfp can be as large as 20%. However, there does not appear to be a small scale spatial correlation between Au-platinoids and pyrite.

4.5 Coronation Hill Critical Observations

Uranium mineralization occurs rarely in a subvertical zone running under the old Uranium pit, to a depth well below that of the planned Au-PGE pit. Significant U is often accompanied by significant Au, though the opposite is clearly not true. Uranium mineralization occurs in conglomerates containing carbonaceous clasts, but also occurs in chloritic zones which alter quartz-feldspar porphyry. In this case, there is no clear redox control like that proposed for most unconformity-related uranium deposits.

Gold mineralization occurs in a series of NNW-trending subvertical bodies which correlate on surface with a series of zones of late distributed brittle fracturing. Displacements on these features are negligible.

On a small scale, gold mineralization occurs in or in indirect association with:

- quartz-(calcite-chlorite-pyrite) veins and breccias which postdate deposition of the various breccia types.
- carbonaceous clasts in breccias.
- uranium-bearing chloritic alteration zones and quartz-chlorite-pitchblende veins.
- polished/sheared chloritic/sericitic rocks and on foliation surfaces.

Gold mineralization can be hosted by type "A", "B" and "c" breccias, dolomitic Koolpin formation, carbonaceous Koolpin Formation, Green Tuffaceous Siltstone, Diorite and Quartz-Feldspar Porphyry. There does not appear to be a strong preference for any single rock type.

On a large scale, Coronation Hill is situated in an area of relatively complex N- and E- trending dip slip faults. It is an area in which sedimentary breccias of various types are common. Breccia types "A", "B" and "C" are all

debris flow deposits, suggesting syndimentary faulting. In other words, Coronation Hill is an area of intense, long-lived faulting during and after sedimentation.

NNW-trending fault-fracture zones which host mineralization show small, predominantly strike-slip displacements, while earlier faults show larger, predominantly dip-slip displacements.

Gold at Coronation Hill does not show a strong spatial association with the sub-El Sherana group or the sub-Katherine River Group unconformity.

There is a slight positive relationship between the occurrence of gold mineralization and the occurrence of chlorite veining and alteration, while there is a slight negative relationship between the occurrence of gold mineralization and the occurrence of hematite alteration and veining. In some cases, chlorite appears to be paragenetically associated with uranium/gold, while in other cases it clearly predated mineralization.

On a large scale, the Coronation Hill area appears to be situated on a dilational jog on the Palette Fault system.

Early chlorite alteration occurs within GTS and diorite in the Coronation Hill area. This is overprinted by a pre-mineralization phase of hematite alteration. A later chlorite alteration overprints early hematite alteration, and this is in turn cross cut by late veins and associated alteration containing coarse specular hematite.

Mineralization at Coronation Hill can be broadly separated into "U-Au-Platinoid" mineralization (occurring in and under the old pit) and "Au-Platinoid" mineralization which is very low in uranium (occurring over the rest of the orebody). Zones of high grade uranium mineralization also contain high grade gold and are often recognizable by their intense chlorite alteration.

4.6 Exploration model

The following significant characteristics could be used to direct exploration for mineralization of the gold-platinoid-only type:

- a) Mineralization at Coronation Hill occurs in dilatant fractures on a north-trending fault jog associated with the main northwest-trending fault system in the South Alligator Valley. The range of fracture geometries expected for another deposit of the same type would be similar to that observed in uranium deposits in the South Alligator Valley.
- b) Mineralization is hosted in a broad range of pre- and post-unconformity rock types. The only rock type in the area which does not host significant mineralization is the quartzitic Capping Sandstone. Thus, the chemical and structural role of the unconformity does not appear to be as important in this deposit type.
- c) Mineralization is associated with green tuffaceous siltstones, quartz feldspar porphyry and Zamu dolerite equivalents which are characteristic of the upper levels of the Koolpin Formation-Gerowie Tuff sequence in the Mundogie region and elsewhere in the South Alligator Valley. This suggests that areas containing rocks which are stratigraphically above the carbonaceous shale- cherty ferruginous shale sequence may be particularly prospective for deposits of this type.

- d) Mineralization is associated with a chlorite-sericite alteration of quartz feldspar porphyry which may be recognizable in surface exposures.
- e) Mineralization is clearly associated with small scale and large scale (eg Callanan's Fault) quartz veining and silicification, in contrast to U-Au-PGE mineralization in the South and East Alligator regions.

4.7 Potential of the Coronation Hill area

Extensions to existing mineralization

The Coronation Hill area occurs in a zone of large scale dilatancy on the northwest-trending Palette Fault system (Valenta 1989; 1990). Within this framework, orebodies should be more extensive vertically than horizontally. Though mineralization at Coronation Hill is in tabular zones, on a large scale they *do* appear to define a pipe-like body with a subvertical long axis. This, combined with the fact that present drilling has failed to close off mineralization at depth, suggests that there is good potential for significant undiscovered mineralization at depth.

The Callanan's fault does not *displace* mineralization. Rather, it is part of the fault mineralizing system, with mineralization both above and below. There is only one drill hole to the north of this fault, and more drilling must be done before areas to the north of the Callanans Fault at depth can be discounted.

Broader potential of the area

The area to the west of Coronation Hill is a "mirror image" of the mineralized area of Coronation Hill, with similar rock types and structures (fig 4). In this area, mixed quartz feldspar porphyry and cherty ferruginous shales are truncated to the east by a fault which brings capping sandstone down to the east. The orientation and timing of this fault is not known, though there is every possibility that this fault is similar in timing to the fault which forms the western boundary of the Coronation Hill mineralized zone. This area warrants further examination on the basis of these characteristics and favourable bleg results.

A number of north-trending faults also cut across the north end of Coronation Hill. Rock types in this area are also similar to those at Coronation Hill, though poor exposure makes it difficult to provide a detailed assessment of this area.

5 El Sherana

Mineralization at El Sherana is hosted in NW-striking, steeply-dipping to subvertical carbonaceous shales (carbonaceous shale) and cherty ferruginous shales (cherty ferruginous shale) of the Koolpin Formation, and to a lesser extent by sandstones, conglomerates and felsic volcanics of the El Sherana Group. In the El Sherana area, uranium mineralization occurs in two broad settings:

At or near the shallow-dipping to subhorizontal South Alligator Group/El Sherana Group unconformity, where it is cut by normal and revers faults. This is the setting of uranium mineralization in the main El Sherana pit. Mineralization in this setting defines a high grade, subhorizontally-pitching "carrot-shaped" body.

In irregular bedding-parallel zones entirely within carbonaceous shale and cherty ferruginous shale of the Koolpin Formation. Uranium orebodies of this type are irregularly distributed from El Sherana West to El Sherana, and often show gentle west pitches. Mineralization often occurs at the contacts between carbonaceous shale and cherty ferruginous shale.

5.1 Structural Setting

El Sherana Group and basement lithologies are exposed in pits and surface outcrops in the El Sherana area. Basement lithologies consist of cherty ferruginous shales, carbonaceous shales and minor bs/gts of the Koolpin Formation. Basement lithologies strike northwest and are subvertical. Detailed underground drilling shows that carbonaceous shales and cherty ferruginous shales occur in irregular alternating layers and lenses (figs 7, 8). Individual layers show significant lateral and vertical thickness changes.

Basement lithologies are unconformably overlain by sandstones, conglomerates and felsic volcanics of the El Sherana Group, with a subhorizontal to gently-dipping angular unconformity (fig 7). Detailed mapping in the El Sherana pit shows a number of different fault orientations, with the two main fault orientations being steep southwest-dipping normal faults and moderate to shallow southwest-dipping later reverse faults (Valenta 1988; 1989). Late faults occurring in the subvertical basement are generally extensional, with shortening parallel to layering and extension in subvertical and northwest-southeast directions. Late faults in basement lithologies take the form of zones of intense foliation, brecciation and gouge formation, often occurring at carbonaceous shale-cherty ferruginous shale contacts.

5.2 Rock Types

Access to drill core at El Sherana has allowed a detailed examination of the characteristics of Koolpin Formation host rocks in the El Sherana area. Unfortunately, poor gold results in recent drilling has made it difficult to assess the small scale controls on gold distribution in this area. The observed concentration of uranium mineralization at carbonaceous shale-cherty ferruginous shale contacts makes it worthwhile to describe in more detail the characteristics of these two rock types.

5.2.1 Carbonaceous Shale

Carbonaceous shales consist of strongly foliated pyritic carbonaceous layers interbedded with varying proportions of siliceous layers and siliceous nodules. Siliceous layers can be up to 2-3 cm in width, while nodules are generally less than 1cm in diameter. Massive carbonaceous pyritic lithologies occur in some cases as well. The fine grained carbonaceous matrix often shows multiple penetrative cleavages, generally at a small angle to layering, while siliceous layers often show penetrative veining and brecciation. Siliceous nodules are often ellipsoidal, with long axes subparallel to cleavage. They are also often fractured and veined. This indicates that formation of siliceous

bands and growth of siliceous nodules occurred prior to or very early during cleavage development. Both the carbonaceous matrix and siliceous beds/nodules are cut by syndeformational quartz veins and breccias.

5.2.2 *Cherty Ferruginous Shales*

Cherty ferruginous siltstone is made up of bands of red, earthy hematitic material interbedded with siliceous layers which are similar in thickness and spacing to those which occur in carbonaceous shales. Siliceous nodules also occur in this rock type. Both ferruginous and siliceous layers show the effects of penetrative brittle deformation, including closely spaced fracturing and veining, indicating that cherty ferruginous shale was already ferruginous and competent prior to deformation.

Contacts between cherty ferruginous shale and carbonaceous shale are often gradational, involving the occurrence of hematitic veins and alteration zones in carbonaceous shales. This, and the similar character and proportion of siliceous layers and nodules, suggests that at least some of the cherty ferruginous shales may have formed as a pre- to early- deformation metasomatic replacement of black shale. It should be pointed out that cherty ferruginous layers are regionally extensive and often correlatable on a small scale over large distances, so any metasomatic replacement must be regional in extent.

The contacts between carbonaceous shale and cherty ferruginous shale are often zones of intense shearing and foliation development within carbonaceous shale and intense brittle deformation within cherty ferruginous shale, so textures indicative of replacement of carbonaceous shale by hematite may have formed during circulation of hydrothermal fluid related to movement on shear zones at these lithological contacts.

Core from recent drilling at El Sherana also contains minor amounts of "bleached shale", which appears to be simply a surface oxidation of carbonaceous shales and chloritic shales and siltstones. Chlorite has a long paragenetic history in the Koolpin Formation in the El Sherana area. It is sometimes clearly pre-deformation, and other times clearly overprints syndeformational veins and occurs as alteration zones around late fractures. There does not appear to be a strong correlation between uranium mineralization and chlorite.

5.2.3 *Distribution of Uranium mineralization*

In El Sherana West and underground, uranium mineralization appears to have been associated with a number of carbonaceous shale-cherty ferruginous shale contacts (fig 8a). Individual stopes were irregular and pitched horizontally to shallow west (fig 9). On a smaller scale, uranium orebodies were made up of veins of massive pitchblende, often with significant associated gold. Zones of minor uranium mineralization in core at El Sherana are associated with late (late to post cleavage) shearing and associated brittle deformation.

The large scale controls on uranium mineralization at El Sherana appear to be both chemical and structural in nature. In this case, competency contrast between carbonaceous shale and cherty ferruginous shale produced permeability and drove fluid flow, and the redox interface between carbonaceous shale and cherty ferruginous shale caused the precipitation of uranium. It is envisaged that oxidized fluids flowed downward through fractured and permeable CFS's, with focussed fluid flow occurring around cross-cutting extensional faults. Zones of maximum

strain incompatibility in this model would have occurred where extensional faults intersected the cherty ferruginous shale-carbonaceous shale contact. In the case of vertical extension (suggested by the occurrence of a steep stretching lineation), intersection zones should be subhorizontal to shallow-plunging.

Structural observations at El Sherana (Valenta 1988; 1989) suggest that there were episodes of both normal and reverse faulting on the unconformity in the main pit. In basement lithologies, associated structures generally take the form of late extensional faults and shear zones. In the case of the main El Sherana pit, permeability was produced by intense faulting on the unconformity, while the redox interface occurred at the contact between El Sherana group lithologies and Koolpin Formation carbonaceous shales.

The contacts in the El Sherana West and underground area are coplanar with the zone of mineralization in the main El Sherana pit (fig 7a). The mineralized zones are subparallel to the main Palette Fault system, but occur approximately 1-200m to the southwest of it (fig 1). Displacements in the El Sherana, subsurface and El Sherana West areas do not appear to be large (eg fig 7). One implication of this is that there may be other El Sherana-style occurrences of mineralization in the area at different stratigraphic levels and lateral locations. Areas which would warrant further exploration encompass Stag Creek in the northwest to High Road in the southeast.

5.2.4 Distribution of Gold Mineralization

Observations of gold mineralization are based solely UUNL assay sections and plans compiled by Porter (1987). PGE's were not assayed in underground fan drilling, but it is notable that the single high gold assay in recent drilling also contained high a high palladium value. The following general observations can be made:

- 1) Gold grades are very high, very patchy and discontinuous. There is often little agreement between adjacent and cross-cutting drill holes, suggesting either assay problems or extremely discontinuous mineralization (eg fig 8b)
- 2) Gold in underground drilling defines two large scale discontinuous trends: a major trend at approximately 820RL/100N; and a minor trend at 960RL/230N (fig 9). These pods appear to plunge 10°-15° in long section, and there may be another stacked pod in and to the south of the El Sherana West pit.
- 3) Gold intersections are more widespread than defined uranium pods, but the zone of gold mineralization corresponds on a large scale to the overall zone of uranium mineralization (fig 9). In section, the carbonaceous shale/cherty ferruginous shale contact does not appear to concentrate gold mineralization to the same extent that it concentrates uranium mineralization (eg fig 8b).
- 4) Gold mineralization occurs in carbonaceous shale, cherty ferruginous shale and bleached shale, and appears to be most common in cherty ferruginous shale (fig 8b).

5.2.5 Recent Exploration

In the last five years the CHJV has drilled five exploration holes in the El Sherana area and has re-entered and sampled old underground adits. Results of these investigations have been poor, but it is worthwhile to assess these results in light of available knowledge on the geology and distribution of gold mineralization.

ES DDH 30 was drilled on the 340E section, and passed to the north of and under the main gold grades shown in the 340E section (Porter, 1987). In this section, the northern contact between carbonaceous shale and cherty ferruginous shale has minor gold shows, while the main gold mineralization was intersected within cherty ferruginous shale near the southern carbonaceous shale/cherty ferruginous shale contact. Grab samples from both #1 and #2 drive rises and stopes gave grades in the 1-20 ppm range.

ES DDH 34 was drilled in the 600E section. It passed to the north of an identified zone of gold mineralization drilled from the 960 level adit, passed to the north of an identified zone of gold mineralization drilled from 820 level, and intersected a 2m zone of 7.16 ppm gold in a zone where gold in this section was not previously intersected.

ES DDH 32 drilled on the 110E section. It passed through a zone of gold mineralization which was drilled from 820 level, but failed to intersect any mineralization. Again, this suggests either a very patchy gold distribution or suspect UUNL assay results.

ES DDH 31 was drilled on the 285E section. It passed close to a zone which intersected high gold values, but failed to contain any mineralization.

ES DDH 33 was drilled on the 980E section. It passed through a zone of detailed fan drilling from 820 level, again with no elevated gold values.

The 960 level and 927 level adits were re-entered and sampled with generally poor results. No gold mineralization was intersected in 927 level drilling, so it is not surprising that adit sampling gave generally poor results. The 960 level adit passes through the smaller of the two large scale zones of mineralization, but again underground drill holes showed generally low values in the vicinity of the adit. Two assays of >10ppm are found near the El Sherana open cut in the 960 adit. Underground drilling shows that the main zone of gold (from present information) is centred around the 750-900 level and 100N. Thus, sampling in the 820 level adit would have been likely to have shown the greatest development of gold mineralization, had it been sampled.

5.3 Summary

The following main points have emerged from this study of the geology and mineralization at El Sherana:

- a) Mineralization in the El Sherana area occurs within northwest-striking, subvertical carbonaceous shales, cherty ferruginous shales and bleached shales of the Koolpin Formation, and to a lesser extent within sandstones, conglomerates and felsic volcanics of the El Sherana Group near the El Sherana Group-basement unconformity.
- b) Cherty ferruginous shales and carbonaceous shales contain similar chert nodules and layers, and often show diffuse contacts in which carbonaceous material appears to be replaced by hematite along fractures and veins. This suggests that cherty ferruginous shales are at least partly a product of metasomatic replacement of carbonaceous shales.
- c) Uranium mineralization at El Sherana occurs in two main settings: i) in shallow northwest-pitching bodies along subvertical carbonaceous shale-cherty ferruginous shale contacts in Koolpin Formation

(eg El Sherana West); and ii) in zones where faults intersect the El Sherana Group unconformity (eg El Sherana main pit).

- d) Gold mineralization occurs in spatial association with uranium orebodies, but also occurs away from uranium mineralization, often within cherty ferruginous shale layers. This suggests a slightly different chemical control on gold precipitation in the area.
- e) Gold grades are high but discontinuous, and define two large scale northwest-pitching trends. These may be associated with the intersections between bedding and steep extensional faults within the basement.
- f) Recent drilling and adit sampling carried out by the CHJV failed to test the area of gold mineralization defined by UUNL underground drilling and adit/stope sampling. The program did show that mineralization may not persist at depth, as was previously suggested by UUNL drilling.

5.4 Exploration Model

U-Au-platinoid mineralization at El Sherana occurs in two main settings: i) In a zone of complex faulting on the El Sherana Group unconformity, above carbonaceous lithologies; and ii) along and near the sheared contacts between carbonaceous shales and cherty ferruginous shales up to 100m below the El Sherana Group unconformity. In both these cases, critical features for identification of further mineralization include proximity to the unconformity, the presence of carbonaceous lithologies and the presence of late subsidiary faults (eg Needham, 1987).

5.5 Potential of the El Sherana area

Using these criteria, it is clear that the El Sherana area shows good potential for more mineralization in the following settings:

- a) In other locations associated with the same NNW-trending subsidiary fault to the main Palette Fault.
- b) In other analogous subsidiary fault zones cutting carbonaceous shales in close vertical proximity to the unconformity.
- c) Au-platinoid-only mineralization in fault/fracture zones near the unconformity above "Kapalga-like" gts-qfp lithologies exposed in basement to the northeast of El Sherana.

Recent CHJV drilling in the El Sherana area tested the downward continuation and/or periphery of known U-Au mineralization at El Sherana. Surrounding areas remain virtually untested at depth.

6 Palette

6.1 Structural Setting

The Palette deposit occurs just to the southwest of the main Palette fault (fig 10), in an area of normal, reverse and strike-slip faulting which cuts the sub-El Sherana Group unconformity and the sub-Kombolgie unconformity.

The following faults have been observed in the Palette area (fig 11):

- a) In section, and from drill hole control (fig 12), it can be seen that the main Palette Fault zone is a wide zone of high strain in South Alligator Group lithologies.
- b) The "#1 adit fault" (fig 11) is a north-trending fault which dips 65° to 70° east and cuts through the main Palette pit. The #1 adit fault shows apparent east-up/dextral displacement, bringing Koolpin Formation in the east into fault contact with Coronation sandstone in the west. This fault hosts the only major uranium mineralization discovered in the Palette area.
- c) The "#5 adit fault" (fig 11) is a fault set which brings green tuffaceous siltstones of the Koolpin formation into fault contact with cherty ferruginous shales, and also separates green tuffaceous siltstones from Coronation Sandstone. This fault set appears to be truncated by the #1 adit fault in the Palette area.
- d) The faults described above are cross cut by the "#2 adit fault" (fig 11), a moderate to shallow southwest-dipping reverse fault which causes a structural doubling of the unconformity immediately to the southeast of the Palette pit. This fault does not host mineralization.
- e) The "Skull Fault" (fig 11) is similar in orientation and displacement to the #1 adit fault, and hosts mineralization in the Skull area. There are a number of minor faults in this orientation between Skull and Palette as well.

The #1 adit fault and the Skull Fault are similar in orientation and displacement to the fault set which hosts mineralization in the Coronation Hill area (fig 2). It is interesting to note that both of these faults are truncated by the Kombolgie Formation, suggesting that their displacement occurred prior to deposition of the Kombolgie Formation.

The section shown in fig 12 has been extrapolated from surface exposures and recent drilling by the CHJV. The #1 adit fault (a) and the Palette Fault Zone (b) bring El Sherana Group rocks down to the southwest under the Scinto Plateau, against rocks of the South Alligator Group. A fault with opposite displacement can be inferred to extend under the Scinto Plateau from exposures at the northwest end of the Plateau. The southwest margin of the Scinto Plateau is defined by a wide (≤25m) zone of siliceous and variably hematitic brecciation, the Clear Springs Fault (d).

6.2 Host Rocks

Mineralization at Palette appears to have been hosted in both basement and cover lithologies. South Alligator Group basement lithologies have been intersected in recent exploration drilling by the CHJV. All basement lithologies drilled in this area are within or near the Palette Fault Zone and show strong foliation development, intense shearing and intense veining in places. The main South Alligator Group lithologies are carbonaceous shales and chloritic siltstones/sandstones.

Carbonaceous Shales are similar to those occurring at El Sherana. They are finely laminated pyritic shales with siliceous interbeds and nodules.

At Palette, highly strained chloritic siltstones and sandstones are common, and are very similar to Green Tuffaceous Siltstones occurring at Coronation Hill. They consist of a fine grained chloritic matrix with chloritic, quartzose and volcanic clasts. The clast to matrix ratio varies from bed to bed and area to area. GTS is also exposed along the road leading to Palette and at the northwest end of the Scinto plateau (see map).

El Sherana Group lithologies in the Palette area consist of hematitic vesicular "basalt" and medium grained grey quartz sandstone overlain in places by quartz feldspar porphyry of the Pul Pul Rhyolite. The faulted nature of most contacts makes it difficult to determine the local stratigraphy, but a regional study of El Sherana Group stratigraphy (Friedmann, 1990) has suggested that vesicular volcanics occur only once, at the base of the El Sherana Group. If this is the case, then the basalt/sandstone sequences must be structurally doubled in the area immediately to the northwest of the northernmost Palette adit.

El Sherana Group lithologies are unconformably overlain by basal conglomerate and sandstone of the Kombolgie Formation. However, this unit has been tentatively correlated with the Kurrundie Sandstone by Friedmann (1990).

6.3 Distribution of Mineralization

Mineralization at Palette is reported to have occurred mainly on the sub-El Sherana Group unconformity and in and around faults near this unconformity. There is very little information available on the detailed distribution of mineralization in the Palette area, so it is difficult to draw concrete conclusions on overall prospectivity and identification of favourable areas. The scant information available suggests that gold and uranium show a positive correlation.

6.4 Palette Drilling Program

The four Palette drill holes were drilled along a single section (fig 12) in an attempt to improve the understanding of a small portion of the Palette area and to test the north-trending fault. Like at Coronation Hill, the north-trending fault separates El Sherana Group and younger rocks from basement lithologies. The Palette drillholes, therefore, test an area which is structurally (and to some extent lithologically) similar to the zone of (U)-Au-PGE mineralization at Coronation Hill. A major difference at Palette is the lack of intrusive quartz feldspar porphyry and diorite. In addition, Palette drill holes contain little evidence of the relatively late quartz-carbonate-chlorite veining of the type which is associated with mineralization at Coronation Hill.

6.5 Potential of the Palette area

Estimation of the potential of the Palette area suffers from: 1) lack of information on the distribution and nature of known uranium and gold mineralization and 2) a very restricted area of coverage by recent drilling.

However, the NNE-trending faults in the Palette and Skull areas do appear to be similar in orientation and timing to those which host mineralization at Coronation Hill. It should be noted that host rocks in the Skull-Palette area are more carbonaceous than those developed at Coronation Hill, suggesting that any new mineralization will contain uranium as well as gold and platinoids. The continuation of these faults under the Scinto Plateau, however, is

likely to occur in dolomitic lithologies similar to those occurring at depth beneath Coronation Hill. This area may therefore be more prospective for gold-platinoid-only mineralization of the Coronation Hill type.

7 The Conservation Zone

7.1 Types of Mineralization

Characteristics of *U-Au-PGE* mineralization and *Au-PGE-only* mineralization are contrasted in table 1. The two main differences between the two end member types are host rocks and mineralization textures. *U-Au-PGE* deposits are hosted mainly in and around carbonaceous shale and cherty ferruginous shale of the Koolpin Formation, though at Coronation Hill mineralization also occurs in sedimentary breccias and in quartz feldspar porphyry. *Au-PGE-only* mineralization, on the other hand, occurs in a broad range of host rocks with different mineralogical makeup and chemical compositions, including qfp, gts, dior, dolomite, sedimentary breccias and cherty ferruginous shale.

Primary *U-Au-PGE* mineralization in the South Alligator Valley takes the form of pitchblende veins, often associated with chlorite alteration, with little or no quartz veining except at late stages (eg Threadgold, 1960). *Au-PGE-only* mineralization at Coronation Hill shows a strong association with quartz-carbonate-chlorite veins. Both of these points suggest that the chemistry of mineralizing fluids and the nature of the chemical control on deposition differs from one type to the other, while the overall similarity in timing and structural controls suggests that the two types were part of the same broad mineralizing event.

The presence of two distinct mineralization types has implications for area-scale prospectivity in the new CZ:

- the two orebody types may occur together at Coronation Hill, but they may occur separately elsewhere.
- *Au-PGE-only* orebodies without uranium will not be detected by radiometric measurements, and are not necessarily associated with conductors which may be detected by electromagnetic methods. The best way to detect orebodies of this type is by geochemical surveys.

7.2 The Role of Structure in Deposit Localization

The role of structure in ore deposit localization in the South Alligator Valley has been dealt with in detail in Valenta (1988; 1989; 1990), which built on the research of Matheson (1960), Johnston (1984), Johnston and Wall (1984), Needham (1987) and Needham and Stuart-Smith (1987). To summarize the results of these publications, heterogeneous deformation on the large scale fault system produces localized zones of dilatancy and permeability which allow the focussed flow of mineralizing fluids (eg Guha et al, 1983; Cox et al, 1987). When metal-bearing fluids interact with the appropriate rock types (or other fluids) in these dilatant zones, they produce ore deposits. Dilatant structures of this type in the South Alligator Valley include:

- 1) Zones of competency contrast (eg cs-cfs competency contrast at El Sherana).
- 2) North-trending dilatant minor faults in extensional settings (eg Palette, Coronation Hill) (cf Sibson, 1987).
- 3) Subhorizontal dilatant structures in contractional settings (eg Rockhole, El Sherana)

The localization of mineralization on minor faults within the major system suggests that minor faults show orientations and geometries which are favourable for fluid focussing during deformation, while major faults show orientations and geometries which are most favourable for accommodation of regional strain (Valenta, 1990b).

7.3 Area-Scale prospectivity

7.3.1 *General*

The new CZ shows a high prospectivity for a number of reasons. It occurs in an area of known large scale alteration, indicating the penetrative passage of large volumes of possibly ore bearing fluids. The characteristics of the recently discovered Coronation Hill gold-platinoid deposit are such that gold-platinoid mineralization alone may not have been discovered by previous exploration in the South Alligator Valley. The area is therefore prospective on a large scale and contains numerous areas with favourable rock types and structure, independent of known prospects. Potential prospects identified below (fig 13) include areas showing favourable rock types and structure, and areas with anomalous results which don't fit U-Au-PGE or Au-PGE-only exploration models.

7.3.2 *Saddle Ridge Northeast*

Saddle Ridge Northeast occurs in a zone of complex faulting on the unconformity separating upper Koolpin - Kapalgia lithologies and sandstones, basalt and quartz feldspar porphyry of the El Sherana Group, in an area between the Palette Fault and the Fisher Fault. The lack of carbonaceous shale in this area means that the occurrence of a uranium deposit is unlikely. On the other hand, the host rocks and structural setting of the area are similar to Coronation Hill. Because of this, the Saddle Ridge Northeast area may have the potential for and Au-PGE-only deposit which would not have been detected by radiometric methods. This assertion is at least partly supported by the occurrence of anomalous BLEG results in the area.

7.3.3 *Pul Pul Hill*

At Pul Pul Hill, the Pul Pul Rhyolite sits unconformably over siliceous dolomites of the Pul Pul Bioherm. Reconnaissance mapping in the area suggests that faulting is common, though the lack of markers in the Pul Pul Rhyolite makes it difficult to trace many faults. Again, this is an area which may contain gold-only mineralization which may not have been detected by radiometric methods.

7.3.4 *Clear Springs*

The Clear Springs Fault in the Scinto Plateau area is a zone of strong silicification. It appears to have been active at the same time as the Palette Fault, yet it shows the same level of silicification shown by the Palette Fault system to the southeast of Coronation Hill, where it is interpreted to be at a higher level in the fluid circulation system (Valenta, 1989). The Clear Springs Fault is an area in which gold assays from the 1990 BMR sampling program have not always been associated with high uranium, once again suggesting the possibility of Au-PGE-only mineralization.

7.3.5 *Stockpile/Flying Fox*

This group of prospects occurs in an area in which Pul Pul Rhyolite unconformably overlies or is in fault contact with the Mundogie Sandstone and the Stag Creek Volcanics. In the Mundogie area, there is good evidence for a regional fault in this position, though it is generally poorly exposed in the South Alligator Valley. Mineralization in the Stockpile/Flying Fox area may be associated with a lateral equivalent of this fault.

7.3.6 *Fisher Fault*

The Fisher Fault defines yet another area in which there is penetrative fracturing cutting host rocks which lack carbonaceous lithologies and are similar to those at Coronation Hill. In the Scinto VI area and along strike, basement lithologies consist of Koolpin-age felsic volcanics, green tuffaceous siltstones and Zamu Dolerite, overlain in places by Coronation Sandstone. Thus, this area contains structures and host rocks similar to those at Coronation Hill, and therefore has potential for Au-PGE-only mineralization which would not have been detected in previous exploration.

8 Conclusions

- 1) The new Conservation Zone shows a high potential for further unconformity-style mineralization of the El Sherana-Rockhole-Palette type, and even greater potential for undiscovered Au-PGE-only mineralization of the type occurring in parts of the Coronation Hill deposit.
- 2) The Coronation Hill deposit is a fracture-controlled unconformity-related U-Au-PGE deposit, with distinctive U-rich and U-poor portions. Mineralization is controlled by NNW-trending fracture zones with relatively small displacements. These zones formed late in the faulting history, probably after deposition of the Kombolgie Formation.
- 3) On a small scale, both types of mineralization often occur in association with veins and breccias with varying proportions of quartz, chlorite and calcite. Veins of this type formed late in the deformation history, and clearly formed the permeable pathways for mineralizing fluids.
- 4) Mineralization at Coronation Hill is persistent through a range of rock types, in contrast to the strong carbonaceous shale association shown by other deposits in the South Alligator Valley. This work has supported the conclusion of Carville et al (1990) that at least some of the quartz feldspar porphyry in the Coronation Hill area must be coeval with the basement, since it is intruded by Zamu Dolerite. Quartz feldspar porphyry and green tuffaceous siltstone may be lateral equivalents of Gerowie Tuff occurring in the Mundogie region. Rocks of this type occur elsewhere in the CZ, and must be considered prospective for Au-PGE-only mineralization.
- 5) Au-PGE-only deposits should occur in relatively competent lithologies which are penetratively fractured in relative proximity to major faults. Possible favourable rock types may include chlorite-rich lithologies such as green tuffaceous siltstone and Zamu dolerite, K-feldspar-bearing lithologies such as quartz feldspar porphyry or calcareous lithologies.

- 6) The Coronation Hill deposit is presently open at depth, and its structural setting suggests that mineralization should pitch subvertically on a large scale, which implies that mineralization should persist at depth for some distance below the unconformity.
- 7) The Coronation Hill West area shows similar structures and rock types to Coronation Hill, and must be considered to be highly prospective for mineralization similar to that developed at Coronation Hill. Other areas which show similar host rocks and structural settings include the Saddle Ridge Northeast area, the Pul Pul Hill area, and the portion of the Fisher Fault occurring within the CZ.
- 8) Gold mineralization at El Sherana occurs around, but often slightly removed from, zones of uranium mineralization. Gold mineralization at El Sherana is generally high grade but patchy and discontinuous. Uranium mineralization is generally concentrated at the contact between carbonaceous shales and cherty ferruginous shales in the El Sherana area, while gold occurs more commonly within cherty ferruginous shales. Both uranium and gold mineralization occur in shallow northwest-pitching bodies, possibly controlled by the geometry of fault/bedding intersections.
- 9) Drilling by the CHJV in the El Sherana did not generally pass through or near zones of known gold mineralization defined from UUNL underground drilling. Thus, while recent drilling failed to find *extensions* to mineralization at El Sherana, it did not test the mineralized zone defined from UUNL drilling. The El Sherana mine area will require much more testing before the nature and distribution of gold mineralization is fully understood. In addition, there has been little testing for extensions of mineralization along and across strike from El Sherana.
- 10) The Cliff Face-Palette-Skull region is a zone of structural and stratigraphic complexity with little subsurface geological and assay control. Recent drilling by the CHJV contributed to geological knowledge about the three dimensional geometry of rock units, but certainly did not test the potential of this region.

9 Acknowledgements

Field work which forms the basis for this report was performed while the author was employed as a contract geologist by the Bureau of Mineral Resources. The following are acknowledged:

- Lesley Wyborn and Liz Jagodzinski for logistical assistance.
- Lesley Wyborn, Stuart Needham, Peter Stuart-Smith, Mike Etheridge, Julio Friedmann, Liz Jagodzinski, Yanis Mieztis, Bill McKay, Aden McKay, Ian Lambert, Gladys Warren, Vic Wall, Rod Page and Andy Wilde for useful geological discussions.
- Dean Carville and Foy Leckie for geological discussions and help, tolerance and consideration in difficult circumstances.
- Mike Sherwood for all sorts of things.
- Jim Kalma, Richard Morse and Matt Noakes for invaluable field assistance

- Draga Gelt for drafting assistance
- Margaret Beckers for manning the fax machine

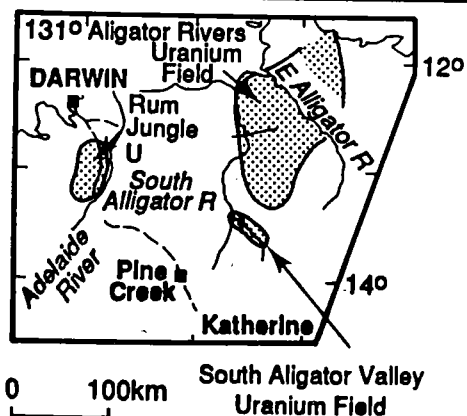
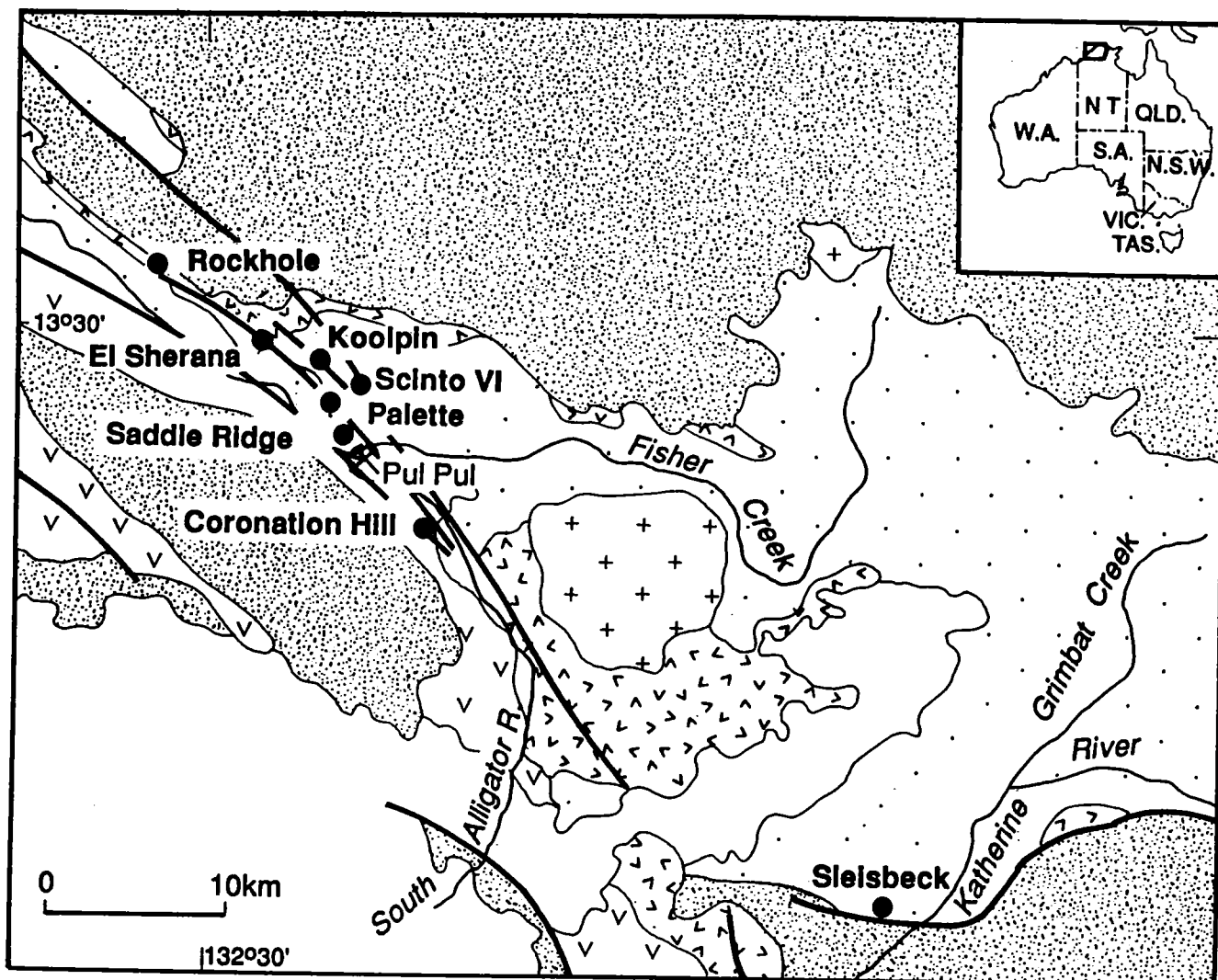
10 References

- Ayres, D.E. and Eadington, P.J., 1975. Uranium mineralization in the South Alligator Valley. *Mineralium Deposita*. 10: 27-41.
- Carville, D.P., Leckie, J.F., Moorhead, C.F., Rayner, J.G. and Durbin, A.A., 1990. Geology and mineralization of the Coronation Hill gold-platinum-palladium prospect, Northern Territory. AusIMM Australian Mineral Deposits Volume.
- Christie-Blick, N.H. and Biddle, K.T., 1985. Deformation and basin formation along strike-slip faults. In Biddle, K.T. and Christie-Blick, N. (eds.), Strike-Slip Deformation, Basin Formation, and Sedimentation: *Society of Economic Paleontologists and Mineralogists Special Publication no. 37*: pp. 1-34.
- Cox, S.F., Etheridge, M.A., and Wall, V.J., 1987. The role of fluids in syntectonic mass transport, and the localization of metamorphic vein-type ore deposits. *Ore Geology Reviews*. 2: 65-86.
- Friedmann, S.J. and J.P. Grotzinger, 1991. Stratigraphy, Sedimentology and Tectonic Evolution of the El Sherana and Edith River Groups, Northern Territory, Australia. BMR Record 1991/108.
- Friedmann, S.J. and J. P. Grotzinger, 1989. Facies and Basin development during sedimentation of the 1.86 Ga El Sherana and Edith River Groups, Pine Creek Orogen, Northern Territory, Australia, Geological Association of America Annual Meeting, Abstracts with programs, 21,
- Guha, J., Archambault, G. and Leroy, J., 1983. A correlation between the evolution of mineralizing fluids and the geomechanical development of a shear zone as illustrated by the Henderson 2 mine, Quebec. *Economic Geology*, 78: 1605-1618.
- Harding, T.P., Vierbuchen, R.C. and Christie-Blick, N., 1985. Structural styles, plate-tectonic settings, and hydrocarbon traps of divergent (transtensional) wrench faults. In Biddle, K.T. and Christie-Blick, N. (eds.), Strike-Slip Deformation, Basin Formation, and Sedimentation: *Society of Economic Paleontologists and Mineralogists Special Publication no. 37*, pp. 51-77.
- Johnston, D.J. and Wall, V., 1984. "Why unconformity-related uranium deposits are unconformity-related." *Abs. Geol. Soc. Aust.* v. 12, 285-287.
- Johnston, J.D., 1984. Structural evolution of the Pine Creek Inlier and mineralization therein, N.T., Australia. Ph.D. thesis, Monash University, Clayton, Victoria, 268pp.
- M. A. Etheridge, R. W. R. Rutland and L. A. I. Wyborn, 1987. Orogenesis and tectonic process in the early to middle Proterozoic of Australia: in A. Kröner, Proterozoic Lithosphere Evolution, American Geophysical Union, Geodynamic Series 17, 115-130
- Matheson, R.S., 1960. Report on holdings of United Uranium, N.L., South Alligator River area, N.T. Unpublished company report.
- Needham, R.S. and Stuart-Smith, P.G., 1985. Stratigraphy and tectonics of the Early to Middle Proterozoic transition, Katherine-El Sherana area, N.T. *Australian Journal of Earth Sciences*, 32: 219-230.

- Needham, R.S., 1987. Review of mineralization in the South Alligator Valley. BMR Record 1987/52.
- Needham, R.S., Stuart-Smith, P.G. and Page, R.W., 1988. Tectonic Evolution of the Pine Creek Inlier, Northern Territory. *Precambrian Research*, 40/41: 543-564.
- Needham, R.S. and P. G. Stuart-Smith, 1987. Coronation Hill U-Au mine South Alligator Valley, Northern Territory, Australian: an epigenic sandstone-type deposit hosted by debris-flow conglomerate. B.M.R. Journal of Australian Geology and Geophysics, 10, 121-131
- Needham, R.S., I. H. Crick and P. G. Stuart-Smith, 1980. Regional Geology of the Pine Creek Geosyncline: in J. Ferguson and A. B. Goleby, Uranium in the Pine Creek Geosyncline.
- Porter, C.A., 1987. Assessment of previous work in the proposed Conservation Zone South Alligator Valley, N.T. Confidential Coronation Hill Joint Venture report, C.R. 5448.
- Sibson, R.H., 1987. Earthquake rupturing as a mineralising agent in hydrothermal systems. *Geology*, 15: 701-704
- Stuart-Smith, P.G., Wills, K., Crick, I.H. and Needham, R.S., 1980. Evolution of the Pine Creek Geosyncline. In Ferguson, J., and Goleby, A.B., (editors), Uranium in the Pine Creek Geosyncline. International Atomic Energy Agency, Vienna. 23-38.
- Threadgold, I.M., 1960. The mineral composition of some uranium ores from the South Alligator River area, N.T. C.S.I.R.O., Melbourne, *Mineragraphic Technical Investigations Technical Paper* 2, 53.
- Valenta, R.K., 1988†. A report on Mineralization and structure in the South Alligator Valley. Unpublished report to the Bureau of Mineral Resources.
- Valenta, R.K., 1989. Structure and Mineralization in the South Alligator Valley, N.T. Part 1 of this volume: *Structural controls on Mineralization of the Coronation Hill Deposit and Surrounding Area*. Record 1991/107.
- Valenta, R.K., 1990a. Structure and Mineralization in the Mungogie and Eastern Stow areas, Kakadu Stage III, N.T. Part 2 of this volume: *Structural controls on Mineralization of the Coronation Hill Deposit and Surrounding Area*. Record 1991/107.
- Valenta, R.K., 1990b. "Structural setting of unconformity related U-Au-Platinoid mineralization in the South Alligator Valley, NT. Abstracts volume, 1990 Australian Geological Convention, Hobart.
- Warren, R.G., and Kamprad, J.L., 1990. Mineralogical, petrographic and geochemical studies in the South Alligator Region, Pine Creek Inlier, N.T. *Bureau of Mineral Resources, Geology and Geophysics, Australia, Record* 1990/54, (114 pp)
- Wall, V.J., and Valenta, R.K., 1990. Ironstone-related gold-copper mineralisation: Tennant Creek and Elsewhere. AusIMM Pacific Rim Congress, Extended Abstracts, 855-863.
- Wilde, A.R., Bloom, M.S., and Wall, V.J., 1989. Transport and deposition of gold, uranium and platinum group elements in unconformity-related deposits. *Economic Geology Monograph*, 6, 637-650.

† The findings of this report are incorporated in Valenta 1989, which is reproduced as part 1 of this record.

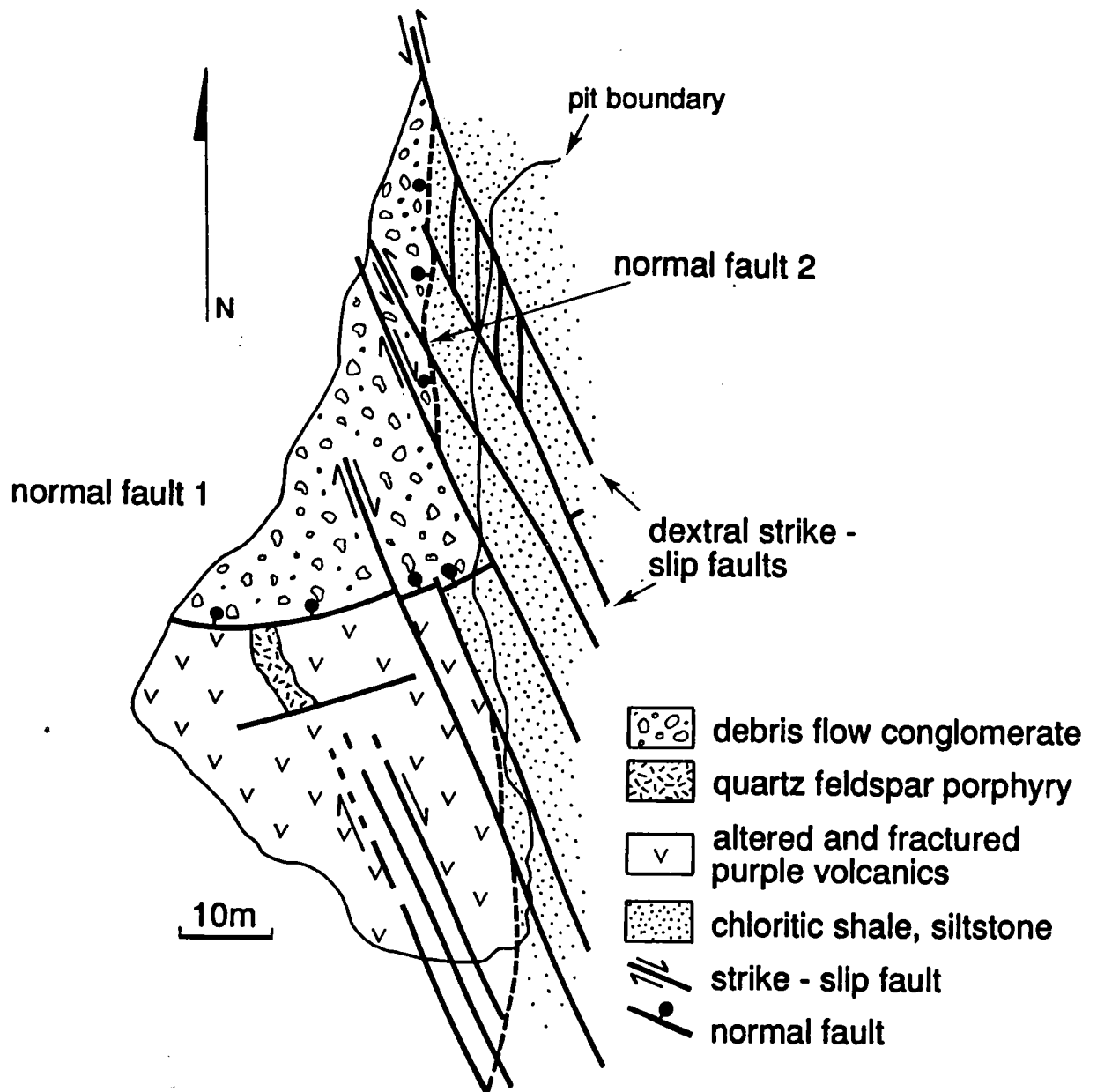
Figure 1. Regional Geology of the South Alligator Valley
(after Needham and Stuart-Smith, 1987)



- Mesozoic, Cainozoic**
Undivided sediments
- Middle Proterozoic**
Sandstone, basalt
- Late Early Proterozoic**
Edith River Group volcanics, sediments
- + Granite
- El Sherana Group volcanics, sediments
- Early Proterozoic**
Undivided metasediments
- Uranium mine

Figure 2. Geological map of the Coronation Hill area (source of data: Author and Noranda/CHJV mapping). Inset shows the detailed geology of the Coronation Hill Uranium Pit.

CORONATION PIT



CORONATION HILL - FAULTS

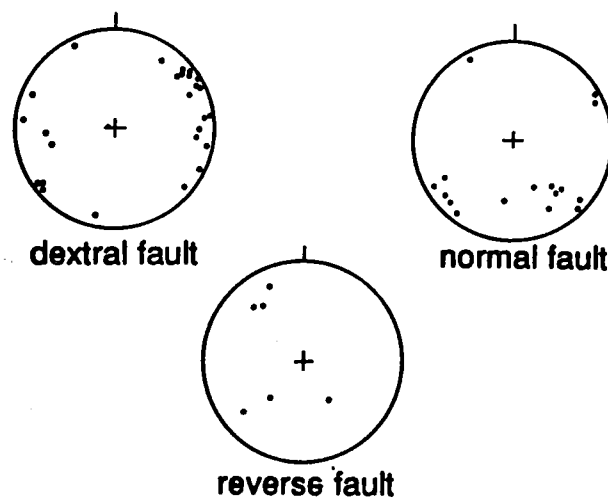
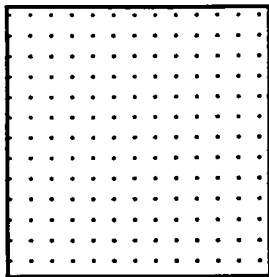


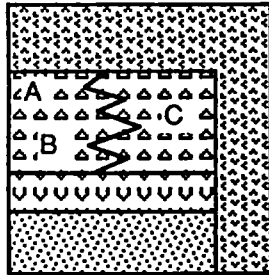
Figure 3. Revised Stratigraphy of the Coronation Hill deposit and nearby area, based partly on CHJV data and interpretation.



capping
sandstone

Kombolgie Sandstone

unconformity



qtz-fs porph
(intrusive and extrusive)

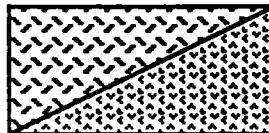
a/b brecc c
brecc

basalt

sandstone

El Sherana Group

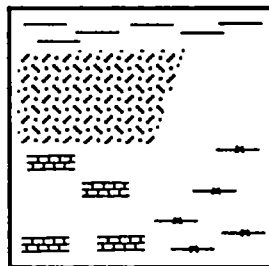
unconformity



diorite

quartz-
feldspar porph.

Zamu dolerite
+
?Gerowie Tuff equivalent?



shale

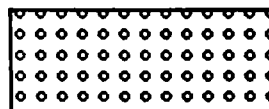
green
tuffaceous
siltstone

carb
shale

siliceous
dolomite

cherty
ferrug
shale

Koolpin
Formation



Mundogie
Sandstone

Figure 4. E-W cross section (6640N) through the Coronation Hill deposit and surrounding area. Note the steep fault on the west side of Coronation Hill, which brings capping sandstone in the east into fault contact with quartz-feldspar porphyry in the west.

6640N SECTION

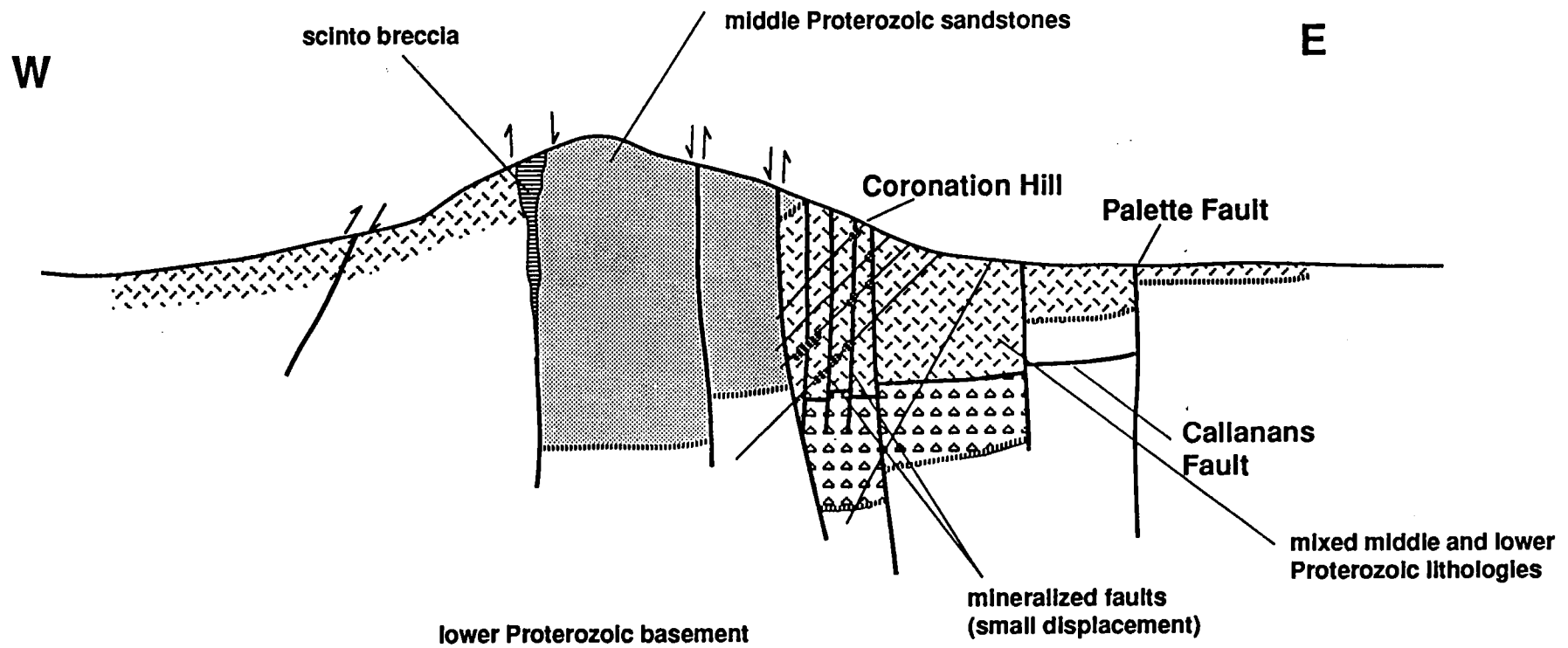
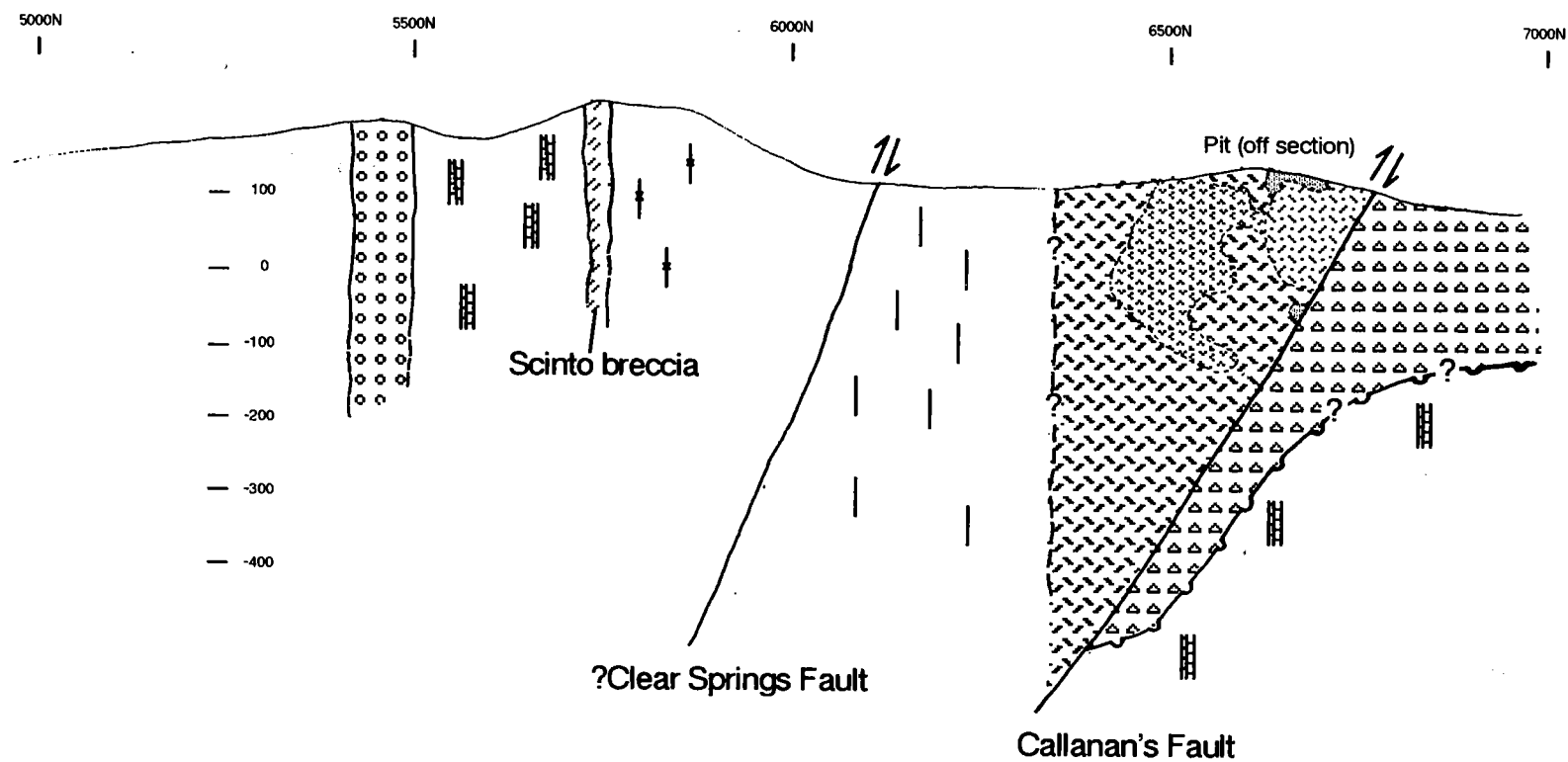


Figure 5. N-S section through the Coronation Hill deposit. See figure 3 for rock units.



Coronation Hill Long Section - 41000E

Figure 6. Textures associated with visible gold. **a)** Specks of visible gold along shear zones cutting chloritic layers in green tuffaceous siltstone. **b)** Polymict hydrothermal breccia in green tuffaceous siltstone. **c)** Quartz-calcite-chlorite vein cutting quartz feldspar porphyry **d)** Late quartz-chlorite seam perpendicular to bedding. **e)** Gold and pitchblende in a quartz-chlorite hydrothermal breccia. **f)** Complex alteration zoning associated with pitchblende seams.

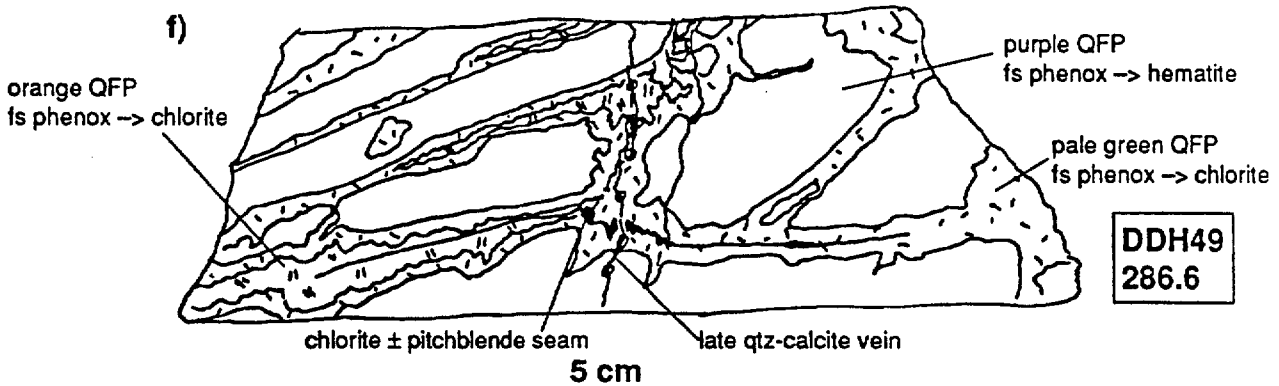
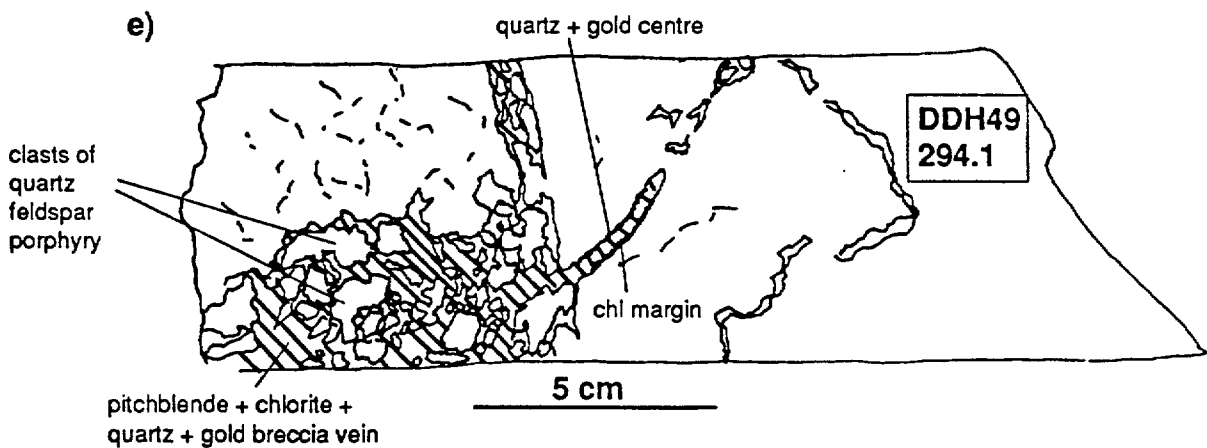
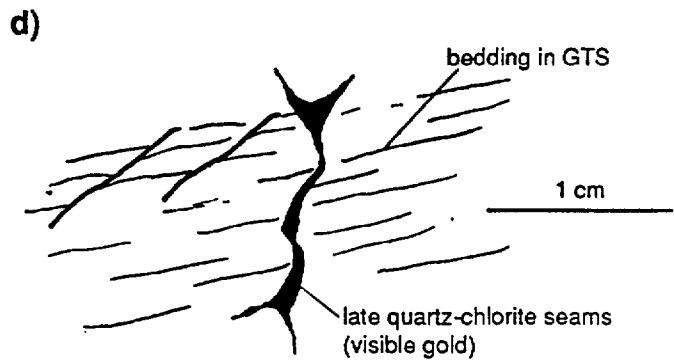
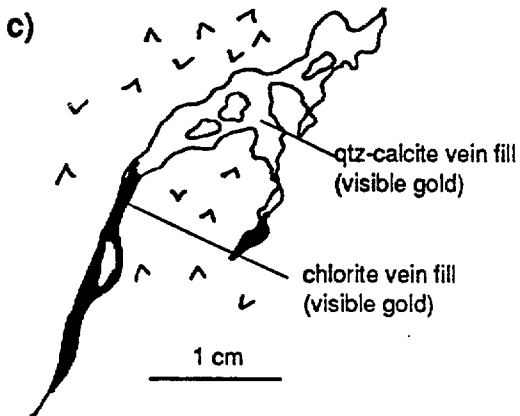
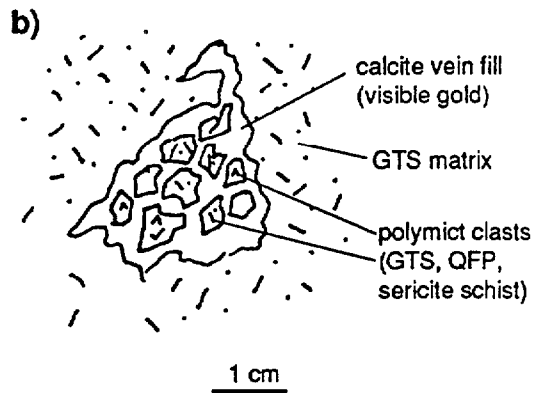
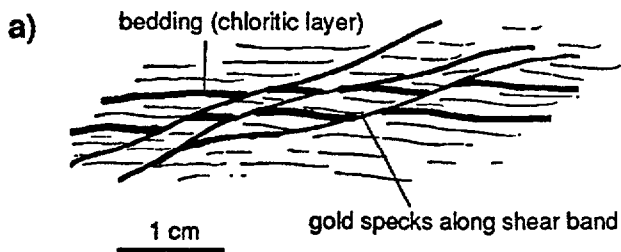


Figure 7A

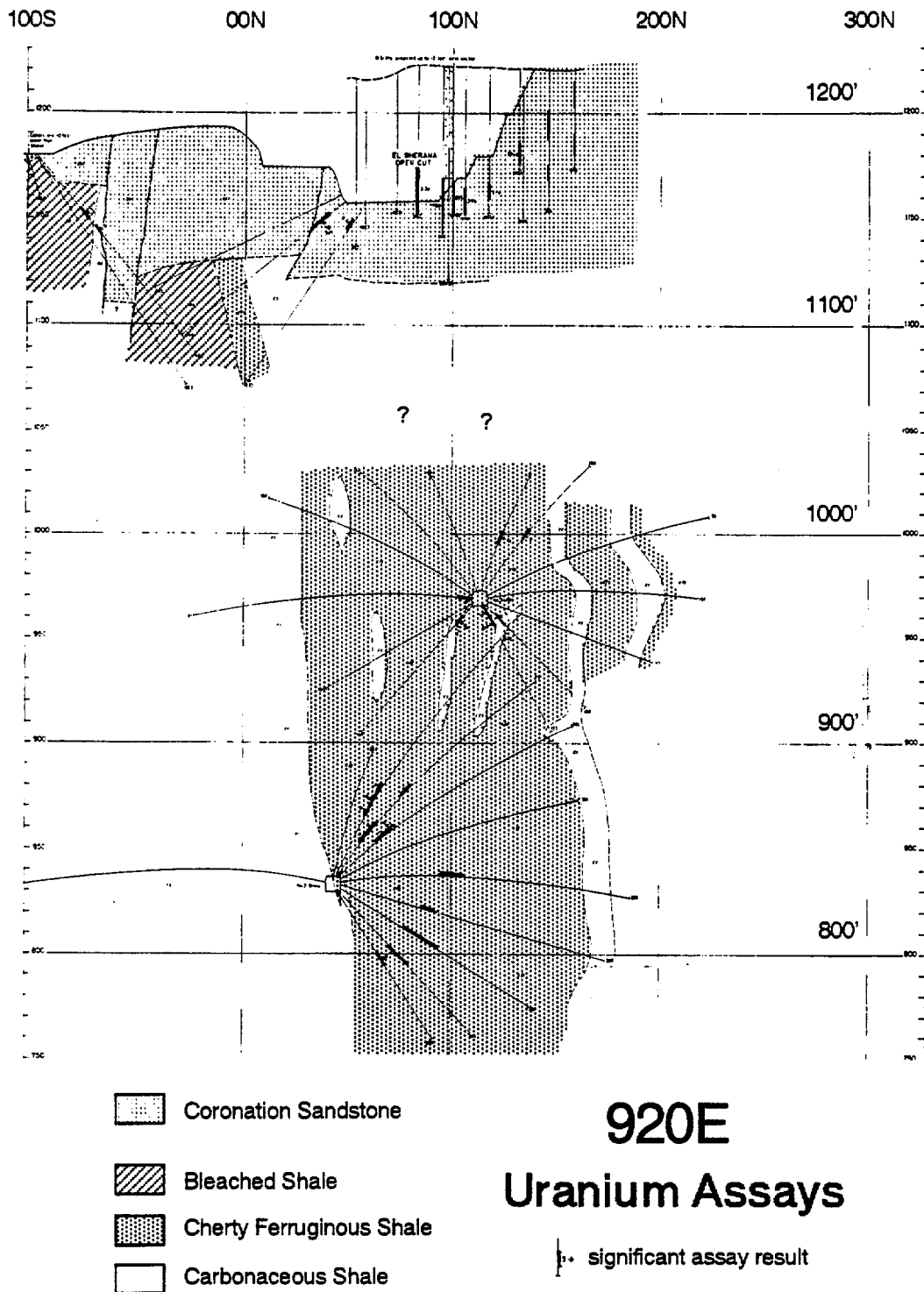


Figure 7. Sections showing gold and uranium distribution in the 920E section at El Sherana. a) Uranium. b) Gold.

Figure 7B

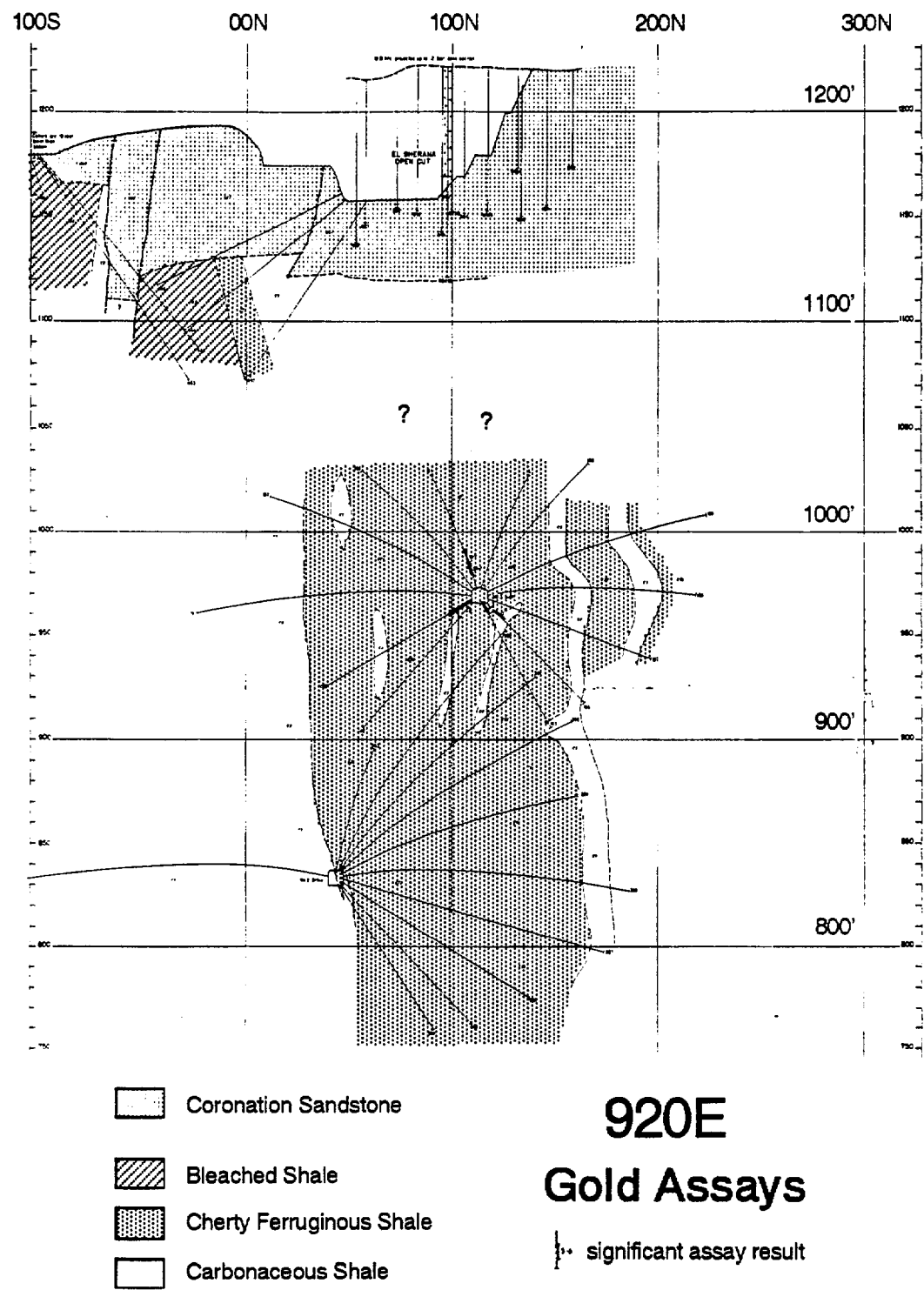


Figure 8A

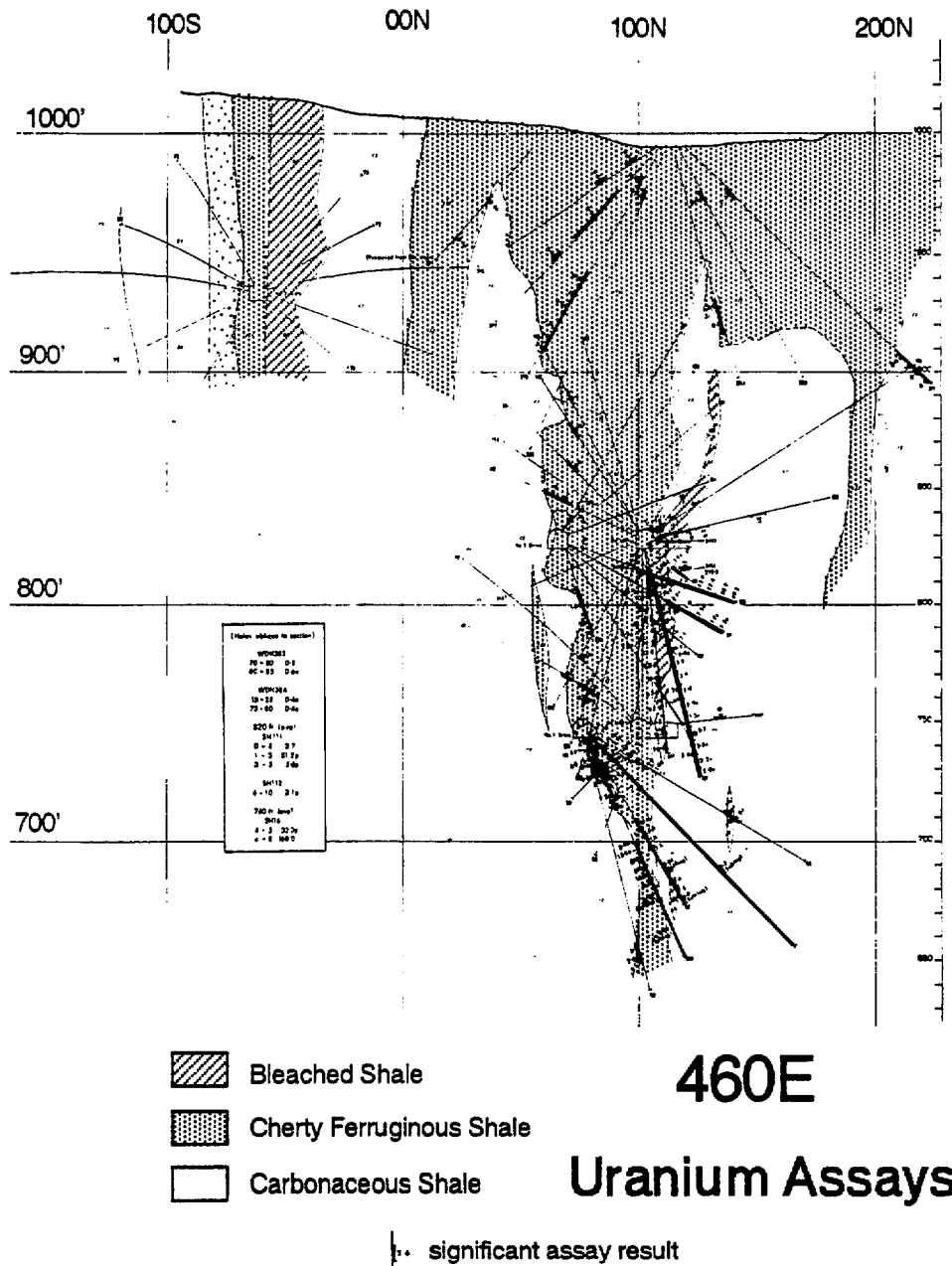


Figure 8. Sections showing gold and uranium distribution in the 460E section at El Sherana. a) Uranium. b) Gold.

Figure 8b

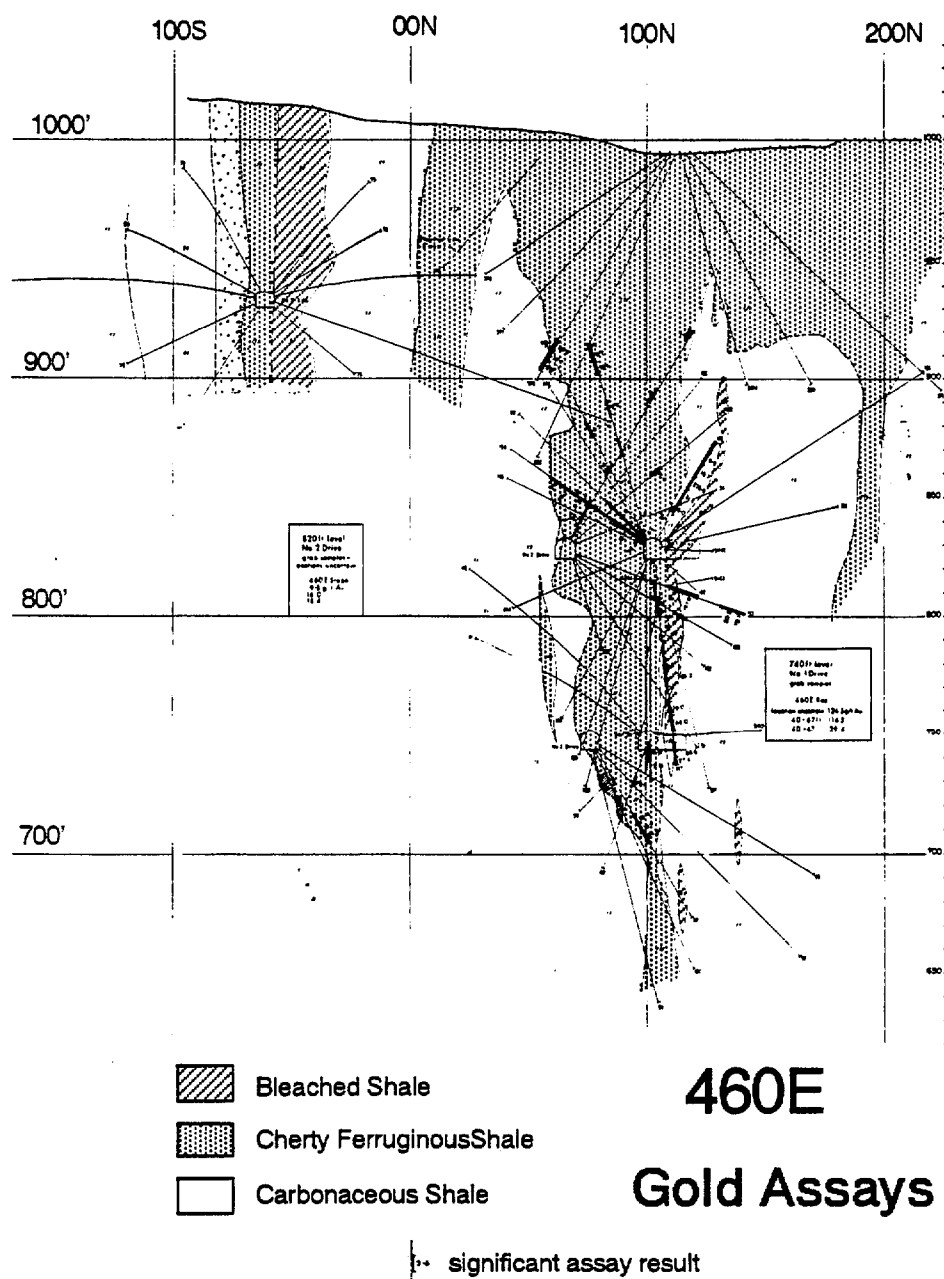


Figure 9. El Sherana line section showing the distribution of gold and uranium mineralization based on the results of UUNL underground drilling. Uranium mineralization in the main El Sherana Pit is projected onto the section.

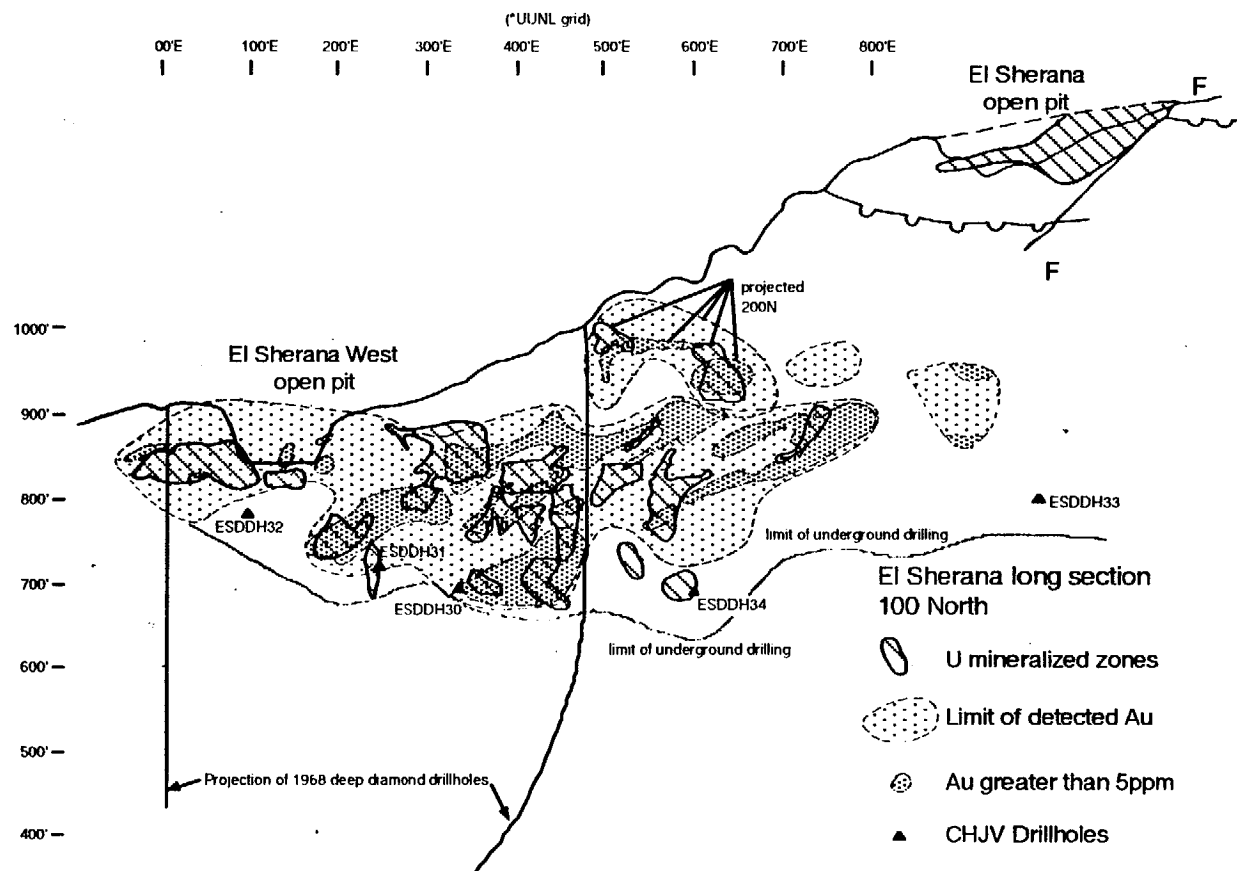
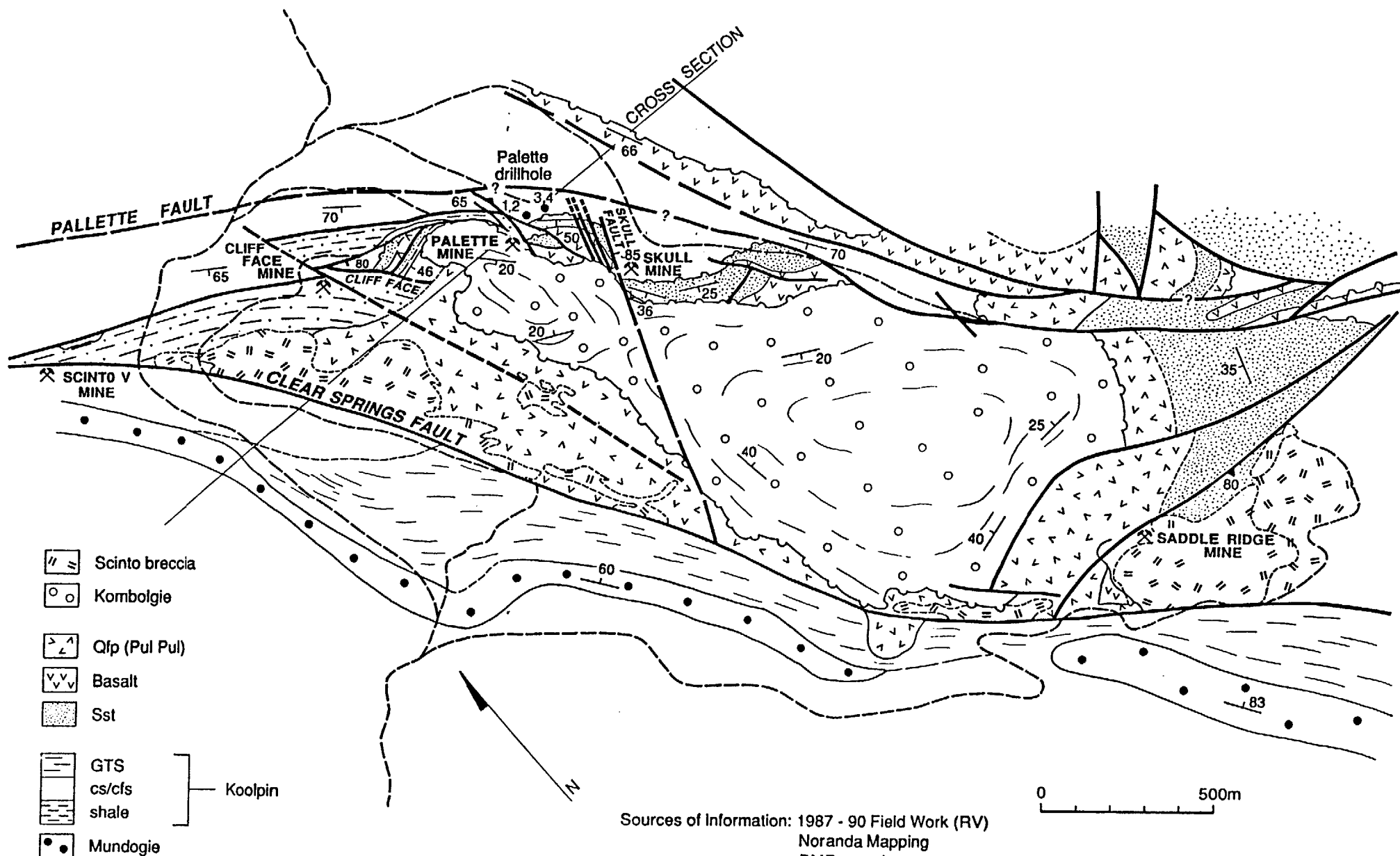


Figure 10. Geological map of the Palette area.



Sources of Information: 1987 - 90 Field Work (RV)
 Noranda Mapping
 BMR mapping
 J. Friedman

Figure 11. An enlargement of figure 10, showing faults referred to in text.

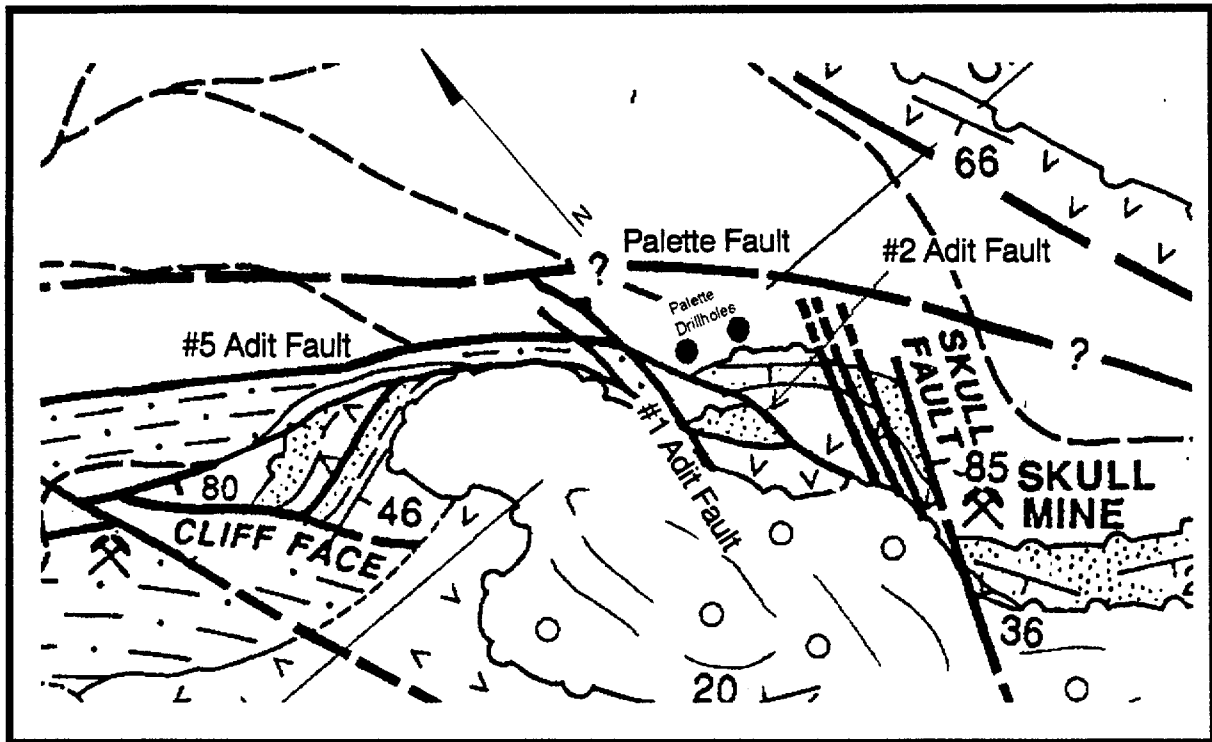
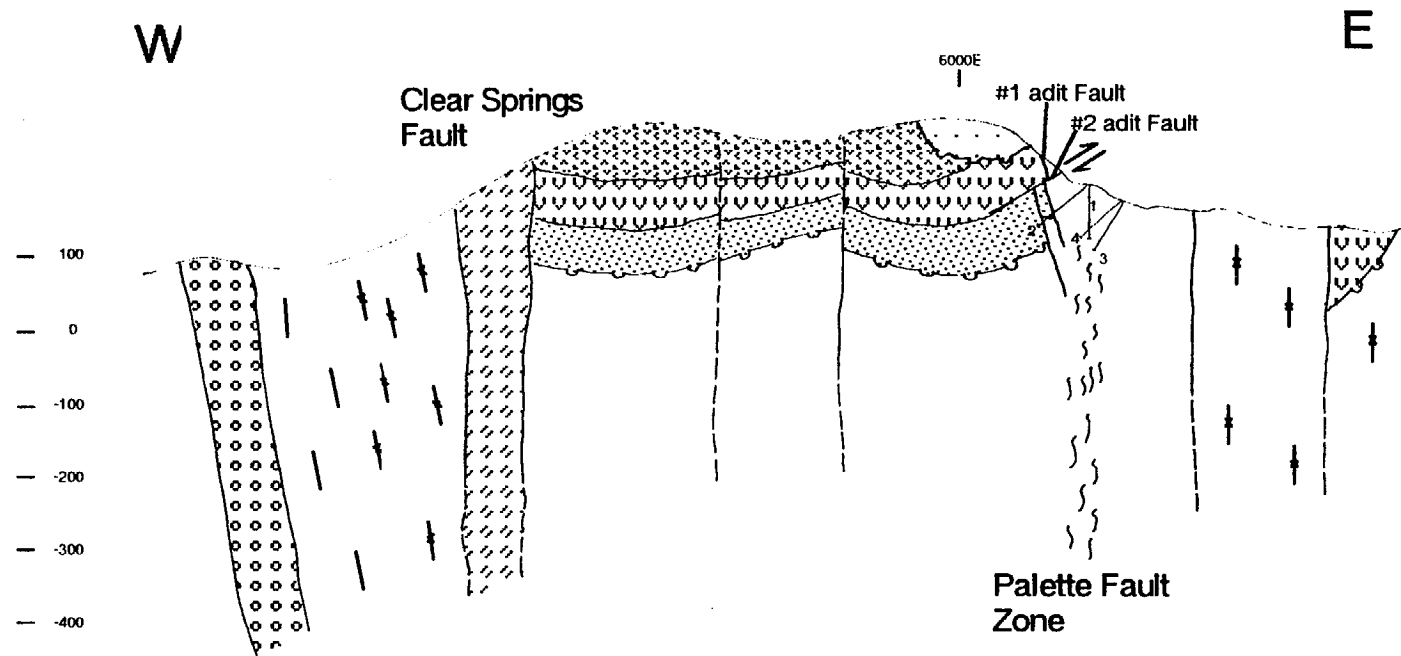
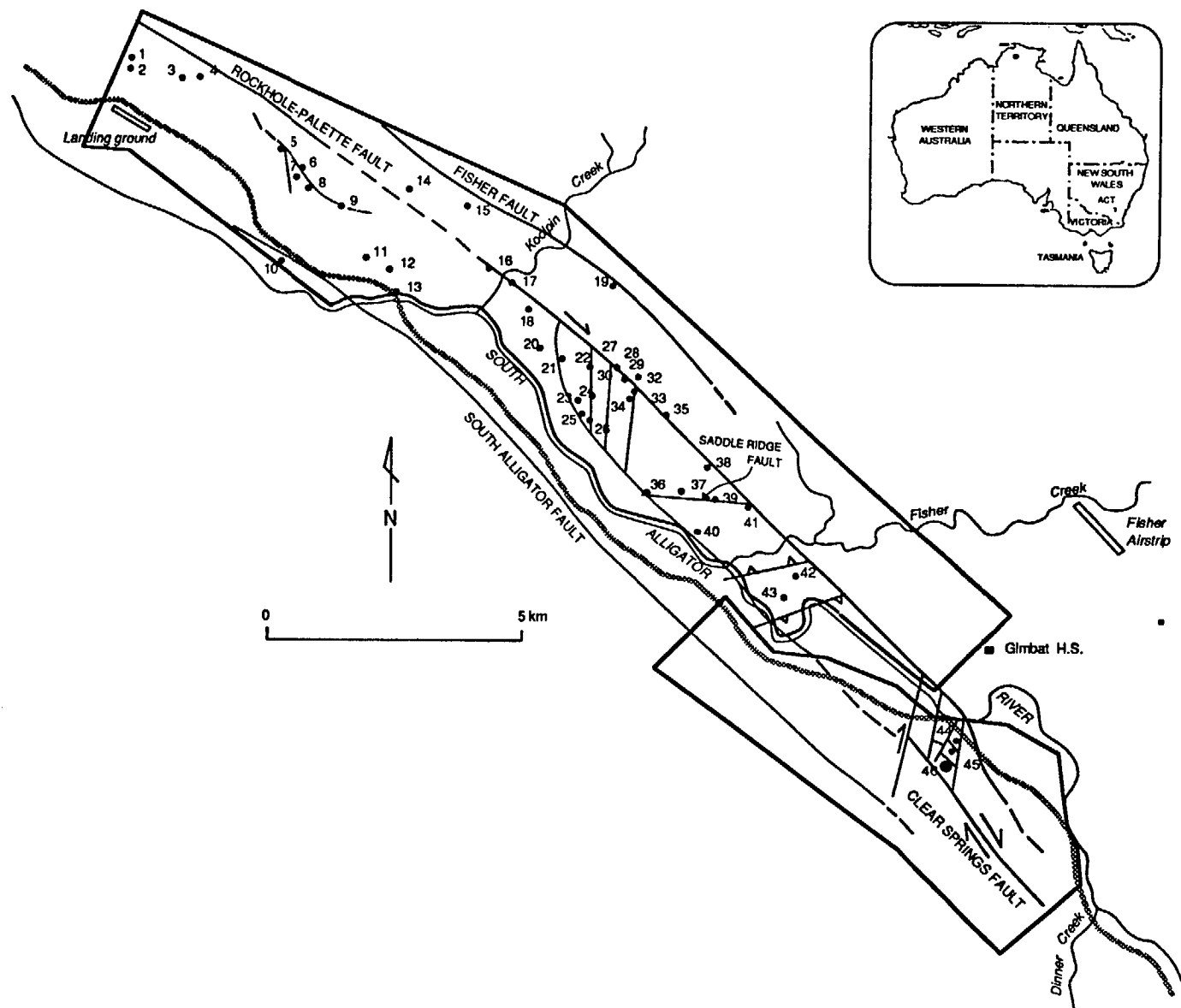


Figure 12. Cross section of the Palette area (see figure 10 for location).



Palette Area Cross Section

Figure 13. A map of major faults and prospects in the new CZ, showing areas referred to in text.



Prospects

- 1 - 9600NW
- 2 - 9200NW
- 3 - Airstrip
- 4 - Airstrip Northeast
- 5 - Stag Creek
- 6 - El Sherana North
- 7 - El Sherana West
- 8 - El Sherana
- 9 - High Road
- 10 - South Alligator Fault
- 11 - Stockpile 1
- 12 - Stockpile 2
- 13 - Flying Fox
- 14 - Charvats
- 15 - Orchid Gully
- 16 - Monolith
- 17 - Koolpin Creek
- 18 - Koolpin East
- 19 - Scinto 6
- 20 - Scinto 5 North
- 21 - Scinto 5 South
- 22 - Cliff Face
- 23 - Scinto 1, No 2 adit
- 24 - Scinto 1, No 1 adit
- 25 - Palms
- 26 - Scinto Camp
- 27 - Palette 5
- 28 - Palette 4
- 29 - Palette 6
- 30 - Palette 1
- 31 - Palette 2
- 32 - Palette 7
- 33 - Palette 3
- 34 - Skull 1
- 35 - Skull 2
- 36 - Clear Springs
- 37 - Saddle Ridge
- 38 - Saddle Ridge NE
- 39 - Saddle Ridge East
- 40 - Saddle Ridge South
- 41 - Saddle Ridge East Extended
- 42 - Pul Pul Hill North
- 43 - Pul Pul Hill South
- 44 - Callanans
- 45 - Coronation Hill
- 46 - Coronation Hill SW

	U-Au-PGE	Au-PGE only
Host Rocks	carbonaceous shale, cherty ferruginous shale, quartz feldspar porphyry	quartz feldspar porphyry, green tuffaceous siltstone, diorite, siliceous dolomites, sedimentary breccias, cherty ferruginous shale
Stratigraphic Setting	above carbonaceous Koolpin Formation	above dolomitic/volcanic Koolpin Formation, intruded by quartz feldspar porphyry
Structural Setting	fracture zones associated with the Palette/Rockhole fault set	fracture zone associated with the Palette fault (?others?)
Mineralization Style	pitchblende veins \pm chlorite- white mica alteration, quartz- absent	quartz-carbonate-chlorite veins, often with chloritic alteration.
Alteration	desilicification, chloritization	minor chlorite, sulphides, silicification
Timing	post-Kombolgie	post-Kombolgie
Structural Control	a) fault bends/intersections b) cfs/cs competency contrast c) unconformity	a) distributed fracturing on north- trending fault jog. b) unconformity
Chemical Control	a) reduction of oxidized fluids from above unconformity by interaction with carbonaceous rocks below unconformity. b) mixing between oxidized fluids carrying U-Au-PGE and CH ₄ -rich fluids c) mixing between saline oxidized metal-bearing fluids and low salinity meteoric or metamorphic fluids	a) reduction of oxidized fluids by interaction with chloritic lithologies. b) titration of slightly acidic metal-bearing fluids to higher pH's by interaction between fluid and calcareous lithologies or K feldspar-bearing lithologies.

Table 1. A comparison of the characteristics of *U-Au-PGE* mineralization and *Au-PGE-only* mineralization.